

**Institut für Experimentelle Genetik
GSF-Forschungszentrum für Umwelt und Gesundheit,
Neuherberg**



Gene expression analysis reveals novel functions of vitamin D and glucocorticoids

Florian Graedler

Vollständiger Abdruck der von der Fakultät Wissenschaftszentrum Weihenstephan für Ernährung, Landnutzung und Umwelt der Technischen Universität München zur Erlangung des akademischen Grades eines

Doktors der Naturwissenschaften

genehmigten Dissertation.

Vorsitzender: Univ.-Prof. Dr. Heinrich H.D. Meyer

Prüfer der Dissertation: 1. Priv.-Doz. Dr. Jerzy Adamski
2. Univ.-Prof. Dr. Hans-Rudolf Fries

Die Dissertation wurde am 21.10.2004 bei der Technischen Universität München eingereicht und durch die Fakultät Wissenschaftszentrum Weihenstephan für Ernährung, Landnutzung und Umwelt am 31.01.2005 angenommen.

Summary	7
Zusammenfassung	9
1. Introduction	11
1.1. Gene expression profiling: Technology development of cDNA microarrays.....	11
1.1.1 Functional genomics	11
1.1.2 Modern analytical methods in functional genomics	11
1.1.3. DNA microarray technology	12
1.1.3.1 The principle	12
1.1.3.2 Oligonucleotide versus cDNA arrays.....	13
1.1.3.3 Protocol development and technical sources of interference.....	14
1.1.3.4 Processing microarray data	15
1.1.3.5 Data interpretation: from single genes to pathways	18
1.1.3.6 Applications of microarray technology and outlook	19
1.1.3.7 Microarray Technology as a tool in Molecular Endocrinology	20
1.2 Vitamin D.....	21
1.2.1 Vitamin D synthesis and metabolism	21
1.2.2 Functions of the vitamin D system	24
1.2.2.1 Molecular mechanism of vitamin D action	24
1.2.2.2 Classical functions of vitamin D: Calcium / Phosphate homeostasis	25
1.2.2.3 Convergent actions of VDR and RXR signalling	27
1.2.2.4 Novel implications of vitamin D action.....	27
1.3 Functions of vitamin D-inducible Cyr 61 in human fetal osteoblasts (hfOB)	29
1.4 Glucocorticoid treatment of insulin-secreting pancreatic β-cells	30
1.5 Aims of the project	31
2. Establishing gene expression profiling with cDNA microarrays; experiments with cell culture systems	32
2.1 Establishing the Technology.....	32

2.1.1 Microarray production.....	32
2.1.1.1 Clone selection	33
2.1.1.2 Printing microarrays.....	33
2.1.2 Sample preparation	39
2.1.2.1 Isolation and purification of RNA	39
2.1.2.2 RNA transcription and labeling	39
2.1.3 Testing the method with cell culture systems: Proof of principle	40
2.2 Gene expression profiling of human fetal osteoblasts after treatment with Cyr61	45
2.3 The mouse cDNA array	50
2.4 Expression profiling of glucocorticoid-treated pancreatic β-cells	52
2.4.1 Experimental set-up	52
2.4.2 Data analysis.....	52
2.4.3 Genes, differentially expressed after glucocorticoid treatment: Discussion.....	54
3. Gene expression profiling of vitamin D receptor knockout (VDRKO) against wild type mouse kidney	57
3.1 Gene expression profiling with cDNA microarrays.....	57
3.1.1 Gene Expression profiles of kidneys from male ND mice: VDRKO compared to WT	57
3.1.2 Gender and diet specific influences on gene expression.....	62
3.1.2.1 Experimental Design.....	62
3.1.2.2 Data processing of single experiments.....	64
3.1.2.3 Different approaches of gene clustering reveal gender-specific effects.....	65
3.1.2.3.1 Hierarchical clustering	65
3.1.2.3.2 Significance analysis of microarray data (SAM).....	69
3.1.3 Genes, differentially expressed in kidneys of male RD mice: VDRKO compared to WT ...	70
3.2 Validation by quantitative PCR and interpretation	73
3.2.1 Genes involved in ion transport and calcium homeostasis.....	74
3.2.2 Nuclear hormone receptors and steroid/cholesterol metabolism.....	78
3.2.3 Cross-talk between nuclear hormone receptors	83
3.2.4 Lipid metabolism and energy supply.....	84
3.2.5 Blood pressure control	90

3.2.6 Cell growth, proliferation, apoptosis and cancer	93
4. Expression analysis of VDRKO and WT mouse heart.....	97
4.1 Microarray experiments: Experimental set-up.....	97
4.2 Analysis of microarray data.....	98
4.3 Annotation of candidate genes	107
4.4 Confirmation of candidate genes by qPCR.....	109
4.5 Discussion of gene expression profiles and assignment of candidate genes to physiological functions and pathways	112
4.5.1 Candidate genes involved in the immune system.....	113
4.5.2 Lipid metabolism and energy mobilization	115
4.5.3 Ion transport processes.....	118
4.5.4 Marker genes for hypertension and cardiac hypertrophy.....	119
4.5.5 Genes induced in ischemic insult and cardiac hypoxia.....	121
5. Conclusions	123
5.1 Establishing microarray technology.....	123
5.2 Treatment of osteoblast with CCN1 induces processes as in bone fracture repair	123
5.3 Pancreatic beta cells respond to glucocorticoid treatment with transcriptional changes characteristic for a pre-diabetic condition	124
5.4 Gene expression profiling of kidneys of mice with inactivated vitamin D receptor (VDRKO).....	124
5.4.1 Influence of covariate factors: Gender and diet	125
5.4.2 Altered gene expression in tissues from normocalcemic VDRKO	126
5.4.3 Ligand-independent action of VDR	126
5.4.4 Non-genomic and genomic actions of vitamin D influence lipid metabolism	126
5.4.5 Vitamin D and growth control / apoptosis.....	127
5.4.6 VDRKO mice and hypertension	127
5.5 Gene expression profiling of VDRKO and WT mouse heart	128

5.5.1 Changes in the immune response in VDRKO mouse heart.....	128
5.5.2 Impaired lipid metabolism in can compromise heart function	129
5.6 Summary	129
6. Methods	130
6.1 Microarray production and analysis	130
6.1.1 Clone selection, storage and verification	130
6.1.1.1 The Human cDNA array	130
6.1.1.2 The Mouse 21k-array.....	131
6.1.2 Template production.....	131
6.1.3 Amplification of probes by PCR.....	131
6.1.4 Printing of DNA microarrays.....	134
6.1.5 Aminoallyl Labeling für RNA Microarrays.....	135
6.1.6 Hybridisation.....	138
6.1.7 Procedure for stringent washing of slides	139
6.1.8 Signal enhancement using dendrimer technology	140
6.1.9 Scanning.....	143
6.1.10 Image processing	144
6.1.11 Data normalisation, filtering and extraction	146
6.2 Quantitative Real-time PCR	152
6.2.1 Principle of relative quantification.....	152
6.2.2 Sample cDNA preparation.....	154
6.2.3 Amplification protocols	155
6.2.4 Primer selection and testing.....	155
6.2.5 Choice of the reference gene	157
6.3 Cell culture conditions	158
7. Materials	159
7.1 Chemicals	159
7.1.1 Chemicals for Microarray analysis	159

7.1.2 General chemicals.....	159
7.2 Buffers and Solutions.....	161
7.3 Kits	161
7.4 Primers.....	162
7.4.1 Primers for microarray analysis.....	162
7.4.2 Primers for qPCR	162
7.5 Hardware.....	164
7.6 Software	164
7.7 Bacterial strains	165
7.8 Cell lines	165
7.9 Media for Cell Culture.....	165
8. Appendix	166
8.1 Frequently used abbreviations.....	166
8.2 Curriculum vitae.....	167
8.3 Publications.....	169
8.3.1 Manuscripts:	169
8.3.2 Posters	169
8.4 Acknowledgements / Danksagung.....	170
9. References	171

Summary

Steroid hormones as Vitamin D and glucocorticoids regulate multiple biochemical pathways and physiological processes. The discovery of nuclear hormone receptors and their mode of action in recent years helped to elucidate the mechanism of steroid-mediated transcriptional control. Disturbances in the control of these complex networks of gene regulation can cause severe diseases. It is therefore of high interest to understand the mechanism of steroid-induced gene regulation on the molecular level. Since it allows monitoring changes in the expression of thousands of genes in parallel, microarray technology was the method of choice to study the influence of glucocorticoids and vitamin D on transcription more in detail.

Establishing cDNA microarray technology was the first task in this project. Microarrays containing cDNA fragments probing for several hundred genes from selected pathways were developed and tested by measuring changes in the transcription profile of cell lines after exposure to steroids. Treatment of human fetal osteoblasts (hfOB) with Cyr61, a factor recently found to be induced by vitamin D in bone tissue culture, activated genes that belong to the Notch and Hedgehog signalling pathways. These pathways were reported to be involved in bone growth and remodelling. The identification of target genes of Cyr61, previously associated with functions during bone fracture repair, shows new signalling pathways controlled by vitamin D and Cyr61 in bone.

The development and production of high-density cDNA arrays with nearly 21.000 probes allowed genome-wide transcriptional profiling in mouse. These microarrays were used to analyse the effect of glucocorticoid treatment of insulin-secreting beta cells of pancreatic islets. Exposure to excessive doses of endogenous and exogenous glucocorticoids previously was shown to cause impaired islet function and diabetes. In this study the direct effect of short-term treatment of beta cells from lean mice with corticosterone, the murine analog of cortisol in humans, was tested for the first time. Corticosterone increased the secretion of insulin and induced genes known as markers for stress conditions, inflammation and a pre-diabetic state.

The main project of this thesis was the analysis of transcriptional regulation by vitamin D *in vivo*. Tissues, especially kidney and heart from wild type (WT) and transgenic mice expressing a transcriptionally inactive vitamin D receptor (VDRKO mice) were analysed for changes in their gene expression profile. Under normal dietary conditions, VDRKO mice develop a phenotype that suffers from severe rickets, hypocalcemia, hyperparathyroidism, alopecia, impaired growth and bone formation. Feeding VDRKO mice with a diet enriched in calcium and phosphate normalises serum calcium and PTH concentrations and partly rescues features of the rachitic phenotype.

The overlapping, antagonistic or synergistic influences of vitamin D, PTH, sex steroids and serum calcium on transcription in kidneys of VDRKO mice were separated by clustering differentially expressed genes according to the gender and diet of the mice. The expression of cytochrome P4504a14 (CYP4 α 14), which is only activated in kidneys from female VDRKO mice, is an example for gender-specific regulation by vitamin D and sex steroids. CYP4 α 14 is involved in the development of several metabolic diseases and hypertension.

The role of vitamin D action in lipid metabolism and in the development of metabolic diseases like adiposity, hypertension or diabetes were clearly reflected in the functional annotations of differentially expressed genes in kidneys from VDRKO mice. Lipogenic genes were significantly up-regulated, apparently through a calcitriol-induced increase of intracellular calcium via VDR-independent mechanisms. Simultaneously, a loss of repression through the vitamin D receptor enhances the expression of uncoupling protein 1 (UCP1). Mitochondrial uncoupling increases the dissipation of energy. A resulting lower efficiency of ATP production can impair insulin signalling. The previously reported activation of the renin-angiotensin system in VDRKO mice was confirmed. In addition, this study identified the induction of a number of marker genes for hypertension and related diseases.

The heart, a non-classical target organ of vitamin D, showed in the case of VDRKO mice changes in gene expression that correspond to the observations in kidney, the key organ of the vitamin D endocrine system. As in kidney, expression of lipogenic genes was significantly increased, together with markers for inflammation, stress response, cardiac hypertrophy and myopathy. Genes associated with the development of hypertrophy and metabolic switching from lipids to glucose and glutamin as energy carriers were activated. Strong induction of calgranulins and vitamin D-binding protein (DBP) show the *in vivo* impact of vitamin D on the immune response in heart for the first time.

All studies in this thesis contribute to the development of microarray technology and its application to investigate the role of steroids in the development of multifactorial diseases. It gives evidence that impairment of the vitamin D endocrine system can affect the regulation of factors controlling central metabolic functions. Novel target genes and pathways regulated by vitamin D through genomic and non-genomic action were identified. The results from this study show that vitamin D is an important element connecting the so far unresolved association between rickets and hypertension, diabetes and cardiovascular diseases.

Zusammenfassung

Steroidhormone regulieren eine große Zahl an biochemischen und physiologischen Vorgängen. Die Entdeckung nuklearer Hormonrezeptoren und die Aufklärung ihrer Wirkungsweise trugen in den vergangenen Jahren dazu bei, Steuerungsmechanismen der Transkription aufzuklären, die von Steroiden reguliert werden. Störungen in der Kontrolle dieser komplexen Netzwerke der Genregulation können schwere Krankheiten verursachen. Es ist daher von großem Interesse, die Mechanismen der Genregulation durch Steroide auf molekularem Niveau zu verstehen. Die Microarray Technologie erlaubt es, Veränderungen in der Expression tausender Gene gleichzeitig zu messen. Sie war daher die Methode der Wahl, um den Einfluß der Steroidhormone Vitamin D und Kortikosteron auf die Transkription näher zu untersuchen.

Die erste Aufgabe in diesem Projekt war die Etablierung der cDNA Microarray Technologie. Zunächst wurden Microarrays entwickelt mit cDNA Fragmenten als Sonden für mehrere hundert Gene aus ausgewählten Signalwegen. Diese wurden durch die Messung von Veränderungen im Transkriptionsprofil von Zelllinien nach der Behandlung mit Steroiden getestet. Fötale menschliche Osteoblasten (hfOB) wurden mit Cyr61 behandelt, einem Faktor, dessen Expression Vitamin D in Knochenzellen induziert. Dadurch wurden Gene aus dem dem Notch- und dem Hedgehog Signalweg aktiviert. Beide Signalwege zeigten in früheren Untersuchungen ihre Bedeutung für den Umbau von Knochengewebe. Die Identifizierung von Zielgenen von Cyr61, dem eine Rolle insbesondere während der Heilung von Frakturen zugeschrieben wurde, zeigt neue Signalwege unter der Kontrolle von Vitamin D und Cyr61 in Knochen.

Die Entwicklung und Herstellung von cDNA Arrays mit knapp 21.000 Sonden ermöglichte eine genomweite Transkriptionsanalyse bei Mäusen. Mit diesen Microarrays wurde u.a. untersucht, wie sich eine Glukokortikoid-Behandlung von Insulin-produzierenden Inselzellen des Pankreas auf deren Expressionsprofil auswirkt. Bereits früher war gezeigt worden, daß die Funktion von Inselzellen stark beeinträchtigt wird, wenn man sie hohen Dosen endogener oder exogener Glukokortikoide aussetzt. In dieser Arbeit wurden zum ersten Mal die direkten Auswirkungen der Behandlung von Inselzellen mit Kortikosteron gezeigt, dem murinen Analog des Kortisols beim Menschen. Die Behandlung mit Kortikosteron verstärkte die Ausschüttung von Insulin und induzierte Gene, die als Marker für Stresszustände, Inflammation und für die Entwicklung von Diabetes bekannt sind.

Das Hauptprojekt in dieser Promotionsarbeit war es zu untersuchen, wie Vitamin D die Transkription *in vivo* reguliert. Gewebe, insbesondere aus Niere und Herz von Wildtyp (WT)-Mäusen und von transgenen Mäusen, die einen auf Transkriptionsebene inaktiven Vitamin D Rezeptor (VDR) exprimieren (VDRKO-Mäuse), wurden auf Unterschiede im Transkriptionsprofil analysiert. Bei normaler Ernährung entwickeln VDRKO Mäuse einen Phänotyp, der schwere Rachitis, Hypokalzämie, Hyperparathyroidismus, Alopecia, sowie Störungen im Wachstum und bei der Entwicklung von Knochen aufweist. Füttert man VDRKO-Mäuse mit einer kalzium-und phosphatreichen Diät, werden die Kalzium- und Parathormon (PTH) Werte im Serum auf Normalniveau gebracht und der rachitische Phänotyp stark abgeschwächt.

Die sich überlappenden, antagonistischen oder synergistischen Effekte von Vitamin D, PTH, Sexualhormonen und Kalzium auf die Transkription in Nieren von VDRKO Mäusen wurden durch das Clustern von Expressionsdaten nach dem Geschlecht und der Diät der Versuchstiere getrennt. Die Expression von Cytochrom P450a14 (CYP4a14), das nur in der Niere weiblicher VDRKO Mäuse aktiviert ist, ist ein Beispiel für geschlechtsspezifische Genregulation durch Vitamin D und Sexualhormone. CYP4a14 ist beteiligt an der Entstehung diverser Stoffwechselkrankheiten und Bluthochdruck.

Die Rolle von Vitamin D beim Lipidstoffwechsel und bei der Entstehung von Stoffwechselkrankheiten, wie Adiposität, Bluthochdruck oder Diabetes spiegelt sich klar in der funktionalen Annotierung differentiell exprimierter Gene in Nieren von VDRKO Mäusen wieder. Gene, die an der Lipogenese beteiligt sind, sind offenbar durch erhöhte intrazelluläre Kalziumkonzentrationen aktiviert. Die Konzentration von Kalzium im Zytosol kann durch Vitamin D durch Mechanismen reguliert werden, die nicht vom Vitamin D Rezeptor abhängen. Gleichzeitig wird durch die fehlende Unterdrückung durch den Vitamin D Rezeptor die Expression des uncoupling protein 1 (UCP1) erhöht. "Uncoupling" in den Mitochondrien verstärkt die Erzeugung von Wärme. Eine folglich geringere Effizienz bei der Produktion von ATP kann die Signalübertragung durch Insulin stören. Eine kürzlich beschriebene Aktivierung des Renin-Angiotensin Systems in VDRKO Mäusen wurde bestätigt. Darüber hinaus wurde in dieser Arbeit die Induktion mehrerer Gene festgestellt, die charakteristisch für Bluthochdruck und verwandte Krankheiten sind.

Das Herz, ein nicht-klassisches Zielorgan von Vitamin D, weist bei VDRKO Mäusen Veränderungen in der Genexpression auf, die gut mit den Daten aus Untersuchungen der Niere korrelieren. Die Niere ist das Schlüsselorgan des endokrinen Systems von Vitamin D. Wie in der Niere, war die Expression von an der Lipogenese beteiligten Genen im Herz erhöht, zusammen mit Markern für Inflammation, Stressantwort, und Herzschwäche. Aktiviert waren auch Gene, die im Zusammenhang mit der Entwicklung von Hypertrophie des Herzens bekannt sind und charakteristisch sind für ein Wechsel im Metabolismus von Lipiden auf Glucose und Glutamin als Energieträger. Die starke Induktion von Calgranulin A und B sowie des Vitamin D-bindenden Proteins (DBP) zeigen erstmalig die Wirkung von Vitamin D auf das Immunsystem im Herzen *in vivo*.

Die Arbeiten in dieser Dissertation sind ein Beitrag zur Weiterentwicklung der Microarray Technologie und zu deren Anwendung in der Erforschung der Rolle von Steroiden bei der Ausbildung multifaktorieller Krankheiten. Es wurde nachgewiesen, daß Vitamin D die Regulierung von Faktoren beeinflusst, die zentrale Funktionen im Stoffwechsel steuern. Es wurden neue Zielgene und Signalwege identifiziert, die durch Vitamin D über genomische und nicht-genomische Mechanismen reguliert werden. Die Ergebnisse dieser Studie zeigen, daß Vitamin D ein bedeutendes Glied in der bislang noch nicht aufgeklärten Verbindung zwischen Rachitis und Hypertonie, Diabetes, sowie mit kardiovaskulären Erkrankungen darstellt.

1. Introduction

1.1. Gene expression profiling: Technology development of cDNA microarrays

1.1.1 Functional genomics

At the beginning of this thesis, worldwide sequencing projects had achieved to decipher the genomes of yeast, *C. Elegans*, and drosophila, as well as over 20 prokaryotic genomes; the human and mouse genomes were expected to follow soon as draft versions. Although studies about the functions of single genes had been done for decades, the sudden wealth of sequence data required new technologies for rapid and massive parallel functional analysis and a new concept of systems molecular biology. Instead of the traditional reductionist approach that simplifies the complexity of organisms by narrowing the focus down to its smallest component parts on molecular level and studying the functions of gene products one-by-one, a more holistic approach was required to understand the interactions and regulatory networks of genes and their protein products in organisms as a whole. Similar to characterising complex electronic circuits by multiple simultaneous measurements of current and voltage at different positions, functional genomics aims to analyze the regulatory networks of tens of thousands of genes, hundreds of thousands of splice variants, protein products, and their post translational modifications. This required not only the development of novel, miniaturised methods of massively parallel analysis; recording, storage, processing of enormous amounts of data created by these methods only started to be possible with the advance of computer technology. The creation of relational databases and bioinformatics tools and algorithms that facilitate statistical data analysis, management and interpretation (Vukmirovic and Tilghman 2000) were prerequisites for the success of new methods and concepts in functional genomics.

1.1.2 Modern analytical methods in functional genomics

Proteins are translated end-products of the information comprised in the genome and thus determine the structure of cells and organisms, catalyse physiological processes at molecular level and transfer signals between compartments. Therefore it seems logical trying to monitor the expression of all proteins to characterise the condition of tissue or of a whole organism. The development of powerful methods for large-scale separation, detection and identification of proteins improved proteomic approaches in functional genomics significantly (Mann 2000). In combination with high-throughput methods to study protein interaction and –localisation, proteomic methods opened a rapidly evolving field of research. The diversity of proteins in terms of physicochemical properties and the complexity of protein structure have nevertheless so far to capture only small fractions of the proteome of cells and organisms at a time and make proteomic studies extremely time-, cost- and labour intensive. For this reason, proteomics still is not very well suited for rapid and comprehensive analysis of biological systems.

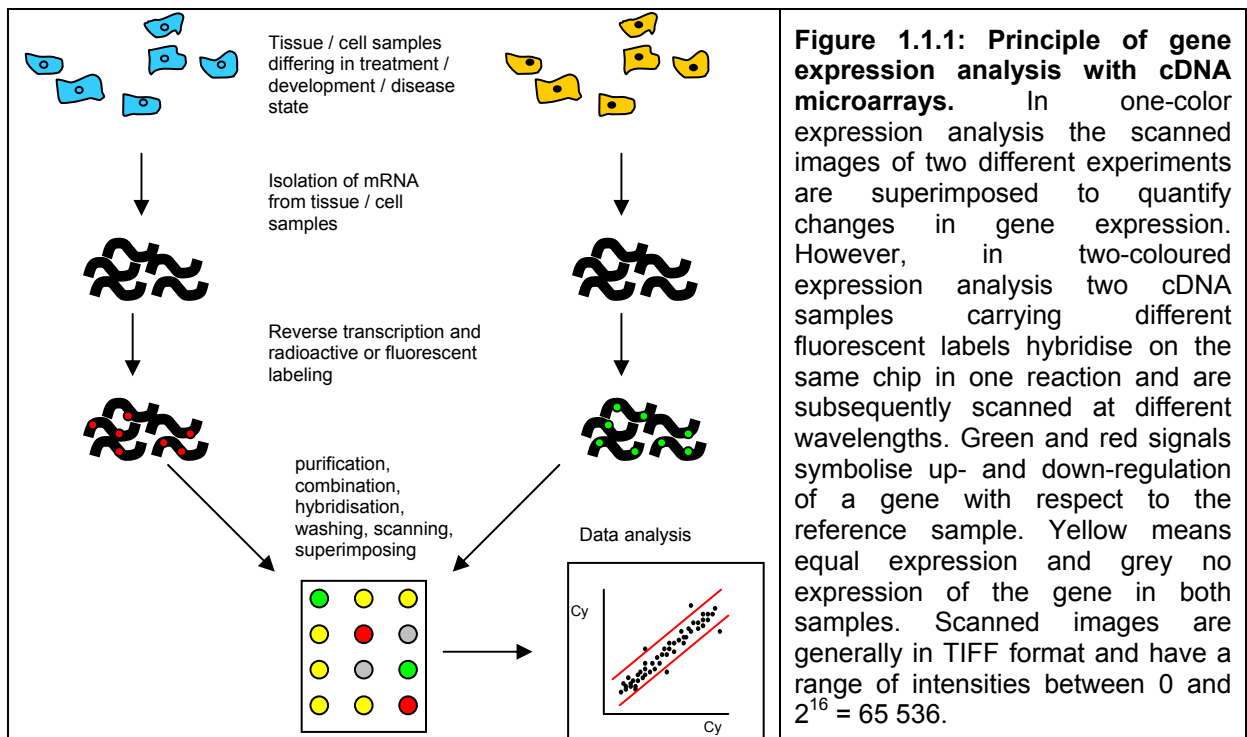
In comparison to proteins, nucleic acids like DNA or RNA are far more uniform and simple and therefore more accessible for biochemical analysis and computational data treatment. Gene expression analysis on transcriptome level has been in practice for about two decades with simple and versatile methods such as Northern Blotting, polymerase chain reaction after reverse transcription (RT-PCR), nuclease protection,

differential display or, more recently, serial analysis of gene expression (SAGE). These methods offer to monitor the expression of smaller or, in the case of SAGE, larger numbers of genes on mRNA level and thus provide powerful means to gain information about the biological state of cells and tissues. Although post-transcriptional events can modify the quantity and nature of protein products, gene expression profiling gives in most cases a good measure on changes in protein production. (Boheler and Stern 2003).

1.1.3. DNA microarray technology

1.1.3.1 The principle

DNA microarray technology has taken up the hybridisation-based principle of nucleic acid analysis from Northern blotting, combined it with PCR-based RNA sample labeling and miniaturisation technologies known from the computer chip technology. The principle of microarray technology is simple and has early been used in blotting and filter techniques (Augenlicht et al. 1987; Southern 2000): Fragments of DNA or oligonucleotides, probing for specific genes are immobilised onto a two- (eg. microscopic glass slides) or three-dimensional (porous membranes) substrate surfaces. The analyte RNA is labelled during reverse transcription by incorporation of nucleotides carrying either radioactive or fluorescent labels. During hybridisation, the labelled RNA products can hybridise specifically to their inverse complementary probes. After a series of washing steps with increasing stringency, scanning of the radioactive or fluorescent signal allows to quantify the relative amount of each mRNA species in the original sample. (see figure 1.1.1).



1.1.3.2 Oligonucleotide versus cDNA arrays

The multitude of different formats and variations of DNA microarrays for gene expression analysis can be grouped into two types: In type one, either synthetically produced long oligonucleotides, 50-120 bp in length, or cDNA fragments amplified by PCR from cDNA plasmid collections with a length varying from 300-2000 bp are deposited onto the substrate surface and chemically immobilized. The length of the immobilised cDNA probe determines the reaction kinetics of the hybridisation process (Stillman and Tonkinson 2001). Probe length also influences the specificity of the measurement and determines the number of fluorescent tags that can be incorporated per molecule (Stears et al. 2003). If reverse transcription of eukaryotic sample mRNA is performed with oligo (dT) primers, the probes should be chosen from a region near the 3' end of genes. Especially the 3' untranslated region promises high specificity and low cross-reactivity between probes.

Since cDNA synthesis by PCR is more accessible to research laboratories than oligonucleotide synthesis, the cDNA approach was chosen for this project. Bacterial cDNA clones are usually the source of probe templates that can be amplified by PCR in high-throughput format with universal primers. cDNA clone sets for microarray production are available from commercial vendors or resource centers like the Resource Center of the German Human Genome Project (RZPD). Initially their quality was compromised by a high degree of redundancy, incorrect sequence assignment, cross-contamination or infection with T1 phage (Halgren et al. 2001). Improvements in laboratory automation technology, cheaper and more efficient sequencing methods and the conclusion of the sequencing of the human, mouse and rat genome have improved the quality of available cDNA clone sets remarkably. This makes expensive and time-consuming quality control steps and clone sequence verification obsolete (section 2.1).

The production of the second type of DNA microarrays uses techniques based on photolithography (Fodor et al. 1991) to synthesize small or medium-sized oligonucleotides (15 - 50 bp) directly on the surface of the substrate. With the help of either photolithographic masks (patented by Affymetrix) or devices containing hundreds of thousands of electronically adressable micromirrors (Singh-Gasson et al. 1999), spots of light can be directed to the location of probe synthesis and selectively deprotect nucleotid building blocks. In a series of automated steps thousands of short oligonucleotides of uniform quality can be synthesised at defined postions of the chip surface. This type of microarrays generally can only be produced in an industrial setting and require standardised platforms for gene expression analysis. The high cost of oligonucleotide arrays and quality problems due to incomplete genome sequencing data and suboptimal procedures of oligonucleotide synthesis initially favoured the use of spotted cDNA arrays in genomic research. As market prices decreased with mass production and the quality of genome-wide oligonucleotide arrays increased significantly, it can be expected that commercially available systems that now offer arrays containing over 500 000 distinct probe features will gradually replace in-house cDNA products. Oligonucleotide arrays have not only great advantages in terms of standardisation and quality control; they also open the use of microarrays for other applications, such as the distinction of alternative splice variants, the detection of single nucleotide polymorphisms (SNPs) or the localisation of target genes in the genome.

The disadvantage in specificity and sensitivity of short oligonucleotides can be compensated by modelling melting conditions of target sequences precisely and by using multiple short sequences per gene in a 'tiling approach'. On Affymetrix arrays each gene is represented by a set of 'perfect match' and 'mismatch' oligonucleotides, the latter with a base exchange in the central position. By subtracting mismatch intensity values from 'match' intensities, an additional quality parameter is calculated that can be used to improve microarray specificity and sensitivity.

With cDNA arrays, amplification of cDNA probes from tens of thousands of bacterial plasmids is prone to cross-contamination or the introduction of tracking errors. Probe delivery onto substrate surfaces in sub-nanoliter volumes with a precision in the range of few micrometers requires extreme care in the control of the environment (temperature, dust, humidity) and the use of sophisticated robotic systems (Rose 2000).

1.1.3.3 Protocol development and technical sources of interference

Miniaturisation, building the potential of microarray technology to perform quickly and with minimal reagent consumption tens of thousands of measurements in one experiment also implies its great vulnerability to technical interferences. Small dust particles, salt crystals or inhomogeneity of the substrate surface coating can skew the detected fluorescence signal of hundreds of probes on a microarray and thus devalue a whole series of experiments and precious sample material. In two-colour expression analysis the probe has to be available in large excess. cDNA fragments of both samples can then hybridise to the probe in a reaction of pseudo first order kinetics. Inhomogeneous spot morphologies, often caused by differences in the shape of spotting pins, in probe concentration and evaporation during the spotting process ('doughnut effect') can partly be canceled out by calculating fluorescence intensity signal ratios of the superimposed scanned images.

Printing cDNA arrays of high quality requires careful matching of available spotting technology with sample buffers, substrate material and the development of protocols for proper array treatment after spotting. This includes rehydration, washing, probe immobilization, blocking, drying, storage, pre-hybridisation, hybridisation and washing (Rickman et al. 2003). Spatial gradients in signal intensities across the slide can arise from inhomogeneous background fluorescence due to residues of labeling dyes, reagents or unbound nucleotides on the array surface. Hybridisation kinetics in a thin film of sample solution between the microarray surface and the cover plate is limited by diffusion and depends on temperature and buffer. Temperature-controlled and sealed hybridisation chambers, equipped with micropumping systems, were therefore developed to guarantee stable conditions and enhance mixing by convection.

Extreme care is not only required for the production of microarrays: During sample preparation and RNA extraction small alterations in the treatment of sample cells or tissues have a strong impact on expression levels and RNA quality. Differences in gene expression between individual organisms of the same genotype introduce variability. Most tissues contain subpopulations of different cell types that can dilute the expression signal of potential target genes or lead to misinterpretations of expression data. Variation between individuals can be smoothed by sample pooling or, preferably by the analysis of larger numbers of biological replicates, which often is impossible because of limited access to sample material (e.g. human tissue biopsies) and the high costs of microarray analysis. Recently developed methods like

laser capture microdissection (Todd et al. 2002) can help to isolate small cell subpopulations from heterogeneous tissue as tumors. This strategy can overcome the problem of signal 'dilution' of genes specifically expressed in these subpopulations. On the other hand, minute amounts of sample RNA require strategies to improve sensitivity. Another problem with small cell numbers is the variability in gene expression between individual cells that only apparently belong to the same histological cell type.

For the labeling step, a large variety of products and protocols is on the market. Radioactive labeling, initially preferred for filter macroarrays for reasons of sensitivity and the large range of linear signal response was increasingly replaced by the less hazardous fluorescent labeling that can be performed in any laboratory and opens options for dual or multicolour labeling. Direct incorporation of labelled nucleotides during reverse transcription follows a simple, fast and straight-forward protocol but requires large amounts of sample RNA and suffers from different incorporation rates between fluorescent labels. Dye-swap experiments and techniques to couple fluorophores to chemically modified nucleotides after cDNA synthesis are strategies to overcome biased dye incorporation. In experiments with sample material from tissue biopsies or mouse primary cells, the amount of available RNA is generally too small for one microarray experiment (let alone the minimum of required experiment repetitions). To meet this problem, techniques of sample RNA amplification, as linear transcription with T7-primers or signal amplification via enzymatic reactions (Karsten et al. 2002) have been developed. In this project, signal amplification was achieved with a technique using fluorophores attached to dendrimeric tree molecules as labels (Stears et al. 2000). Recent publications even report microarray experiments with samples from laser capture microdissections in the range between ten and few hundred cells (Feldman et al. 2002; Xiang et al. 2003).

Although academic and commercial laboratories invested immense efforts to overcome these problems, there is still no gold standard for the production and use of microarrays of high quality. As a consequence, each laboratory has to invest time and effort to establish its own protocols, adapt them to the respective requirements of projects, the available instrumentation, workforce and budget. Only a carefully worked-out workflow, strict quality control of array production, processing and data analysis can guarantee consistent results from cDNA microarray experiments. This is the reason why many research institutions tend to either establish a core microarray facility as a central service institution or switch to commercial systems that have continuous support from service and development.

1.1.3.4 Processing microarray data

The overview about technical considerations on microarray experiments above underscores that this technology still is far away from being suited for routine analysis without expert knowledge. But once the large amounts of gene expression data from technically successful experiments are produced, the real challenge is to analyze these data, filter out noise, extract interesting 'target' genes, tendencies, or sample classes and interpret their function or allocate them to functional properties and pathways.

Having scanned the hybridised microarray and recorded the image in TIFF format, the following work steps are data acquisition, pre-processing, analysis and interpretation.

Data acquisition generally includes the localisation of probe spots on the array image, the definition and subtraction of the background, as well as the integration of light intensity signals. In the case of two-colour experiments two images of the array are recorded at different wavelengths and superimposed. The mean intensity ratio for each probe spot is calculated and linked to the respective probe annotation. The resulting data are saved as tab-delimited text files and imported into spreadsheets and data analysis software. Spot finding and the definition of feature boundaries generally occurs by laying a pre-defined grid of the drafted spot positions over the image. This image can first be manually adjusted to (often pin-defined) sub-grids and then automatically adapted to the exact shape of each spotted feature. Each spot position of the grid has an identifier that can be linked to the respective probe sequence and gene annotation, stored in a database (or an Excel spreadsheet for small non-commercial applications). Commercially available software often contains algorithms to identify and flag signals suspected to be artefacts, such as dust particles (by assessing the roundness and uniformity of the spots) or to exclude signals below a certain intensity threshold. Success and ease of data acquisition strongly depends on the quality of spotted arrays, signal intensities, substrate fluorescent background and scanner settings.

The extracted raw data then are imported to a commercial or open source program for data pre-processing and analysis. Among the open-source packages are BASE, developed at Lund University (Saal et al. 2002), TM4 from the TIGR Institute for Genomic Research (Saeed et al. 2003) or Bioconductor (Dudoit et al. 2003). Bioconductor is a versatile and extremely flexible collection of applications for microarray data analysis based on the statistical package R that requires some programming experience. The TM4 package, a modular collection of programmes for microarray data acquisition, pre-processing, analysis, storage and management is powerful and user friendly and was predominantly used in this project.

All experimental steps to acquire microarray gene expression data introduce some systematic bias, like differences in printing between pins, different efficiencies of dye incorporation during reverse transcription or slightly unbalanced concentrations of sample RNA, among others. A great part of this bias in dye intensity signals or spatial variations within one slide or between arrays can be removed by mathematical transformations. Global normalisation over the overall intensity of all probe signals is a simple method that was widely used in early microarray experiments. It is based on the assumption that the expression of the vast majority of genes (>95%) does not change between two experimental conditions. This means that (after excluding outliers and noise at low signal intensities) a normalisation factor N can be calculated and the individual expression ratios adjusted so that the overall expression ratio is equal to one (Quackenbush 2002). The assumption of an overall constant level of gene expression is not valid for small microarrays containing selected genes of common pathways or experiments causing drastic effects on the overall metabolism of the organism (e.g. heat shock experiments with yeast (van de Peppel et al. 2003)) and does not account for systematic, nonlinear or intensity-dependent effects. Global shifts in gene expression can be detected and quantified with RNA spikes added to the samples in different concentrations. The complementary probes detecting the spike RNA species on the array have to be foreign to the genome of the respective organism, like plant-specific genes for mouse arrays. Non-linear normalisation algorithms like locally weighted linear regression analysis (LOWESS) can help to reduce intensity-dependent effects. Local normalisation approaches can help to

correct for spatial variations, such as different spot morphologies between sub-grids (pin groups) (Colantuoni et al. 2002).

After normalisation, filtering algorithms help to exclude noisy data, generally in the low range of signal intensities. This reduces the amount and complexity of data and saves computing time and memory during analysis. Most packages offer the possibility to set a fixed intensity threshold or a percentage cut-off, below which data elements are discarded. More refined algorithms calculate the local background and its standard deviation and only retain data that differ from their local background by a pre-set confidence level, e.g. 95% (Quackenbush 2002). Filtering out data that behave differently in replicate experiments, dye swap experiments and averaging over replicates can further contribute to the elimination of false positives and to reduce data complexity.

The ultimate goal of each expression profiling experiment is the extraction of a small list of 'candidate genes' that change in expression between biological conditions. The simplest way of selection is to set an arbitrary threshold of $\log_2(\text{ratio intensities})$, and to define gene probes that are changed in signal intensity more than two- or fourfold as differentially expressed. Although used in many early microarray experiments, this approach does not account for the structure of the data set which can change from experiment to experiment and tends to either include false positive results, or to qualify many regulated genes as not differentially expressed. Changes in variability due to the nature of samples, experimental conditions or decreasing signal intensity can be taken into account with the definition of a local Z-score. Z is calculated as the ratio of the difference between a data point and the local mean and the local standard deviation of a subpopulation of data points within a sliding window around this data point (Quackenbush 2002).

Many studies have shown the necessity of replicates in microarray experiments (Pan et al. 2002). Technical replicates are intended to filter out noise between experiments with the same sample material, introduced by experimental conditions, whereas biological replicates should reflect the biological variability between individual organisms, cell culture batches or tissue samples. Normalised and filtered data sets from replicate experiments can be imported into data analysis software, such as the multi experiment viewer (MEV) of the TM4 package. All data of a series of experiments can be assembled in a multi-dimensional expression matrix, with each experiment forming a vector and each expression ratio a coordinate. Visualisation of $\log_2(\text{ratio intensities})$ is done by translating the values into a colour code, giving a direct and intuitive impression about the structure of gene expression profiles from multiple experiments.

In the microarray studies within this project, the main question was to find genes that characterise the difference between samples representing two different conditions: Treated versus untreated cells or tissue from knockout vs. wild type mice. In one study, the influence of other, 'covariate' factors, such as sex and diet on the changes in expression profile was under investigation. The direct comparison between two biological conditions requires the use of filtering methods rather than gene clustering. Traditional parametric tests, such as versions of the two-sample t-test can be used to filter out differentially expressed genes. T-tests assume normal distributions, which are generally not given in microarray data and confidence levels of 99% still can mean 200 false positives in the case of an experiment with microarrays containing 20.000 probes. Therefore, nonparametric statistical methods, such as the

significance Analysis of Microarrays (SAM) were developed (Tusher et al. 2001; Zhao and Pan 2003).

To interpret complex expression matrices, a number of methods were developed to group candidate genes or experiments into clusters, making 'order' in apparently random data collections. Clustering algorithms can be divided into supervised and unsupervised methods, depending on whether any additional information about the nature of samples or experiments determines the pattern according to which genes or experiments are sorted or whether the clustering process serves to find a structure in the data without any a priori input.

Widely used unsupervised methods for microarray data analysis are principal component analysis, k-means clustering or hierarchical clustering and network determinations, like Boolean, Bayesian or relevance networks to determine gene-gene or gene-phenotype interactions. While the latter methods are only relevant in the case of large data sets comprising many experimental conditions, k-means (Soukas et al. 2000) and hierarchical clustering (Eisen et al. 1998; Iyer et al. 1999) are simple, iterative methods to assign genes or experiments to groups with similar expression patterns. Although not taking into account more sophisticated associations such as negative correlations (like p53 suppressing a number of genes), they are useful to get a quick visual impression of overall similarities in expression patterns in a set of experiments.

1.1.3.5 Data interpretation: from single genes to pathways

The output of most data analysis procedures is a list of candidate genes that characterise through their pattern of expression a certain phenotype, the reaction to drug treatment or distinguish diseased from normal tissue. Gene annotation is a crucial factor necessary to interpret the biological meaning behind these lists of genes, for hypothesis building and for establishing strategies to validate these conclusions with additional experiments. Candidate genes have to be identified through the probe sequence and connected with a unique and universal gene identifier. By searching databases, this gene identifier can be linked with information about promoter elements, intron-exon structures, splice variants and functions and structure of protein products. Valuable information can also include homologous genes in other organisms. Links to other databases contain literature references, further expression data, gene-protein or protein-protein interactions. During the preparation of this thesis there have been substantial improvements in the quality and accessibility of gene annotation data. Nevertheless, missing annotations, redundancy and unsystematic nomenclature in databases that often lack links and compatibility among each other still make data interpretation a difficult and time-consuming endeavour. The Gene Ontology (GO) consortium tries to address some of these problems by assigning genes and gene functions to a standardized and structured set of terms that can be linked to public databases.

GenMapp is an open, web-based software platform that enables the user to import candidate gene lists resulting from expression profiling studies and to assign them to GO functional categories. It also allows to create models for regulatory pathways (Dahlquist et al. 2002; Doniger et al. 2003). Home-made cDNA arrays require the assignment of all probes to reference mRNA sequences by alignment tools like BLAST and the storage and curation of all data concerning probes, reference

sequences and gene product annotations in a database. Commercial microarray platforms generally offer their clients to use web-based data bases, which are regularly updated and linked to other public or commercially available resources.

The success story of public databases containing genome sequencing (GenBank, dBEST, TIGR) or mapping (LDB, CHCL) data has raised the demand to implement similar platforms to share data from gene expression profiling experiments to exploit this wealth of information more efficiently. Although there are already examples of expression databases from large scientific institutions, consortia and industry, the quantitative nature of expression data, the multitude of different microarray technology platforms and simply the lack of standards for experimental design and data analysis have so far impeded a similar success story for gene expression databases (Becker 2001).

To address the lack of standardisation for the publication of gene expression data, the Microarray Gene Expression Database Group (MEGD), a consortium of leading research institutions like the European Bioinformatics institute (EBI) and the National Institutes of Health (NIH) created a standard format for the design and annotation of microarray experiments called Minimum Information About a Microarray Experiment (MIAME). MIAME is supposed to facilitate the exchange of microarray data and the establishment of public expression data repositories (Brazma et al. 2001). The concept of MIAME has been complemented by the development of the universal data format MAGE-ML (microarray gene expression markup language) and tool kits to integrate MAGE-ML into different microarray platforms (Spellman et al. 2002). While large commercial microarray platforms like Affymetrix implemented the export of microarray data from end-user databases in a format according to the MIAME standards, some scientific journals require already the submission of microarray data according to MIAME guidelines.

1.1.3.6 Applications of microarray technology and outlook

Microarray technology has the potential that enables the researcher to perform in one experiment tens of thousands of measurements simultaneously and to establish gene expression profiles that precisely can characterise the state of a cell or an organism. Since the first publication of a gene expression profiling study of colon biopsies with 4000 cDNA probes immobilized on nylon membranes (Augenlicht et al. 1987) and the first microarray printed on glass (Schena et al. 1995), the number of published studies using this technique rose dramatically. At the beginning of this project most publications focused on the technical aspects of microarray technology. Later the focus shifted towards methods and strategies for data analysis and interpretation. Applications of microarray technology include all aspects of functional genomics, like the classification of tumors, the finding of disease marker genes for medical diagnostics, studies about the function and metabolism of drugs on molecular level or the characterisation of developmental stages in cellular and embryonic development.

Beyond gene expression profiling, the principle of massive parallel testing with large sets of probes immobilized in high-density array elements was extended to applications in comparative genome hybridisation analysis (CGH) to study gene duplications or deletions and in genotyping studies to analyse probes from a set of individuals for thousands of SNPs in one experiment. Further assays in microarray

format were developed to study protein expression with antibody arrays or the interaction of proteins with other proteins (MacBeath 2002), organic molecules, carbohydrates (Wang, D. et al. 2002) or peptides (Robinson et al. 2002).

In the near future more sensitive and robust techniques for signal detection will be developed, like colorimetric measurement of products of enzymatic reactions similar to ELISA formats (Lau et al. 2002) or detection by resonance light scattering (RLS) (Bao et al. 2002). The development of microfluidic lab-on-chip technologies (Lau et al. 2002) will help to make microarray technologies more robust and open their way to applications in fully integrated assays and routine diagnostic tests suitable for unskilled users.

Just at the time the writing of this thesis was concluded the first diagnostic test based on microarray technology got the CE mark for admission in the European Union. The "Amplichip", a cooperation product from Roche Diagnostics and Affymetrix Inc. provides a rapid test to distinguish variations of cytochrome CYP2D6 and CYP2C19 genes in blood samples. As these enzymes play an important role in the metabolism of widely prescribed drugs, the test can give valuable information helping to adjust the optimum dose for each drug and patient and to avoid hazardous reactions of slowly metabolising phenotypes. The development of genetic assays for clinical use can therefore be seen as an important step towards individualised drug treatment (Newswire 2004).

1.1.3.7 Microarray Technology as a tool in Molecular Endocrinology

Hormones like estrogen or vitamin D act by binding to nuclear receptors. Liganded receptors translocate into the nucleus, bind to specific DNA sequence elements and activate or suppress transcription. The protein products of genes regulated by hormone action can activate various functions and initiate signalling pathways in target tissues, which might regulate the production of the steroid itself. The analysis of complex networks of gene regulation requires highly parallel measurement technologies as gene expression profiling with microarrays or quantitative real-time PCR (Soulet and Rivest 2002; Amsterdam et al. 2003; Otsuki et al. 2003).

1.2 Vitamin D

Vitamin D has been discovered as preventive agent against rickets, a defect in bone development due to impaired calcium homeostasis, endemic in the rapidly growing and polluted industrial cities of 19th century Europe. It was soon observed that both, diet supplementation with cod liver oil, as well as sunbathing, can cure rickets (Lin and White 2004), indicating that the vitamin can be ingested or synthesized in the body during sun exposure.

1.2.1 Vitamin D synthesis and metabolism

Feeding UV-B-irradiated skin to rats with rachitic symptoms cured these animals. This and finally the discovery of the chemical structure of the therapeutic agent in cod liver oil showed that the anti-rachitic substance from nutritional and endogenous sources was identical. Depending on the dietary source, the hormonal precursor can be either in the form of vitamin D₃ (cholecalciferol) or as vitamin D₂ (ergocalciferol) with a slightly modified carbohydrate side chain of the secosteroid core. In the skin Vitamin D₃ is synthesised by photochemical derivatisation of 7-dehydrocholesterol (Jones et al. 1998). The precursors of the active forms of vitamin D, cholecalciferol and ergocalciferol, are activated by the same cytochrome P450 enzyme system (figure 1.2.1). As cutaneous photochemical synthesis of vitamin D accounts for more than 90% of the average human vitamin D requirement (Holick 2003), it is unsurprising that vitamin D supply strongly depends on skin pigmentation (Clemens et al. 1982), geographical latitude and season (Webb et al. 1988). The application of sunscreens containing UVB blockers dramatically decreases vitamin D synthesis (Matsuoka et al. 1988). The conversion of ergosterol to previtamin D₂, a process that efficiently absorbs harmful UVB irradiation even in primitive organisms as diatoms, has been proposed to have functioned as a sunscreensing system in early stages of evolution before the ozone layer in the stratosphere was formed. (Holick 1989). A curiosity in this context are studies showing the impact of different dress styles of women in islamic countries on circulating levels of vitamin D (Alagol et al. 2000; Mishal 2001).

Both, vitamin D₃ and vitamin D₂ undergo a two-step activation process, catalysed by enzymes of the cytochrome P450 family, vitamin D₃-25 hydroxylase (CYP27) in the liver, followed by a second hydroxylation through 25-hydroxyvitamin D₃-1 α -hydroxylase (CYP1 α) in renal proximal tubular cells (figure 1.2.1). Both vitamin D-activating cytochrome P450 hydroxylases and the catabolic 25-hydroxyvitamin D₃-24-hydroxylase (CYP24), which initiates the degradation of calcidiol 25(OH)D₃ and the active hormone calcitriol 1,25(OH)₂D₃ are located in the inner mitochondrial membrane of the respective cells in liver, kidney and several vitamin D target tissues. To avoid pathologic effects of vitamin D deficiency or -toxicity, both, activation by CYP1 α and catabolism by CYP24 in kidney and target tissues are tightly controlled by transcriptionally regulated feedback loops. An important role in the homeostatic control of renal 1,25(OH)₂D₃ production has parathyroid hormone (PTH). PTH synthesis in turn is controlled by serum concentrations of calcium and phosphate (see the scheme in figure 1.2.2).

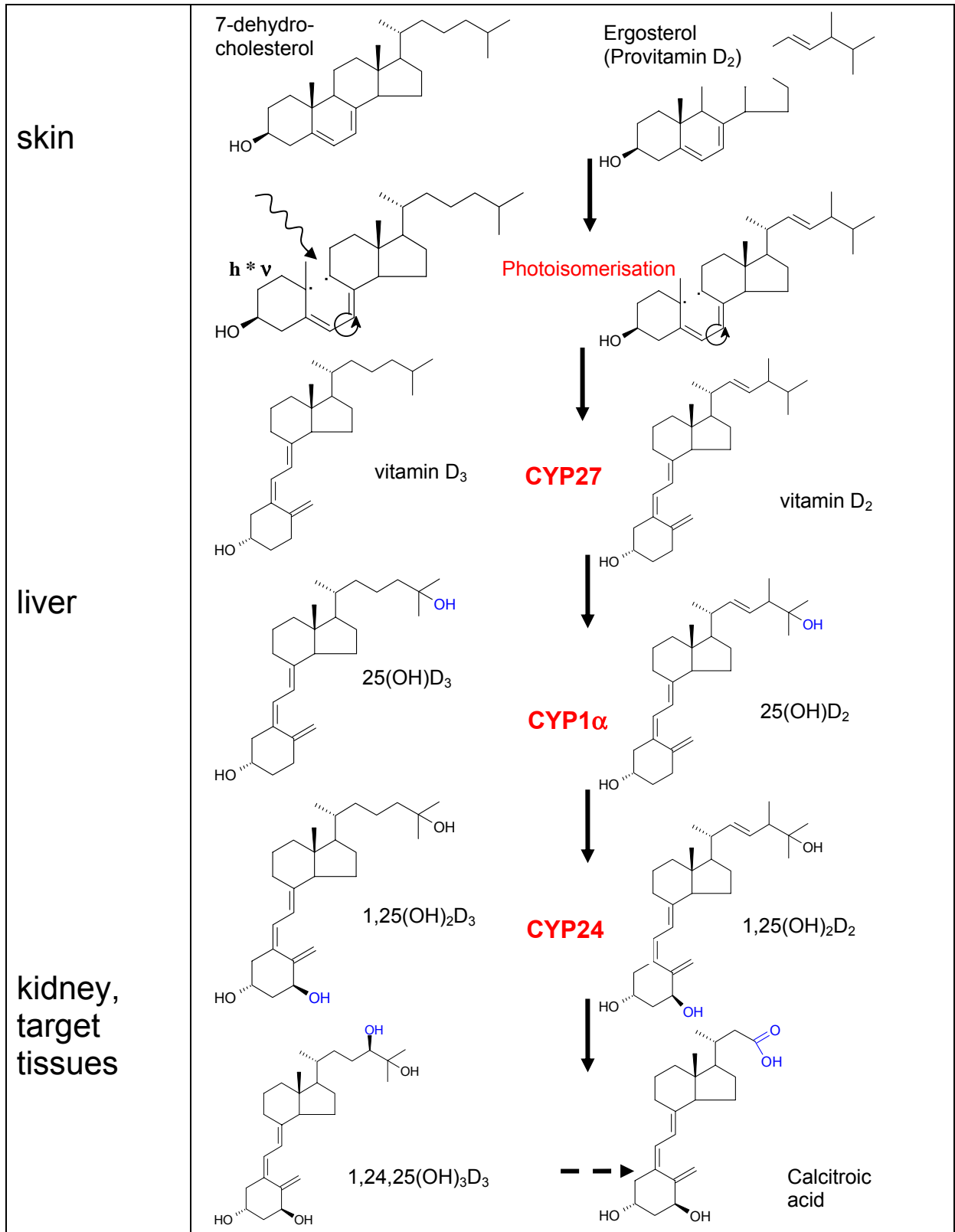
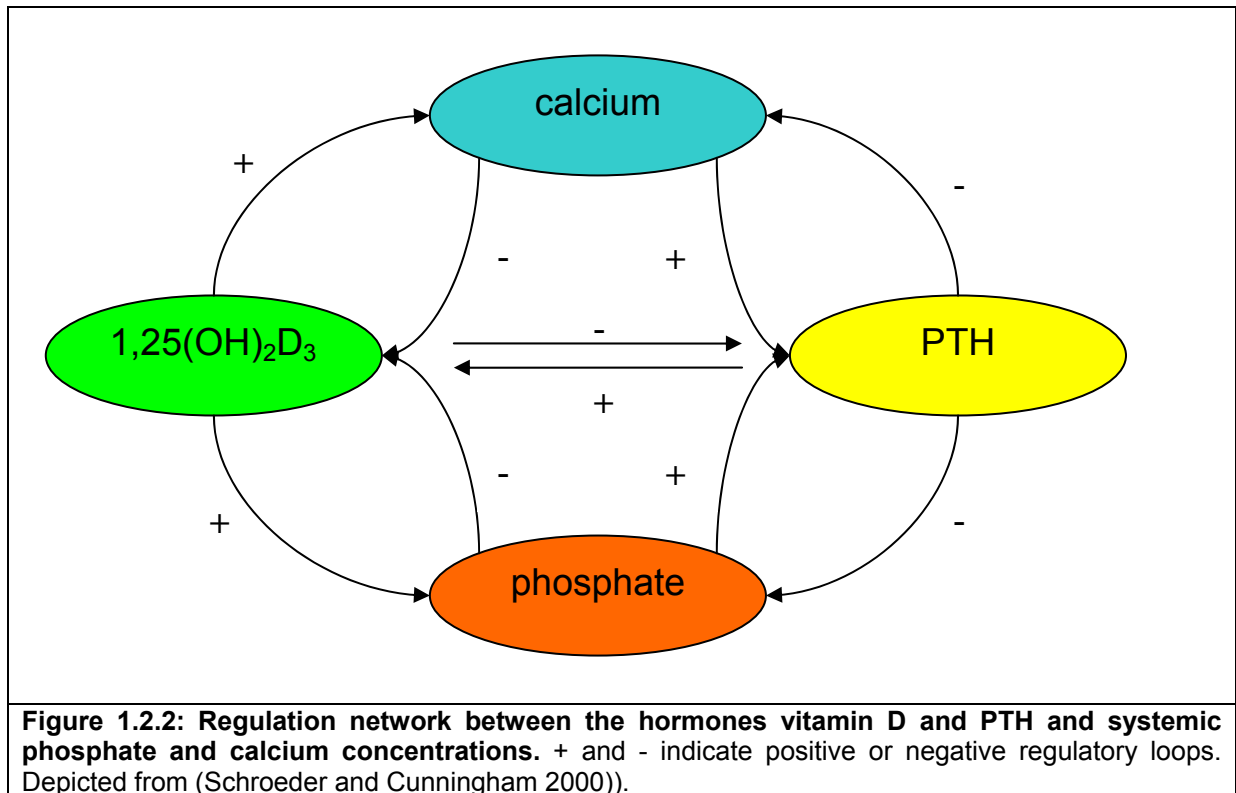


Figure 1.2.1: Vitamin D Metabolism. Starting from 7-dehydrocholesterol (top, left) or ergosterol (top, right), UV-B irradiation in the skin breaks one carbon bonding of ring B and induces photoisomerisation and H-shift to vitamin D₃ (left) or vitamin D₂ (right). In hepatocytes, mitochondrial CYP27 catalyses the hydroxylation of vitamin D_{3/2} at position 25 to 25(OH)D_{3/2}, the predominant circulating vitamin D metabolite, before CYP1 α catalyses a second hydroxylation at the 1 α position, forming the active hormone 1,25(OH)₂D_{3/2} in renal tubular cells and, to a smaller extent, in other vitamin D target tissues. CYP24 competes with CYP1 α for substrate and hydroxylates either 1,25(OH)₂D_{3/2} or 25(OH)D_{3/2} at position 24 and initiates the catabolic pathway of vitamin D, which leads to excretable calcitroic acid.



Vitamin D₃ can be either stored in adipose tissue or metabolised to its major circulating form 25(OH)D₃, which is mainly bound to vitamin D binding protein of serum (DBP). Circulating levels of 25(OH)D₃ are approximately 500-1000 times higher than those of the active hormone, which is reflected by its longer half-life time of 12-19 days (Zittermann 2003). The half-life time of vitamin D metabolites is strongly dependent on binding to DBP and re-absorption of the vitamin D-DBP-complex in the renal proximal tubule by an endocytotic mechanism, mediated by megalin. Megalin binds, apart from vitamin D-DBP, vitamin A - retinol binding protein (RBP), PTH, insulin EGF, cytochrome c, lysozyme and prolactin. It is expressed at the brush border of renal proximal tubular cells and accelerates tubular re-absorption of vitamin D-DBP from the glomerular filtrate, thus avoiding urinary wasting of the hormone or its metabolites (see figure 1.2.3 below). Modulation of circulating 25(OH)D₃ and 1,25(OH)₂D₃ concentrations and half-life times by changing DBP or megalin expression levels offers - apart from regulation by the expression of vitamin D-metabolizing enzymes - another means to regulate the amount of bioavailable active hormone in target tissue. The hypothesis of the importance of "free" (unbound) concentrations of active vitamin D in target tissues rather than total circulating levels of hormone metabolites has recently been supported by studies with transgenic mouse models with targeted deletion of vitamin D carrier proteins (White and Cooke 2000). The results from these studies correlate with altered transcription profiles in organs of vitamin D knock-out (VDRKO) mice as observed here (see discussion in chapter 2.2).

Another modification of the "classical" view of the endocrine vitamin D system is the discovery of the expression of vitamin D-activating CYP1 α and -catabolising CYP24 in tissues other than kidney. These tissues were previously identified as calcitriol target tissues, such as prostate, colon, skin or bone. In these tissues, that express the vitamin D receptor (VDR), local hormone activation from circulating precursor 25(OH)D₃ can regulate vitamin D signalling in an autocrine or paracrine fashion,

independent from systemic levels of the active hormone (Cross et al. 2001; Tangpricha et al. 2001).

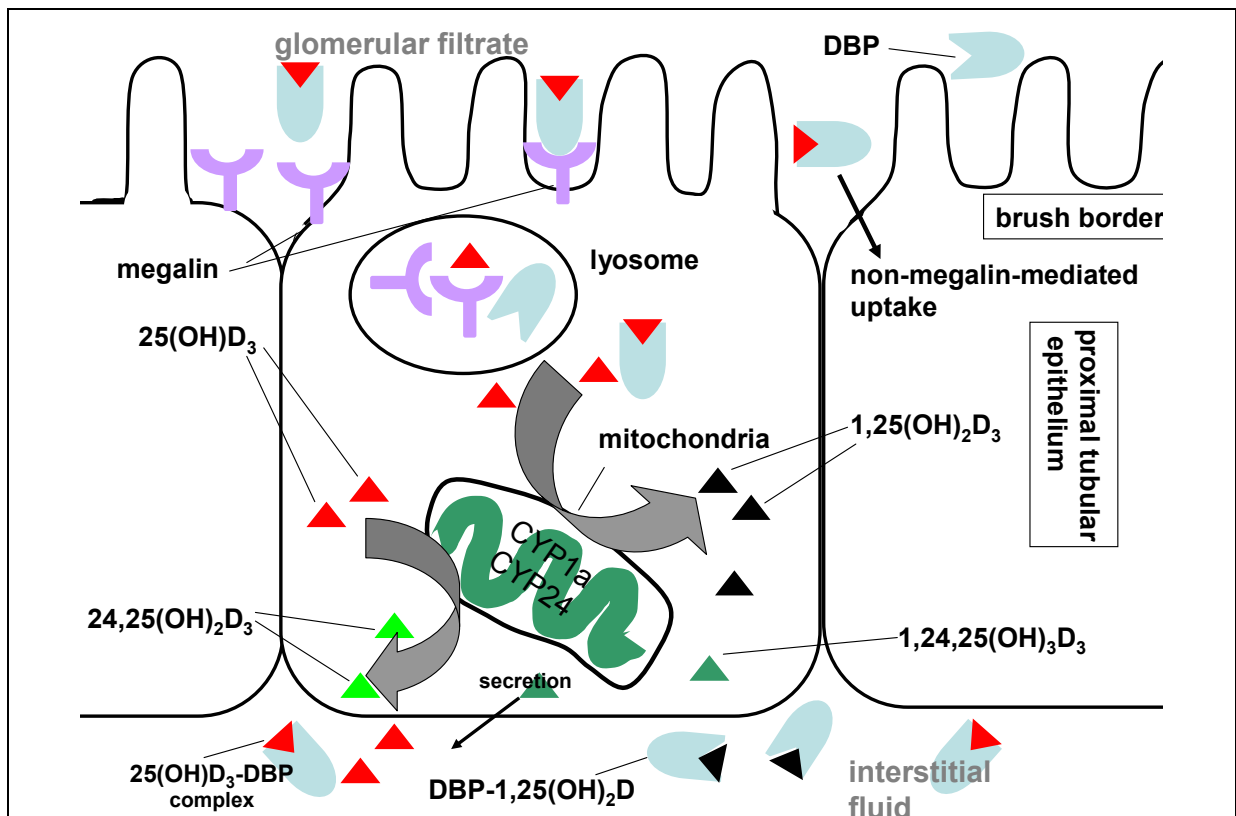


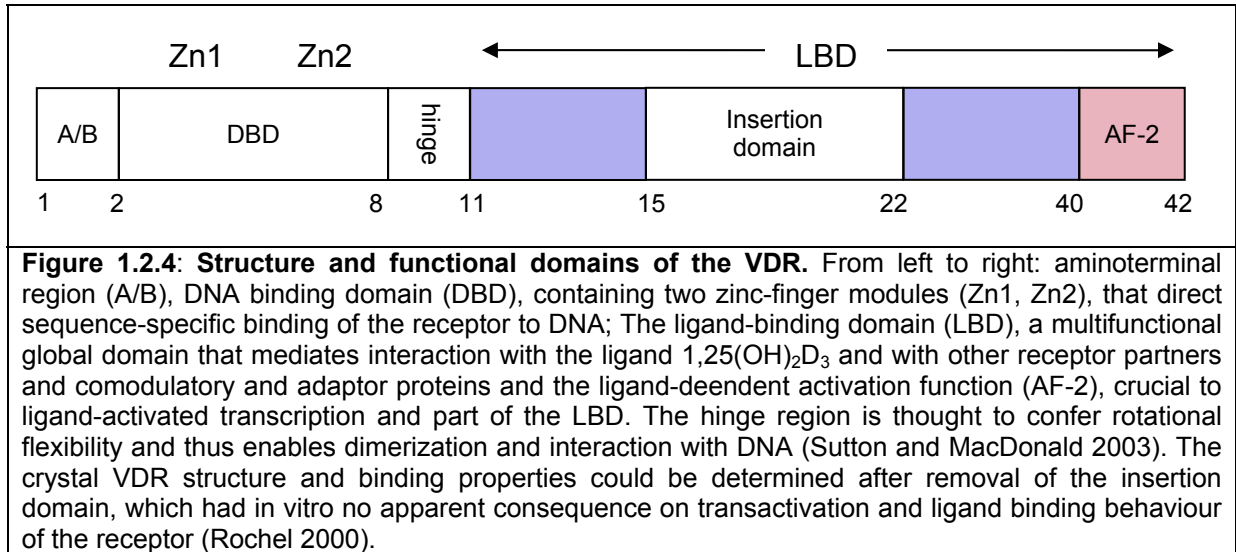
Figure 1.2.3: Model of megalin-mediated endocytosis of 25(OH)D₃, activation and catabolism in renal proximal tubular epithelium, adopted and modified from (White and Cooke 2000). The multifunctional clearance receptor megalin is expressed at the brush border of proximal tubular epithelium of kidney. 25(OH)D₃ (red triangles), complexed by DBP (light blue) is filtered through the glomerulus and re-absorbed into renal tubular epithelial cells mainly by endocytosis, mediated by megalin (Singh-Gasson et al.) and to a smaller extent through megalin-independent processes. Inside the lysosomes, the vitamin is released from its protein carriers and the components are released into the cytosol. 25(OH)D₃ can then either be secreted directly into the interstitial fluid, or metabolised by mitochondrial CYP1 α and CYP24 to the active hormone 1,25(OH)₂D₃ (black triangles) or to 24,25(OH)₂D₃ (bright green triangles). Hydroxylation by CYP24 initiates the immediate catabolism of a part of the active 1,25(OH)₂D₃, to 1,24,25(OH)₃D₃ (dark green triangles), which is then further metabolised to calcitroic acid. The other part is secreted and can be transported to vitamin D target tissues, after binding to DBP that circulates in excess concentrations.

1.2.2 Functions of the vitamin D system

As mentioned above, vitamin D was discovered for its anti-rachitic function nearly a century ago. In recent years, fast advances in the exploration of vitamin D-mediated functions were made. Nevertheless, in most cases the molecular mechanisms, underlying the pleiotropic functions of this hormone, still await explanation.

1.2.2.1 Molecular mechanism of vitamin D action

Activation of vitamin D-responsive target genes requires the binding of the vitamin D receptor (McDonnell et al. 1987), a member of the nuclear hormone receptor family, that includes the retinoid acid receptor (RAR), thyroid hormone receptor (RXR), peroxisome proliferator activated receptor (PPAR), farnesoid X receptor (FXR), and orphan receptors like Nurr, Nur77 (TR3), and others.



In the cytosol of target cells, the vitamin D receptor binds to its ligand, $1,25(\text{OH})_2\text{D}_3$ and translocates to the nucleus, where it heterodimerises with retinoid X receptor, RXR. Here the VDR/RXR complex binds to specific sequences in the promoter region of target genes, the so-called vitamin D responsive elements (VDRE), and recruits basal transcription factors and co-regulators to either enhance or suppress the rate of gene transcription by polymerase II. Binding of $1,25(\text{OH})_2\text{D}_3$ to the receptor has been shown to change the VDR conformation at the carboxylated end, permitting interaction of the AF-2 domain with coactivators like SRC-1. This in turn can bind to transcriptional integrators, such as calcium-binding-protein (CBP) and p300, which have histone acetylase activities and can release histones from DNA by acetylation. The remodelling of genomic DNA opens the promoter region of target genes to the transcriptional machinery and increases the rate of transcription (Jones et al. 1998).

Apart from genes that are activated by VDR action, there are also genes repressed by vitamin D, like PTH or interleukin IL-2. Transcriptional repression may be caused by disrupting the binding of up-regulatory transcription factors by the interaction of VDR-RXR with downregulatory response elements. The other possibility is the interaction of VDR-RXR with co-repressor proteins, which, like in the case of the silencing mediator of retinoic acid and thyroid hormone receptor (SMRT), activate histone acetylases. Deacetylated histone can bind to the promoter regions of target genes and shut off transcription.

1.2.2.2 Classical functions of vitamin D: Calcium / Phosphate homeostasis

As explained above, the role of vitamin D in regulating the concentration of calcium in blood and the occurrence of rachitic diseases led to the discovery of the vitamin D endocrine system. Impairments in the vitamin D system are today established as causes for osteomalacia and calcitriol and its analogs are widely used therapeutic agents against osteoporosis, secondary hyperparathyroidism (HPT) and psoriasis (Wu-Wong et al. 2004). To study the biological background of diseases caused by derangements in the vitamin D system more in detail, mouse models with ablated functions of the vitamin D-activating CYP1 α and the vitamin D receptor (VDRKO) were created. While in CYP1 α $-/-$ mice levels of active $1,25(\text{OH})_2\text{D}_3$ are

close to the limit of detection, in VDRKO mice the active hormone is produced in excess but cannot modulate transcription. To date, four different VDRKO mouse lines were established. Two of these lines express a dysfunctional VDR that can bind the ligand hormone but lost its ability to bind to vitamin D responsive elements (VDRE) in the promoter region of target genes due to a deletion of the first zinc finger binding domain. In both cases, the animals showed after weaning symptoms similar to humans with hereditary rickets and the severeness of the phenotype was progressing with age. While effects like hypocalcemia, hyperparathyroidism and bone disease in both mouse models could be rescued with a diet rich in calcium ("rescue diet", RD,(Erben et al. 2002) some symptoms appeared to be independent of calcium supply.

The balance of calcium is predominantly controlled by the concerted action of kidney, intestine and bone. For intestinal calcium absorption and renal calcium reabsorption the calcium ions have to be transferred across an epithelial cell wall. In VDRKO mice these transport processes are impaired, resulting in calcium losses by urinal excretion.



Figure 1.2.5: Mice under investigation in this study. From left to right: Homozygous Vitamin D receptor knockout (VDRKO) mouse, heterozygous VDR (+/-) mouse, wild type VDR (+/+) mouse. Since the the heterozygous VDR (+/-) mouse showed no pronounced phenotype, the gene expression experiments focused on comparisons between VDRKO and WT mice. Note that the VDRKO mouse develops hair loss after 3 months.

Some features of the VDRKO mouse phenotype, like growth retardation, were at least partly normalised with a calcium-rich diet (Erben et al. 2002). Nevertheless, differences between WT and VDRKO animals persisted in the average size and relative weight of organs like kidney and heart (own observations and (Li et al. 2002). Further known differences between the VDRKO phenotype and WT mice encompass metabolic functions, blood pressure and in the efficiency of endochondral ossification (Li et al. 1997; Erben et al. 2002).

1.2.2.3 Convergent actions of VDR and RXR signalling

Among the most obvious calcium-independent features of the VDRKO phenotype is alopecia, which did not occur in CYP1 α $-/-$ mice and could not be rescued neither by 1,25(OH) $_2$ D $_3$ deprivation nor by calcium supplementation (Sakai and Demay 2000; Sakai et al. 2001). Moreover, selective ablation of retinoid X receptor alpha RXR α in the keratinocytes of the epidermis and hair follicles results in the same hair phenotype as observed in VDRKO mice (Li, M. et al. 2001). As in VDRKO mice, the onset of alopecia appears to be due to a defect in the anagen phase of the second hair cycle. This shows that hair growth, independent of hormone ligands, depends on the function of the VDR-RXR receptor heterodimer. Binding of unliganded VDR with RXR has been shown to increase import rates of VDR into the nucleus considerably and appears to be a prerequisite for ligand-independent functions of the vitamin D receptor (Prufer and Barsony 2002).

The ability of nuclear hormone receptors to heterodimerise, like VDR, RXR, but also thyroid hormone receptor (TR), peroxisome proliferator-activated receptor (PPAR), liver-X-receptor (LXR) and orphan receptors, supports the hypothesis that hormone signalling pathways might interact through nuclear receptors. Evidence for this hypothesis gave the observation that retinoic acid and vitamin D can inhibit terminal differentiation of growth plate chondrocytes induced by thyroid hormone (Ballock et al. 2001). In pluripotent myeloid cells vitamin D can trigger differentiation to monocytic cells and repress transcriptional activation of retinoic acid-responsive genes (Bastie et al. 2004).

Apart from the creation of transgenic animal models with mutated steroid hormone receptors and intercrossing of these mutants, gene expression analysis can give valuable information about possible synergistic or antagonistic influences of vitamin D action on signalling of other hormones.

1.2.2.4 Novel implications of vitamin D action

The discovery of the expression of nuclear vitamin D receptors in tissues that are not directly involved in calcium metabolism, like heart, stomach, pancreas, brain, skin, gonads and activated B and T lymphocytes stimulated the search for non-calcemic biological functions of vitamin D (Mathieu et al. 2001; Wu-Wong et al. 2004) The ability of vitamin D to down-regulate hyperproliferative cell growth has been observed in a range of in vitro studies with tumor cells and was the rationale to use 1,25(OH) $_2$ D $_3$ and analogs to treat the skin disorder psoriasis (Kragballe et al. 1988). The association between vitamin D supply the progression of cancer growth was confirmed by epidemiological studies on breast and prostate cancer (Krishnan et al. 2003; O'Kelly and Koeffler 2003).

The suspected role of vitamin D in functions of the immune system was established by rescuing phenotypes of mouse models. These models were determined to develop autoimmune diseases, like type 1 diabetes (Deluca and Cantorna 2001), rheumatoid arthritis (Cantorna et al. 1998) and multiple sclerosis (Cantorna et al. 1996). Treatment of these mice with vitamin D prevented or attenuated the development of the diseases. The risk of non-obese diabetic (NOD) mice to develop type 1 diabetes was reduced by 80% through dietary vitamin D supplementation

(Gregori et al. 2002), a finding that was recently corroborated by a study with humans (Hypponen et al. 2001).

The association between factors controlling endogenous vitamin D production, like exposure to UVB irradiation, skin pigmentation, latitude and season or dietary vitamin D supplementation and the down-regulation of blood pressure (Krause et al. 1998) was substantiated in studies with a hypertensive mouse model showing the impact of vitamin D on the rennin-angiotensin system (Li, Y 229).

In spite of the wealth of investigations supporting the direct or indirect impact of vitamin D in many physiological functions there is still little known about the mechanisms by which the hormone mediates these processes on molecular level. In contrast to the synthesis of circulating $25(\text{OH})\text{D}_3$ the renal production of the active form $1,25(\text{OH})_2\text{D}_3$ is stable and tightly controlled by Ca, PTH and phosphate homeostasis through a complex, interrelated enzymatic system (see figure 1.2.1 above). This apparent independence of vitamin D signalling from systemic $25(\text{OH})\text{D}_3$ concentrations, raised the question, how it is possible that circulating levels of hormonally inactive forms of vitamin D influence these biological processes (Holick 2004).

Recent findings of the expression of enzymes catalysing vitamin D production and – catabolism in extra-renal tissues, suggesting the existence of autocrine and paracrine mechanisms of vitamin D action might be one key to answer this question. In prostate cancer cells, for example, the expression of vitamin D-activating CYP1 α was shown to be markedly reduced, compared to benign hypertrophied or normal prostate cells (Schwartz et al. 1998).

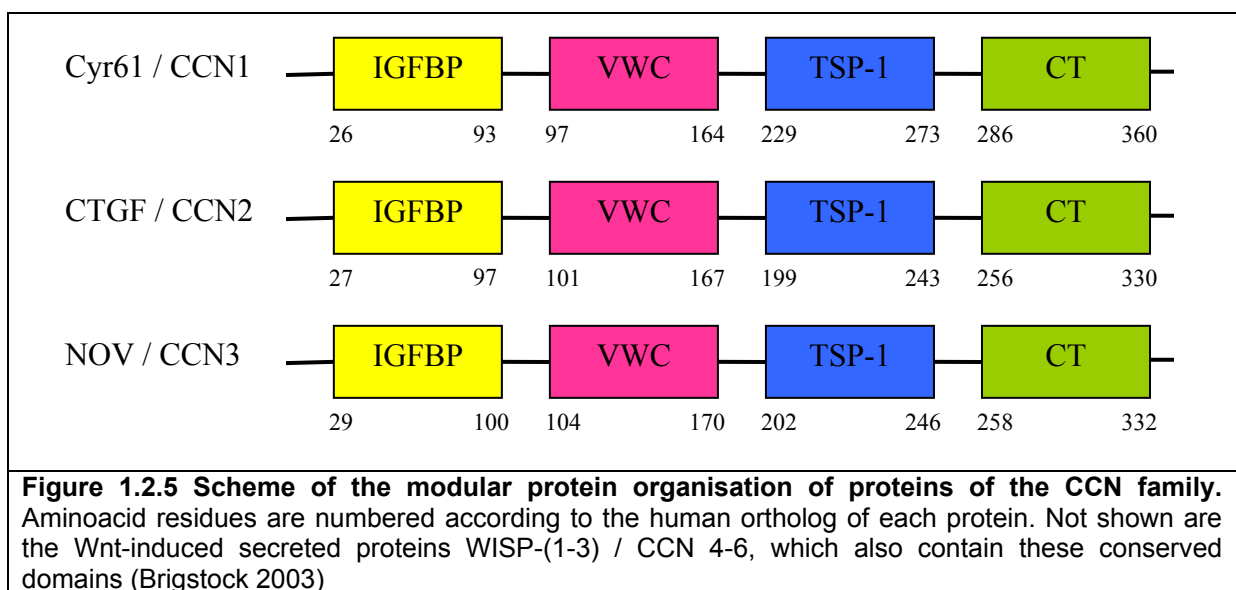
Another recent finding gives further emphasis on the question how vitamin D and its metabolites can act specifically in target tissues of certain individuals: New World primates from the American continent, living in the Los Angeles zoo suffered with a strongly elevated incidence from rachitis, compared to African Old World primates under identical conditions. Measurements of serum concentrations of $25(\text{OH})\text{D}_3$ and $1,25(\text{OH})_2\text{D}_3$ in rachitic New World primates resulted in surprisingly elevated levels of the hormone and its precursor with respect to non-rachitic animals. In electromobility shift assays using vitamin D-responsive DNA sequence elements (VDRE) as probe, nuclear extracts of Old World primates showed only the VDR-RXR complex bound to the DNA, whereas assays with extracts from New World Primates exhibited an additional band from a protein that competed with the receptor for VDRE binding. Two of these VDRE binding proteins (VDRE-BPs), that when overexpressed confer vitamin D resistance, have been to date identified in primates, one in humans (Chen et al. 2000). To compensate at least in part for the inhibiting effect of VDRE-BPs, New World primates also express elevated levels of a recently discovered class of intracellular vitamin D binding proteins (IDBPs) that promoted the delivery of the vitamin D ligand to the receptor and enhanced transactivation of vitamin D-responsive genes. It turned out that IDBPs can particularly activate the transcription of vitamin D-activating CYP1 α . IDBPs belong to the Hsp70 family of chaperones and appear to have a major impact on vitamin D trafficking also in humans (Adams et al. 2003)

Further insights into the transcriptional networks and biochemical pathways responding to vitamin D can be provided now and in the near future by studies

employing novel tools of functional genomics like microarray technology as in the project presented here.

1.3 Functions of vitamin D-inducible Cyr 61 in human fetal osteoblasts (hfOB)

Cysteine-rich protein 61, recently renamed CCN1, belongs together with connective tissue growth factor (CCN2) to a recently characterised family of modulators of hormonal signalling pathways. CCN proteins were reported to stimulate mitosis, adhesion, apoptosis, extracellular matrix production, growth arrest and migration and contain four conserved sequence modules. These highly conserved modules are known from other proteins, like a insulin-like growth factor (IGF)-binding domain, a von Willebrand type C domain, a thrombospondin-1 and a cysteine-rich C-terminal domain (Brigstock 2003).



Gene expression profiling of VDRKO mouse kidney and heart in this study showed differential regulation of CCN1 and CCN2 in organs of animals with ablated VDR function in comparison to wild type animals (see chapter 3 and 4). In tumor biopsies and breast cancer cell lines both proteins have been found up-regulated (Babic et al. 1998; Babic et al. 1999) and were shown to promote cell adhesion and angiogenesis. The closely related proteins CCN3 (Nov) and CCN5 (WISP-2) support cell adhesion in osteoblasts (Kumar et al. 1999) and vascular smooth muscle cells (Ellis et al. 2000), respectively, the latter pointing at an important role of CCN proteins in atherosclerosis. As blood monocytes have a central role in atherosclerosis and wound healing, it is interesting to note that they adhere to Cyr-61 (CCN1) and CTGF(CCN2), which were both found strongly up-regulated in arteriosclerotic lesions (Schober et al. 2002).

CCN1 was described as an immediate early gene which is expressed in osteoblasts in response to treatment with active vitamin D (Schutze et al. 1998). Vitamin D regulates bone growth not only by controlling calcium homeostasis; In vitro studies showed that $1,25(\text{OH})_2\text{D}_3$ also has an indirect influence on osteoclast differentiation via VDR-mediated expression of RANKL in co-cultured osteoblasts (Takeda et al. 1999; Kitazawa and Kitazawa 2002). Apart from previously identified vitamin D-responsive genes with functions in bone remodelling, like osteopontin and

osteocalcin (Haussler et al. 1995; Christakos et al. 2003), CCN1 appears to have central regulatory functions in chondrogenesis and fracture repair (Hadjiargyrou et al. 2000).

Gene expression profiling of the established human osteoblastic cell line hfOB with and without treatment with CCN1 was intended to further clarify the role of Cyr61 in these processes via transcriptional regulation and to identify signalling pathways involved in CCN1-mediated bone remodelling (see section 2.1). Alterations in the gene expression of Cyr61-treated cell lines also might give further insights into signalling pathways triggered by CCN1.

1.4 Glucocorticoid treatment of insulin-secreting pancreatic β -cells

Similar to vitamin D, glucocorticoids are steroid hormones that, by binding to nuclear receptors can mediate changes in gene expression. Glucocorticoid action influences functions as metabolism and inflammation, which qualifies them as target substances for therapeutic treatment. Chronic exposure to elevated levels of glucocorticoids can have negative effects on metabolic functions, connected with impairment of insulin secretion from pancreatic β -cells and the development of diabetes (Lenzen and Bailey 1984).

The β -cells of the pancreatic islets of Langerhans have a key function in the control of glucose metabolism through the production and secretion of insulin. The release of insulin from intracellular storage vesicles is a fast process controlled by ATP production, activation of ATP-dependent potassium channels, membrane depolarization and the opening of voltage-dependent calcium channels (Ashcroft et al. 1994). long-term adaption of insulin synthesis depends on nutrient state and is controlled by transcriptional processes (Itoh and Okamoto 1980).

An important role in the activation of the hormonal precursor (cortisone in humans, dehydrocorticosterone in rodents) of the glucocorticoid receptor ligand (cortisol in humans, corticosterone in rodents) has 11 β -hydroxysteroid dehydrogenase 1 (11 β -HSD1). 11 β -HSD2 catalyzes the reverse reaction. The systemic effects of glucocorticoid excess concentrations resulting in insulin resistance and hyperglycemia have been studied in detail, whereas direct effects of glucocorticoid actions on β -cells remain unclear and the subject of debate. Long-term treatment of pancreatic islets from normal (Lambillotte et al. 1997) and obese (Khan et al. 1992); (Delaunay et al. 1997) mice with glucocorticoids resulted in a decrease of insulin production, a process that can be reversed by 11 β -HSD1 inhibitors. Mice that overexpress the glucocorticoid receptor in pancreatic islets develop diabetes (Davani et al. 2000). Short-term treatment of pancreatic islets from lean mice, however, was observed to increase the secretion of insulin in response to glucose challenging (Hult 2004). The analysis of transcriptional changes that go along with stress through glucocorticoid treatment of β -cells was expected to give further insights into mechanisms causing the impairment of insulin secretion, glucose metabolism and diabetes.

1.5 Aims of the project

The first goal in this thesis was the development of a small cDNA microarray containing probes that represent genes involved in steroid biosynthesis, cholesterol metabolism and bone development. Protocols for probe selection, amplification and microarray printing were established and optimised for efficient chip production, using liquid-handling robotic systems. Methods for RNA extraction from tissue and cell cultures had to be optimised for small amounts of samples. Achieving strong fluorescent signal intensities with limited quantities of sample RNA was the motivation for testing and optimizing different strategies for fluorescent labeling and array hybridisation. The proof for the functioning of the method had to be given by monitoring changes in gene expression patterns of osteoblast precursor cells during differentiation. However, with small numbers of selected genes normalisation was difficult and the possibilities to find novel pathways of gene regulation were limited. Therefore, it was decided to upscale the arrays to about 2000 probes.

Exploring the impact of hormone treatment on gene regulation and differentiation of an established line of human osteoblasts (hfOB) was the motivation for expression profiling experiments with cells treated with dexamethasone, estradiol and vitamin D. Vitamin D was shown previously to induce the expression of cysteine-rich protein 61 (Cyr61) in osteoblasts. Changes in gene expression of hfOB in response to elevated concentrations of Cyr61 were therefore expected to unveil new target genes and pathways in the putative role of Cyr61 in bone remodeling.

Ambitions to perform genome-wide expression profiling experiments and the aim to monitor the expression of target genes of hormones and hormone receptors in animal models resulted in the production of a mouse microarray containing nearly 21.000 cDNA probe fragments. The functioning of this upscaled high-density array had to be tested with RNA samples from osteoblast-like mouse cell lines and mouse tissue. With this mouse cDNA array it was intended to identify target genes induced by cortisol in primary cells extracted from the pancreas of lean mice, which might characterise the induction of a pre-diabetic state.

A transgenic mouse model with a transcriptionally inactive vitamin D receptor (VDRKO) was chosen to further investigate the pleiotropic effects of the secosteroid and its nuclear receptor on transcriptional level. Comparison of the expression profiles of organs from VDRKO and WT mice should elucidate the molecular base of "classical" and novel functions of vitamin D. This included the regulation calcium homeostasis in kidney, as well as the impact of vitamin D signalling on physiological functions like blood pressure control and energy turnover. Metabolic diseases like diabetes, hypertension or cardiac hypertrophy only recently were connected with vitamin D action (Zemel 1998; Zemel 2002). Novel functions of vitamin D were especially expected to be found by gene expression analysis of organs from VDRKO mice with restored systemic serum calcium levels. The analysis of mouse heart, a non-classical vitamin D target organ was especially promising to find novel pathways of the vitamin D signalling system. The regulation of target genes, identified in these studies, had to be confirmed by other methods, like quantitative real-time PCR and further analyzed and interpreted in their biological context.

2. Establishing gene expression profiling with cDNA microarrays; experiments with cell culture systems

The most time-consuming step in this project was the establishment of microarray technology. Although the principle appears to be simple, the miniaturisation of the technique, which makes the massive parallel detection of thousands of transcripts possible, opens many sources for interference. Technical interferences can distort gene expression profiles systematically or impede the functioning of the method completely (see introduction). Protocols, published by the TIGR Institute for Genomic Research (Hegde et al. 2000), Mark Schena (Schena et al. 1996) and the group of Pat Brown (Brown 1999) gave valuable advice, but had to be adapted according to the available instrumentation, reagents and the experimental settings of the respective study. In section 2.1, an overview over the different steps of microarray production, labeling protocol development, array post-spotting treatment, hybridisation and washing will be given. The proof of principle for the functioning of the method is described in section 2.2, where established lines of osteosarcoma, osteoclast- and osteoblast-like cells were treated with steroids to initiate differentiation. Gene expression profiles from different stages of differentiation were monitored with microarray technology according to the protocols established before.

Section 2.3 shows the first successful attempt to find changes in transcription of an human fetal osteoblast cell line, established by T. Spelsberg and the collaborating N. Schütze, after treatment with the vitamin D-induced angiogenic factor Cyr61 (CCN1). In this experiment it was possible to identify several genes and pathways that to date were not primarily associated with physiological functions in bone. The small number of pre-selected genes, on the other hand, complicated normalisation and restricted the validity of interpretation, since each pathway only was represented by single or few regulated candidate genes. Therefore and because of the resources of the Institute of Experimental Genetics (IEG) in mouse genetics it was decided to scale up microarrays. In collaboration with the group of Dr. J. Beckers, a microarray that covers almost 21.000 probes a large part of the mouse genome (section 2.4) was produced. In section 2.5, a brief description of a microarray study of gene regulation in β -cells of mouse pancreatic islets will be given, before and after treatment with glucocorticoids. This project was carried out in collaboration with M. Hult and U. Oppermann from the Karolinska Institute in Stockholm.

2.1 Establishing the Technology

2.1.1 Microarray production

The guideline for establishing the technique was the development of cDNA arrays containing selected genes and gene families involved in steroid and cholesterol metabolism, which was subsequently complemented by adding genes from a Unigene library containing genes expressed in cartilage and bone tissue (see methods).

The creation of cDNA microarrays included the following steps:

1. selection of target genes presented on the array
2. design /selection of the probes (cDNA fragments / ESTs), according to
 - position within the gene (3', UTR)
 - length of the probe (melting conditions)

- check for redundancy, cross hybridisations
- 3. storage, amplification and administration of clones
- 4. verification of probe identity
 - by PCR
 - by re-sequencing / BLAST search
- 5. amplification of probes by PCR
- 6. purification / concentration
- 7. selection of microarray substrate- and spotting buffer chemistry and-technology
- 8. development / optimization of post-spotting protocols

2.1.1.1 Clone selection

All of these steps had to be carefully optimised and matched. The selection of clones containing cDNA probe fragments is described in the methods part. Due to the incomplete sequencing of the human (and mouse) genome and the suboptimal management of *E.coli* clones at the German Resource Center RZPD at the beginning of the project, the clone annotations were often incomplete or wrong. Therefore probe length and -identity had to be verified by PCR / agarose gel electrophoresis and sequencing. This time-consuming and expensive procedure was done for ca. 1100 clones by the author and the collaborating partners Dr. Johannes Kappler and Holger Laux, former members of the GSF Institute of Molecular Pathology, who were involved in the development of a human cDNA array, leading to a common publication (Kappler et al. 2003). At a later stage the percentage of clones with "true identity", acquired from the RZPD rose from initially 70% to about 90%, so that it was decided to stop re-sequencing of all clones and limit it to selected candidate genes, identified by microarray analysis. Cross-contamination during the amplification of *E.coli* clones from glycerol stocks and clone management in Excel sheets were further potential sources of error.

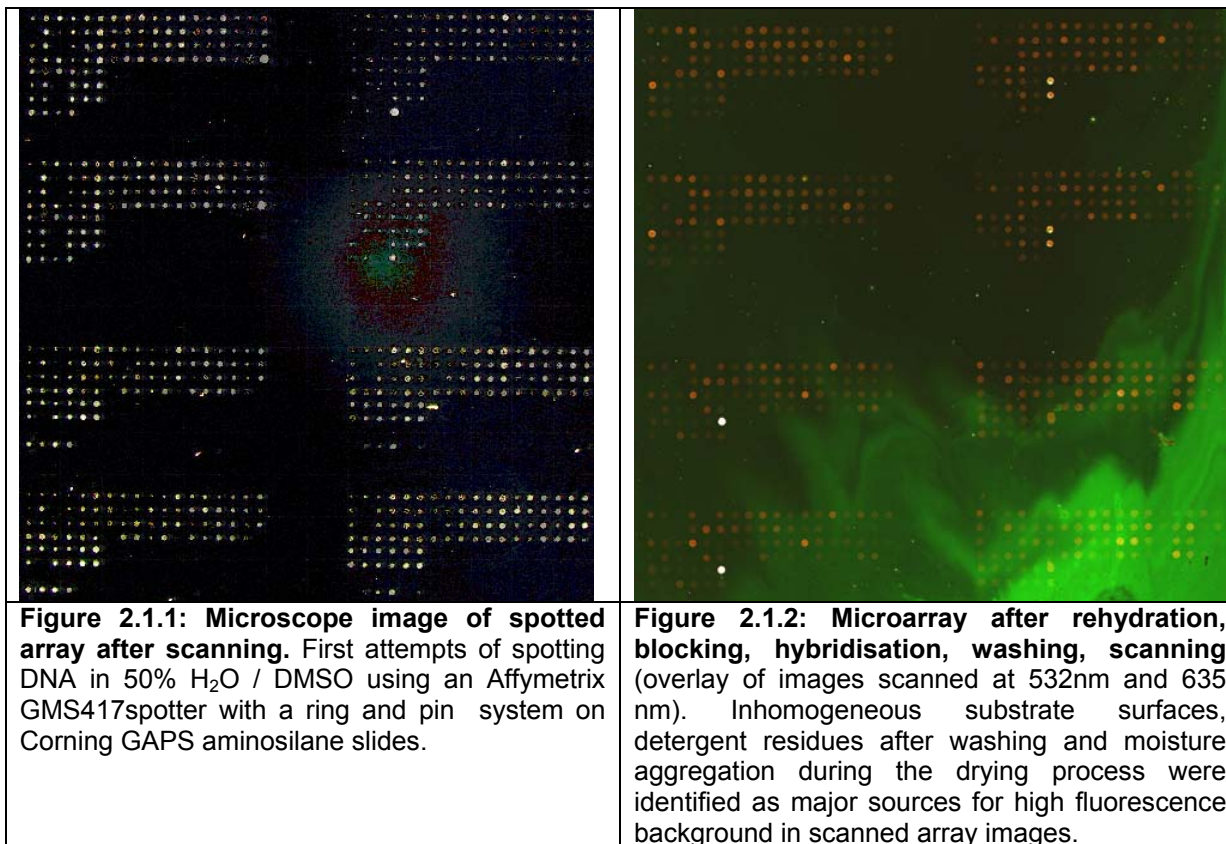
While the detailed procedure of probe amplification, quality control and concentration is described in the methods part, some important results of multiple experiments performed to optimise microarray production will be summarised in the following.

2.1.1.2 Printing microarrays

A crucial step in cDNA microarray technology is the spotting of cDNA probes onto the substrate, generally microscope glass slides coated with a surface that allows the DNA to bind strongly by covalent or ionic bonding. Coated glass substrates have to

- have a homogeneous, stable surface coating (even after intensive washing and hybridisation steps)
- exhibit a low background fluorescence at the (532nm.(Cy3) and 635nm (Cy5))
- have a big DNA binding capacity
- be stable against the binding of DNA or contaminants after spotting ("blocking")
- be matched to the spotting buffer properties (hydrophobicity, ionic strength, etc.)
- be chemically stable during storage

The result of the first attempts of printing microarrays with a GMS 417 robotic spotter on Corning aminosilane-coated glass substrates is shown below, as it is a good example for typical problems in microarray production:

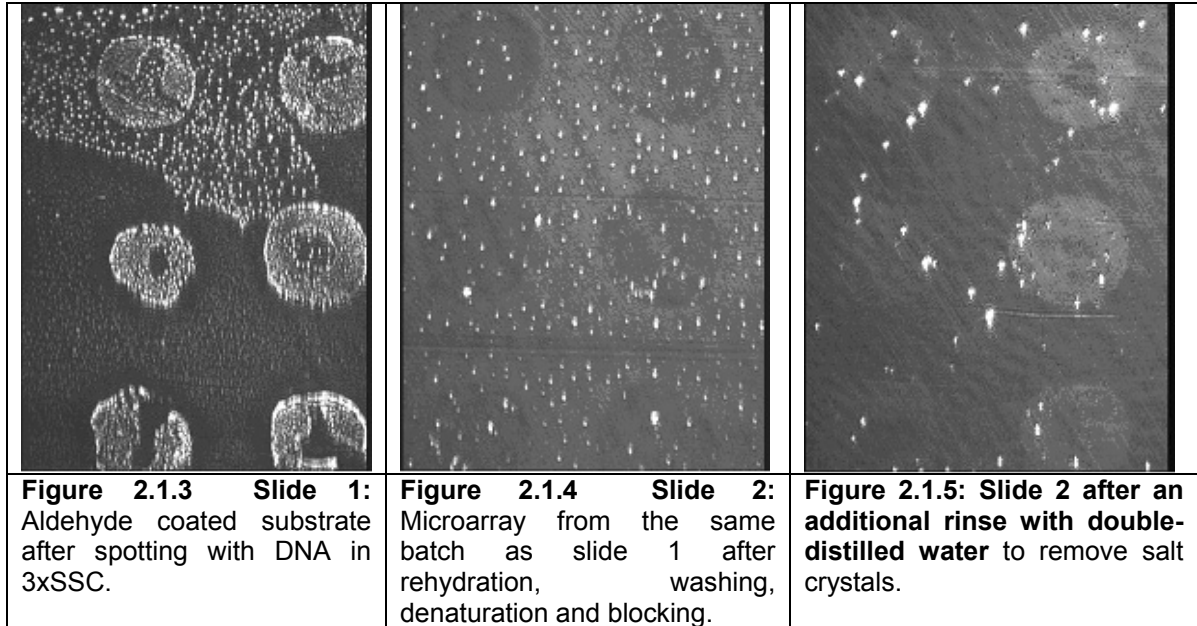


Among the multitude of products on the market, a selection of surface chemistries and buffers were tested. Hybridisation conditions, blocking and washing steps were optimised to achieve good spot homogeneity, high probe density and low background fluorescence. Microarray quality after spotting, washing and hybridisation can be evaluated visually from microscope or scanned fluorescence images.

Figure 2.1.1 and 2.1.2 above show typical problems that have to be overcome by careful protocol optimization: Irregular spot morphology (left) and high background fluorescence (right). Aminoallyl-coated slide surfaces have a relatively low binding capacity and tend to lose probe material during washing steps. Different approaches to assess the quality of spotted arrays were tested. With light microscopy only salt crystals from the spotted sample buffer are visible. Therefore, further experiments were done with spotting buffers containing a dye (e.g. bromophenol blue) and with fluorescently labeled oligonucleotides.

Although visual quality control can deliver a good impression of array quality, quantitative assessments are less subjective and preferable for long-term batch-to-batch quality control. One method to test spotting quality, used in this work, was the hybridisation of labeled oligonucleotides onto cDNA probes that were amplified with universal primers (M13). Additional quality control spots (e.g. arabidopsis genes) on the array and spiking the hybridisation samples with homologous cDNA species that do not cross-hybridise with the sample cDNA (e.g. mouse, human) can be used as reference for transcript quantification and data normalisation.

Another way to quantify unlabelled DNA on the array surface directly and without and dye incorporation is scanning with imaging ellipsometry. This method is based on the phase shift in light diffracted at a surface consisting of layers of different materials:



The images 2.1.3-5 above were obtained by scanning aldehyde-coated slides, spotted with a Biorobotics Migrogrid II spotter (split-pin technology). The slides were scanned directly after spotting (slide 1), after post-spotting treatment (slide 2) and hybridisation (slide 3, not shown here). The microarrays were produced and treated by the author, the images recorded by Kerstin Fuchs and Matthias Vaupel (Nanofilm Inc., Göttingen) with an Ellipsometer EP³ (Hippler 2004). The white crystals are salt residues from the buffer evaporating instantly after deposition on the surface. The spots show inhomogenous morphologies, often with a hole in the middle ("donought effect") that can complicate image analysis and signal integration. These donought holes, resulting from the mechanical force applied by the pin during sample deposition can partly be removed by exposing the spotted arrays to a humid atmosphere after spotting (rehydration), a step which also improves binding of DNA strands to the surface coating.

The re-hydration has to be performed in an atmosphere with controlled humidity. Best results were obtained with rehydration in the atmosphere over a solution of 50% (v/v) of glycerol in water for 48 hours at room temperature in closed containments, like empty pipette tip boxes, sealed with film. Scanning ellipsometry even can detect differences in the thickness of cDNA spots before and after hybridisation and thus give an estimate for the hybridisation efficiency (see Figure 2.1.7 above).

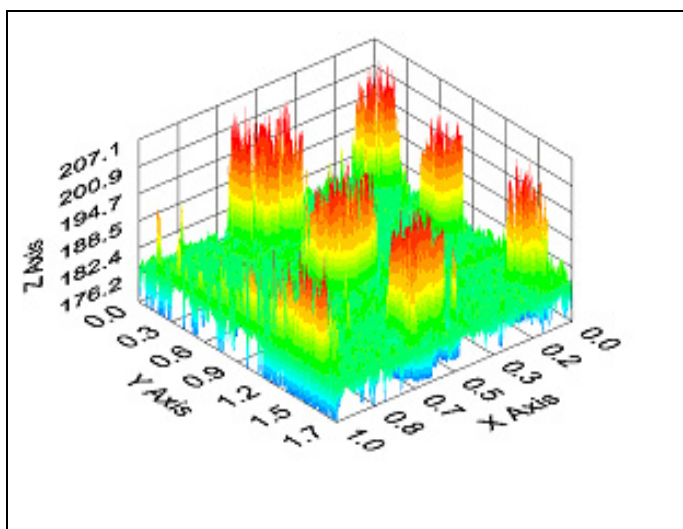


Figure 2.1.6: 3D-map of microarray after spotting (slide 1), scanned with imaging ellipsometry. This image can serve to assess the spot morphology and give a rough estimate of the quantity of DNA deposited on the array.

	slide 2	slide 3
	thickness[nm]	thickness[nm]
position 1		
spot 1-1	5.89	4.33
spot 1-2	3.42	3.82
position 2		
spot 1-1	1.55	3.18
spot 1-2	0.97	2.69
position 3		
spot 1-1	5.15	8.65
spot 1-2	1.74	9.83
position 4		
spot 1-1	6.86	7.55
spot 1-2	6.47	9.47

Figure 2.1.7: Thickness of DNA spots before (slide 2) and after (slide3) hybridisation. With exception of position 1, spot 1-1, the thickness of the DNA layer increases considerably with hybridisation.

To obtain uniform spot morphologies, it turned out to be vital to match the pin shape, spotter technology, surface chemistry and spotting buffer. Solid pins have to dip into the buffer reservoir each time before depositing the solution droplet (ca. 0.2-0.6 μL) onto the surface. As this slows down the spotting process considerably, the ring and pin-technology was developed: A small ring of steel wire dips into the solution which is kept in the ring by surface tension. The solid pin can then repeatedly punch small droplets out of this liquid film and deposit it onto the substrate, before the ring has to be reloaded.

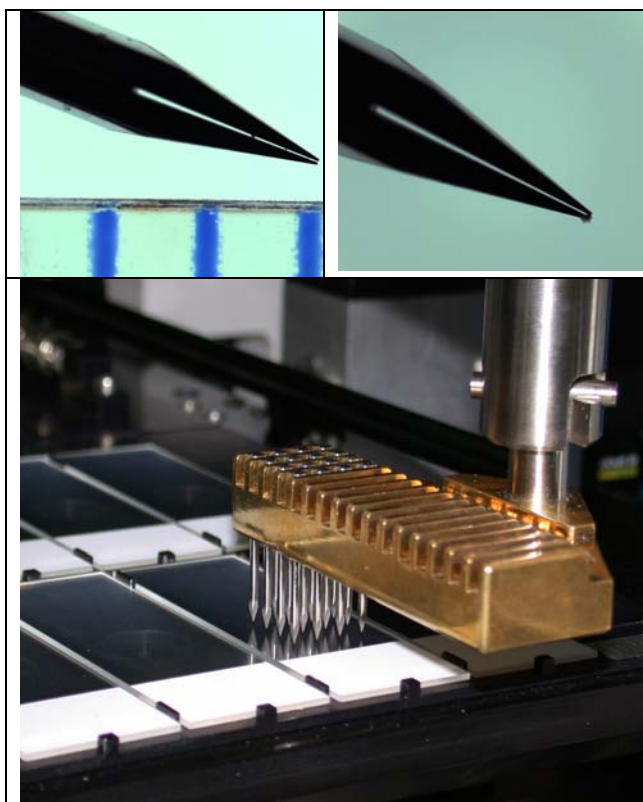


Figure 2.1.8: Printing with split-pin technology. Top left: Tip of a split pin, below scale in mm. Top right: Tip of split pin, clogged with salt crystals. Corrosion and bended tips promote clogging of the capillary channel within the tip with solid residues of the probe solution, which can result in hundreds of missing spots on each microarray. Below: Set of 4x4 split pins installed in the spotting robot (Microgrid MG II). The pins stick loosely in the holder and can move up when the slide is contacted. Exact positioning of the tool and optimization of printing speed and pin washing conditions are essential to obtain regular spot morphologies on the array.

Solid pin technologies combine long pin operating times with extremely small sample volumes, which makes evaporation a big issue. It is therefore important to take the vapour pressure of the spotted solution into account. Temperature and humidity control during the deposition of probe solutions onto the slide surface an important issue to be considered before installation of the spotting robot. Since these installations were not available during this project, the addition of hydrophilic solvents with low boiling point (e.g. 50% DMSO) or high salt concentrations (e.g. 3M betaine) were tested to reduce the evaporation rate and thus improve spot morphology.

Whereas 50% DMSO in water worked fine for the ring-and pin system, used to print the first microarrays in this study (compare figure 2.1.1, 2.1.2), split pin printing is more suited for buffers with high salt concentrations, like 3M betaine (Diehl et al. 2001) or 3xSSC + 0,1% Triton-X. Whereas solid pins are preferred for membrane printing, split pins, which can take up enough probe solutions for 100 spots or more (which means 100 slides can be spotted at a time), are mostly used to print high density microarrays on glass substrates. Due to the small dimensions of the capillary, split pin tips can be bent or clogged with buffer residues very easily, which can result in the loss of hundreds of spots per pin and array. Since pins are a constant problem in microarray production, spotting robots allowing contact-less printing have been developed.

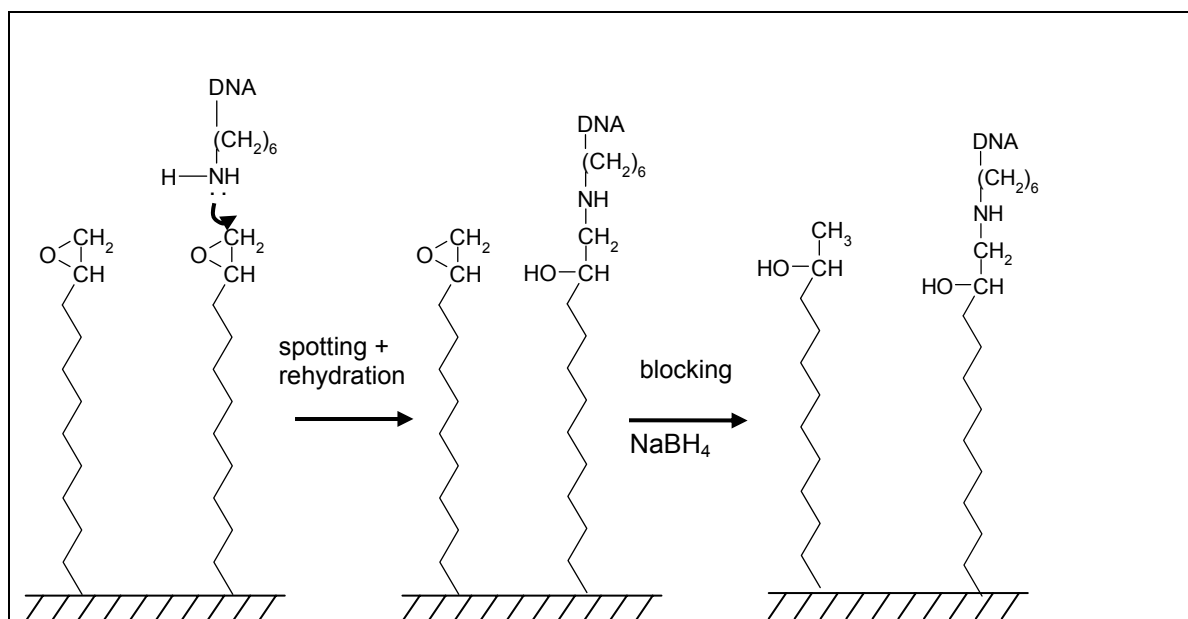


Figure 2.1.9: Process of covalent binding of cDNA probes to the microarray substrate surface, here with a coating containing reactive epoxy groups. The cDNA probes, amplified with primers containing C6-aminolinkers, can react during spotting or rehydration in a nucleophile attack with the epoxy groups of the coating and thus form a covalent bonding. During post-spotting slide treatment, unbound cDNA is washed off and free epoxy groups are reduced with a sodium borohydrate solution to alcohol. This "blocking" process helps to avoid further unspecific binding of DNA during hybridisation, which would raise background fluorescence.

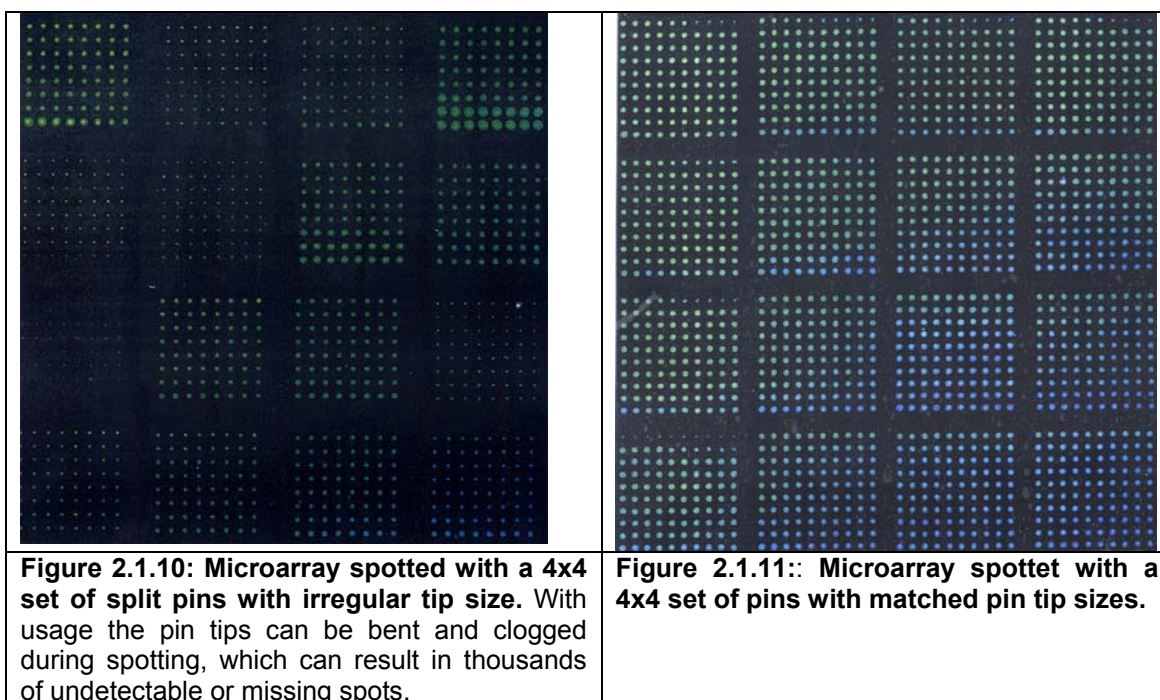
Figure 2.1.9 shows the mechanism of covalent binding of amino-linked cDNA probes to epoxy groups of the surface coating of glass substrates. Covalent binding of amino-linked probes to aldehyde surface coatings, as used later for the mouse arrays is similar via formation of a Schiff base. Covalent probe binding proved to be more stable and gave better signal intensities than ionic binding, like in the case of aminosilane - coated substrates.

Surfactants are used to modulate the surface tension of the deposited droplets to obtain regular, round-shaped spots. Buffers with high water content and high ionic strength form very small, round droplets on hydrophobic substrate surfaces. These droplets can be displaced before drying, upsetting during analysis the grid laying and feature localisation process. Extremely hydrophilic surfaces can produce large spots that might merge and mix spotting products. Microporous polymer coatings have, similar to membranes, high probe binding capacities and are suited for radioactively labeled samples. With fluorescence detection, membranes have the disadvantage of a high and irregular fluorescent background, limiting sensitivity and the linear range of detection. Below a selection of surface coatings is shown, that were tested within this project:

Table 2.1.1: Different surface / buffer chemistries that were tested during method development. The best results were obtained with aldehyde and epoxy-coated slides.

coating / name	company	binding	recommendable buffer	price [€ / piece]
poly-L-lysinated POLY-PREP	Sigma	ionic	50% DMSO, or 3M phosphate buffer	0,6
amino-silanated CMT	Corning	ionic	50% H ₂ O / DMSO (ring & pin) or betaine-SSC	17,00
aldehyde CSS silyated	CEL Assoc. Inc.	covalent -NH ₂	3xSSC or 3M betaine	1,10
epoxy QMT	Quantifoil	covalent -NH ₂	Quantifoil SP1 or 3xSSC+0.1% Triton-X	4,00
microporous polymer FAST	Schleicher & Schüll	ionic 3-D	1x SSC	ca. 10.-

Another important issue in microarray spotting is the pin shape and quality. Solid pins are generally more stable than split pins and pins made from titanium are more robust than those made from stainless steel.



Although only pins from renowned suppliers (Biorobotics Inc., Telechem Inc.) were used, which go through stringent quality control before delivery, it turned out to be beneficial to test and match pin sets before printing.

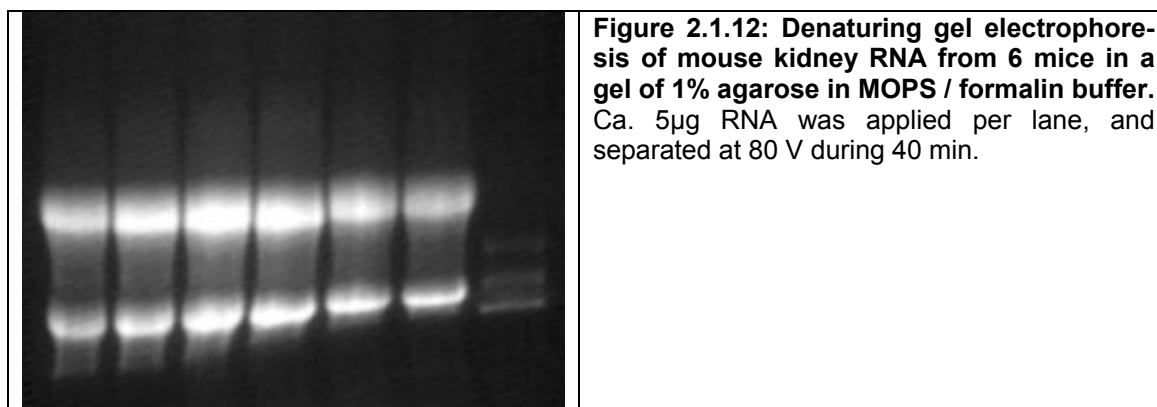
Pin tips were inspected under the microscope and test spottings performed as in figure 2.1.10-11 with different buffer solutions containing bromophenol blue. Regular cleaning by ultrasonication in a sequence of washes including water, water + detergent, water, double-distilled water and 80% ethanol, as well as quality control of split pin tips under the microscope proved to be necessary to achieve consistent array quality.

2.1.2 Sample preparation

2.1.2.1 Isolation and purification of RNA

Different protocols for messenger or total RNA extraction from tissue or cells were tested. Since RNA quality is crucial for the success of microarray experiments, and sample cells or tissue often are limited, a combined method for liquid extraction (phenol-chloroform) and on-column clean-up was chosen to obtain pure total RNA. Extraction of mRNA with either resin or magnetic beads attached to a oligo(dT) capture sequence is unnecessary and might introduce additional bias.

RNA quality was checked both by spectrophotometry and gel electrophoresis on denaturing formamid/fomaldehyde/MOPS gels (see methods).



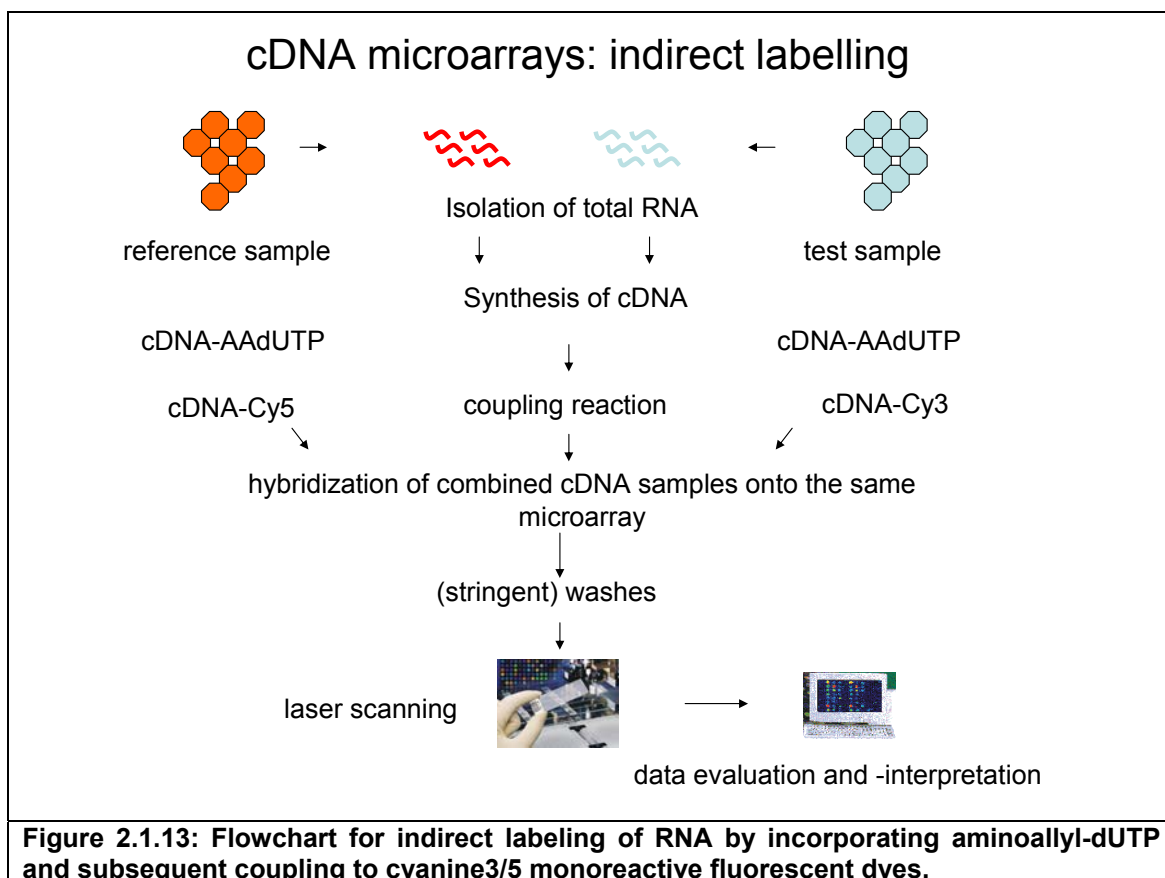
For quality control of minute amounts of RNA many users recommend analysis by microfluidic lab-on chip systems, like the Agilent bioanalyzer 2100 that allows precise analysis of sample amounts below 1ng of RNA. This system was tested during this project, as well, but the high cost of consumables favoured conventional gel electrophoresis.

2.1.2.2 RNA transcription and labeling

Direct incorporation of nucleotides, labelled with cyanine 3/5 fluorophores was tested, but resulted in poor sensitivity due to steric hinderance of bulky fluorophores in the process of enzymatic reverse transcription. Stable rates of dye incorporation, more sensitivity in comparison to direct labeling and low consumable costs were the motivation to use a protocol for indirect cDNA labeling. As shown in figure 2.1.13, this protocol includes the incorporation of aminoallyl-dUTP during reverse transcription,

followed by chemical coupling of the cDNA product with cyanine dyes in the form of succinimidyl ester esters (see methods).

Other methods were tested to work with small amounts of sample RNA, like dye incorporation catalysed by enzymatic reaction (NEN) or the incorporation of fluorophores attached to organic molecules consisting of self-assembled dendrimeric trees (see methods).



The use of commercially available kits for RNA labeling results in high cost without having any advantages over the use of self assembled compounds. Nevertheless, strict quality control and fresh chemicals showed to be vital, especially in the case of dyes, aminoallyl dUTP and DMSO that degrade quickly if exposed to light, heat or humidity.

2.1.3 Testing the method with cell culture systems: Proof of principle

Once protocols for probe DNA production, purification, spotting, rehydration, blocking, washing, RNA extraction and labeling, hybridisation and washing were developed and optimised, the method was first tested with commercially available RNA from mouse brain and testis (figure 2.1.14). Printing of replicate probes on the same array, which was done in early microarray experiments of this study, turned out to be not necessary. For large arrays and the use of several pins, replicate printing can help to account for spatial variation due to concentration gradients during hybridisation and irregular spot morphology, but complicates data analysis.

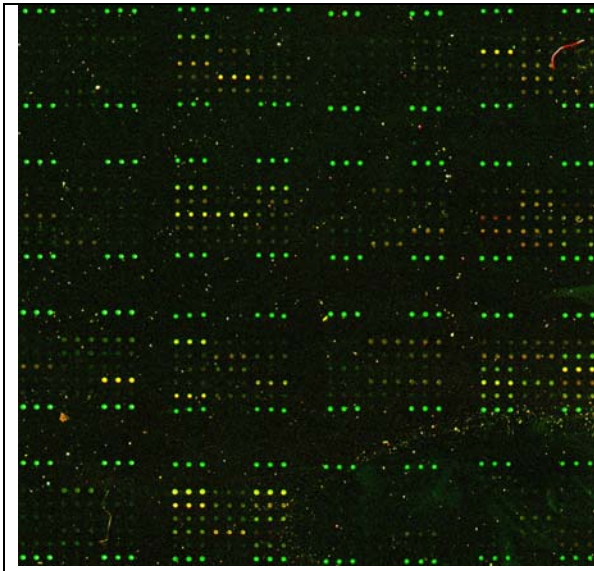


Figure 2.1.14: First successful test for a microarray experiment with in-house produced microarrays: Dual channel overlay of brain (Cy3: green) and testis (Cy5: red) cDNA hybridised on a chip containing human ESTs and Arabidopsis thailania negative control genes. All spots were printed in triplicates.

Further tests were done with cell culture systems, which were expected to change significantly in gene expression after treatment. Human osteoblast-like MG63 osteosarcoma cells are known to express nuclear hormone receptors (Mahonen and Maenpaa 1994). Treatment of MG63 cells with dexamethasone or active vitamin D stops proliferation and induces a differentiation program, similar to that known from maturing osteoblasts during calcification (Stewart et al. 1999; Walsh et al. 2001). Differentiation along the osteoblastic lineage is characterised by changes in the expression of marker genes, like osteocalcin, osteopontin, type I collagen and alkaline phosphatase (Mahonen et al. 1998). Like osteoblasts, steroid-treated osteosarcoma cells start to agglomerate, building so-called nodules. These nodules get covered with extracellular matrix proteins and apatit crystals, initiating calcification in bone tissue. Except from treatment with 10^{-8} M dexamethasone, the MG-63 cells were grown for the same time under the identical conditions before harvesting and RNA extraction.

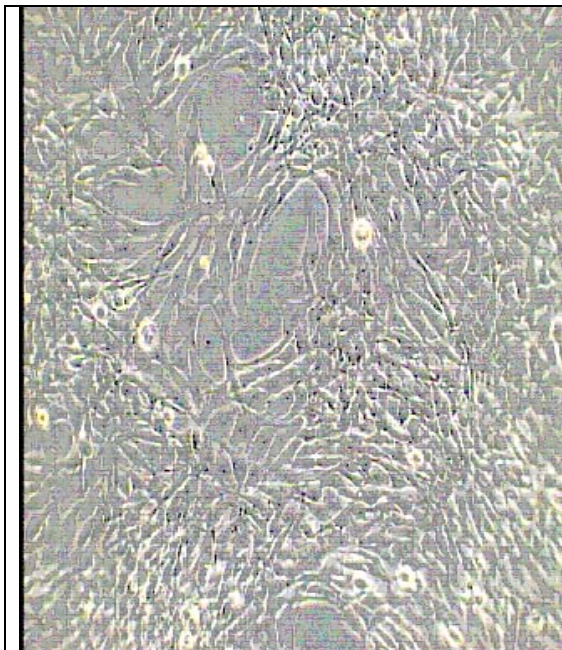


Figure 2.1.15: MG-63 osteosarcoma cells 90% confluent without dexamethasone treatment. Light microscope image enlargement 1:200.

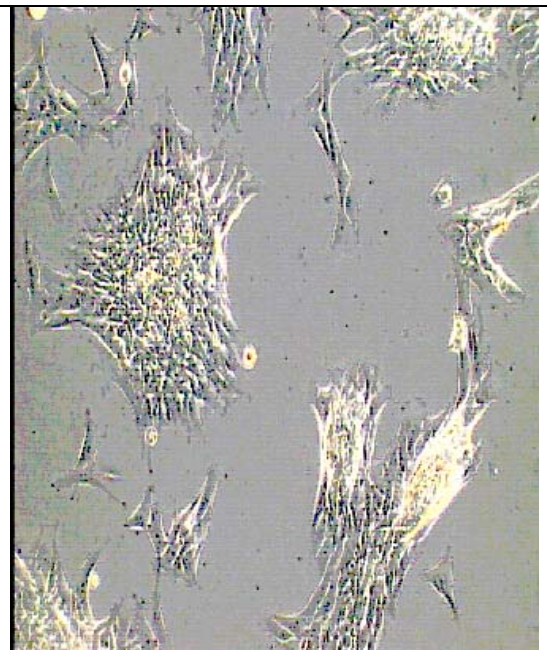


Figure 2.1.16: MG-63 cells after 48h treatment with dexamethasone. The cells aggregate to nodules and excrete matrix proteins. Enlargement 1:200.

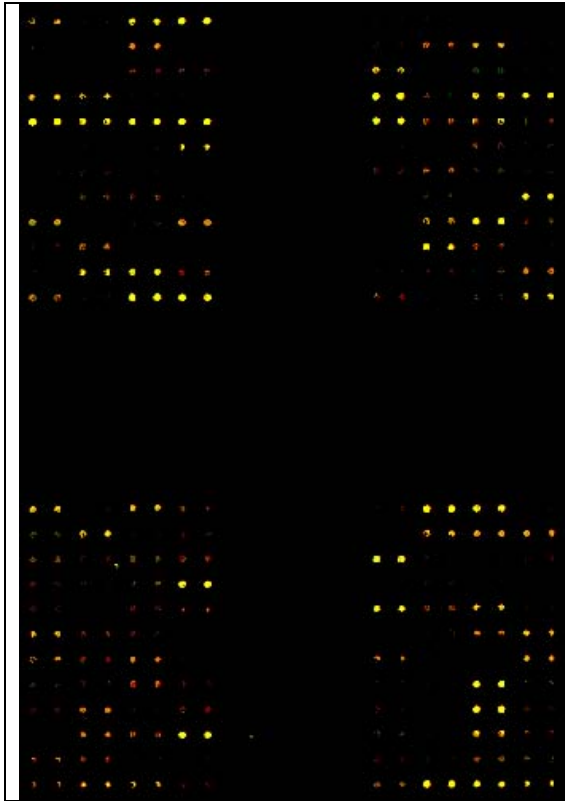


Figure 2.1.17: Control experiment: Self-self hybridisation of RNA from untreated MG-63 osteosarcoma cells on a chip containing cDNA probes from 192 genes. Each cDNA probe was spotted in duplicate.

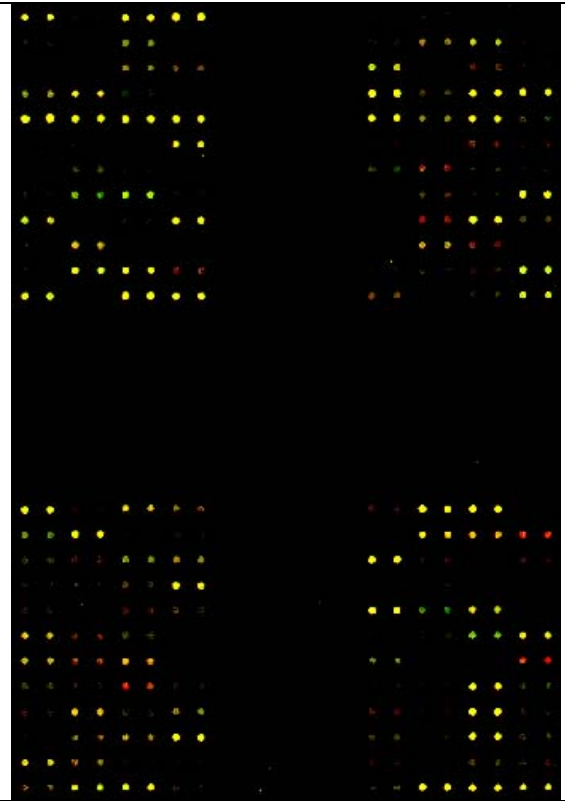


Figure 2.1.18: Hybridisation of dexame-thasone-treated cells (48h) against untreated MG-63 cells. Treated cells were labeled with cyanine 5, untreated with cyanine 3.

Epoxy coated slides (Quantifoil), spotted with amino-linked DNA probes that bind covalently to the surface, gave excellent signal-to noise ratios of fluorescence intensities and a low background (see pictures 2.1.17 and 2.1.18 above) The experiments with dexamethasone-induced, differentiated MG-63 cells and untreated cells show clear differences in gene expression. A control experiment (figures 2.1.17 and 2.1.19) shows equal fluorescence signal intensities for both (Cy3 and Cy5) channels, resulting in yellow spots in the dual colour overlay.

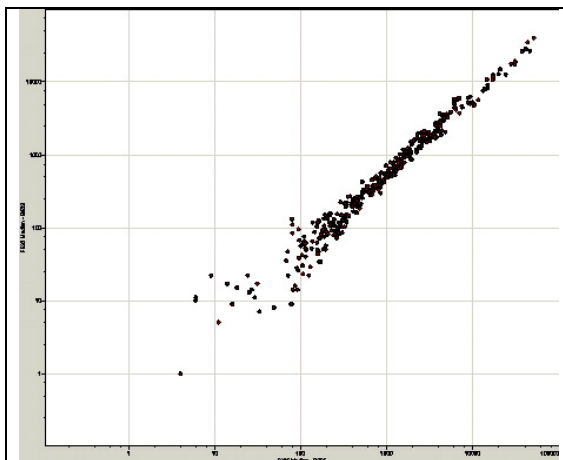


Figure 2.1.19: No data spreading in the control experiment. Scatterplot showing signal intensities from a self-self hybridisation (control experiment) of RNA from untreated cells on a logarithmic scale.

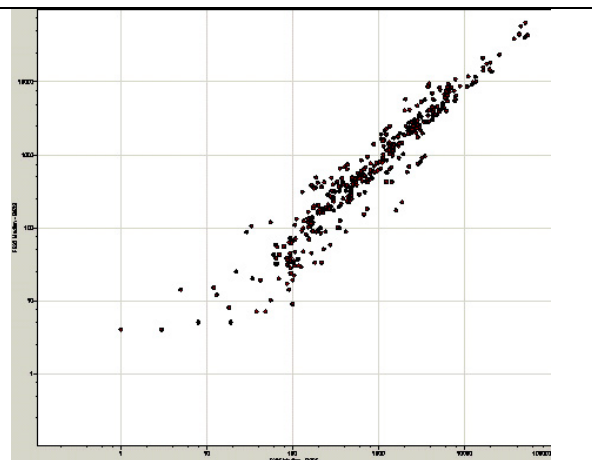


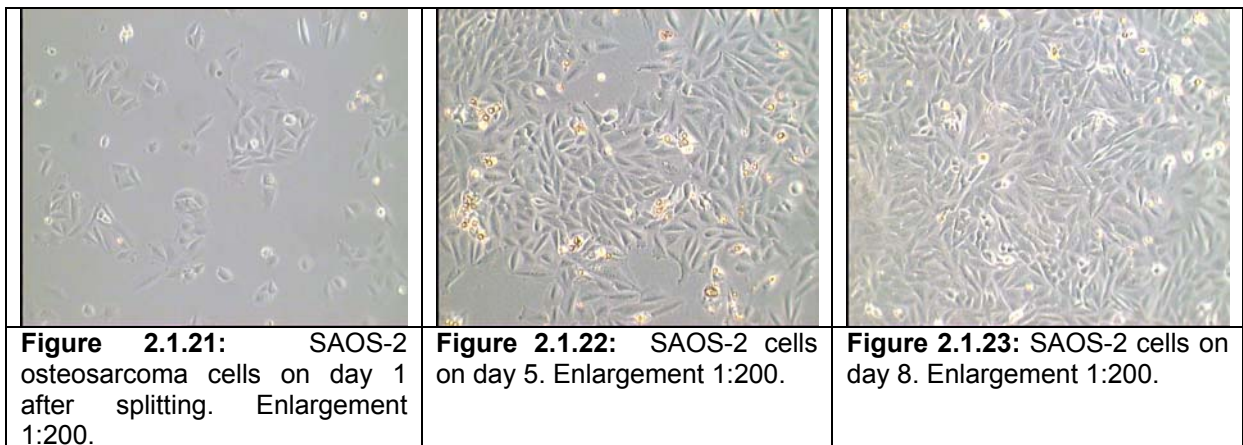
Figure 2.1.20: Spreading due to differential expression. Scatterplot of intensity signals from treated (Cy5) MG-63 cells hybridised against untreated (Cy3, reference) MG-63 cells.

Although the overlay of the images of an hybridised microarray scanned at both channels gives a valuable first impression on whether or not the experiment worked at all, a graph with both intensities plotted against each other on a logarithmic scale provides more quantitative information about

- the balance of the two channels (if we assume that the majority <95% of the genes show no difference in expression level, then most of the genes should group around the 45 degree axis. A parallel shift towards the y (Cy5) or the x (Cy3) -axis indicates an imbalance artifact that might result from different total RNA sample amounts, dye incorporation rates, fluorescence efficiencies or scanning laser intensities. This kind of imbalance can be corrected by normalisation algorithms.
- the fraction of differentially expressed genes
- the homogeneity of spotting, hybridisation and washing conditions across the slide

In simple experimental set-ups (e.g. direct comparison of two samples) and small arrays the scatter plot can help to identify directly differentially expressed genes, although in general the comparison of experimental replicates and statistical analysis gives more solid results.

Differently treated osteoblast-like mouse osteosarcoma SAOS-2 (Rao et al. 1998), and osteoblast-like MC3T3 cell lines served to test the performance of the mouse 21K-array developed at a later stage.



Gene expression profiling of osteoblast-like cell lines at various differentiation stages was successful as a tool to test the feasibility of the technique. Nevertheless it was difficult to obtain consistent and biologically meaningful results for several reasons:

- The limited number of probes on the array (initially 400) was too small to find a significant number of differentially expressed genes that could serve as a characteristic expression "fingerprint" for the stage of differentiation. The small number of biologically related genes made approaches of global normalisation difficult, as in this case the assumption of null regulation across all genes is not any more valid

- The available cell lines changed their differentiation behaviour with every passage, which hampered reproducibility of experiments
- Treatment of osteoblast-like cells with steroids in vitro resulted in strong morphological changes, and produce changes in the expression profile but whether this has any significance for in vivo systems, remains questionable, as many studies have shown previously (Gurlek and Kumar 2001).

As differentiation is a dynamic process that is very sensible to any influence on growth conditions and that changes the expression profile continuously, monitoring gene expression requires a very well-controlled cell culture system and many replicate microarray experiments to acquire consistent data. Since this was not possible within this project it was decided to carry out microarray studies with RNA samples from the established system of human fetal osteoblasts (hfOB), as obtained from the laboratory of Dr. N. Schütze, Würzburg. In a second collaboration primary pancreatic beta cells, obtained from the laboratory of Prof. Udo Oppermann, Karolinska Institute, Stockholm, Sweden, were treated with glucocorticoids, as (section 2.4).

2.2 Gene expression profiling of human fetal osteoblasts after treatment with Cyr61

Cystein-rich protein 61 (Cyr61, CCN1) belongs, together with connective tissue growth factor (CTGF, CCN2) to the immediate-early CCN gene family that regulate angiogenesis, tumor growth, placentation, implantation, endochondral ossification and fracture / wound repair (Brigstock 2003). It was shown to be induced in osteoblasts by treatment with vitamin D and seems to have functions in bone fracture repair (Schütze et al. 1998; Lechner et al. 2000). It therefore was decided to study the Cyr61-induced changes of osteoblastic gene expression to reveal unknown downstream targets of vitamin D signalling and to further clarify the role of the hormone and Cyr-61 in bone growth and fracture repair.

Although the cell culture work was done in parallel by the author of this work, the data presented here were produced from RNA that was provided from the laboratory of Dr. Norbert Schütze, University Hospital of Orthopaedic Research, Würzburg, Germany. The author of this work carried out the work connected with microarray design and production, sample labeling, microarray experiments and data analysis. Confirmation experiments by semi-quantitative RT-PCR were done in Dr. Schützes laboratory.

Human fetal osteoblasts (hfOB), obtained from the TC Spelsberg, (Harris et al. 1995) were grown in phenol red free medium supplemented with charcoal-stripped FCS. After amplifying the cells under equal conditions, the cells were split into aliquots and treated with Cyr-61 for 0, 6, 24 and 48 hours before harvesting and extraction of total RNA.

In a series of gene expression profiling experiments using the human array with ca. 1900 PCR products (representing ca. 1000 genes), hfOB treated with Cyr61 were compared to untreated hfOB cells. Some genes were represented by several cDNA probes on the chip which ensures data security but makes quantification difficult. Only one pair of dye swap experiments with hfOB, treated with Cyr61 for 24 hours before harvesting, delivered results. Therefore the array experiments can only be regarded as a rough screen to select for genes that are differentially expressed. Candidate genes were selected in the case of >2-fold regulation after 24 hours of treatment with Cyr61 and verified by semi-quantitative RT-PCR. RT-PCR was then used to analyse changes in expression of identified candidate genes at other timepoints (Schütze, N. 2003; Schütze, N. G., F; Kunz, M; Balling, S; Hendrich, C; Eulert, J; Adamski J; Jakob F 2003; Schütze, N. G., F; Kunzi-Rapp, K; Jaschinski, D; Balling, S; Hendrich, C; Eulert, J; Adamski, J; Jakob, F 2004).

Microarray experiments with hfOB on Peroxy-coated slides (Quantifoil, Germany) obtained homogenous signal distributions and very good signal-to noise ratios, with low background, compare figures 2.2.1-2 below. While this proofed the quality of previously developed and optimised protocols for array production, blocking, washing and hybridisation, there were problems to obtain consistent successfully labelled cDNA. It later turned out that changing quality of monoreactive cyanine dye and aminoallyl-dUTP was the reason why labeling failed in many occasions (Amersham 2002). This is especially critical in the case of limited sample RNA amounts. It was therefore decided to switch to the more sensitive, but time consuming and cost-intensive method of labeling with dendrimers (see methods).



Figure 2.2.1: Dual colour image: Hybridisation of RNA from hfOB, treated (Cy5) for 24 hours with 10^{-8} M Cyr-61 against untreated (Cy3) hfOB. All 1900 probes were spotted in duplicate.

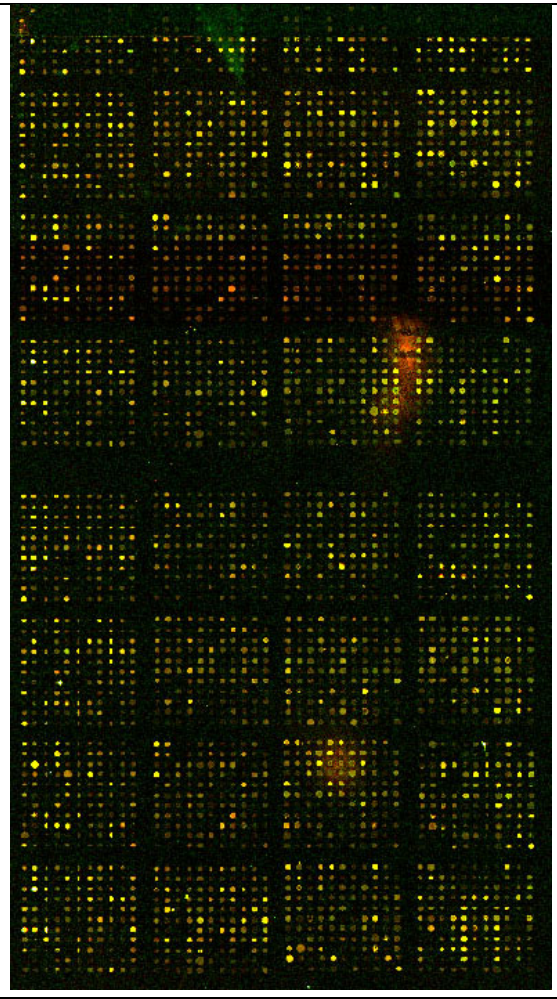
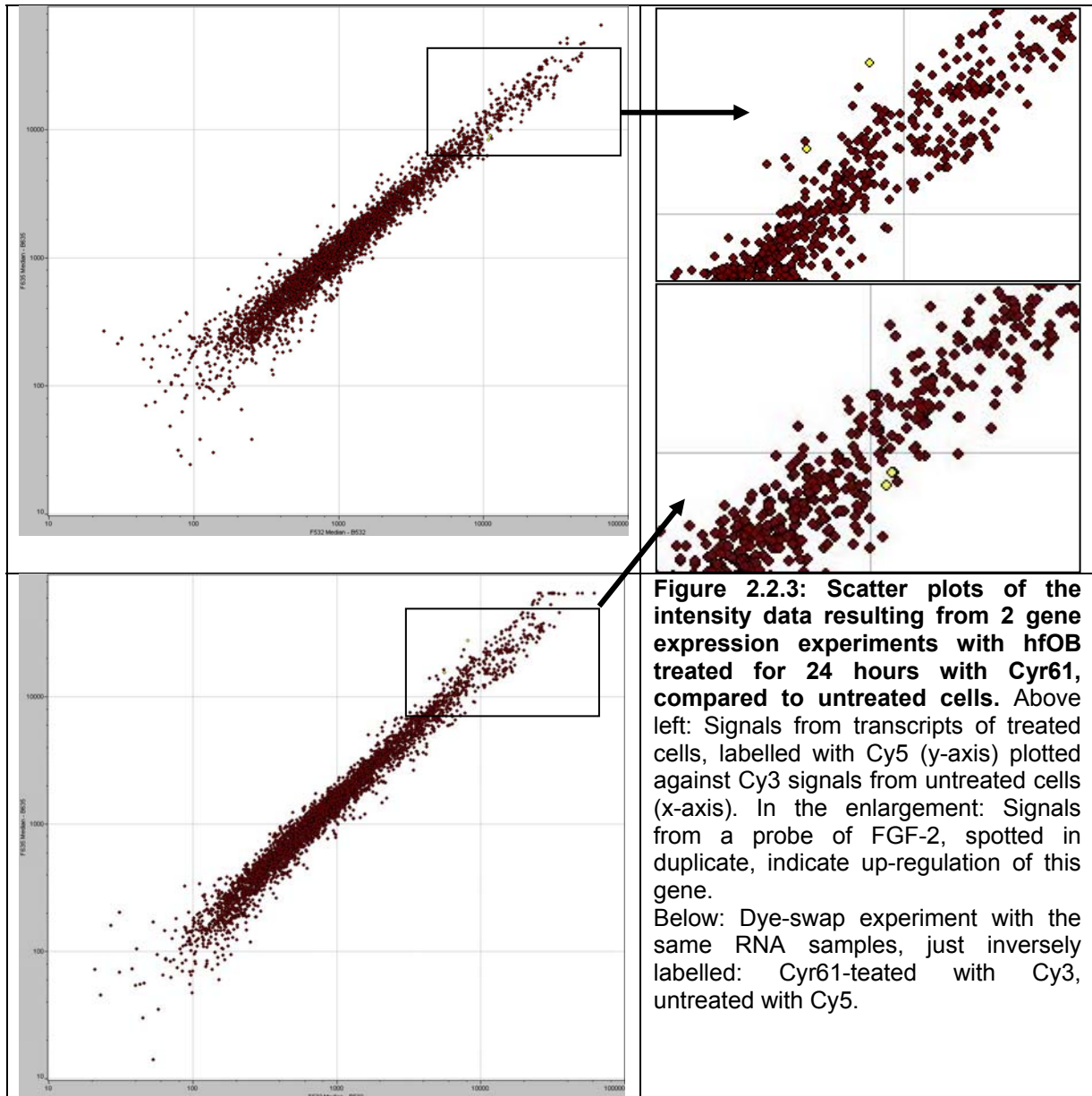


Figure 2.2.2: Dye swap experiment with the same sample RNA as in the hybridisation shown in picture 1.3.1 but with inverse labeling.

Since the differentially expressed genes had to be extracted from the data of only two successful experiments, statistical analysis was impossible. The data were subjected to global linear normalisation and genes represented by duplicate probes that were both regulated by a factor greater than 2 were selected as candidates for verification by quantitative PCR. In figure 2.2.3 the principle of dye-swap experiments is explained, as used in experiments with Cyr61-treated hfOB cells. Dye swap experiments were used to exclude artifacts due to different dye chemistries. The representation of each DNA probe by two spots on the human cDNA array helped to find artefacts due to spatial differences in printing or in hybridisation conditions.

Among the 20 candidate genes selected for verification, 15 could be verified by RT-PCR. In two cases RT-PCR gave signals too low to be quantified and in only three cases regulation was detected. Although a higher number of experimental repetitions would have been desirable to increase statistical data significance, a confirmation rate of 75% of candidate genes showed the potential of the method even under difficult conditions as restricted sample material.



As expected from previous studies, a large fraction of the genes regulated by treatment of hfOB with Cyr61 were involved in growth and differentiation (see table 2.2.1).

Of especial interest is the up-regulation of the Notch Receptor and its downstream effector Hey1 and Hes2. Notch-2 is a transmembrane protein with an extracellular domain containing multiple EGF-like repeats that can interact with other EGF-like transmembrane proteins, such as Delta, Jagged or Serrate (Baron et al. 2002). This interactions cause the proteolysis of the intracellular domain of Notch, which initiates signal transduction via a cascade of cytosolic and nuclear proteins, such as Hes2, and has been shown to have multiple functions in embryonic development and cell fate (Lai 2004; Rida et al. 2004). Notch-2 and its ligand Delta-1 have an important role in the development of chicken limbs (Crowe et al. 1999). Further evidence for a role of Notch signalling in bone and cartilage was given by the observation that Notch-2 and Notch-activating "A-Disintegrin and Metalloproteinase (ADAM)-10" are co-expressed in neonatal rat tibiae and osteoblast-like human cell lines (Dallas et al. 1999).

Table 2.2.1: Genes that were identified as induced or suppressed in hfOB after treatment with Cyr61 for 24 hours by microarray analysis and subsequent confirmation by RT-PCR. Confirmation experiments by RT-PCR were carried out by the group of Dr. N. Schütze, Würzburg.

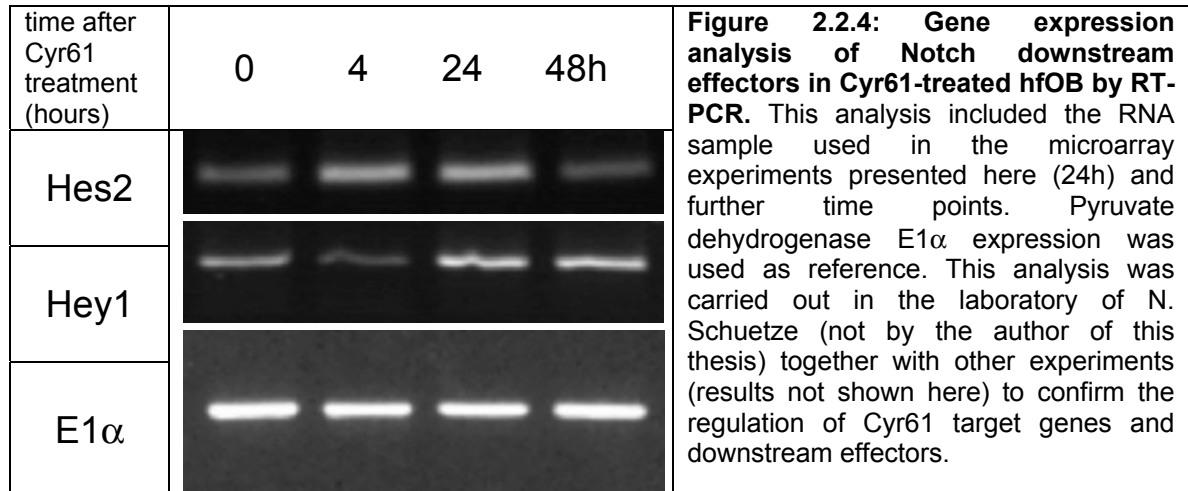
Gene name	Genbank accession	Function	RT-PCR
up-regulated			
patched 2	AF091501	receptor for hedgehog proteins signal transduction	confirmed
vitronectin	X03168	cell adhesion, integrin ligand	no effect
SKN	X77366	transcription factor	confirmed
IGF2	NM 000612	growth, proliferation	confirmed
Notch-2	M15800	receptor, cell differentiation, signal transduction	confirmed, small effect
Indian hedgehog	U59748	ligand for patched, signal transduction	too little PCR product
Gli3	M57609	transcription factor	confirmed
HD	L12392	huntington-disease gene	confirmed, small effect
Mal	M15800	T-cell differentiation factor	confirmed
down-regulated			
gadd45	M60974	growth control, DNA repair, genomic stability, cell cycle control	confirmed
inhibin a	M13436	differentiation-inducing factor	no effect
IGFBP5	A1244014	proliferation, signal transduction	confirmed
BMPR1A	Z22664	receptor, signal transduction	confirmed
Tau	J03778	microtubuli-associated	confirmed, small effect
MR	M16801	mineralcorticoid receptor	confirmed
RPSKA5	AF090421	ribosomal S6 protein kinase	no effect
PYGL	AF046785	unknown	too little PCR product
NF2	AA991180	tumor suppressor, membrane organisation	confirmed
EST	AA991180	unknown	confirmed
EST	A1962658	unknown	confirmed, small effect

Notch-2 and its ligand Delta-like-1 (Dll1), essential for somite segmentation and condensation of sclerotomes (Koizumi et al. 2001), were reported to be dependent on the expression of presenilin1. Presenilin1-deficient mice showed severe defects in the axial skeleton and impaired ossification of vertebral bones, confirming the role of Notch signalling in the transition of cartilage tissue to bone.

The anabolic effect of Notch signalling on bone formation was further corroborated by the observation that expression of the Notch cytoplasmic domain in murine osteoblast-like MC3T3 cells stimulated the formation of calcified nodules (Tezuka et al. 2002). In mesenchymal C3H10T1/2 cells and in primary human mesenchymal stem cells Notch enhanced differentiation along the osteoblastic lineage. Simultaneously it suppresses adipocyte development, a finding that has been challenged by a similar *in vitro* study published recently (Sciaudone et al. 2003).

A recently published study has shown that Notch signalling, activated either by site-specific overexpression of PTH/PTHrP receptors in osteoblasts of transgenic mice or by treatment of WT mice with PTH, induces an increase of the production of hematopoietic stem cells in bone marrow and increases the number of osteoblasts and trabecular bone formation *in vivo* (Calvi LM 2003). This effect is suppressed by inhibition of the cleavage of the Notch intracellular domain through γ -secretase inhibitor.

Vitamin D suppresses PTH secretion (while increasing intestinal calcium uptake). The effect of PTH on Notch signalling indicates that the systemic effect of vitamin D on bone formation can be different from direct local effects through Cyr61-mediated activation of Notch signalling in bone tissue. This underscores the necessity to test models of vitamin D / Cyr61 function in osteoblasts, based on *in vitro* studies, in a physiological context *in vivo*.



Several genes known from hedgehog signalling pathways, like Indian hedgehog (Ihh), Gli3 and patched 2 were found up-regulated in Cyr61-treated hfOB. Hedgehog proteins are known to promote osteogenic differentiation of osteoblast precursor cells (Nakamura et al. 1997), stimulate bone fracture repair (Ito et al. 1999) and cartilage formation (Ito et al. 1999). BMPR1A, which was down-regulated after Cyr61-treatment, has a role in bone formation by osteoblasts, as well as in bone resorption (Mishina et al. 2004) through osteoclasts.

Gadd45 was previously known for its role in cell cycle control and induction with DNA damage (Takekawa and Saito 1998) in response to environmental stress and seems to link the cell-survival promoting NFκ-B pathway to apoptosis via JNK (Papa et al. 2004). In a gene expression study of osteoblast precursor cells Gadd45 was found up-regulated in later stages of differentiation, when proliferation already had stopped. In the context of fracture repair this process might be reversed, which would confirm the role of Cyr61 in bone suggested previously (Hadjjargyrou et al. 2000). IGF binding protein IGFBP5, down-regulated after Cyr61 treatment of hfOB is up-regulated in chondrocytes at later differentiation stages (Sekiya et al. 2002).

This microarray study confirmed the role of Cyr61 in bone remodelling and its potential to support fracture repair, which is evaluated currently (Schütze, N. 2004). The involvement of several signalling pathways in this process, like Notch or Ihh has been suggested and can now be investigated more in detail. This will also include gene expression analysis with microarrays covering the full genome.

2.3 The mouse cDNA array

As the production of cDNA arrays is extremely time consuming and requires large material resources, the production of a microarray was limited to 1900 probes. The production of microarrays covering a large part of a mouse genome became achievable with the acquisition of a sequence-verified cDNA clone set with database annotations from Lion Biosciences. In collaboration with the group of Dr. Johannes Beckers these chips were produced and hybridised according to protocols that were previously developed for the smaller human arrays.

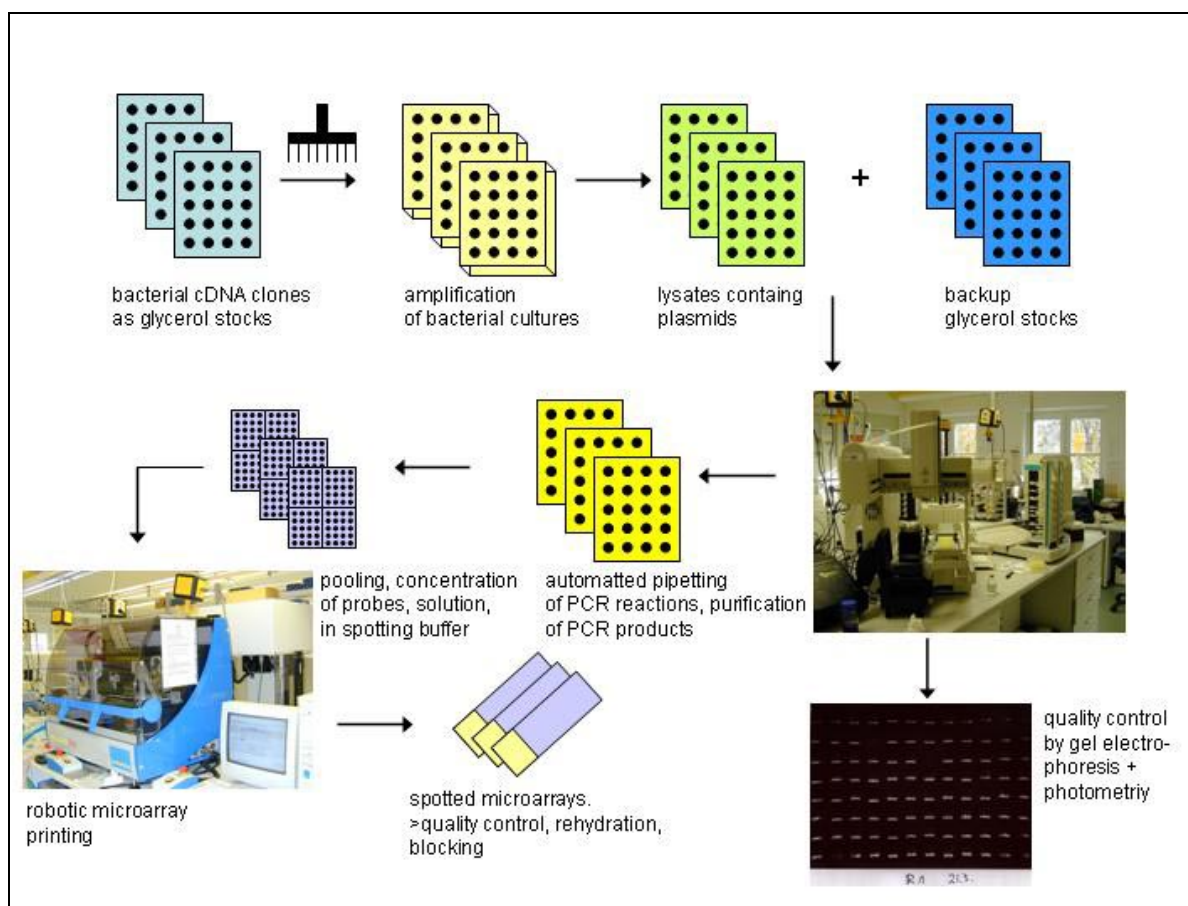
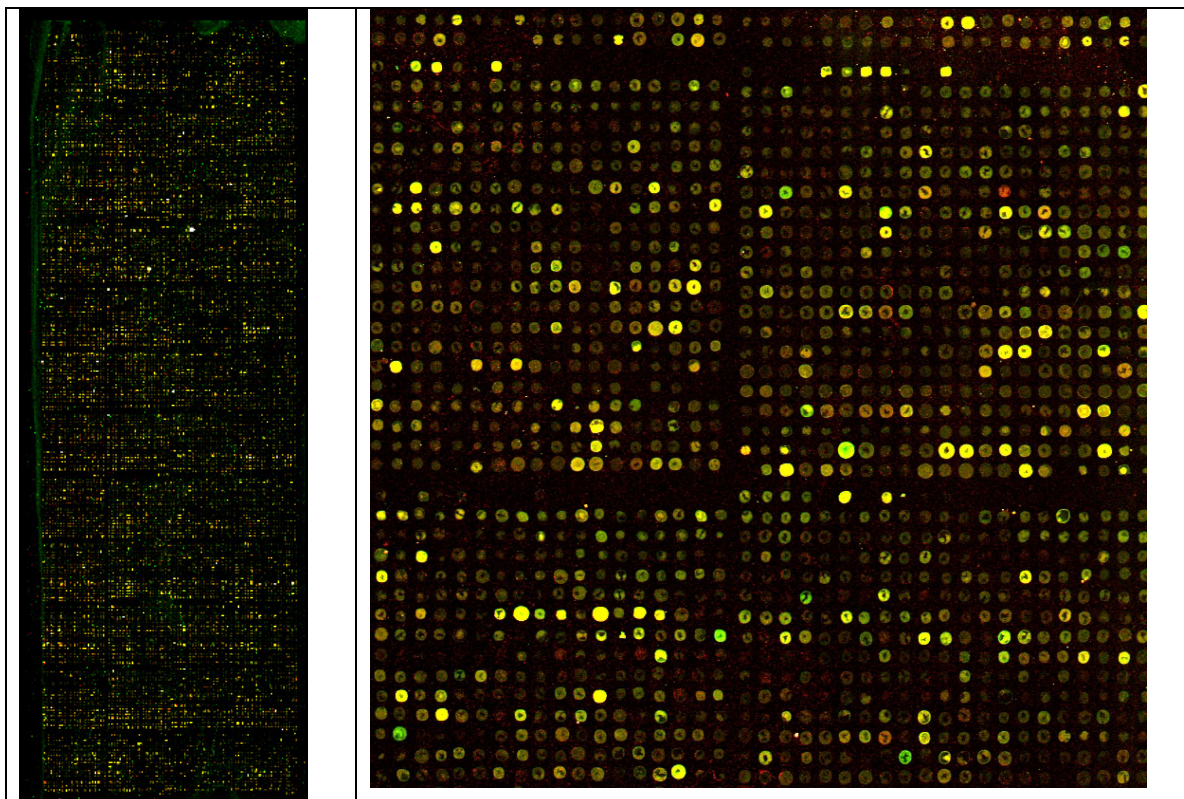


Figure 2.3.1: Workflow scheme of the production of 21K mouse microarrays. To cope with the large numbers of clones, PCR reactions (ca 70.000), the protocols developed before had to be up-scaled and automated with liquid-handling robotics. Workflow organisation according to an efficient logistic scheme was necessary to allow the cooperation of several co-workers and storage of intermediate products during the process of microarray production.

The scheme of microarray production in figure 2.3.1 above gives an overview of the main steps in microarray production. Bacterial clones were transferred into 96-well plates with LB-culture medium with 96-needle stainless steel combs that easily can be desinfected after use. All pipetting steps were done either with 8- or 12-channel pipettes or with a liquid-handling robot. Automation of pipetting processes can not only increase the speed but also helps to avoid pipetting errors. Bacterial lysates served as templates for PCR reactions. Previous experiments showed that the minimum concentration of probe DNA in the spotting buffer has to be 200ng/ μ l. To obtain enough DNA probe material (ca. 10 μ g/probe), three PCR reactions of 100 μ L were pooled and purified on columns, as described in the methods section. Quality control steps, including agarose gel electrophoresis and photometric concentration measurements were introduced before and after the purification of PCR products.

Before printing, the DNA was dried in vacuum driers, re-dissolved in spotting buffer and transferred into low-volume 384-well plates. The workflow was organised to maximize throughput and to allow the storage of intermediate products.



Figures 2.3.2 and 2.3.3: Mouse array with 20736 spotted cDNA fragments (mouse 21K array). The pictures show an overlay of scanned images of an array hybridised with vitamin D-receptor knockout (VDRKO) mouse kidney (Cy5), hybridised against WT (Cy3) kidney. The PCR products were spotted with a set of 48 split pins in 3xSSC on aldehyde-coated slides using the Migrogrid 2 spotter from Biorobotics. The enlargement of a small section shows parts of four 21x21 spot subgrids.

The genome-wide mouse array was spotted on aldehyde-coated glass substrates from Cell Associates with a 48 needle pin head for split pins from Telechem Inc., using the MigrogridPro Spotter from Biorobotics Inc. The array contains 48 pin subgrids of 21x21 spots. A data base, obtained from Lion Biosciences AG, contained probe annotations including the probe sequence, Unigene reference mRNA identifiers and further information regarding gene function and genomic location. These data had to be associated with the microarray spotting grid coordinates for later evaluation of gene expression data.

The use of this genome-wide arrays opened possibilities to apply the potential massive parallel gene expression profiling and pathway finding to explore the influence of hormone function on gene regulation, in glucocorticoid-treated pancreatic β -cells.

2.4 Expression profiling of glucocorticoid-treated pancreatic β -cells

Glucocorticoid hormones regulate essential physiological functions, like glucose metabolism and inflammation by binding to nuclear receptors (see introduction). Hyperglycemia, insulin resistance and development of diabetes type 2 were associated with an excess of endogenous or exogenous glucocorticoids, but the direct function of glucocorticoid hormone action on insulin-secreting β -cells is under debate. To gain further insights into these processes on transcriptional level, the effect of short-term treatment of pancreatic β -cells from lean mice was studied by microarray analysis.

2.4.1 Experimental set-up

Our collaboration partners Malin Hult and Prof. Udo Oppermann (Karolinska Institute, Stockholm, Sweden) isolated pancreatic islets from V57BL/6J mice and split them into four aliquots of 6-7 mice each. Two of the aliquots were treated overnight with 200nM corticosterone, the murine analog of cortisol, followed by extraction of total RNA from all samples according to the procedure described in methods and sent to the author of this work.

Total RNA, extracted from corticoid-treated and untreated pancreatic β -cells was transcribed into cDNA and labelled with cyanine 3/5 fluorophores attached to dendrimers, using a modified Genisphere kit and protocol (see methods). The labelled cDNA products, resulting from 5 μ g total RNA of treated and untreated cells, respectively, were combined and hybridised over night on 21k-mouse arrays. Raw data were acquired and extracted with the GenePix software, version 4.0 (Axon) and annotated with the gene IDs contained in the mouse arrayBase databases A and B from Lion Biosciences.

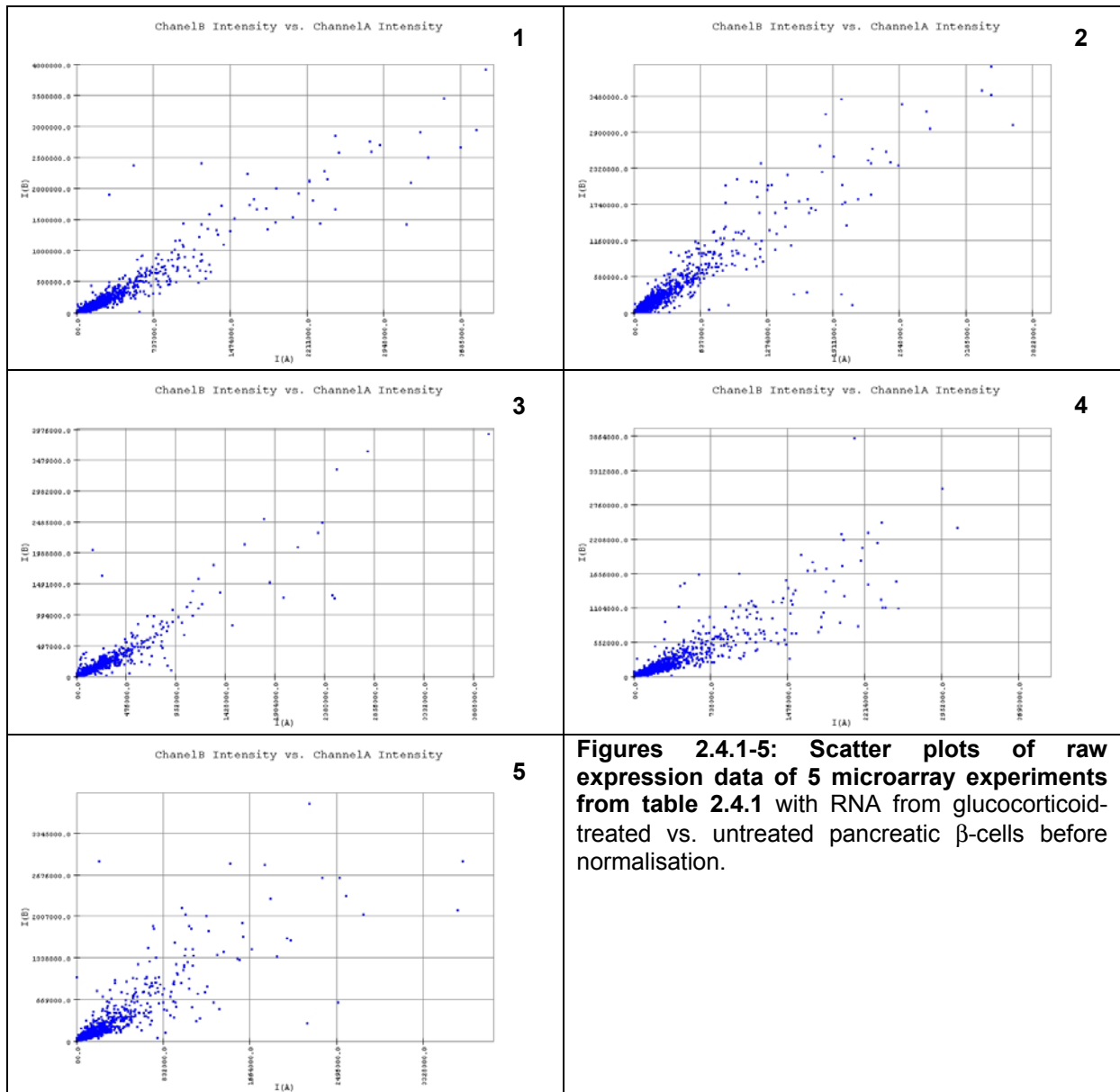
Table 2.4.1: Set-up of dual-channel microarray experiments, comparing gene expression between cortisol-treated and untreated murine pancreatic β -cells. From the left: Experiment number, labeling of samples, dye swap, name of result data file.

experiment #	Cyanine 3	Cyanine 5	dye swap	.gpr file
1	1, untreated	2, treated	no	20_NN.gpr
2	2, treated	1, untreated	yes	21_NN.gpr
3	4, treated	3, untreated	yes	opp1.gpr
4	3, untreated	4, treated	no	opp2.gpr
5	4, treated	3, untreated	yes	opp3.gpr

In total, 5 hybridisations were done with two sets of treated (sample 2, 4) and untreated (samples 1, 3) cells. To exclude artefacts arising from the different labeling chemistries, dye swap experiments were included, exchanging the labeling dye cyanine 3 with cyanine 5 and vice versa (see table 2.4.1).

2.4.2 Data analysis

Microarray raw data were imported for normalisation and filtering into MIDAS, a component of the TM4 software package, provided by the TIGR Institute (Saeed et al. 2003). Data from a series of experiments were all treated in MIDAS according to the same protocol: First, the data underwent a blockwise locally weighted linear regression (LOWESS) analysis procedure. This non-linear normalisation method helps to remove systematic intensity-dependent effects on the $\log_2(\text{ratio intensity})$ distribution within each experiment (Park et al. 2003).



Figures 2.4.1-5: Scatter plots of raw expression data of 5 microarray experiments from table 2.4.1 with RNA from glucocorticoid-treated vs. untreated pancreatic β -cells before normalisation.

After normalisation, data with intensities below 10.000 units (ranging from 0 to $2^{16} = 65.535$) were discarded. Since variability in the measured $\log_2(\text{ratio intensity})$ values increases as intensities decrease, differentially expressed values were selected, using an algorithm that calculates the local standard deviation of each array element. As a measure for differential expression, a local Z-score was calculated by dividing the $\log_2(\text{ratio})$ values $[\log_2(T_i)]$ by the local standard deviation $\sigma_{\log_2(T_i)}^{local}$. Differentially expressed values can then be automatically extracted by setting the Z-score threshold to 1, 1.5 or 1.96, depending on the statistical level of confidence to be obtained. Here we chose a Z-score of 1.96 and a 95% level of confidence, reducing the number of potentially differentially expressed genes from 20.952 to only 17.

This Z-score selection has been shown to be more reliable than setting rigid global $\log(\text{ratio intensity})$ levels for the extraction of differentially expressed data (Quackenbush 2002). Further confirmation was obtained by comparing biological and technical repeats of the array experiments and dye swap experiments. Data from multiple experiments were compared and processed with the software Multi Experiment Viewer (MEV) developed by the TIGR institute. The MEV package allows

for log-ratios of intensity values to be visualized in a vector matrix and to be treated with different clustering algorithms, e.g. hierarchical clustering (Eisen et al. 1998). By comparing technical and biological repeats, as well as dye swap experiments (see table 1 above), artefacts arising from different labeling chemistries or spotting and washing conditions were excluded and thus the number of candidate genes for differential expression reduced to 12:

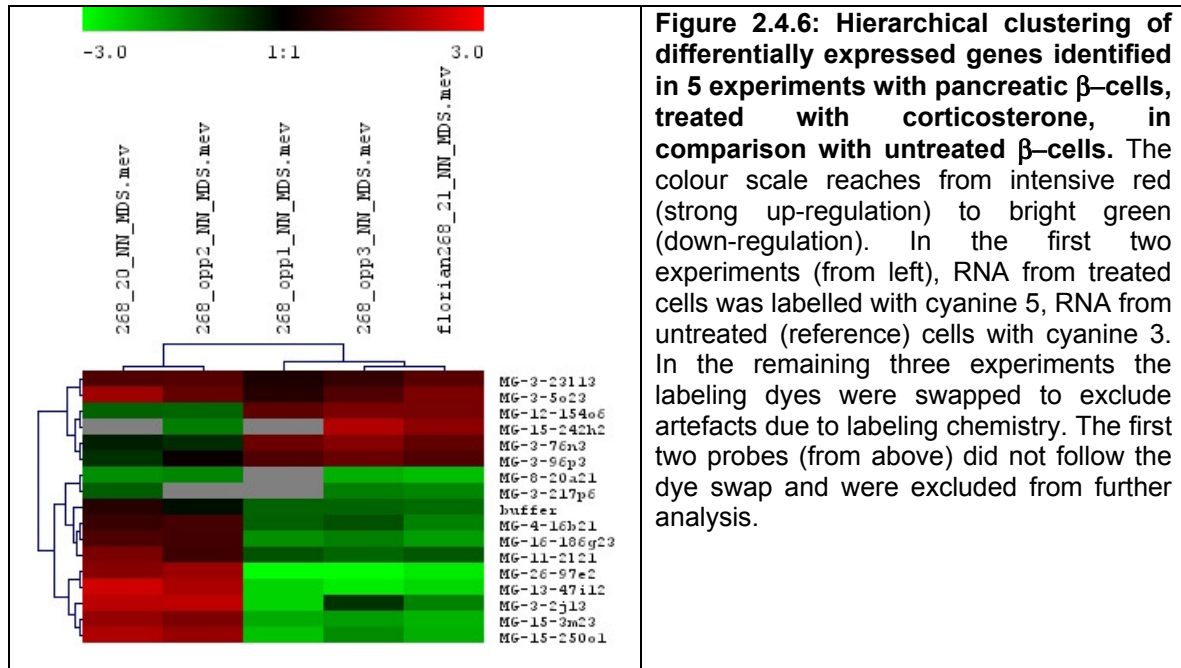


Figure 2.4.6: Hierarchical clustering of differentially expressed genes identified in 5 experiments with pancreatic β -cells, treated with corticosterone, in comparison with untreated β -cells. The colour scale reaches from intensive red (strong up-regulation) to bright green (down-regulation). In the first two experiments (from left), RNA from treated cells was labelled with cyanine 5, RNA from untreated (reference) cells with cyanine 3. In the remaining three experiments the labeling dyes were swapped to exclude artefacts due to labeling chemistry. The first two probes (from above) did not follow the dye swap and were excluded from further analysis.

2.4.3 Genes, differentially expressed after glucocorticoid treatment: Discussion

Our collaborating partners Malin Hult and Prof. Udo Oppermann, Karolinska Institute, Stockholm analysed the data obtained from these five microarray experiments according to a different, less stringent procedure. They came to a list of the 100 most differentially expressed candidate genes, including the genes contained in table 2.4.2 above. From this list they selected 9 candidate genes for confirmation experiments by quantitative real-time PCR, including *Itmap*, *Fabp4*, *Hsbp1*, *Fkbp5* and *Serpina 12*, all of which could be confirmed.

In contrast to islets of ob/ob obese mice, glucocorticoid treatment of pancreatic islets from lean mice for 18-22h increased insulin secretion significantly (3-fold). Increased secretion of insulin was inhibited with the mineralcorticoid receptor antagonist RU486. Treatment with the hormone precursor dehydrocorticosterone amplified the expression of the activating enzyme 11 β HSD1. Concomittant with increased insulin secretion in response to stimulation by glucose, Hult et al. found the up-regulation of a number of genes involved in insulin secretion, such as amiloride sensitive cation channel, phosphatidylinositol 3-kinase (PI3), PI3-interacting growth factor receptor-binding protein 10 (*Grb10* (Deng et al. 2003) or the metabolic enzyme lipoprotein lipase (*Lpl*) (Hult 2004).

Table 2.4.2: List of differentially expressed genes in pancreatic islet cells after corticoid treatment. Here a Z-score filtering of 1.96 (95% confidence) was applied and dye-related artifacts were excluded.

	mean	error of mean	genbank ID	locus linkGene ID	short name	name
up-regulated	6.41	2.69	NM_010492	15893	Ica1	islet cell autoantigen 1
	5.61	0.91	NM_026535	68054	Serpina12 /Api	ser/cys proteinase inhibitor
	3.99	0.61	NM_008491	16819	Lcn2	lipocalin 2
	3.89	1.48	NM_008411	16433	Itmap1	integral membrane-associated protein 1
	3.67	0.54	NM_013560	15507	Hspb1/25	heat shock protein 1
	2.68	0.75	NM_010220	20363	SEPP1	selenoprotein P, plasma, 1
	2.15	0.37	BX639727	14229	Fkbp51	FK506 binding protein 5
	2.09	0.47	BQ932872	319269	EST	n.a.
down-regulated	mean	error of mean	genbank ID	locus link	short name	name
	0.64	0.23	NM_009366	21807	Tgfb1i4	TGFB1 induced transcript 4
	0.53	0.17	NM_007837	13198	Ddit3	DNA-damage inducible transcript 3
	0.42	0.04	NM_009363	21785	TFF2	trefoil factor 2 (spasmolytic protein 1)
	0.30	0.05	NM_013655	20315	Cxcl12	chemokine (C-X-C motif) ligand 12

Among the candidate gene with the strongest up-regulation was found α -1 proteinase inhibitor (Serpina12, Api). Api, an acute-phase protein mainly secreted by hepatocytes, but also locally produced in pancreas, lung and intestine, has been shown to be specifically expressed in cell-cell junctions of microvascular endothelial cells (MEC) of the islets of Langerhans (Lou 1999), distinguishing them from endothelia of other organs. Api expression in MEC accounts not only for reduced proliferation rates and trypsin resistance; it was found to be specific to a pre-diabetic phenotype in islets of non-obese diabetic (NOD) mice. Api is up-regulated by treatment of MEC with the anti-inflammatory cytokine interleukine IL-10, whereas interleukin IL-1 β or the onset of diabetes suppresses Api expression (Papaccio 2002). Pro-inflammatory IL-1 β was among the strongest down-regulated genes found in this study (Hult 2004). Moreover, other studies connected Api to a role as immune effector by modulating lymphocyte proliferation and cytotoxicity. It was reported to inhibit revascularization of transplants and to accelerate autoimmune disorders including diabetes (Sandler 1998). A recently published study on NOD mice, transfected with human Api through recombinant adeno-associated virus vector mediated gene delivery, showed the potential of Api to reduce significantly the frequency of overt type 1 diabetes (Song 2004).

Highly up-regulated in corticoid-treated islets was islet cell Ag69 (ICA69), an auto-antigen target by self-reactive T-cells in human and murine diabetes. ICA69 NOD knockout mice develop autoimmune diabetes with the same rate as wild type NOD mice, showing that ICA69 is not an obligate auto-antigen in the development of diabetes (Winer 2002). FK506 binding protein 5 (FKBP51) is a high molecular weight immunophilin that binds to the immunosuppressant drug FK506. FKBP51, a component of the unliganded high affinity glucocorticoid receptor (GR) complex, lowers in the case of its overexpression the affinity of GR to its ligand and is likely to cause glucocorticoid resistance (Denny et al. 2000). In the case of pancreatic islets that were exposed to high concentrations of glucocorticoids, overexpression of FKBP51 appears to confer protection against corticosterone-induced stress.

Among the activated genes was also heat shock protein 1/25 (Hsp1/25), known to protect cells against oxidative stress in models of intestinal epithelial injury (Ropeleski et al. 2003). The product of the Integral membrane-associated protein-1 (Itmap) gene localizes to zymogen granule membranes in pancreas and was found to attenuate the severity of pancreatitis, a mortal inflammatory disease leading to the autodigestion of the pancreas (Imamura et al. 2002). Lipocalin 2 (LCN2) is another acute phase protein that was recently characterised as a marker gene for inflammatory bowel disease (Dooley et al. 2004). Up-regulation of LCN2 after treatment of islet cells with glucocorticoids may be interpreted as a stress signal similar to those characterising inflammatory conditions. Trefoil peptides are known as tumor markers in cancers as adenocarcinoma (Argani et al. 2001) and were observed as up-regulated during inflammation. Treatment of experimentally induced intestinal inflammations with trefoil factor 2 (TFF2) was recently reported to have a beneficial effect and to attenuate other markers of inflammation (Soriano-Izquierdo et al. 2004). Down-regulation of TFF2, as observed here in pancreatic islets after treatment with glucocorticoids can therefore be interpreted as indicator for a pro-inflammatory state.

Up-regulation of a series of genes with functions in the response to stress and inflammatory response (Hult 2004) indicates the triggering of a strong transcriptional reaction to the stress signal mediated by corticosterone in pancreatic islets. This stress response, in combination with enhanced insulin secretion characterises a hyperresponsive state. This condition was previously characterised as pre-diabetic and can progress to the onset of glucose insensitivity. Up-regulation of Api further supports the diagnosis of a pre-diabetic state.

3. Gene expression profiling of vitamin D receptor knockout (VDRKO) against wild type mouse kidney

Kidneys not only have a central role in vitamin D biosynthesis (see introduction), but are target organs of vitamin D action and express the nuclear vitamin D receptor (VDR) in high concentrations. The physiological functions of kidneys comprise mineral ion homeostasis, blood pressure control and multiple endocrine functions and transport processes, which can be affected by vitamin D.

Differences in the gene expression profiles of kidneys from wild type (WT) and vitamin D receptor knockout (VDRKO) mice can help to further clarify gene regulation underlying these functions of vitamin D signalling. Since vitamin D action is tightly coupled with calcium metabolism and since vitamin D-controlled processes were reported in many cases to be influenced by sex steroids, animals of different gender and raised with diets, containing normal or high calcium concentrations, were included in the study. In the following chapter 3.1, first the experimental design of two microarray studies will be described, together with different strategies of data analysis and the resulting data presented in tables. In the part 3.2 these results will be analysed in detail, together with confirmation experiments with quantitative real-time PCR (qPCR). qPCR also was used to analyse changes in gene expression of additional genes or conditions, not included in the microarray analysis. Expression data of these genes might complement data from microarray experiments in the search of physiological functions and pathways regulated by vitamin D and its receptor.

3.1 Gene expression profiling with cDNA microarrays

In two entirely different experimental set-ups, using different data analysis tools and strategies, the influence of VDR ablation on gene expression profiles in kidney was studied. The set of experiments described below aimed at a direct comparison of VDRKO and WT kidneys from male mice fed with a standard diet (Erben et al. 2002).

3.1.1 Gene Expression profiles of kidneys from male ND mice: VDRKO compared to WT

5 male age-matched vitamin D receptor knockout (VDRKO) mice and 5 wild type (WT) mice from the same strain were sacrificed and dissected. From each animal a set of organs, containing liver, spleen, kidney and femur were retained, immediately snap-frozen in liquid nitrogen and stored at -80° C.

For RNA extraction, frozen kidneys were grounded to powder with a dismembrator and RNA was extracted according to the protocol described in methods section 5. As mentioned in the introduction, printed cDNA arrays change significantly in quality and performance, making it difficult to obtain larger numbers of microarrays that deliver data of similar quality. Therefore and because of financial restrictions, pooled RNA samples from 5 VDRKO animals were compared with a pool from 5 WT animals, in awareness that sample pooling causes some loss of information (Churchill 2002). RNA was transcribed to cDNA, substituting 50% of d(TTP) with aminoallyl-dUTP, purified and labelled with monoreactive cyanine 3/5 according to protocols in methods section 5. To exclude artefacts caused by varying experimental conditions, the experiments were repeated four times, including two dye swap experiments. As

one dye swap experiment gave signal-to-noise ratios that in average were much lower than those in the other three experiments and since intensity distribution across the slide was inhomogeneous, it was excluded from further analysis. The images were scanned at 635nm and at 532nm on an Axon scanner and image analysis was performed with the use of GenePix software. The raw data output of GenePix of the three remaining experiments were visualized as intensity scatter plots, with intensity signals of channel Cy5 (VDRKO) plotted against intensities from channel Cy3 (WT, reference).

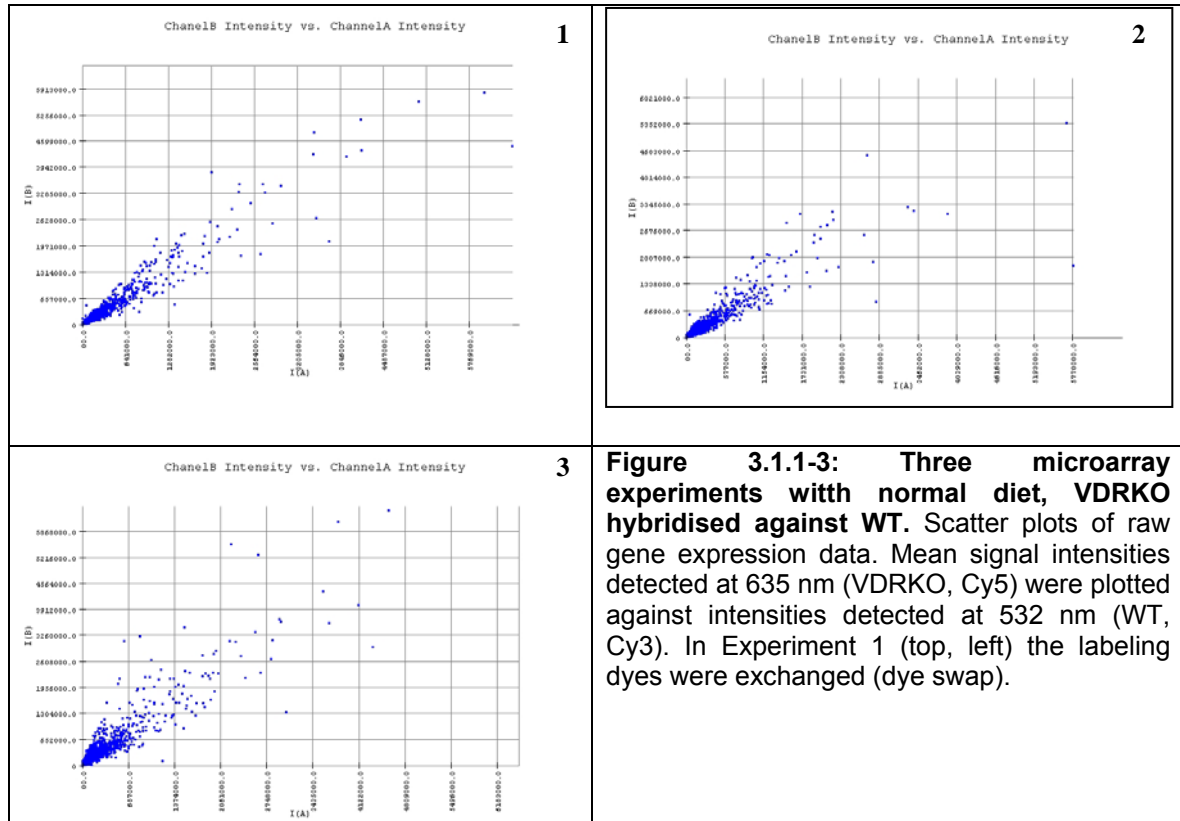


Figure 3.1.1-3: Three microarray experiments with normal diet, VDRKO hybridised against WT. Scatter plots of raw gene expression data. Mean signal intensities detected at 635 nm (VDRKO, Cy5) were plotted against intensities detected at 532 nm (WT, Cy3). In Experiment 1 (top, left) the labeling dyes were exchanged (dye swap).

Raw data were analysed using a program in a MATLAB environment, designed by A. Drobyshev (GSF Institute of Experimental Genetics, AG J. Beckers). This program allows the import of raw data files containing the results of several experiments. After excluding signals, identified and flagged as artefacts or below a pre-set intensity threshold, global normalisation is applied by setting the median $\log_2(\text{ratio intensities}) = 0$. Furthermore, signal intensity ratios can be corrected for dye swap experiments and results filtered for genes that appear differentially expressed in all experiments.

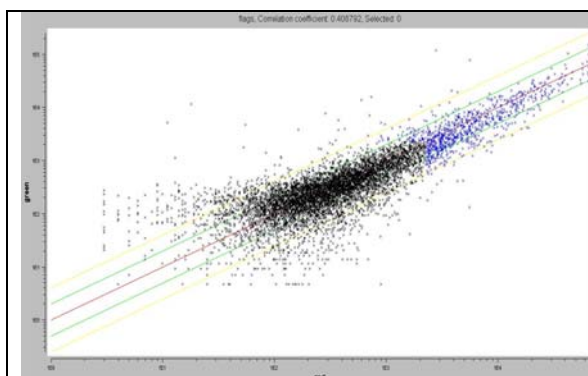


Figure 3.1.4: Scatter plot of a microarray experiment after global normalisation. As variability generally increases with decreasing signal intensity, data below a certain threshold (in black) were excluded from further analysis.

Linear normalisation all $\log(\text{ratio intensity})$ values works well for technically perfect experiments and is generally superior to normalisation relative to the expression of pre-defined "housekeeping genes". On the other hand, it does not account for non-linear signal intensity distribution. Rigid intensity thresholds, as applied in the example shown in figure 3.1.4 and the introduction of dye-swap experiments can help to exclude false positive values, but also results in increased rates of false negative results. Especially gene expression data in the lower range of expression and fluorescence signal intensity, as transcription factors, nuclear receptors or growth factors, often are neglected by global normalisation and filtering with intensity thresholds.

The data output was exported as a list of genes, ranked according to the number of relative fold change in gene expression. A nice feature of this program is the visualization of the corresponding images for each spot next to its fold change ratio and its absolute mean fluorescence intensity value, which gives an immediate impression of the quality of data and allows to easily identify artefacts (e.g. distorted intensity signals due to background, scratches, doughnut spots etc.). The limitations in the use of this program are its inflexibility and the lack of more sophisticated methods for normalisation and data analysis.

Table 3.1.1: Fraction of the differentially regulated genes extracted from three microarray experiments with male ND VDRKO vs. WT mouse kidney, as received after linear normalisation and data filtering, using a MATLAB routine. In this example, the regulation of two genes, CYP4B1 (MG-12-3e4) and calbindin D9K (MG-12-3f11) is shown, which are both down-regulated in VDRKO mouse kidney compared, to WT. Experiment 1 was a dye swap experiment, i.e. the labeling dyes were exchanged. For each gene in each experiment the mean intensity ratio, the mean absolute fluorescence intensity value of Cy5 (left spot in the picture) and fluorescence intensity pictures of the respective spot, scanned at 635 nm (Cy5, left) and at 532 nm (Cy3, right) are shown.

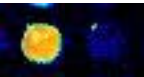
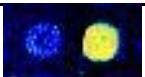
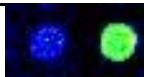

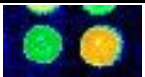

Lion ID	experiment 1 (dye swap)	experiment 2	experiment 3
MG-12-3e4	41,9 37742 	46,0 546 	49,0 572 
MG-12-3f11	16,3 64921 	14,0 3464 	16,8 3420 

Table 3.1.1 shows two candidate genes on the top of a list of genes, identified as differentially expressed. The complete list of the top 42 up-regulated and 43 down-regulated genes (ranked according to fold regulation VDRKO vs. WT) with annotations describing names and putative biological functions is given in tables 3.1.2 and 3.1.3 below. Although the method of data analysis and extraction is somewhat crude in comparison to other methods (see chapter 3.1.2 and 4), it can provide solid results, given that the quality of input data (the scanned images) is good, i.e. if there are no gradients in signal intensity or background fluorescence across the slide. This was proven with the validation of selected microarray results by quantitative real-time PCR (qPCR). The analysis results from qPCR and microarray studies in tables 3.1.2-3 will be discussed in section 3.2.

Results & Discussion: VDRKO mouse kidney

Table 3.1.2: Genes up-regulated in male ND VDRKO vs. WT mouse kidneys. The error of the mean from the three microarray experiments was calculated as the standard deviation, divided by the square root of the number of repeats (N=3).

Lion	Genbank	Function	Functional keywords	mean	error
MG-12-229d11	BC010711	n.a.	n.a.	69.87	33.94
MG-4-3p22	M63550	Immunoglobulin g1 (kappa light chain) fab' fragment	Immunoglobulin V region	46.27	27.99
MG-12-184j5	AK050078	2-Hydroxyphytanoyl-CoA lyase	lipid metabolism	6.67	0.67
MG-6-61p12	BM124941	Cell Death Activator CIDEA	apoptosis;	11.40	5.63
MG-8-46e22	AK075843	Apolipoprotein E precursor (Apo-E).	VLDL; Chylomicron; HDL; Lipid transport; Heparin-binding	14.83	10.33
MG-3-116f20	BC010711	erythropoietin regulated EST, clone ERG 8.2	n.a.	6.27	1.19
MG-12-171j2	AK034169	Pte2a-pending: Peroxisomal acyl-CoA thioesterase 2A	serine esterase; hydrolase;	4.73	0.53
MG-12-146c2	AK029029	Long Chain Fatty Acyl Elongase	ELOVL family member 6, elongation of long chain fatty acids	4.63	0.72
MG-14-3j13	AW209037	Ceruloplasmin precursor (ferrioxidase)	ferrioxidase, transport and binding proteins	4.77	0.68
MG-14-2c21	AY044241	Glutamine synthetase (EC 6.3.1.2) (Glutamate--ammonia ligase).	fatty acid and phospholipid metabolism	3.93	0.35
MG-4-5e2	U16818	UGT1	Glycosyltransferasel; Microsome; Transmembrane	3.80	0.21
MG-3-27f11	BF384201	Apolipoprotein E precursor (APO-E).	HDL; Plasma; Signal; Lipid transport	3.93	0.48
MG-6-21i12	AW411843	cAMP-dependent 3',5'-cyclic phosphodiesterase 4B (DPDE4).	cAMP; Hydrolase; Central intermediary metabolism	7.63	3.65
MG-8-14b1	NM_027219	Serum Protein MSE55	Rho GTPase binding 1 (Cdc42ep1)	4.23	0.71
MG-8-70n14	AK028008	Monoglyceride Lipase (Mgll)	lipid metabolism	4.53	0.84
MG-16-143m3	NM_025522	;Retinal short-chain dehydrogenase/reductase 4	dehydrogenase/reductase (SDR family)	3.63	0.48
MG-16-127o18	NM_010357	Gsta4; Glutathione S-transferase, alpha 4	fatty acid metabolism	4.00	0.74
MG-6-44m9	BE991974	Creatine Kinase, B chain (B-CK).	Kinase; Transferase;	3.77	0.57
MG-3-37o2	BI694083	Lysozyme C, 1,4-beta-N-acetylmuramidase C	Bacteriolytic enzyme; Glycosidase; Hydrolase; Signal;	2.97	0.27
MG-6-3e12	BM211923	Creatine Kinase, B chain (B-CK).	Kinase; Transferase;	2.93	0.23
MG-12-212p20	AK086805	Mrpl23;Mitochondrial ribosomal protein L23	n.a.	3.17	0.43
MG-12-252p13	NM_011817	growth arrest and DNA-damage-inducible 45 gamma (Gadd45g),	growth arrest and DNA-damage-inducible 45 gamma	2.63	0.08
MG-16-5g10	AF127033	Fatty acid Synthase	NADP; Phosphopantetheine; Transferase; fatty acid synthesis	3.27	0.47
MG-12-197n17	AK052746	Nphs2; Nephrosis 2 homolog, podocin (human)	Retaining proteins in glomerular filtration; slit diaphragms	3.23	0.39
MG-6-48g14	BI738553	pyruvate kinase, m2 isoenzyme	Glycolysis; Magnesium; Kinase; Class Energy metabolism	3.33	0.57
MG-6-49i5	AW491617	Lynx1 protein	GPI-anchor; T-cell; Antigen	2.47	0.11
MG-6-25b9	NM_023805	N system amino acids transporter NAT-1	Transmembrane; Hypothetical protein;	2.83	0.54
MG-12-255b22	NM_008182	Glutathione S-transferase GT41A (GSTA2)	lipid metabolism, ROS	2.53	0.15
MG-3-2m2	BF449796	lipocalcin-type prostaglandin-D-synthase	Lipocalin; Signal; Glycoprotein; (PGDS2, PGDS)	2.93	0.50
MG-12-169a2	AI426654	Bumetanide-sensitive sodium-(potassium)-chloride cotransport	Transport and binding proteins	2.63	0.29
MG-6-2a22	BI733315	pyridoxal pyridoxine vitamin B6 kinase	Pyridoxine kinase (EC 2.7.1.35) (Pyridoxal kinase).	2.63	0.29
MG-6-22h16	BC012400	3-ketoacyl-CoA thiolase A, acetyl-CoA acyltransferase A	Fatty acid and phospholipid metabolism	2.30	0.07
MG-12-247c4	AF020519	Aqp2;Aquaporin 2	Transport and binding proteins	2.33	0.11
MG-8-21b10	AI255996	annexin VI (lipocortin VI), chromobindin 20, calelectrin, calphobindin-II (CPB-II)	Repeat; Annexin; Calcium/phospholipid-binding;	2.57	0.33
MG-6-54h14	BM249584	ATP-citrate (pro-S)-lyase	Phosphorylation; Lipid synthesis; ATP-binding; Lyase	2.30	0.12
MG-15-277e23	AK009103	K0137A04-3 NIA Mouse Hematopoietic Stem Cell	Flavoprotein; Oxidoreductase; Carotenoid biosynthesis	2.50	0.21
MG-6-32g12	BB023497	GTP-RHO binding protein 1 (Rhopilin). GRBP	n.a.	2.57	0.32

Results & Discussion: VDRKO mouse kidney

MG-16-5p18	BB214612	cytochrome C oxidase COX VIIA-M, COX7A; COX7AH; COX7A1	Oxidoreductase; Mitochondrion; Energy metabolism	2.57	0.36
MG-4-4k2	NM_007388	Acp5: Acid phosphatase 5, tartrate resistant	osteoclast differentiation	2.50	0.25
MG-16-51o13	NM_010174	fatty acid binding protein 3, muscle and heart FABPH1; FABP3	FABPH1; FABP3	2.63	0.36
MG-6-56a1	BC013551	Down syndrome candidate region 1 (Dscr1), calcipressin 1, calcineurin inhibitor	calcium-mediated signalling	3.17	1.07
MG-3-40e12	BF165048	macrophage migration inhibitory factor (MIF), (DER6)	Cytokine; MIF; glycosilation inhibiting	2.07	0.04

Table 3.1.3: Genes down-regulated in male ND VDRKO vs. WT mouse kidneys.

Lion	Genbank	Name	Function	mean	error
MG-12-3e4	BC008996	cytochrome P450 4B1 (CYPIV1).	Oxidoreductase; Endoplasmic reticulum; Microsome; Heme	0.022	0.001
MG-12-3f11	AF136283	Vitamin D-dependent calcium-binding protein (calbindin D9K)	S100D; CALB3 Calcium-binding;	0.064	0.004
MG-6-43b23	BE862147	submandibular gland CRL-1734 SCA-9 clone 15	n.a.	0.078	0.019
MG-12-20411	A55281	carboxylesterase (EC 3.1.1.1)	Transport and binding proteins	0.121	0.006
MG-3-27116	BC005532	MNCb-1930 protein	Hydrolase;	0.121	0.012
MG-11-1e9	AA822938	transthyretin precursor (prealbumin)	Retinol-binding; Albumin; Vitamin A; Thyroid hormone; transport	0.118	0.025
MG-8-25c3	BM233324	Alpha-2-antiplasmin precursor/ inhibitor SERPINF2; PLI	Serine protease inhibitor; Serpin; Signal; Glycoprotein	0.123	0.016
MG-12-3o12	AI098151	aspartoacylase (aminoacylase, ACY-2)	Hydrolase	0.150	0.005
MG-12-140f13	NM_028048	SLC13A1; NAS1 Slc13a1;Solute carrier family	inner membrane; mitochondrion; energy production	0.139	0.026
MG-12-214a17	NM_153193	Hsd3β2; 3β-Hydroxysteroid dehydrogenase-2	androstenedione production, dihydrotestosterone metabolism	0.134	0.032
MG-12-286p16	NM_009470	Uromodulin precursor (Tamm-Horsfall urinary glycoprotein)	calcium-binding EGF-like domain	0.166	0.009
MG-12-133f3	AK048574	similar to h.s. protein phosphatase 1, regulatory (inhibitor) subunit	n.a.	0.163	0.016
MG-14-89d5	AK086788	Phf3: PHD finger protein 3	n.a.	0.209	0.007
MG-12-162d20	NM_010006	CYP2D-9; CYP2D9 Cytochrome P450 2D9	n.a.	0.184	0.024
MG-3-34k9	BM115102	metastasis-associated protein MTA1.	transcription factor, histone deacetylase	0.210	0.015
MG-3-16p4	BB746263	ornithine decarboxylase structural	ODC	0.237	0.010
MG-12-263n6	AW049778	Myocyte-specific enhancer factor 2D, Cml4	MEF2D protein, Cml4	0.251	0.013
MG-16-186g23	NM_009155	selenoprotein P plasma 1	selenium binding	0.281	0.007
MG-12-255i3	AB072395	topoisomerase I-binding RS protein (TOPORS)	expressed sequence AW105885	0.256	0.047
MG-8-33p4	BF018814	Serpina1d; serine/cysteine proteinase inhibitor, clade A, 1d	Hydrolase; Signal-anchor	0.294	0.005
MG-6-48k13	NM_133206	zinc ring finger protein 1, Rnf42, Zrfp1	alkyldihydroxyacetonephosphate synthase, peroxisomal precursor	0.279	0.022
MG-12-274i8	NP_084177	Akr1c21: aldo-keto reductase family 1, member C21	aldo-ketoreductase	0.287	0.013
MG-12-247j17	NM_023455.2	camello-like 4 Cml4	neg. regulation of cell adhesion; fatty acid & phospholipid metabolism	0.311	0.018
MG-16-3f6	BB698820	FK506 binding protein 5 (Fkbp5)	hormonal activation of the glucocorticoid receptor, chaperone	0.200	0.080
MG-12-219i14	BC024450	similar to:acetyl-Coenzyme A synthetase 3	hypertension-associated	0.317	0.015
MG-12-30d2	U52842	Slc22a6;Solute carrier family 22 member 6	kidney-specific transport protein	0.338	0.010
MG-6-3n18	BC009158	mitochondrial import inner membrane translocase subunit TIM9 B. fractured callus expressed transcript 1, Fxc1	Translocation;Mitochondrion; Transport; Protein transport	0.304	0.027
MG-73-7m21	Mm.44170	Vdr;Vitamin D receptor	transcription factor	0.282	0.038
MG-12-258e15	Mm.2409	Adh1;Alcohol dehydrogenase 1 (class I)	NAD; Oxidoreductase; Zinc;	0.345	0.007
MG-15-151d1	NM_008621	Mpp1;Membrane protein, palmitoylated	calmodulin-dependent; Scgf;Stem cell growth factor	0.312	0.023
MG-8-28d11	M75717	Serpina1e: serine /cysteine) proteinase inhibitor	Serine protease inhibitor; Serpin; Signal; Glycoprotein	0.329	0.021
MG-19-2c13	NM_009349	thioether S-methyltransferase (TEMT)	Methyltransferase; Transferase;	0.358	0.013
MG-3-77p17	AB078618	KIAA0707 protein (KIAA0707)	mCACH-1 mRNA for cytosolic acetyl-CoA hydrolase	0.359	0.021

Results & Discussion: VDRKO mouse kidney

MG-6-34b12	AK014649	D-lactate dehydrogenase, ferricytochrome c oxidoreductase (D-LCR)	Energy metabolism; Flavoprotein; FAD;	0.315	0.052
MG-12-278g10	NM_133732	PTD012 homolog	n.a.	0.387	0.022
MG-12-249l16	BC018252	Transport; Sodium transport; Symport; Glycoprotein	Na dependent-phosphate cotransporter	0.270	0.078
MG-12-134p11	NM_009203	Slc22a2;Solute carrier family 22 (organic cation transporter)-like 2	RST; Transport; Transmembrane; Glycoprotein	0.406	0.006
MG-12-152e20	U09418	Bile acid receptor (Farnesoid X-activated receptor)	Nr1h4;Nuclear receptor subfamily 1, group H, member 4	0.391	0.014
MG-3-140l14	BE634628	a-helical protein (HCR)	n.a.	0.376	0.042
MG-8-12h24	NM_008062	glucose-6-phosphate 1-dehydrogenase X (G6PD)	glucose metabolism	0.361	0.046
MG-12-194m5	AK047211	hypothetical gene supported by AK047211	Nr1h4: nuclear receptor subfamily 1, group H, member 4	0.344	0.091
MG-3-37f4	BC004801	isopentyl-diphosphate isomerase (IPP isomerase)	Isomerase; Isoprene biosynthesis;	0.300	0.079
MG-12-1i13	BM069222	selenoprotein X 1 (selenoprotein R)	n.a.	0.390	0.033

3.1.2 Gender and diet specific influences on gene expression

Gene expression profiling of ND VDRKO and WT mouse kidney in the previous chapter confirmed studies from other authors (Li et al. 2003) and extended the list of new genes that are directly or indirectly regulated by VDR. The impact of PTH, calcium, phosphate and sex steroids on vitamin D signalling increases the number of genes that are potentially differentially expressed in VDRKO mice and diffuse direct and indirect effects of VDR action.

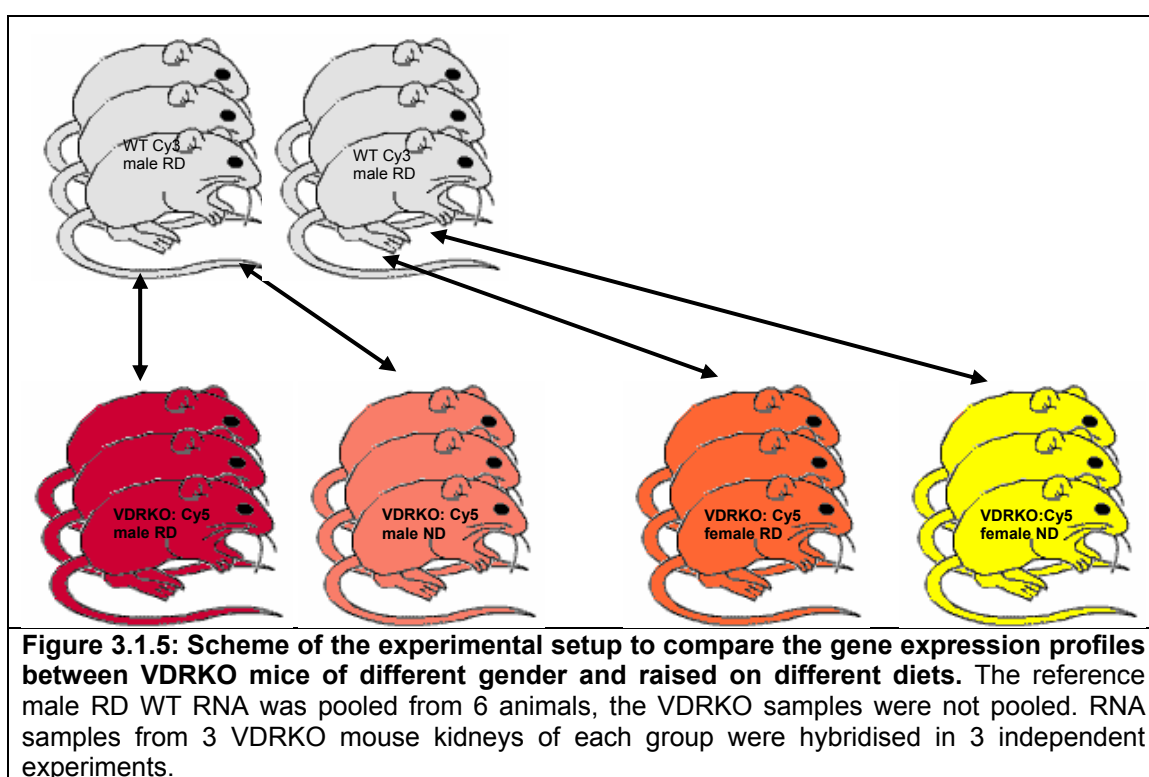
To clarify this bewildering picture of competing influences on transcription, an additional set of microarray experiments was designed, including mice raised on a diet enriched in calcium and phosphate (rescue diet, RD). RD that was shown to normalise serum calcium and PTH levels and to rescue many of the features of the VDRKO phenotype (Li et al. 1998a; Erben et al. 2002). As sex steroids were shown to have partially overlapping functions with vitamin D and since they might contribute to the modulation of gene expression profiles, both male and female animals were analysed separately in the following expression study. In chapter 3.1.2.1, the experimental design and different strategies of data analysis are discussed and results presented in tables. In chapter 3.2 these data, together with gene expression data from ND mouse kidney presented in the previous section, were grouped according to physiological function, compared with results from confirmation experiments by qPCR and discussed in more detail in the context of data from literature.

3.1.2.1 Experimental Design

Like in the experiments with mice raised on normal diet, in this study the in-house produced 21K mouse cDNA array was used for direct comparison between two conditions. In the following experimental setup, three parameters (sex, diet, genotype) were included, defining $2^3 = 8$ conditions (e.g. male, rescue diet, VDRKO). An approach to compare all these different conditions with each other is to use a common reference RNA.

The use of a common reference RNA implies several problems: In the case of no expression of a gene in the reference RNA the signal ratio becomes infinity. High expression levels lead to saturation effects during hybridisation and scanning. Therefore, the reference RNA should contain all transcript species expressed in the

samples in the medium concentration range. Indirect comparisons of samples via a common reference require more hybridisations as direct comparisons to obtain the same amount of information. In the case of bad technical reproducibility experiments with of microarrays from different batches (like in this case self-spotted cDNA arrays) and restrictions on sample material and budget this can be a problem. A compromise between the direct comparison and the reference RNA setup was the strategy to profit from both approaches: Pooled kidney RNA from 6 age-matched male WT mice raised on rescue diet (RD) was chosen as reference. Against this common reference, kidney RNA samples from 4 groups of age-matched VDRKO mice, each consisting of 3 individuals, were hybridised. Within these groups, RNA from VDRKO animals was not pooled, but hybridised in separate experiments to acquire information about the variation between individual animals. This approach allows a direct comparison of gene expression between RD male VDRKO vs. WT mouse kidney and gives information about the influence of sex and diet on transcriptional regulation by the vitamin D receptor.



For complex experimental set-ups, where multiple, interrelated sample subclasses are to be expected, clustering algorithms can help to elucidate an inner structure of expression matrices and group the genes (or experiments) according to function (pathways, conditions, etc.).

The twelve gene expression profiling experiments with VDRKO kidneys from 12 animals and one control experiment were performed on one day to provide equal hybridisation and washing conditions. Like in previous gene expression studies, a test hybridisation with male RD WT RNA, hybridised against itself was performed to check the array quality. All arrays in this study were printed in one batch. cDNA from VDRKO and WT kidneys were labelled indirectly with Cy3 or Cy5, respectively (protocol see methods). The labelled reference cDNA was mixed and aliquoted to exclude differences due to varying labeling efficiencies or irregular sample recoveries

after purification. In the table below the experiments and the nature of VDRKO kidney samples are listed:

Table 3.1.4: Nature of the mouse kidneys used in the experiments series analysed below. The number 268 represents the microarray batch number, experiment 268_1 was a confirmation experiment, where the reference RNA was hybridised against itself. In all experiments, RNA from VDRKO mouse kidney was labelled with cyanine 5, the pooled reference RNA from WT mouse kidney with cyanine 3.		
experiment number	sex	diet
268_1 MDS control	male	rescue diet
268_2 MDS - 268_4 MDS	female	normal diet
268_5 MDS - 268_7 MDS	male	rescue diet
268_8 MDS - 268_10 MDS	female	rescue diet
268_11 MDS - 268_13 MDS	male	normal diet

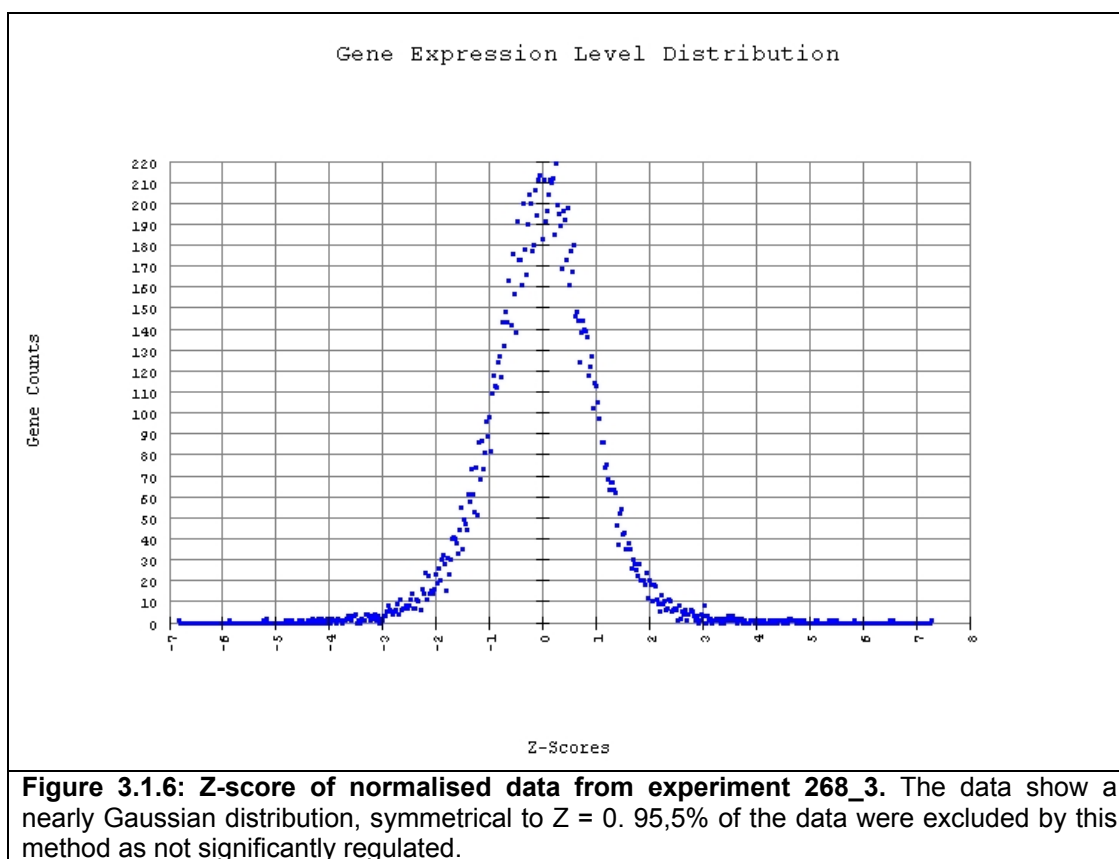
3.1.2.2 Data processing of single experiments

The raw data were acquired and quality-controlled using the GenPix software package. Exported .gpr data files were converted into .mev text files using the GenPix converter and imported into MIDAS (see methods). All 13 data sets were then treated independently, using the same MIDAS procedure:

1. Trimming of signals below 10.000 units
2. Blockwise LOWESS normalisation, employing a smoothing parameter of 0,33.
3. Selecting values that indicate differential expression: Using a sliding window algorithm, genes of a subpopulation of 500 that are less regulated than two standard deviations of log(ratio intensity) values were flagged and excluded from later analysis.

After filtering out data from spots with irregular morphologies (e.g. artefacts from dust particles, scratches), values in the very low intensity range were excluded. The remaining data were then normalised to compensate for differences in the amounts of starting RNA, labeling efficiencies, sample recovery after purification, or in the detection of fluorescence intensity signals. Instead of selecting genes according to their rank in the relative fold change, as in chapter 3.1.1, an intensity-dependent Z-score value was calculated for each gene. Genes were selected if the Z-score for differential expression exceeded the local standard deviation of a data population around the respective data point. In the series of experiments with VDRKO mouse kidney a Z-score threshold of 2 was chosen, which means that selected genes are differentially expressed with 95,5% confidence. Taking all filtering steps together, the number of datapoints (genes) in this experiment series was reduced from 21168 to 175.

Figure 3.1.6 shows a typical example of the Z-score distribution of normalised data from a hybridisation of kidney RNA from a female ND VDRKO mouse against the common reference:



3.1.2.3 Different approaches of gene clustering reveal gender-specific effects

Filtered data from all experiments were loaded into the Multi Experiment Viewer (MEV, see methods). In MEV data from multiple experiments can be loaded and gene expression ratios of all genes and experiments translated into a colour code and represented in a gene expression matrix. Genes or experiments can be represented as vectors in a multidimensional space, and clustered in groups according to these distances. Since this requires considerable computer memory resources and calculation time, it is necessary to extract significantly regulated genes before and thus reduce the amount of data input. The expression matrix of twelve experiments was first analysed for outliers, experiments that differed significantly in the distribution of gene expression from the other experiments in the respective group. The scanned microarray images of these experiments showed an inhomogeneous fluorescent background. These experiments were excluded from further analysis.

3.1.2.3.1 Hierarchical clustering

Hierarchical clustering of VDRKO mouse kidney experiments show that the experiments cluster according to sex and diet of the animals. The influence of gender on the gene expression profile outweighs diet and other parameters. Like previous gene expression profiling experiments with VDRKO mouse kidney (Li et al. 2003) this series shows that more genes are down-regulated by VDR ablation than activated.

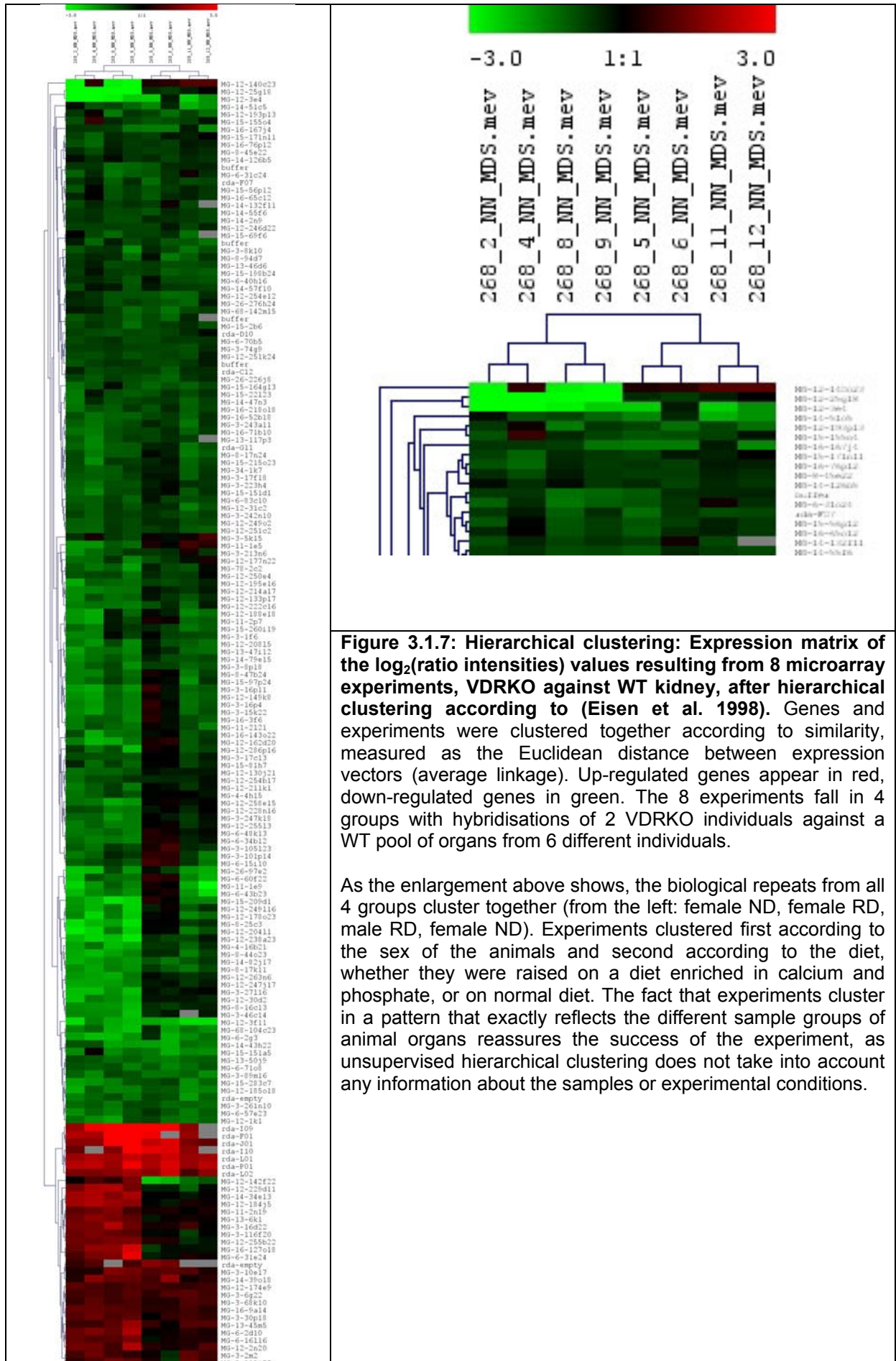


Figure 3.1.7: Hierarchical clustering: Expression matrix of the $\log_2(\text{ratio intensities})$ values resulting from 8 microarray experiments, VDRKO against WT kidney, after hierarchical clustering according to (Eisen et al. 1998). Genes and experiments were clustered together according to similarity, measured as the Euclidean distance between expression vectors (average linkage). Up-regulated genes appear in red, down-regulated genes in green. The 8 experiments fall in 4 groups with hybridisations of 2 VDRKO individuals against a WT pool of organs from 6 different individuals.

As the enlargement above shows, the biological repeats from all 4 groups cluster together (from the left: female ND, female RD, male RD, female ND). Experiments clustered first according to the sex of the animals and second according to the diet, whether they were raised on a diet enriched in calcium and phosphate, or on normal diet. The fact that experiments cluster in a pattern that exactly reflects the different sample groups of animal organs reassures the success of the experiment, as unsupervised hierarchical clustering does not take into account any information about the samples or experimental conditions.

Subdividing the expression matrix of differentially expressed genes into groups with common regulation is a valuable help to interpret gene function in the biological context.

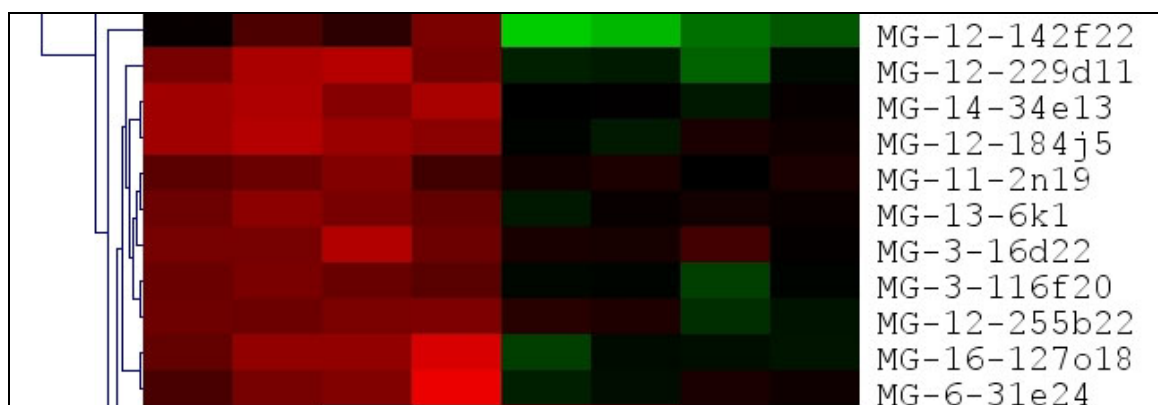


Figure 3.1.8: Fraction of the matrix after hierarchical clustering, showing genes that were differentially regulated according to phenotype and sex of the mice. This group of candidate genes was up-regulated only in female VDRKO mouse kidney, whereas in male VDRKO kidney, the genes were either equally expressed or down-regulated, as in the candidate gene ID MG-12-142f22 (CYP4 α 14), on the top.

Figure 3.1.8 shows a group of gene candidates, differentially expressed between VDRKO and WT and between male and female mice, irrespective of the diet. Strongly up-regulated in females and down-regulated in male VDRKO kidney was clone ID MG-12-142f22, containing a 3' fragment of the mRNA of mouse CYP4 α 14. The identity of the genes represented in the expression matrix in figure 3.1.8 above is shown in table 3.1.5 below:

Table 3.1.5: Annotations of the candidate genes from figure 3.1.8: Genes up-regulated in VDRKO kidney from female mice, relative to male WT.			
Lion ID	Genbank ID	gene name	abbreviation
MG-12-142f22	NM_007822	cytochrome P450 family 4 subfamily a polypeptide 14	CYP4 α 14
MG-12-229d11	n.a.	n.a.	n.a.
MG-14-34e13	NM_007620	Cbr1: carbonyl reductase 1	Cbr1
MG-12-184j5	NM_019975	2-hydroxyphytanoyl-CoA lyase	Hpcl
MG-11-2n19	NM_008340	insulin-like growth factor binding p., acid labile subunit	Igfals, ALS
MG-13-6k1	NM_007599	capping protein (actin filament), gelsolin-like	Capg
MG-3-16d22	XM_358306	ATP-binding cassette, sub-family C (CFTR/MRP), 3	Abcc3, Mrp3
MG-3-116f20	X82564	n.a.	n.a.
MG-12-255b22	NM_008182	glutathione S-transferase, alpha 2 (Yc2)	Gsta2
MG-16-127o18	NM_010357	glutathione S-transferase, alpha 4	Gsta4
MG-6-31e24	NM_010357	glutathione S-transferase, alpha 4	Gsta4

Above a table of candidate genes that were up-regulated only in female VDRKO mouse kidney. Gsta4 appears twice, as it is represented on the chip by two distinct cDNA fragments. Glutathione-S-transferases, in their majority localized in the cytosol and in mitochondria, have an important role in cellular protection against chemical and oxidative stress (Robin et al. 2003). Endogenous oxidative stress is caused by the production of reactive oxidative species (Del Arco et al.), by-products of lipid peroxidation or steroid hormone synthesis and metabolism (Rapoport et al. 1995). Gsta2 was found expressed in steroidogenic organs, like bovine and human kidney,

especially in the epithelial cells of proximal convoluted tubules and the thick descending loop of Henle, the loci of vitamin D synthesis (Rabahi et al. 1999).

CYP4 α 14, a member of the closely related CYP4 α and CYP4b families (Heng et al. 1997), was slightly up-regulated in female VDRKO mouse kidney, whereas it was found to be down-regulated in male VDRKO mouse kidney, like CYP4 β 1, which will be discussed later in chapter 3.2. Both, CYP4 α and CYP4b enzyme families are involved in fatty acid metabolism. CYP4 α proteins, which can be induced by peroxisomal proliferators, are mainly expressed in kidney. They mediate the oxidation of arachidonic acid to 20- and 19-hydroxyeicosatetraenoic acid (20- and 19-HETE). Eicosanoids are implicated in the regulation of renal salt excretion and vascular tone (Muller et al. 2004). In VDRKO mice, both electrolyte homeostasis (Erben et al. 2002) and vascular tone (Li 2003) were found to be heavily impaired. The creation of a transgenic mouse lacking CYP4 α 14 expression, however, has shown that in spite of the high degree of homology to 20-HETE-producing rat CYP4A2, not murine CYP4A14 but its homologue CYP4A12 is responsible for the synthesis of 20-HETE. In a gender-dependent manner, CYP4 α 14 (-/-) mice suffer from hypertension (Holla et al. 2001). CYP4 α 14 (-/-) mice exhibit elevated plasma levels of androgens, which increases expression of CYP4 α 12 and thus enhances the biosynthesis of of prohypertensive 20-HETE (Holla et al. 2001; Skott 2003). The prohypertensive effect of CYP4 α 14 ablation appears only in male mice and was not found in castrated or in female CYP4 α 14 (-/-) mice, indicating that CYP4 α 14 might be a factor involved in gender differences in the regulation of blood pressure, as observed in rodents and humans (Reckelhoff 2001).

Down-regulation of CYP4A14 in male VDRKO RD mouse kidney (microarray experiments: (0.32 +/- 0.12)-fold, qPCR: (0.67 +/- 0.05)-fold) might contribute to the development of hypertension in these animals, like a number of other factors, pointed out in section 3.2. In female RD mice, however, CYP4 α 14 was found (2.10 +/- 0.64)-fold up-regulated, as well as in kidneys from male ND VDRKO mice ((1.64 +/- 0.19)-fold), pointing at a complex regulation of CYP4 α 14 expression by vitamin D, androgens and calcium.

Gelsolin-like macrophage-capping protein (Capg), also up-regulated in female VDRKO mouse kidney, is a member of the gelsolin-like protein family which remodel actin fibers by uncapping the barbed ends (Bubb et al. 2003). Recently, Capg was ascribed protective effects in vascular endothelial cells experiencing hemodynamic shear stress and might help to avoid the development of atherosclerotic lesions (Pellieux et al. 2003). Proteins of the gelsolin-like family cooperate with vitamin D-binding protein (DBP) that was also found to be up-regulated in both VDRKO mouse kidney and heart, see discussion later in chapter 3.2 and 4. Both proteins form the so-called actin-scavenger system, responsible for rapid depolymerization and clearance of actin fibers from the bloodstream (Otterbein et al. 2002).

3.1.2.3.2 Significance analysis of microarray data (SAM)

As the expression of significant number of genes, differentially regulated in VDRKO mouse kidney appears to be sex-dependent, supervised methods of class-specific clustering as SAM can be used to differentiate between VDRKO expression profiles of male and female mouse kidneys.

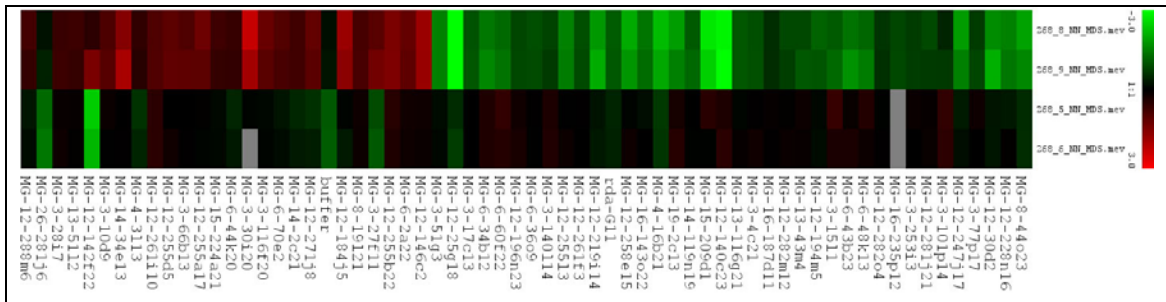


Figure 3.1.9: Data analysis by SAM: Significant candidate genes with differential expression between female (first two experiments from above) and male VDRKO kidneys (below), both hybridised against pooled RD male WT kidney cDNA. As usual, red means up-regulation, green down-regulation of the respective gene. The genes were selected and clustered according to SAM, with the most significant genes (highest delta values, lowest false discovery rate FDR) in the middle.

In Figure 3.1.9 and 3.1.10 the results from the analysis of two experiments with kidneys from VDRKO male and two from VDRKO female mice (all RD) were clustered according to gender-specific expression by SAM (see also section 4). The list of candidate genes, differentially expressed according to genotype and gender, contains most of the genes identified by hierarchical clustering, together with additional genes only down-regulated in female VDRKO mouse kidneys, compared to WT. The delta table in figure 3.1.10 below shows how clearly gene expression of a group of genes is influenced by gender.

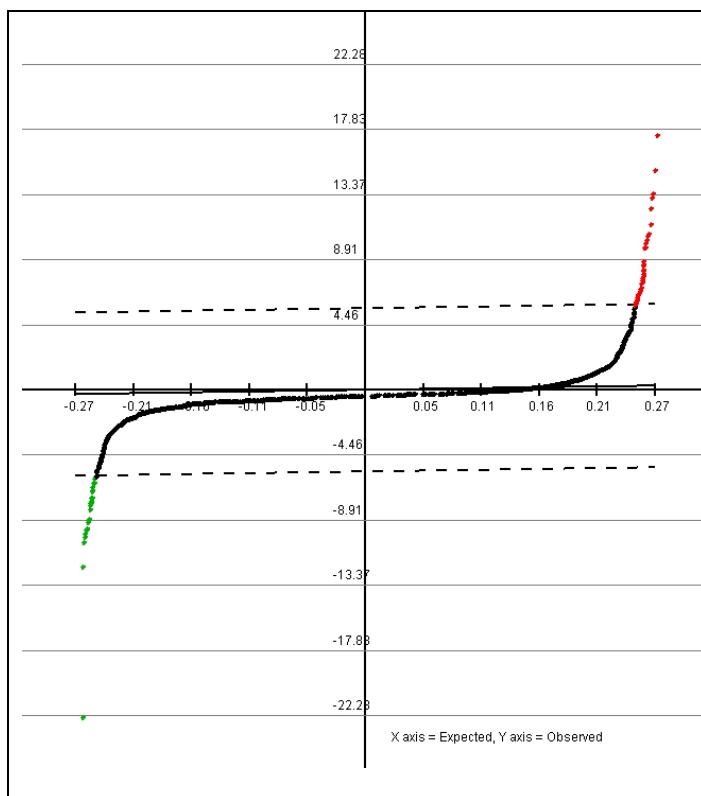


Figure 3.1.10 SAM Delta plot: Subclassification of genes, differentially expressed genes in VDRKO (against WT) mouse kidney according to the sex of animals by SAM (all raised on rescue diet which normalises blood calcium levels). Even when choosing a very stringent delta threshold of 5.57, still 64 candidate genes were identified, 38 of them with a positive (down-regulated in female vs. male VDRKO), 26 with a negative delta score.

A large set of genes was found to be involved in fatty acid metabolism, energy supply and blood pressure, which is known to be dependent on serum and intracellular calcium content, as well as on sex hormones. Since genes regulating lipid synthesis and lipid catabolism are involved, there seems to be a general activation of lipid turnover in VDRKO mice. This observation is in accordance with the fact that both male and female VDRKO mice showed a significantly decreased growth in body mass after weaning (Erben et al. 2002).

Among the genes down-regulated specifically in kidneys of female VDRKO mice was CYP7b1, involved in cholesterol metabolism, Acyl-CoA synthase, regulating lipid metabolism, or Zn-alpha2 glycoprotein-1 α (Azgp1), reported to be a candidate gene for the regulation of body weight (Gohda et al. 2003). CYP7B1 also has a key function in the catabolism of 5 α -androstane-3 β ,17 β -diol, which, by binding to the estrogen receptor β (ER β), can suppress the expression of the androgen receptor (AR) and androgen-controlled growth processes (Weihua et al. 2002). In kidneys from male VDRKO mice, CYP7b1 was found up-regulated in both qPCR and microarray experiments, which might indicate a dependence of CYP7B1 expression on serum androgen levels (see also figure 3.2.9). Up-regulated in kidneys from female VDRKO mice were Apolipoprotein E (ApoE) or growth arrest-specific protein 1 (Gas-1), the latter involved in cell cycle control and apoptosis (Evdokiou and Cowled 1998).

As gene regulation is of enormous complexity, the influence of secondary effects had to be minimised to find out genes that are directly dependent on VDR action. The short duration of the estrous cycle in mice might be an important factor that can influence the gene expression profiles between female individuals. For this reason data interpretation in part 3.2 will focus on expression profiles of kidneys of male, age-matched animals, all raised on a diet that rescues the otherwise decreased blood calcium concentration and normalises systemic PTH levels.

Although hierarchical clustering is a useful means to visualize data structure and quality, the large number of genes in comparison to the small number of experiments makes it often difficult to analyse dendrogram structure and the co-regulation of related genes in detail.

3.1.3 Genes, differentially expressed in kidneys of male RD mice: VDRKO compared to WT

Another way of ordering genes according to their expression pattern is K-means clustering (see methods), where genes are iteratively distributed over a given number of clusters. This method of subdividing candidate genes into groups is especially valuable when there is an *a priori* hypothesis about the number of conditions (Soukas et al. 2000), as here with animal groups with different diets and gender. More rigid methods, as T-test grouping or SAM are valuable to differentiate between sample groups with large differences, (VDRKO - WT, colour flip experiments, see expression profiling with VDRKO heart, chapter 4), but failed in the case of more subtle differences, as were found between animals of the same genotype, age and sex but raised on different diets. In the following, candidate genes identified as differentially expressed in kidneys of normocalcemic, male VDRKO mice with respect to kidneys

from WT mice and were grouped together by K-means clustering of 3 microarray experiments with RNA extracted from organs of three individuals.

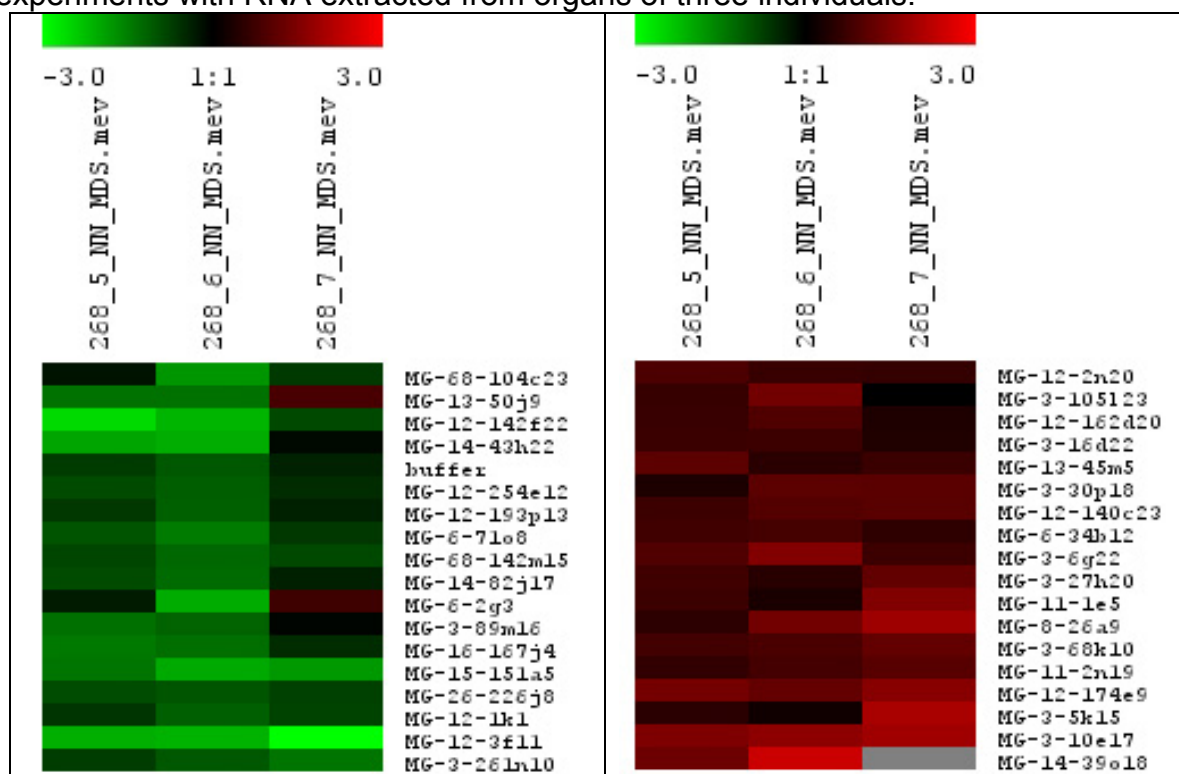


Figure 3.1.11: Strongly down-(left) and up-regulated (right) genes in microarray experiments with male VDRKO mouse kidney VDRKO against WT, clustered by K-means clustering. The RNA from 3 male age-matched animals, raised on rescue diet (RD) was hybridised against pooled male RD WT kidney RNA from 6 individuals. As in previous experiments with female mice and mice raised on normal diet, the number of down-regulated genes exceeded the number of up-regulated genes. Down-regulated genes were split into two clusters (the second cluster with smaller fold change values is not shown here). Since experiment 268_7 differed significantly from the other two experiments, it was not included into the evaluation of the mean fold change values of gene expression shown in tables 3.1.6-7 below.

Table 3.1.6: Genes up-regulated in VDRKO vs. WT kidney of male mice raised on a diet rich in calcium and phosphate. The mean fold expression values are average ratios VDRKO / WT in three experiments with kidney RNA from 3 different animals.

mean fold expression	error	Genbank ID	abbreviation	name
3.88	1.17	NM_009463	UCP1	uncoupling protein 1
3.27	0.26	NM_178373	Fsp27	fat specific gene 27
2.66	0.22	BC014692	Cpn1	carboxypeptidase N, polypeptide 1
2.56	0.64	NM_007606	Car-3	carbonic anhydrase 3
2.21	0.92	NM_008574	Mcsp	mitochondrial capsule selenoprotein
2.17	0.38	NM_007751	Cox8b	cytochrome c oxidase, subunit VIIIb
1.96	0.16	AF159298	Pde1a	phosphodiesterase 1A, calmodulin-dependent
1.93	0.49	NM_146057	Dap	death-associated protein
1.92	0.13	NM_007825	CYP7b1	Cytochrome P450, 7b1.
1.85	0.29	NM_009171	Shmt1	serine hydroxymethyl transferase 1 (soluble)
1.79	0.16	NM_008340	ALS; ALBS; IGFALS	insulin-like growth factor binding protein acid labile subunit
1.74	0.21	NM_000583	Snrpb, Cc, VDB	small nuclear ribonucleoprotein B, group specific component
1.73	0.46	NM_177304	Enpp6	ectonucleotide pyrophosphatase/phosphodiesterase 6
1.68	0.10	NT_039308	Gc, DBP	Gc group specific component
1.66	0.09	NM_027570	Ldhd	Ldhd lactate dehydrogenase D
1.62	0.19	NM_010006	CYP2d9	Cytochrome P450, 2d9.
1.54	0.11	BC048825	Abcc3	ATP-binding cassette, sub-family C (CFTR/MRP), member 3

Table 3.1.7: Genes down-regulated in male VDRKO vs. WT kidney of mice raised on a diet rich in calcium and phosphate. The mean fold expression values are average ratios VDRKO / WT in three experiments with kidney RNA from 3 different animals.

mean fold expression	error	Genbank ID	abbreviation	name
0.19	0.04	AF136283	Calb3	calbindin 3, (vitamin D-dependent calcium binding protein)
0.25	0.01	BC003205	Cyr61	cysteine rich protein 61
0.30	0.04	BC004770	Nr4a1	nuclear receptor subfamily 4, group A, member 1
0.32	0.12	NM_007822	CYP4 α 14	CYP4 α 14
0.39	0.00	AV318245	Cyr61	cysteine rich protein 61
0.49	0.10	NM_010591	AP-1, Junc, c-jun	Jun: Jun oncogene
0.49	0.07	AW049671	Leng8-pending	mCG118268 leukocyte receptor cluster (LRC) member 8
0.50	0.08	AV298856	dtr	diphtheria toxin receptor
0.51	0.04	NM_008597	Mglap	matrix gamma-carboxyglutamate (gla) protein
0.52	0.23	BC054782	Hspa1a /HSP70A1	heat shock protein 1A
0.54	0.03	NM_133808	Hdlbp	high density lipoprotein (HDL) binding protein
0.56	0.06	BC014696	Cml3	camello-like 3
0.57	0.07	NM_139065	n.a.	similar to APOBEC-1 stimulating protein [Homo sapiens]
0.57	0.10	NM_008509	Lpl	Lpl: lipoprotein lipase
0.58	0.01	NM_175403	n.a.	n.a.
0.59	0.16	BC059826	ODC	ornithine decarboxylase
0.60	0.16	NM_009895	Cish; Cis, F17, F23	cytokine inducible SH2-containing protein
0.60	0.18	NM_145443	n.a.	cDNA sequence BC016226
0.61	0.09	NM_026268	Dusp6	dual specificity phosphatase 6
0.61	0.25	BC008996	CYP4 β 1	cytochrome P450, family 4, subfamily b, polypeptide 1
0.62	0.09	NM_011066	Per2	period homolog 2
0.62	0.03	NM_009637	Aebp2	Aebp2: AE binding protein 2
0.63	0.06	NM_145942	Hmgcs1	Hmgcs1: 3-hydroxy-3-methylglutaryl-Coenzyme A synthase 1
0.63	0.12	NM_007788	Csnk2a1	casein kinase II, alpha 1 polypeptide
0.64	0.06	NM_009114	S100A9/MRP14	S100 calcium binding protein A9 (calgranulin B)
0.65	0.11	NM_026455	n.a.	Similar to AP47 protein - mouse
0.66	0.11	NM_145932	Osta; OSTalpha	organic solute transporter alpha
0.67	0.05	AK005531		similar to male sterility protein 2-like
0.68	0.11	NM_146067	Slco3a1, Anr1; Slc21	solute carrier organic anion transporter family, 3a1 (Slc21a11)
0.68	0.07	NM_178684	PMP3, PRP3	proline-rich protein MP-3
0.70	0.01	NM_015804	Atp11a	ATPase, class VI, type 11A
0.71	0.09	NM_019778	Oda8, Zfp288	zinc finger protein 288
0.71	0.04	NM_025278	Gng12	Gng12: guanine nucleotide binding protein (G protein), gamma 12
0.71	0.06	NM_145942	Hmgcs1	Hmgcs1: 3-hydroxy-3-methylglutaryl-Coenzyme A synthase 1
0.71	0.13	NM_175417	NaGLT1	androgen-dependent expressed protein; NaGLT1
0.71	0.05	NM_009621	Adamts1	disintegrin-like metalloprotease (reprolysin type) with thrombospondin type 1 motif, 1
0.72	0.07	AK018780	n.a.	n.a.
0.72	0.12	NM_011756	Ttp, Gos24,, Zfp-36	zinc finger protein 36, tristetraprolin (TISII, Nup475, TIS11D)
0.72	0.04	AK037717	n.a.	major histocompatibility complex region containing the Q region of class I.
0.73	0.02	NM_023908	A2D, A2LG, A2RP	A2lp: ataxin 2 related protein
0.73	0.05	NM_178607	Rnf24	Rnf24: ring finger protein 24
0.74	0.16	NM_025435	Ngg1 interacting	homolog to: homo sapiens Ngg1 interacting factor 3 like 1 binding protein 1.
0.74	0.10	NM_013749	Tnfrsf12a, Fn14, HPIP, TweakR	tumor necrosis factor receptor superfamily, member 12a
0.74	0.09	NM_023792	Pank, Pank1a, Pank1b	Pank1: pantothenate kinase 1
0.75	0.08	NM_172404	Ccbl1	cysteine conjugate-beta lyase
0.76	0.11	NM_146067	n.a.	n.a.

Results & Discussion: VDRKO mouse kidney

0.76	0.03	NM_030113	Arhgap10	Rho GTPase activating protein 10
0.76	0.06	NM_029166	n.a.	n.a.
0.77	0.08	NM_144916	TM6P1	fasting-inducible integral membrane protein TM6P1
0.77	0.07	NM_027992	n.a.	n.a.
0.78	0.12	NM_023799	Mgea5	meningioma expressed antigen 5 (hyaluronidase)
0.78	0.05	NM_021534	Pxmp4, Pmp24	peroxisomal membrane protein 4
0.78	0.17	NM_007570	Btg2, Pc3, TIS21	Btg2: B-cell translocation gene 2, anti-proliferative
0.79	0.11	NM_013650	S100A8	S100 calcium binding protein A8 (calgranulin A)
0.79	0.03	NM_015804	Atp11a	ATPase, class VI, type 11A
0.79	0.08	NM_026170	n.a.	n.a.
0.79	0.09	NM_015763	Lipin1	Lpin1: lipin 1
0.81	0.13	NM_181277	Col14a1	procollagen, type XIV, alpha 1
0.82	0.12	NM_008529	Ly6e	lymphocyte antigen 6 complex, locus E
0.82	0.04	NM_177093	Gp1ba	similar to:glycoprotein 1b, alpha
0.83	0.21	NT_039590	Hmgcr	Hmgcr: 3-hydroxy-3-methylglutaryl-Coenzyme A reductase
0.83	0.12	NM_019490	Vdp	vesicle docking protein
0.84	0.17	NM_010633	Kist, Kis	Kist: Kinase interacting with leukemia-associated gene (stathmin)
0.84	0.07	NM_015762	Txnrd1, TR, TR1, Tgr	thioredoxin reductase 1
0.84	0.13	NM_010492	ICA69	islet cell autoantigen 1
0.85	0.10	NM_178577	V-SERA 1	n.a.
0.85	0.04	NM_007700	IKK1, Chuk1, IKK[a]	Chuk: conserved helix-loop-helix ubiquitous kinase

Candidate genes listed above were identified as differentially expressed in kidneys from normocalcemic animals. With a diet enriched in calcium, phosphate and lactose (rescue diet, RD), serum calcium levels were increased to normal values, cancelling out the losses through impaired renal calcium re-absorption with increased intestinal calcium uptake. A number of secondary effects of hypocalcemia altering gene expression, like elevated serum concentrations of PTH were excluded by dietary means, resulting in increased body weight and bone mineralization. Other physiological features of the VDRKO phenotype, like alopecia, hypertension or impaired growth plate formation remained and are reflected on transcriptome level in the lists of genes differentially expressed in tables 3.1.6-7 above (Erben et al. 2002).

3.2 Validation by quantitative PCR and interpretation

Gene expression analysis helped to identify substantial numbers of candidate genes for VDR-mediated differential expression of either unknown function, with functional annotations from studies in a different biological context and others that were previously identified as being involved in vitamin D-dependent biological processes and metabolic pathways. Although the latter group of known VDR-dependent genes among the candidate genes lists is well represented (Li et al. 2003) and confirms the validity of the gene expression studies in this project, it was decided to confirm gene expression data of selected genes experimentally with an independent method based on a different principle of analysis. Like in a number of recently published gene expression studies with microarrays (Hofmann et al. 2002; Zou et al. 2002; Madsen et al. 2004), sensitivity, accuracy, throughput capacity and relatively moderate costs were the criteria that made quantitative real-time PCR (qPCR) the method of choice. In the following, some of the candidate genes resulting from microarray experiments described in section 3.1 were grouped according to their putative function and selected members of these groups were validated by qPCR. In expression studies of VDRKO / WT mouse kidney with qPCR the sample cDNA was generally transcribed

from pooled total RNA of kidneys from 5 animals of each genotype (VDRKO and WT) and diet (normal diet, ND and calcium /phosphate-enriched diet RD). Confirmation experiments with qPCR were made with samples from other animals than those used for microarray experiments, which gives the data additional validity.

3.2.1 Genes involved in ion transport and calcium homeostasis

The regulation of genes involved in calcium and phosphate homeostasis in kidney and intestine is a prominent and well described function of VDR action. It is therefore not surprising that a large percentage of the genes that were identified as differentially expressed in VDRKO kidney can be related to the intestinal absorption, renal reabsorption, transport and signalling of calcium, phosphate and other ions. As calcium and PTH have in many cases antagonistic or synergistic effects on VDR-controlled gene expression, changes in the expression profiles between mice raised on different diets are of special interest (see introduction).

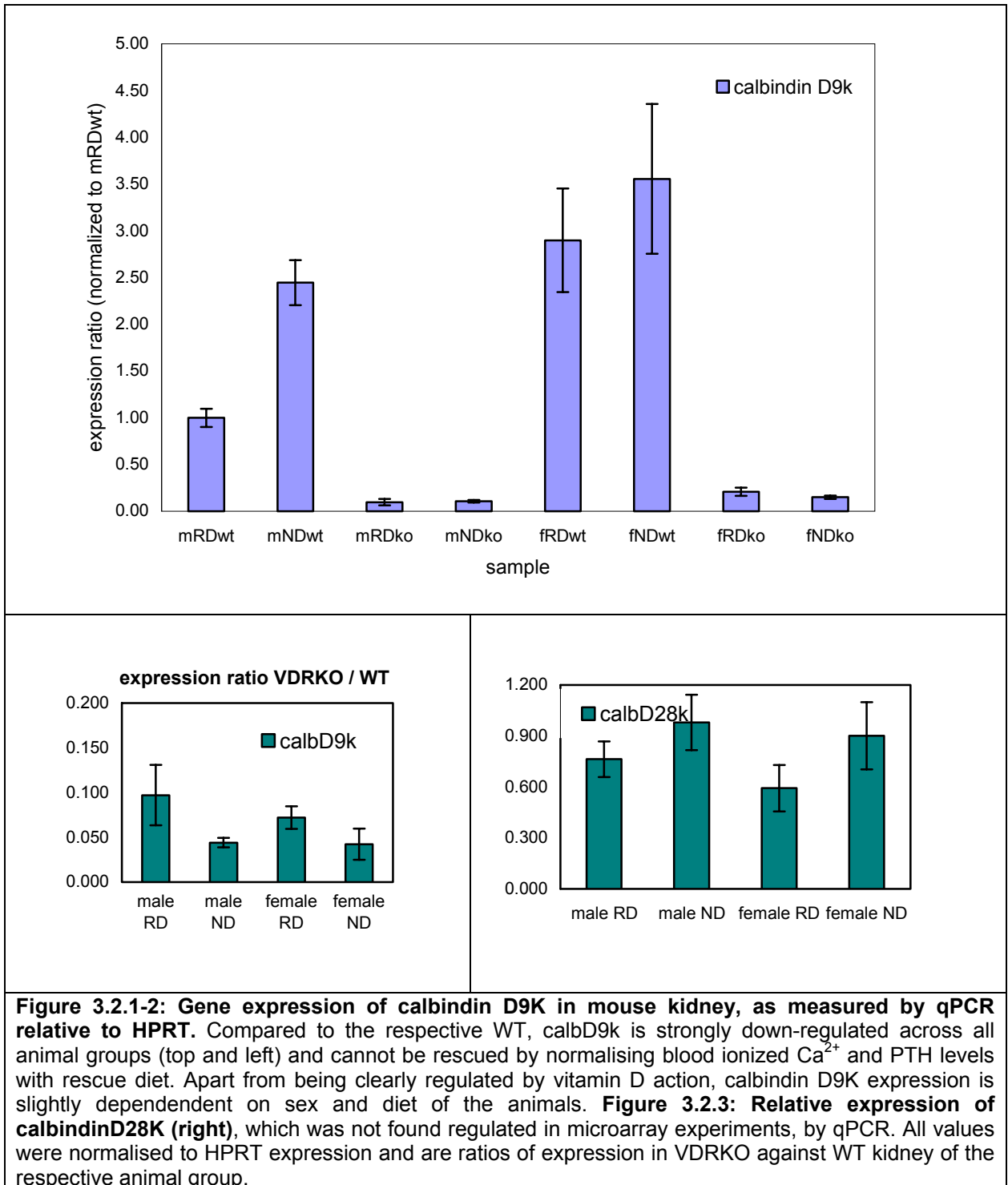
Table 3.2.1: Differentially expressed genes in male VDRKO vs. WT mouse kidney that have functions in electrolyte homeostasis. On the top, results from experiments with organs from mice raised on rescue diet (RD), below results from normal diet (ND) mice.

array RD	error	Lion ID	Genbank ID	name	function
0.194	0.041	MG-12-3f11	AF136283	Vitamin D-dependent calcium-binding (calbindin D9K)	intracellular calcium buffer, transport
0.513	0.043	MG-68-142m15	NM_008597	matrix gamma-carboxyglutamate (gla) protein	calcium ion binding; role in vascular calcification
0.665	0.114	MG-12-185o18	NM_145932	organic solute transporter alpha	steroid transport
array ND	error	Lion ID	Genbank ID	name	function
0.064	0.004	MG-12-3f11	AF136283	Vitamin D-dependent calcium-binding (calbindin D9K)	intracellular calcium buffer, transport
0.139	0.026	MG-12-140f13	NM_028048	SLC13A1; NAS1;solute carrier family	Na-SO ₄ -cotransport, renal reabsorption
0.166	0.009	MG-12-286p16	NM_009470	Uromodulin precursor (Tamm-Horsfall urinary glycoprotein)	calcium-binding EGF-like domain
0.270	0.078	MG-12-249i16	BC018252	Slc17a3, Npt4	Na dependent-phosphate cotransporter
0.338	0.010	MG-12-30d2	U52842	solute carrier family 22, member 6	kidney-specific transport protein
0.406	0.006	MG-12-134p11	NM_009203	Rst; OAT4L; URAT1; Slc22a12	Transport; Transmembrane
2.333	0.108	MG-12-247c4	AF020519	Aqp2;Aquaporin 2	Transport and binding proteins
2.633	0.294	MG-12-169a2	AI426654	BSC1 butenamide-sensitive Na/K/Cl cotransporter 2	Transport and binding proteins

During renal calcium reabsorption the calcium ions have to pass a barrier of endothelial cells. On the apical side of this cell wall, which consists of the lining cells of the distal convoluted tubule and the connecting tubule, epithelial calcium channels, consisting of the two homologous isoforms TRPV5 and TRPV6 (previously called ECAC1 and ECAC1) enable the entry of calcium ions across the plasma membrane. In the cytosol, free calcium is bound to calbindins, consisting of calbindinD9k and calbindin D28k, which act as intracellular calcium buffers and facilitate the transport of calcium in the cytosol by diffusion (Hoenderop et al. 2002).

Calbindin D9K belongs to the S100 family of calcium-binding proteins that bind 2 Ca²⁺ ions in their EF-hand domains. It is expressed in kidney, intestine and placenta, organs involved in calcium homeostasis. Transcriptional induction of kidney calbindin D9K by vitamin D has been known for a long time (Thomasset et al. 1982). In VDRKO mice calbindin D9K mRNA and protein levels are drastically reduced and expression can not be induced by 1,25(OH)₂D₃ treatment, a fact that has been observed in all lines of VDRKO mice (Li et al. 1998b; Erben et al. 2002). As shown in previous studies, calbindin D9k was significantly down-regulated in male and female

VDRKO mice, an effect that could not be rescued in RD mice with normalised serum ionized calcium levels. The strong down-regulation of this gene was seen in all microarray experiments with VDRKO / WT mouse kidney and intestine and served as quality control to assess the performance of data analysis.



Impaired renal reabsorption, as observed as increased calcium urinary excretion rates of VDRKO mice on a diet enriched in calcium and phosphate was attributed to decreased calbindin D9K expression (Li, Y. C. et al. 2001). Calbindin D28K, which has been detected previously in tissues like brain, uterus, lung and pancreas, was not significantly reduced by VDR ablation and did not appear as differentially expressed in microarray experiments (see figure 3.2.3).

Data of calbindinD9K expression resulting from microarray experiments were well in line with the results from experiments with qPCR (figures 3.2.1-3). While VDRKO and WT mice on normal diet express similar amounts of calbindin D28K mRNA, its expression in RD mouse kidney seems to be slightly suppressed, indicating calcium-dependent regulation of calbindin D28K expression. Measurements of calbindin expression in kidneys of 25-hydroxyvitamin D₃-1 α -hydroxylase knockout (CYP1 α KO) mice showed that the expression of calbindin D28K, but not of calbindin D9K, could be rescued with a calcium/phosphate-enriched rescue diet (Hoenderop et al. 2002). Recent studies on calcium channel TRPV5 - ablated mice with elevated systemic serum levels of 1,25(OH)₂D₃ and normal (!) calcium concentrations in blood showed down-regulation of calbindin D28K and up-regulation of vitamin D-dependent calbindin D9K. These mice compensate impaired reabsorption in the distal convolution with increased intestinal calcium absorption rates. While the latter is clearly a result of elevated serum vitamin D levels, it shows that calbindin D28K expression, independent of vitamin D status, has to be linked to apical calcium influx through TRPV5 calcium channels.

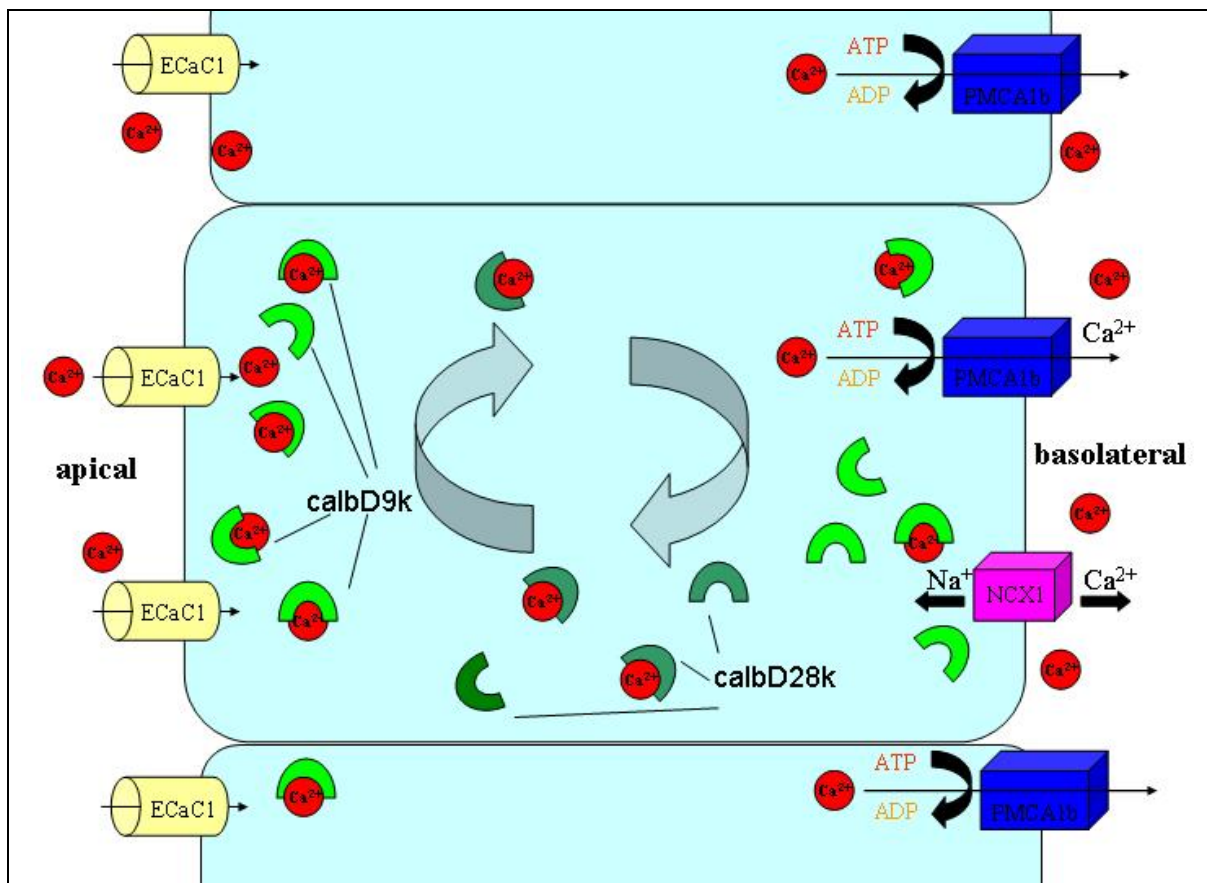


Figure 3.2.4: Model of renal calcium reabsorption, as proposed by Hoenderop et al. in cells lining the distal part of the nephron. Calbindins serve as a cytosolic calcium buffer that facilitates calcium transport by diffusion. Immunofluorescence confocal microscopy studies showed that while calbindin D28K was uniformly distributed in the cytosol, calbindin D9K was localised along the apical and the basolateral membrane, which might indicate a transport function for Ca²⁺ ions along the plane to and from the few scattered membrane Ca-channels (Hoenderop et al. 2002).

Apart from calbindin D9K, a number of organic solute carriers (SCL) were found down-regulated in VDRKO mouse kidney. Members of the SCL protein family often are involved in the transport of steroids and eicosanoids across cell membranes, like organic solute transporter alpha (Seward et al. 2003), or have themselves regulatory

functions, like in the case of the recently characterised uncoupling proteins UCP4 and UCP5. In normal diet hypocalcemic VDRKO animals, renal vasopressin-sensitive aquaporin Aqp2 was significantly up-regulated by (2.33 +/- 0.11)-fold. Aqp2 was recently observed to be suppressed in the collecting duct of hypercalcemic rats exposed to elevated levels of vitamin D (Wang, W. et al. 2002), which suffered from impaired water re-absorption and increased urine output. In the same rats, type 1 butenamide-sensitive Na-K-2Cl cotransporter (BSC-1) was down-regulated in the apical membrane of rat thick ascending limbs after treatment with vitamin D. Up-regulation of BSC-1 in VDRKO ((2.63 +/- 0.29)-fold) mice corroborates a VDR-mediated transcriptional control of this gene.

Down-regulation of the phosphate/sodium cotransporter Npt4, as observed in ND VDRKO vs. WT mouse kidney at (0.21 +/- 0.08) was also observed in kidneys of mice lacking hepatocyte nuclear factor 1a (HNF1 α). Interestingly, the kidney phenotype of the HNF1 α mice that suffer from defective cholesterol and bile acid metabolism is somewhat similar to the VDRKO phenotype, as both have defects in renal proximal tubule reabsorption. (Cheret et al. 2002). Disruption of the closely related Na-PO₄ cotransporter Npt2 resulted in hypophosphatemia and activation of 1,25(OH)₂D₃ synthesis by increased expression of CYP1 α (Tenenhouse et al. 2004).

Apart from sodium/phosphate cotransporter, sodium/sulfate cotransporter mRNA was significantly down-regulated in ND VDRKO mouse kidney (0.14 +/- 0.03)-fold. Similar to other membrane transport proteins, NaS1 (SCL13A1) is located in the apical membrane of the renal proximal tubule and mediates sulfate (SO₄) reabsorption from the glomerular filtrate. NaS1 expression was significantly decreased in vitamin D deficient rats (Fernandes et al. 1997), which had significantly lower plasma sulfate levels and increased rates of urinary SO₄ excretion. Feeding a diet rich in calcium and lactose, normalising plasma calcium and parathyroid levels, could not rescue sulfate homeostasis. Normalisation of NaS1 mRNA and protein expression, as well as normal sodium and sulfate reabsorption only was possible by vitamin D supplementation, showing that vitamin D regulation of NaS1 is a direct effect and not mediated by calcium or PTH. The promoter region of NaS1, transiently transfected into opossum kidney cells, was activated by vitamin D via a VDR-mediated mechanism (Beck and Markovich 2000). Similar results were obtained recently *in vivo* in experiments with VDRKO mice (Bolt et al. 2004).

Podocin, encoded by the gene NPHS2, has important functions in the ultrafiltration of plasma in the renal glomerulus. NPHS2 was significantly up-regulated in kidneys from male (ND) VDRKO mice with respect to WT mice. Microarray experiments delivered a mean up-regulation in VDRKO mouse kidney by (3.23 +/- 0.29) -fold, measurements by quantitative real-time PCR (2.54 +/- 0.32)-fold, whereas in normocalcemic (RD) mice NPHS2 expression was even slightly down-regulated (qPCR: 0.77 +/- 0.08)-fold. Mutations in the NPHS2 gene can lead to the steroid-resistant nephrotic syndrome, a group of kidney disorders, characterised by early childhood onset of proteinuria, rapid progression to end-stage renal disease and focal segmental glomerulosclerosis (Boute et al. 2000; Karle et al. 2002). Deletions of NPHS2 in mice resulted in a severe phenotype resembling human renal disease, leading to the death of NPHS2 *-/-* mice shortly after birth due to renal failure and massive mesangial sclerosis (Roselli et al. 2004). Podocin is specifically expressed in podocytes, visceral epithelial cells located in the glomerular filtration barrier, where it presumably has its role as scaffolding protein. It builds the microstructure of slit diaphragms and attaches the cytoplasmic extensions of podocytes (foot processes)

to the glomerular basement membrane. Effacement of foot processes due to NPHS2 ablation leads to focal and segmental glomerulosclerosis and leakage of proteins across the filter into the membrane, a condition occurring in the course of diabetes, renal mass reduction and diabetes (Ichikawa and Fogo 1996). While these disease conditions were connected with missing expression of podocin, the up-regulation in VDRKO kidney might be a compensatory reaction and its physiological significance of NPHS2 has yet to be elucidated.

3.2.2 Nuclear hormone receptors and steroid/cholesterol metabolism

As pointed out previously in chapter 1, the VDRKO mice, objects of this study, expressed a vitamin D receptor lacking a zinc finger domain required for DNA binding and transcriptional regulation (Erben et al. 2002). In VDRKO mice raised on normal diet, truncated VDR was identified as down-regulated to (0.28 +/- 0.04)- fold (mean over 3 microarray experiments).

Increased expression of VDR at elevated levels of 1,25(OH)₂D₃ was observed previously (McDonnell et al. 1987; Strom et al. 1989). Interestingly, these studies showed that, while total receptor concentration increased with vitamin D administration, the level of unliganded VDR remained stable, indicating an important role of the unliganded receptor. Down-regulation of the mutated VDR in VDRKO mouse kidneys in spite of the increase in systemic vitamin D shows that VDR expression is regulated via the transcriptional activity of the receptor itself.

The lack of transcriptional activity of liganded VDR/RXR disrupts metabolic feedback loops that control the activity of enzymes involved in vitamin D synthesis and - metabolism, such as 25-hydroxyvitamin D₃ 1 α -hydroxylase (CYP1 α) (Takeyama et al. 1997), or 24-hydroxylase (Chen and DeLuca 1995). Disruption of this negative feedback loops in VDRKO mice result in dramatically elevated systemic levels of active vitamin D, as observed previously in an independently created VDRKO mouse strain (Yoshizawa et al. 1997) and in the strain which was investigated in this study (Erben et al. 2002).

The elevated expression of 25-hydroxyvitamin D₃ 1 α -hydroxylase was confirmed in this study by quantitative real-time PCR (see Figure 3.2.5 below). In the case of both diets, expression levels of CYP1 α were dramatically increased in VDRKO mouse kidney with respect to WT (ND: 158,4 +/- 10,7-fold, RD: 5,4 +/- 1,1-fold). This indicates a control of CYP1 α expression by both, vitamin D via a VDR-mediated mechanism and by circulating levels of calcium/PTH.

Each value given here in Figure 3.2.5 and in other qPCR measurements on gene expression in kidney was calculated from 4 parameters, describing relative gene expression of the target and reference gene in VDRKO and WT mouse kidney. Each of these parameters in turn was calculated from 3 individual measurements. The error bars here were calculated by Gaussian error progression (see methods).

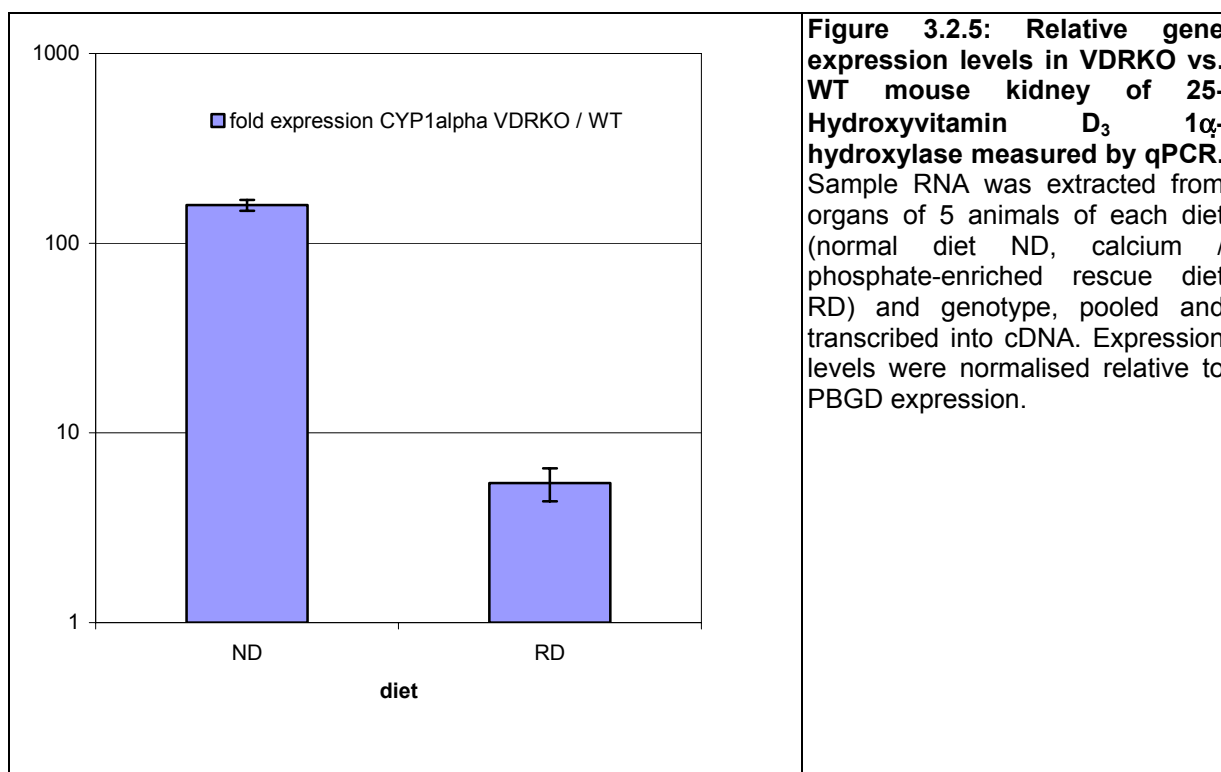


Figure 3.2.5: Relative gene expression levels in VDRKO vs. WT mouse kidney of 25-Hydroxyvitamin D₃ 1 α -hydroxylase measured by qPCR. Sample RNA was extracted from organs of 5 animals of each diet (normal diet ND, calcium / phosphate-enriched rescue diet RD) and genotype, pooled and transcribed into cDNA. Expression levels were normalised relative to PBGD expression.

Figure 3.2.6 shows the relative mRNA expression levels of genes, identified in microarray experiments of section 3.1 as differentially expressed in VDRKO vs. WT mouse kidney and the results from validation experiments by qPCR. These genes have putative functions in processes involved in steroid biosynthesis, transport and in cholesterol metabolism.

One of the most significantly down-regulated genes across all groups of animals was cytochrome P450 β 1 (CYP4 β 1). CYP4 β 1 was up to present reported to be involved in bladder carcinogenesis, liver detoxification and activation of procarcinogenic hydrocarbons in kidney (Imaoka et al. 1995; Imaoka et al. 2001b). In a phylogenetic study (Heng et al. 1997) CYP4 β 1 was shown to be related to cytochrome 4a14 (CYP4 α 14) which has functions in fatty acid metabolism (Guan et al. 1998) and protection against reactive oxygen species in mitochondria. The expression of both genes is down-regulated in VDRKO and appears to be androgen-dependent (Imaoka et al. 2001a). A recently published study showed that CYP4 β 1 is induced in corneal epithelial cells in response to hypoxia and that it has a role in the metabolism of arachidonic acid to eicosanoids, which in turn are involved in inflammatory response, vasodilation and angiogenesis (Mastyugin et al. 2004). Promoter analysis of the CYP4 β 1 gene revealed binding sites for transcription factors such as HIF-1, NF κ B and AP-1.

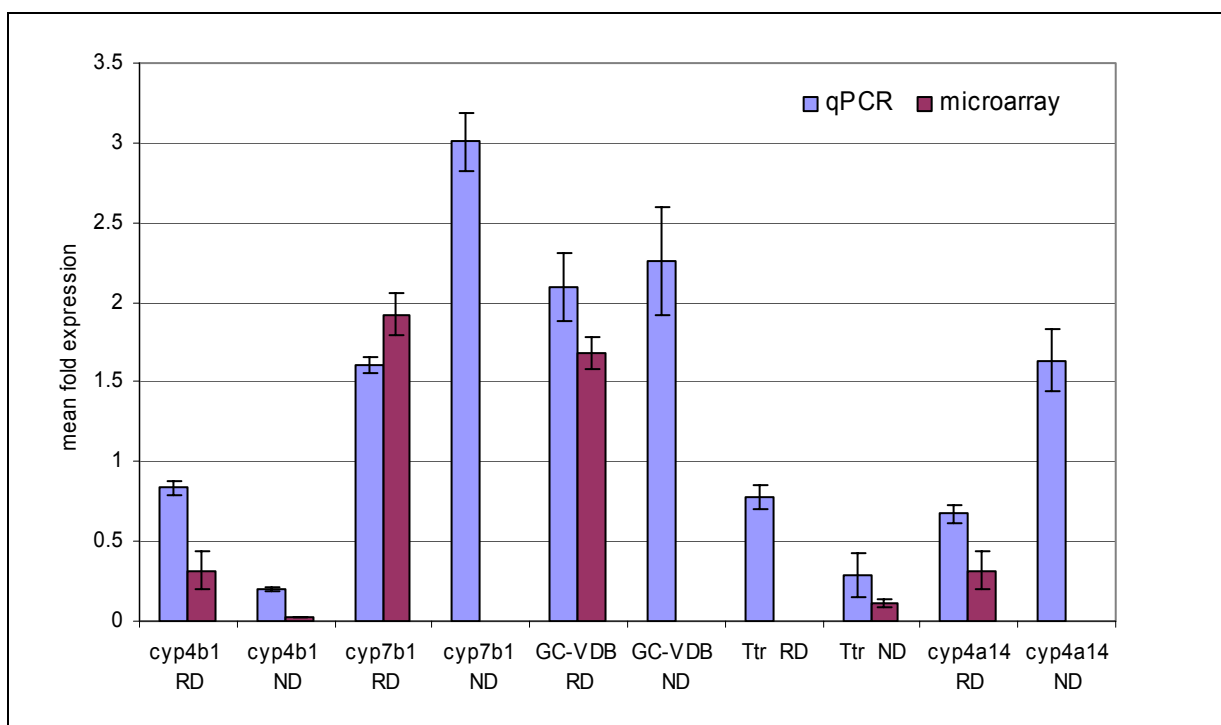


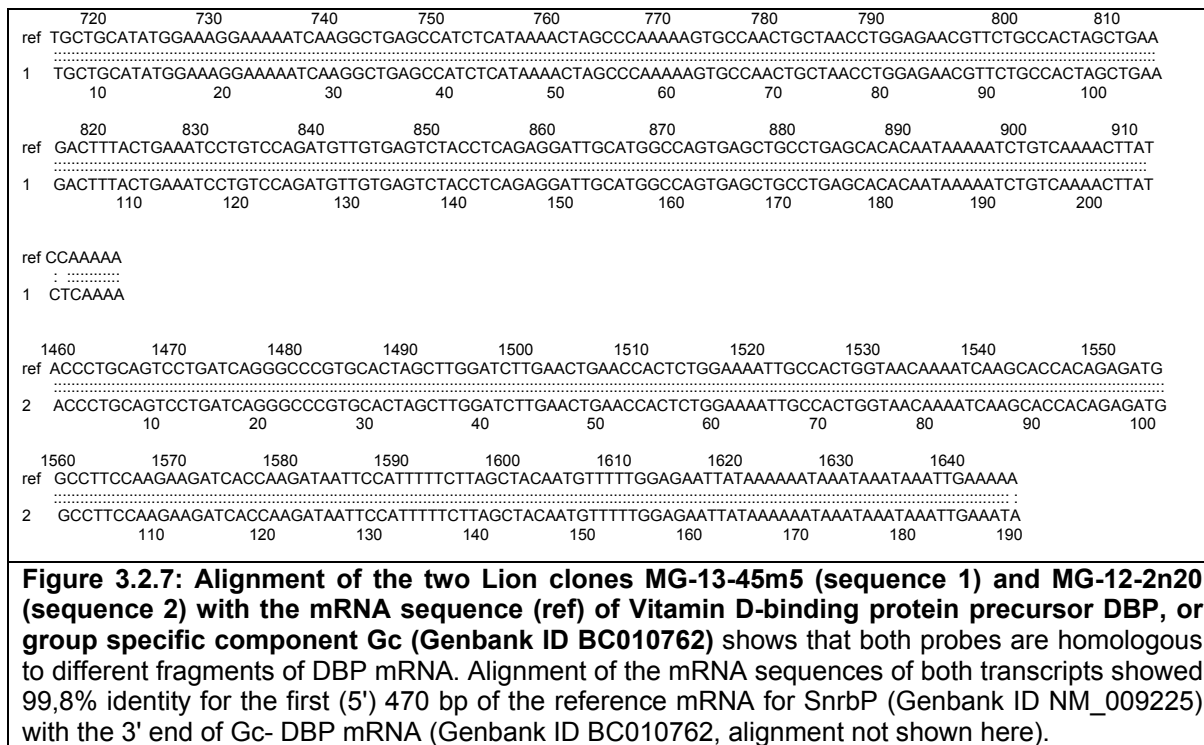
Figure 3.2.6: Comparison of two methods for gene expression analysis: Relative gene expression VDRKO / WT in mouse kidney from male animals raised on normal (ND) and rescue (RD) diet, measured by microarray analysis and quantitative real-time PCR (qPCR). qPCR data were measured relative to PBGD expression in pooled RNA from organs of 5 individuals, as described before. Microarray data were generated from experiments with kidney RNA pooled from 5 animals in the case of normal diet mice or from separate experiments with RNA from 3 different individuals in the case of rescue diet mouse kidney. Up-regulated genes have mean relative expression values above 1, down-regulated genes <1. All values are the means of 3 independent experiments. Note that only in the case of cytochrome CYP4 β 1 there are microarray data for ND and RD VDRKO vs. WT animals, as this gene was strongly down-regulated kidney from animals of all groups of diets and gender and therefore always appeared as candidate gene.

The oxysterol 7 α -hydroxylase gene CYP7b1 is widely expressed in many tissues and mediates the catabolism of cholesterol via oxysterols to bile acid via a mechanism alternative to the classical pathway (Wu et al. 1999; Wu and Chiang 2001). In this pathway, initiated by CYP7A1 in liver, cholesterol is first hydroxylated by mitochondrial 27-hydroxylase to 27/25-hydroxysterol, which is then further hydroxylated by CYP7b1. CYP7b1 $-/-$ mice show elevated levels of 27/25-hydroxysterol, which in turn regulates cholesterol biosynthesis through liver orphan receptor (LXR), steroidogenic factor 1 and sterol response element binding protein (SREBP) (Brown and Goldstein 1997).

Down-regulated in VDRKO mice is transthyretin (Ttr, prealbumin), a carrier protein for tyrosine and retinol. In the latter case of retinol Ttr acts through binding to retinol-binding protein (RBP) (Monaco 2000). In kidney the Ttr-RBP complex prevents losses of retinol through glomerular filtration and thus controls vitamin A availability in serum.

While retinol transporting Ttr is down-regulated, two candidate genes, coding for vitamin D-binding proteins were both found up-regulated in VDRKO mouse kidney, independent of nutritional calcium intake and confirmed by qPCR (see figure 3.2.6 above): Small nuclear ribonucleoprotein B (Snrpb, Lion ID: MG-13-45m5) and vitamin D-binding protein (DBP, or group specific component, Gc, MG-12-2n20). The Lion database attributes the probes to two different genes on mouse chromosome 2 and

5. BLAST search for the probe sequences against the NCBI mouse transcriptome delivers the same cDNA hits, like Genbank accession ID BC010762, group specific component Gc or Vitamin D-binding protein precursor DBP. Alignment by BLAST with the ENSEMBL mouse genome delivers for both cases the same ENSEMBL cluster ENSMUSG00000035540 for Gc-DBP, located on chromosome 5. This leads to the conclusion that the two probes in the Lion data base represent the same gene.



Vitamin D-binding protein (DBP), initially named group-specific component of serum, is highly expressed multifunctional glycoprotein of the albumin / alpha-fetoprotein family, that was reported as a carrier for sterols, especially calcidiol 25(OH)D₃ and its active form calcitriol 1,25(OH)₂D₃ in serum. Studies of the DBP gene proximal promoter show that the expression of DBP depends on the expression level of the enhancing hepatocyte nuclear factor 1α (HNF1α) relative to its inhibiting isoform HNF1b. It was reported that DBP plasma concentration is about 20-fold higher than that of circulating vitamin D metabolites and that over 85% of both calcidiol and calcitriol are bound to DBP, leaving only 0.4% of free active vitamin D and the rest bound to other serum proteins (White and Cooke 2000). Apart from its role as steroid carrier, DBP was found to have functions together with gelsolin (see section 4) in the actin scavenger system, protecting the cardiovascular system from damage through clogging of F-actin filaments. In the immune response system, DBP promotes monocyte differentiation, macrophage activation and chemotaxis of phagocytic cells (White and Cooke 2000). DBP null-mutants did not show a pronounced phenotype when fed with a normal diet, although they had significantly decreased serum levels of 25(OH)D₃ and 1,25(OH)₂D₃, compared with WT animals. However, when subjected to a diet deficient in vitamin D, they showed a phenotype comparable to VDRKO or CYP1a^{-/-} mice, with secondary hyperparathyroidism, hypocalcemia and osteomalacia (Safadi et al. 1999). These findings support the 'free hormone' hypothesis, relating hormone activity to its unbound availability in plasma rather than to its total concentration. This conclusion was corroborated by the observation that DBP^{-/-} mice had shorter half-life-times of circulating vitamin D and thus were resistant to vitamin D toxicity.

Studies on a recently created site-directed megalin $-/-$ mouse that expresses megalin in all tissues except of kidney revealed a crucial role of the endocytic receptor megalin for reabsorption of DBP-bound $25(\text{OH})\text{D}_3$ in renal proximal tubular cells and its conversion to $1,25(\text{OH})_2\text{D}_3$ by 1α -hydroxylase in the mitochondria (Lehste et al. 2003). Similar to DBP $-/-$ mice, kidney megalin $-/-$ mice on a normal diet had a very mild phenotype, but showed severe hyperparathyroidism, hypocalcemia and osteopathy, when subjected to a diet deficient in vitamin D.

Since DBP increases the half-life time and thus circulating concentration of vitamin D, it can be supposed that vitamin D signalling negatively controls DBP expression via the VDR. In VDRKO mice the mutated VDR lost this feedback control function, which results in elevated expression of DBP, as observed in this study. Up-regulation of DBP and CYP1 α means that both, longer half-life-times and biosynthesis rates increase the level of $1,25(\text{OH})_2\text{D}_3$ in VDRKO mice.

In this context it is interesting to note that megalin also functions in renal re-absorption of transthyretin, a carrier protein for both retinol-binding protein and thyroxine in proximal tubules, again connecting vitamin D-, retinol- and thyroxin-dependent pathways (Sousa et al. 2000). Down-regulation of transthyretin expression was observed in gene expression profiling of ND VDRKO vs. WT mouse kidney. This result was confirmed by qPCR for mice subjected to both diets, but down-regulation was stronger in the case of ND mice (figure 3.2.6). As explained before, only a selection of candidate genes identified in microarray gene expression studies was confirmed by qPCR. A complete list of confirmed and unconfirmed differentially expressed genes with functions in retinoid or steroid biosynthesis and nuclear receptors can be found in table 3.2.2a-b.

Table 3.2.2a: Nuclear hormone receptors and genes involved in cholesterol and steroid metabolism, identified as differentially expressed in VDRKO vs. WT mouse kidney of normocalcemic animals on a calcium-rich rescue diet.

fold change RD	error	Lion ID	Genbank ID	abbreviation	name	function
0.31	0.04	MG-15-151a5	BC004770	Nr4a1/Nur77/TR3	nuclear receptor subfamily 4, group A, member 1 (NGFI-B)	nuclear hormone receptor
0.63	0.06	MG-8-17k11	NM_145942	Hmgcs1	Hmgcs1: 3-hydroxy-3-methylglutaryl-Coenzyme A synthase 1	cholesterol biosynthesis
0.68	0.11	MG-12-222c16	NM_146067	Slco3a1, Anr1, Slc21a11	MJAM; OATP-D, androgen regulated protein 1	organic anion carrier
0.71	0.06	MG-6-57e23	NM_145942	Hmgcs1	Hmgcs1: 3-hydroxy-3-methylglutaryl-Coenzyme A synthase 1	cholesterol biosynthesis
0.83	0.21	MG-8-94d7	NT_039590	Hmgcr	Hmgcr: 3-hydroxy-3-methylglutaryl-Coenzyme A reductase	cholesterol biosynthesis
1.54	0.11	MG-3-16d22	BC048825	Abcc3	ATP-binding cassette, sub-family C (CFTR/MRP), member 3	canalicular bile acid transport
1.62	0.19	MG-12-162d20	NT_039308	CYP2d9	Cytochrome P450, 2d9	n.a.
1.68	0.10	MG-12-2n20	NM_009225	Gc, DBP	group specific component	vitamin D-binding protein
1.74	0.21	MG-13-45m5	NM_009225	Snrpb, Cc, VDB	small nuclear ribonucleoprotein B, group specific component	regulation of transcription, vitamin D binding protein
1.924	0.128	MG-12-140c23	NM_007751	CYP7b1	Cytochrome P450, 7b1.	cholesterol metabolism

Table 3.2.2b: Nuclear hormone receptors and genes involved in cholesterol and steroid metabolism, identified as differentially expressed in VDRKO vs. WT mouse kidney of animals on normal diet

fold change ND	error	Lion ID	Genbank ID	abbreviation	name	function
0.022	0.001	MG-12-3e4	BC008996	CYP4β1	cytochrome P450 4B1 (CYP1VB1).	Oxidoreductase; Endoplasmic reticulum; Microsome; Heme
0.118	0.025	MG-11-1e9	AA822938	Ttr	transthyretin precursor (prealbumin)	Retinol-binding; Albumin; Vitamin A; Thyroid hormone; Transport
0.134	0.032	MG-12-214a17	NM_153193	Hsd3β2	3β-Hydroxysteroid dehydrogenase-2	steroid metabolism
0.200	0.080	MG-16-3f6	BB698820	Fkbp5	FK506 binding protein 5	hormonal activation of the glucocorticoid receptor, chaperone
0.282	0.038	MG-73-7m21	Mm.44170	VDR	Vdr; Vitamin D receptor	transcription factor
0.287	0.013	MG-12-274i8	NM_029901	Akr1c21	aldo-keto reductase family 1, member C21	n.a.
0.344	0.091	MG-12-194m5	AK047211	Nr1h4, FXR	hypothetical gene supported by AK047211	Nr1h4: nuclear receptor subfamily 1, group H, member 4
0.345	0.007	MG-12-258e15	NM_007409	Adh1	Alcohol dehydrogenase 1 (class I)	NAD; Oxidoreductase; Zinc;
0.391	0.014	MG-12-152e20	U09418	Nr1h4, FXR	Bile acid receptor (Farnesoid X-activated receptor)	Nuclear receptor subfamily 1, group H, member 4
3.633	0.481	MG-16-143m3	NM_025522	11β-HSD, Dhhrs7	Retinal short-chain dehydrogenase/reductase 4	retinoic acid biosynthesis
3.800	0.21	MG-4-5e2	U16818	UGT1	UDP glucuronosyltransferase	glucuronate metabolism

According to table 3.2.2a-b above a number of genes were found to be down-regulated especially in VDRKO mice vs. WT raised on normal diet, which are involved in retinoic acid biosynthesis and transport, like transthyretin precursor, retinal short-chain dehydrogenase 4 and alcohol dehydrogenase 1. Among the differentially expressed genes also are genes involved in steroid metabolism, like Hsd3β2 and aldo-ketoreductase 1 C21. Whether the regulation of these genes is mediated by both VDR and / or calcium needs further investigation. Mutations in the Hsd3b1 and Hsd3β2 genes have recently been associated with increased hereditary and sporadic prostate cancer susceptibility (Chang et al. 2002).

3.2.3 Cross-talk between nuclear hormone receptors

Retinoic acid, in its all-trans or the 9-cis form is the ligand for the nuclear hormone receptors RAR and RXR, which dimerise in vivo with RXR like VDR, thyroid hormone receptor (TR) and peroxisome proliferator-activated receptors (PPAR). These heterodimers can bind to specific cis-acting elements within promoter or enhancer regions and modulate gene transcription. Various studies have shown that retinoic acid, 1,25-(OH)₂D₃ and other ligands of nuclear hormone receptors can mutually enhance or inhibit transcriptional activity, like RAR- and RXR-ligands in the regulation of aromatase transcription (Yanase et al. 2001). Retinoic acid inhibits and 1,25-(OH)₂D₃ promotes transcription of PPAR_γ and pre-adipocyte differentiation (Hida et al. 1998; Kawada et al. 2000).

Cross-talk between nuclear receptors might also be the explanation for the observed down-regulation of farnesoid X receptor (FXR, Nr1h4), which is represented on the array by two Lion clones that were regulated by nearly identical fold change values (see table 3.2.2). FXR, another heterodimerisation partner of RXR, binds to specific primary and secondary bile acids and regulates the activity of enzymes involved in cholesterol and lipoprotein metabolism (Anisfeld et al. 2003). FXR null mice show elevated serum bile acid, cholesterol and triglyceride levels (Sinal et al. 2000). When challenged with cholic acid, FXR action inhibits via the activation of the orphan nuclear receptor SHP the expression of liver cytochrome P4507A, which controls the

main, neutral pathway of cholesterol catabolism. In this context, the elevation of CYP7B1 in VDRKO mouse kidney by (1.94+/-0.13)-fold is remarkable, as CYP7B1 controls the alternative acidic bile acid pathway in extrahepatic tissues.

While cholesterol catabolism along the acidic bile acid pathway seems to be up-regulated in kidney from VDRKO mice on normal diet, two genes with functions in cholesterol biosynthesis, 3-hydroxy-3-methylglutaryl-Coenzyme A synthase 1 (Hmgcs1) and 3-hydroxy-3-methylglutaryl-Coenzyme A reductase (Hmgcr) were down-regulated in RD mouse kidney. Another FXR target gene with increased expression in both VDR ND and FXR null mice is apolipoprotein E. Impaired expression of genes involved in pathways controlled by the nuclear hormone receptors RXR, FXR and PPAR in VDRKO mice strongly indicate cross-talk between transcriptional pathways, controlled by these receptor and VDR. This conclusion is supported by numerous previous studies, (Makishima et al. 2002; Adachi et al. 2004), that found activation of VDR by bile acids in colon, which previously had been identified as classical ligands of FXR, like the lithocholic acid (LCA). High-fat diets increase colon LCA concentrations and can promote colorectal cancer (Owen et al. 1987), which in turn was shown to be reversed by VDR action (Garland et al. 1999). VDR, activated by LCA and/or 1,25(OH)₂D₃ upregulates the expression of cytochrome P4503A, which detoxifies LCA in colon.

3.2.4 Lipid metabolism and energy supply

Apart from genes involved in bile acid signalling and metabolism, the largest group of candidate genes identified as differentially expressed in VDRKO vs. WT mouse kidney was involved in lipid metabolism and energy production (see tables 3.2.3-4, below). Regulation of pathways of lipid metabolism by vitamin D, by vitamin d-responsive receptors and by calcium has been observed in many studies. These include epidemiological studies on the (negative) influence of dietary calcium intake on body weight (Davies et al. 2000) and body fat index in humans (Carruth and Skinner 2001). Experiments with transgenic mouse models showed a clear association between calcium channel activation by vitamin D, intracellular calcium concentrations and lipogenesis (Zemel et al. 2000; Shi et al. 2001a).

The body weight of VDR null mice is significantly reduced in comparison to WT littermates (Erben et al. 2002), but can be raised to almost normal levels by feeding a diet rich in calcium and phosphate. Apart from symptoms of increased energy turnover, especially in ND VDRKO mice, pancreatic insulin secretion was reported to be impaired in ND and RD VDRKO mice (Zeitz et al. 2003). On molecular level, some of the genes involved in steroid and cholesterol metabolism discussed above also have major functions in lipid metabolism, especially those involved in bile acid signalling and transport.

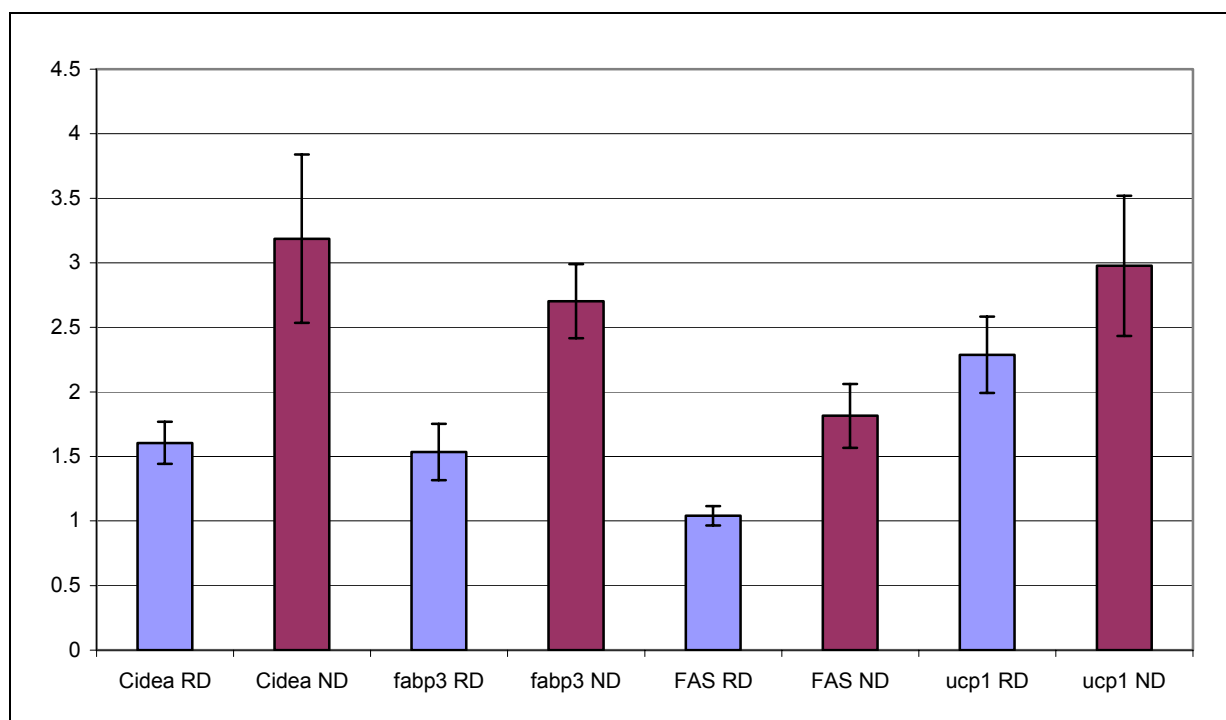


Figure 3.2.8: Relative gene expression VDRKO vs. WT of genes involved in lipid metabolism. Results of confirmation experiments by qPCR of relative gene expression levels in VDRKO / WT mouse kidney of selected genes that were identified by microarray gene expression profiling. All parameters were measured in triplicates and gene expression was normalised, relative to PBGD expression. Relative VDRKO / WT gene expression levels in ND mice are represented in purple columns, blue columns stand for RD mice.

As shown in previous experiments, genes found up- or down-regulated in microarray experiments, could be confirmed in independent experiments by qPCR, although the number of relative fold change might differ between the methods. Since verification and detailed discussion of all genes involved in lipid metabolism and energy production is impossible, the focus was directed to genes known as key regulators that can be related in signalling cascades to other regulated candidate genes. Of special interest is the comparison of the influence of diet that determines serum calcium, phosphate and PTH levels on gene expression.

Among the genes involved in fatty acid and energy metabolism, differentially expressed in VDRKO mice (see table 3.2.8) is lipin 1, slightly down-regulated by (0.79 +/- 0.09)-fold. Lipin was identified as the gene responsible for symptoms of human lipodystrophy in mice carrying mutations in the alleles, *fld* and *fld*^{2j} (Peterfy et al. 2001). Lipodystrophy is a metabolic disease leading to dramatically reduced adipose tissue mass, acquired insulin resistance and increased susceptibility to arteriosclerosis, symptoms found in a milder form in VDRKO mice. In vitro studies have shown that lipin expression is required during initial stages of adipogenesis and induces key adipogenic factors, such as PPAR γ and CCAAT enhancer-binding protein ((C/EBP) α) (Phan et al. 2004).

Fatty acid synthase (FAS), a key enzyme of lipogenesis was significantly up-regulated in kidneys of VDRKO mice raised on normal diet (3.27 +/- 0.47-fold in microarray experiments, 1.82 +/- 0.25-fold in qPCR), whereas it was unchanged in VDRKO mice raised on a rescue diet rich in calcium and phosphate. An increase of FAS through VDR inactivation is in accordance to the observation of Hang Shi et al. (Shi et al. 2001b): Human adipocytes were treated with 1,25(OH)₂D₃, which resulted in a rapid increase of intracellular calcium [Ca]_i, followed by increased FAS

transcription and decreased lipolysis, mediated through a VDR-independent mechanism. This experiment based on previous studies that related metabolic disorders of obesity and insulin resistance to elevated levels of $[Ca]_i$ (Draznin et al. 1988; Byyny et al. 1992). Increased dietary calcium, administered to aP2-agouti, a mouse model for human obesity and insulin resistance, suppressed serum levels of active $1,25(OH)_2D_3$, which in turn decreased adipocyte $[Ca]_i$ and FAS mRNA expression and protein production (Shi et al. 2001a). This effect of $[Ca]_i$ on FAS expression was mimicked by treating adipocytes with KCl, thus increasing calcium influx through voltage gated channels and inhibited by the Ca^{2+} -channel blocker nitrendipine (Xue et al. 1998). Alternatively, the vitamin D derivative $1\alpha,25$ -dihydroxylumisterol₃ (1α -(OH)₂-lumisterol₃), an agonist for a putative vitamin-D-responsive membrane Ca^{2+} -channel, has the same effect as $1,25(OH)_2D_3$ on the activation of calcium influx. This effect was antagonized by $1\beta,25$ -dihydroxyvitamin D₃ ($1\beta,25$ -(OH)₂D₃), which has no effect on VDR-mediated transcription (Shi et al. 2001b).

As pointed out previously, serum levels of $1,25(OH)_2D_3$ are significantly increased in VDRKO mice due to the disruption of VDR-mediated feedback loop on the expression of vitamin D-activating (CYP1 α) and -metabolizing enzymes (24-hydroxylase). The observed increase of FAS expression in ND VDRKO kidney cells fits well to the model proposed by Shi, Zemel et. al. for $[Ca]_i$ -controlled lipogenesis by FAS, given that it is stimulated by $1,25(OH)_2D_3$ through nongenomic, VDR-independent action. In VDRKO mice raised on a calcium / phosphate-enriched rescue diet, PTH levels, strongly elevated in ND VDRKO mice, were normalised to WT levels (Erben et al. 2002). However, the vitamin D-activating CYP1 α was still up-regulated in VDRKO compared to WT, but to a far smaller extent (ND: 158,4 +/- 10,7-fold, RD: 5,4 +/- 1,1-fold, determined by qPCR, see figure 3.2.4). Both PTH and $1,25(OH)_2D_3$ were reported to cause rapid, non-genomic increase of $[Ca]_i$ in epithelial cells (Picotto 2001) and adipocytes (Shi et al. 2001b). Decreased levels of both calciotropic hormones may be the reason for normalised FAS transcription in VDRKO mice raised on a rescue diet.

In ND mice, lipogenic genes were differential at higher fold expression values. For both diets significantly up-regulated in mice with dysfunctional VDR was uncoupling protein 1 (UCP1), coding for the first described member of the gene family of mitochondrial uncoupling proteins. UCP1 is predominantly expressed in mitochondria of rodent and human embryonic brown adipose tissue (BAT). To a lesser extent it is also expressed in tissues of high energy expenditure, like kidney, skeletal muscle and heart. In BAT, UCP1-mediated uncoupling allows proton backflow from the mitochondrial intermembrane space into the matrix, by-passing the ATP-synthase complex. This leads to non-shivering thermogenesis and thus constitutes an important mechanism for heat generation in newborn, cold-acclimated, hibernating and overfed mammals (Jezek and Garlid 1998; Jezek et al. 2004). UCP1 catalyzes the transport of the anionic heads of fatty acids in the lipid membrane bilayer from one to the other side of the membrane, where they become protonated and return to the other membrane side by a flip-flop mechanism and thus lower the efficiency of the proton gradient generated by the respiratory-chain in ATP production (Jezek et al. 1998; Jezek 1999).

Recently, the discovery of the isoforms UCP2-5, which are about 60% homologous to UCP1, and reports about the role of UCPs in reactive oxygen species (Del Arco et al.) formation, prevention of atherosclerosis, participation in inflammation, body

weight control and diabetes type 2 led to rapidly increased scientific interest in the mechanism and function of mitochondrial uncoupling. In their studies about the regulatory role of vitamin D-controlled $[Ca]_i$ in de-novo lipogenesis and lipolysis with aP2-agouti transgenic mice, the group of MB Zemel observed activation of UCP2 expression by high calcium diets (Shi et al. 2001a). Treatment of human adipocytes with $1,25(OH)_2D_3$ showed that inhibition of UCP2 transcription was mediated by vitamin D and could not be mimicked or inhibited by the VDR nongenomic agonists or antagonists. Knockout of nuclear VDR via antisense oligonucleotides showed that UCP2 inhibition by vitamin D was VDR-dependent and was not regulated via $[Ca]_i$. If we assume a similar regulation of the closely related UCP1, this might explain why UCP1 was strongly up-regulated in mice with disrupted VDR activity, independent of the diet, serum vitamin D and $[Ca]_i$ levels.

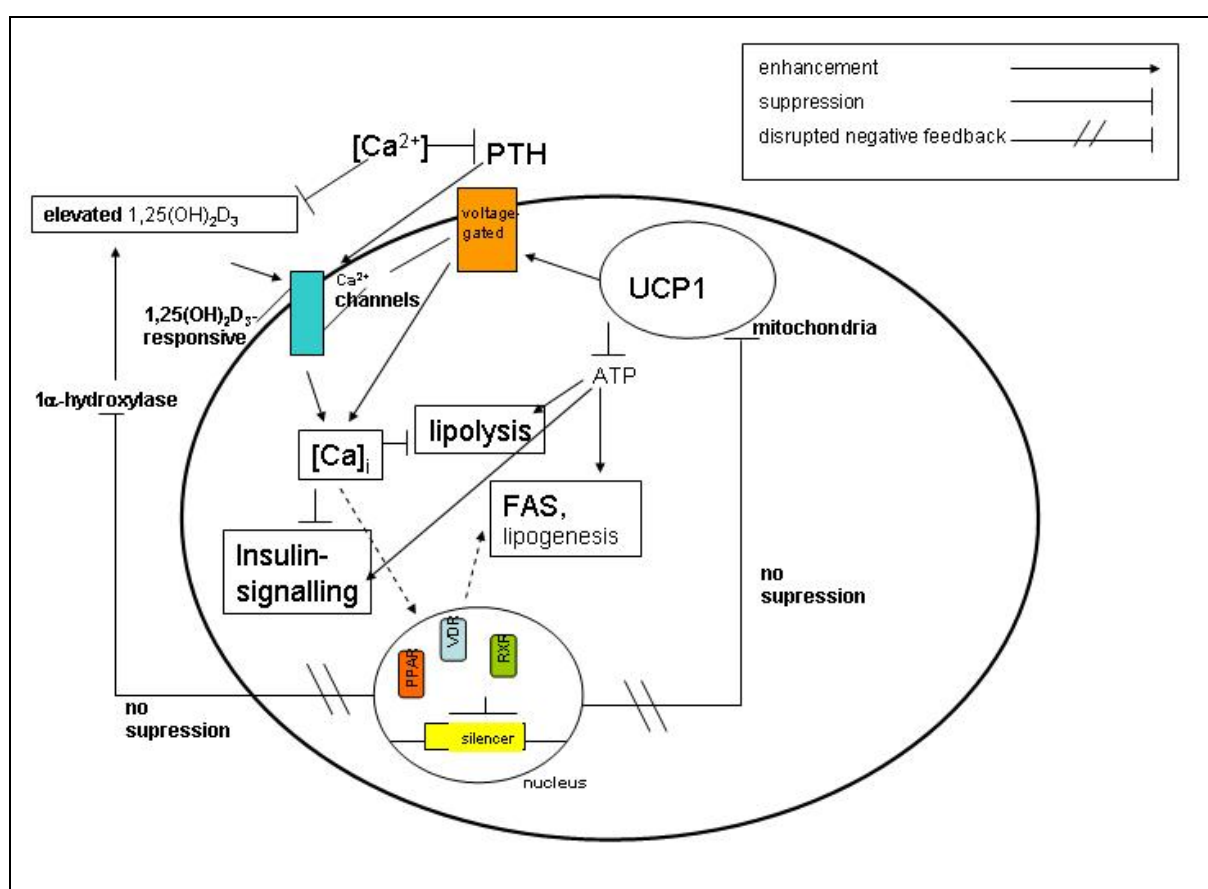


Figure 3.2.9: Scheme describing mechanisms of altered lipid and energy metabolism in cells of VDRKO mice with dysfunctional VDR. Low serum $[Ca^{2+}]$, increased PTH levels and a disrupted negative feedback loop for 1α -hydroxylase lead to increased production of active vitamin D and Ca^{2+} influx through calcium channels, in response to $1,25(OH)_2D_3$, $1\alpha,25(OH)_2lumisterol_3$ or PTH. Elevated $[Ca]_i$ stimulates lipogenesis and FAS expression and inhibits lipolysis and insulin signalling. Non-functional VDR, competing with PPAR and other nuclear hormone receptor for RXR, can not mediate suppression of UCP1 transcription by $1,25(OH)_2D_3$, which leads to increased uncoupling and decreased production of ATP and ROS. ATP in turn is needed for lipogenesis, lipolysis and insulin signalling. This scheme is a modified version of a model proposed by Zemel et al. (Zemel 2004), extended by the author of this thesis.

Promoter analysis of the 5' upstream region of the UCP1 gene and transfection assays identified peroxisome proliferator-activated receptor α (PPAR α) and RAR/RXR as potent inducers (Barberá, MJ 1486). As already discussed before, there is mounting evidence for cross-talk between nuclear hormone receptors. Vitamin D receptor has been shown to repress PPAR α signalling in a ligand-dependent manner (Sakuma et al. 2003). In VDRKO mouse kidney, the truncated VDR

apparently is unable to inhibit induction of UCP1 expression by PPAR α independent from the diet.

Cidea, as well as fat specific protein 27 (Fsp27), members of the CIDE family of proteins, were strongly up-regulated in ND and RD VDRKO mouse kidney. Overexpression of Cidea was reported to cause caspase-independent cell death (Inohara et al. 1998), whereas ablation of the Cidea gene resulted in lean mice, resistant to obesity, with increased expression of UCP1 (Zhou et al. 2003). UCP1 and FSP27 were both strongly up-regulated in kidney and heart from VDRKO mice. One explanation might be that activating factors like PPAR α and the lack of suppression through VDR outweigh attenuation of UCP1 expression by Cidea. Increased expression of Cidea might also be secondary to the activation of mitochondrial uncoupling, induced by a feedback loop mechanism. Recently it was shown that the protein products of the Cidea gene binds to UCP1 and inhibits uncoupling (Lin and Li 2004).

In any case, there are many indications of activated lipid turnover in VDRKO mice. Activation of both, lipogenesis and lipid catabolism is also indicated by the up-regulation of cytosolic acetyl-CoA hydrolase (CACH) in ND VDRKO kidney, providing free cytosolic CoA for lipid metabolism (Matsunaga et al. 1985; Suematsu et al. 2002). Since VDRKO mice, especially in the case of hypocalcemic mice on a normal diet have a lean phenotype, supports the conclusion that UCP1 might have an important role connecting vitamin D signalling and obesity. The fact that the expression of a number of genes involved in lipid metabolism cannot be normalised by dietary means, crosstalk between nuclear receptors and proven nongenomic actions of vitamin D contradict the hypothesis that inactivation of VDR might abrogate both, genomic and non-genomic actions of vitamin D (Erben et al. 2002) on metabolic processes.

A recently published study showed that uncoupling itself has dual effects on lipogenesis: By activating voltage-gated calcium channels, mitochondrial uncouplers increase $[Ca]_i$ in a dose-dependent manner, an effect that can be blocked by the non-specific calcium channel antagonist lanthanum (Sun and Zemel 2003). While elevated $[Ca]_i$ promotes FAS expression as pointed out before, decreased ATP production through uncoupling can lead to an inhibition of energy-dependent processes like lipolysis (HSL phosphorylation) or *de novo* lipogenesis by FAS and other lipogenic enzymes, an effect that can be reversed by addition of ATP (Sun and Zemel 2003). ATP, a universal energy carrier, is required for a multitude of cellular processes and needed for insulin signalling. Increased concentrations of cytosolic calcium were reported to decrease insulin sensitivity and glucose uptake and therefore were related to insulin resistance and diabetes type 2. Glucose challenging of pancreatic cells from the same VDRKO mouse resulted in lower insulin secretion rates, in comparison to WT littermates (Zeitz et al. 2003). Oral administration of 1,25(OH) $_2$ D $_3$ was able to protect non-obese diabetic mice, an animal model for insulin-dependent type 1 diabetes (IDDM) from the onset of the disease (Zella et al. 2003). Expression of VDR and CYP1 α in activated T-lymphocytes are further indications for a role of vitamin D signalling in the development/protection of the autoimmune disease IDDM.

Table 3.2.3a: Candidate genes up-regulated in RD VDRKO / WT mouse kidney, putatively involved in lipid metabolism / energy production.

mean fold expression	error	RD	Genbank ID	abbreviation	name	function / keywords
3.88	1.17	MG-14-39o18	NM_009463	UCP1	uncoupling protein 1	mitochondrial brown fat uncoupling protein
3.27	0.26	MG-3-10e17	NM_178373	Fsp27	fat specific gene 27	apoptosis inducing
2.21	0.92	MG-3-5k15	NM_008574	Mcsp	mitochondrial capsule selenoprotein	n.a.
1.96	0.16	MG-3-68k10	AF159298	Pde1a	phosphodiesterase 1A, calmodulin-dependent	up-regulated in response to pressure overload
1.92	0.13	MG-12-140c23	NM_007825	CYP7b1	cytochrome P450, 7b1.	cholesterol metabolism
1.79	0.16	MG-11-2n19	NM_008340	ALS; IGFALS	insulin-like growth factor binding protein acid labile subunit	cell adhesion, IGF-binding
1.54	0.11	MG-3-16d22	BC048825	Abcc3	ATP-binding cassette, sub-family C (CFTR/MRP), member 3	canalicular bile acid transport
0.31	0.05	MG-6-34b12	AK014649	D-LCR, Ldhd	D-lactate dehydrogenase, ferricytochrome c oxidoreductase	Energy metabolism; Flavoprotein; FAD
0.32	0.12	MG-12-142f22	NM_007822	CYP4a14	CYP4a14	indirectly regulates blood pressure
0.49	0.10	MG-16-167j4	NM_010591	AP-1, Junc, c-jun	Jun: Jun oncogene	activates C/EBPbeta

Table 3.2.3b: Candidate genes down-regulated in RD VDRKO / WT mouse kidney, putatively involved in lipid metabolism / energy production.

0.50	0.08	MG-6-71o8	AV298856	Dtr, DTS, HB-EGF	diphtheria toxin receptor	up-regulation by IGF-1, essential for normal heart function
0.52	0.23	MG-6-2g3	BC054782	Hspa1a /HSP70A1	heat shock protein 1A	vitamin D signalling, protection against myocardial infarction
0.54	0.03	MG-26-226j8	NM_133808	Hdlbp	high density lipoprotein (HDL) binding protein	lipid binding
0.56	0.06	MG-12-1k1	BC014696	Cml3	camello-like 3	carbohydrate transport and metabolism
0.57	0.07	MG-12-254e12	NM_139065	n.a.	similar to APOBEC-1 stimulating protein [Homo sapiens]	heterogeneous nuclear ribonucleoprotein R
0.57	0.10	MG-14-82j17	NM_008509	Lpl	Lpl: lipoprotein lipase	lipid metabolism
0.61	0.09	MG-15-164g13	NM_026268	Dusp6, MKP3	dual specificity phosphatase 6	PI3/Akt pathway
0.77	0.08	MG-12-249o2	NM_144916	TM6P1	fasting-inducible integral membrane protein TM6P1	n.a.
0.78	0.05	MG-16-76p12	NM_021534	Pxmp4, Pmp24	peroxisomal membrane protein 4	n.a.
0.79	0.09	MG-14-57f10	NM_015763	Lpin1	Lpin1	lipid metabolism
0.84	0.13	MG-26-97e2	NM_010492	ICA69	islet cell autoantigen 1	ICA69(null) nonobese diabetic mice develop diabetes

Table 3.2.4a: Candidate genes down-regulated in ND VDRKO / WT mouse kidney, putatively involved in lipid metabolism / energy production.

mean fold expression	error	ND	Genbank ID	abbreviation	name	function / keywords
0.12	0.01	MG-12-204i1	A55281	ES-4	liver / kidney carboxylesterase 4, microsomal palmitoyl-CoA hydrolase	esterases and lipases
0.30	0.03	MG-6-3n18	BC009158	TIM9 B.	mitochondrial import inner membrane translocase subunit TIM9 B.	mitochondrion; transport
0.31	0.02	MG-12-247j17	Mm.154782	Cml4	camello-like 4 Cml4	cell adhesion; fatty acid / phospholipid metabolism
0.32	0.05	MG-6-34b12	AK014649	D-LCR, Ldhd	D-lactate dehydrogenase, ferricytochrome c oxidoreductase	energy metabolism; Flavoprotein; FAD;
0.32	0.02	MG-12-219i14	BC024450	HXM-A	acetyl-CoA synth. 3, xenobiotic/medium-chain fatty acid:CoA ligase	hypertension-associated, lipid transport / -metabolism
0.36	0.02	MG-3-77p17	AB078618	Cach	cytosolic acetyl-CoA hydrolase	lipid metabolism
0.36	0.06	MG-8-12h24	NM_008062	G6PD	glucose-6-phosphate 1-dehydrogenase X	carbohydrate metabolism

3.2.4b: Candidate genes up-regulated in ND VDRKO / WT mouse kidney, putatively involved in lipid metabolism / energy production.						
6.45	1.6	MG-8-46e22	AK075843	Apo-E	apolipoprotein E precursor	VLDL; HDL; lipid transport; heparin-binding
11.40	5.6	MG-6-61p12	BM124941	CIDE-A	cell death activator CIDE-A	apoptosis, regulation of energy dissipation
7.63	3.7	MG-6-21i12	AW411843	DPDE4	cAMP-dependent 3',5'-cyclic phosphodiesterase 4B	cAMP; Hydrolase; Central intermediary metabolism
6.67	0.67	MG-12-184j5	AK050078	Hpcl	2-hydroxyphytanoyl-CoA lyase	peroxisome, lipid metabolism
4.73	0.53	MG-12-171j2	AK034169	Pte2a	Pte2a-pending: peroxisomal acyl-CoA thioesterase 2A	serine esterase; hydrolase
4.63	0.72	MG-12-146c2	AK029029	ELOVL6	long chain fatty acyl elongase	elongation of long chain fatty acids
4.53	0.84	MG-8-70n14	AK028008	Mgll	monoglyceride lipase	n.a.
4.00	0.74	MG-16-127o18	NM_010357	Gsta4	Gsta4; Glutathione S-transferase, alpha 4	fatty acid metabolism
3.93	0.35	MG-14-2c21	AY044241	Glul, GS, Glns	glutamate-ammonia ligase (glutamine synthase)	fatty acid and phospholipid metabolism
3.93	0.48	MG-3-27f11	BF384201	APO-E	apolipoprotein E precursor (APO-E).	HDL; Plasma; Signal; Lipid transport
3.33	0.57	MG-6-48g14	BI738553	Pkm2, Pk3	pyruvate kinase 3, m2 isoenzyme	glycolysis; energy production, stimulated by insulin
3.27	0.47	MG-16-5g10	AF127033	Fas	fatty acid synthase	fatty acid synthesis
3.17	0.43	MG-12-212p20	AK086805	Mrpl23	mitochondrial ribosomal protein L23	n.a.
2.93	0.50	MG-3-2m2	BF449796	PGDS2, PGDS	prostaglandin-D synthase, glutathione-independent PBG synthase	Lipocalin; Glycoprotein
2.63	0.08	MG-12-252p13	NM_011817	Gadd45g	growth arrest and DNA-damage-inducible 45 gamma (Gadd45g).	putative function in the regulation of body weight
2.63	0.36	MG-16-51o13	NM_010174	FABPH1; FABP3	fatty acid binding protein 3, muscle and heart	lipid transport
2.57	0.33	MG-8-21b10	AI255996	CPB-II, annexin VI	lipocortin VI, chromobindin 20, calelectrin, calphobindin-II	calcium/phospholipid-binding;
2.57	0.36	MG-16-5p18	BB214612	COX7A	cytochrome C oxidase	oxidoreductase; mitochondrion; energy metabolism
2.53	0.15	MG-12-255b22	NM_008182	Gsta2	glutathione S-transferase GT41A	fatty acid metabolism
2.30	0.07	MG-6-22h16	BC012400	Acaa1	acetyl-Coenzyme A acyltransferase 1, 3-ketoacyl-CoA thiolase A	fatty acid and phospholipid metabolism
2.30	0.12	MG-6-54h14	BM249584	Acly	ATP citrate lyase	phosphorylation; lipid synthesis; energy production

3.2.5 Blood pressure control

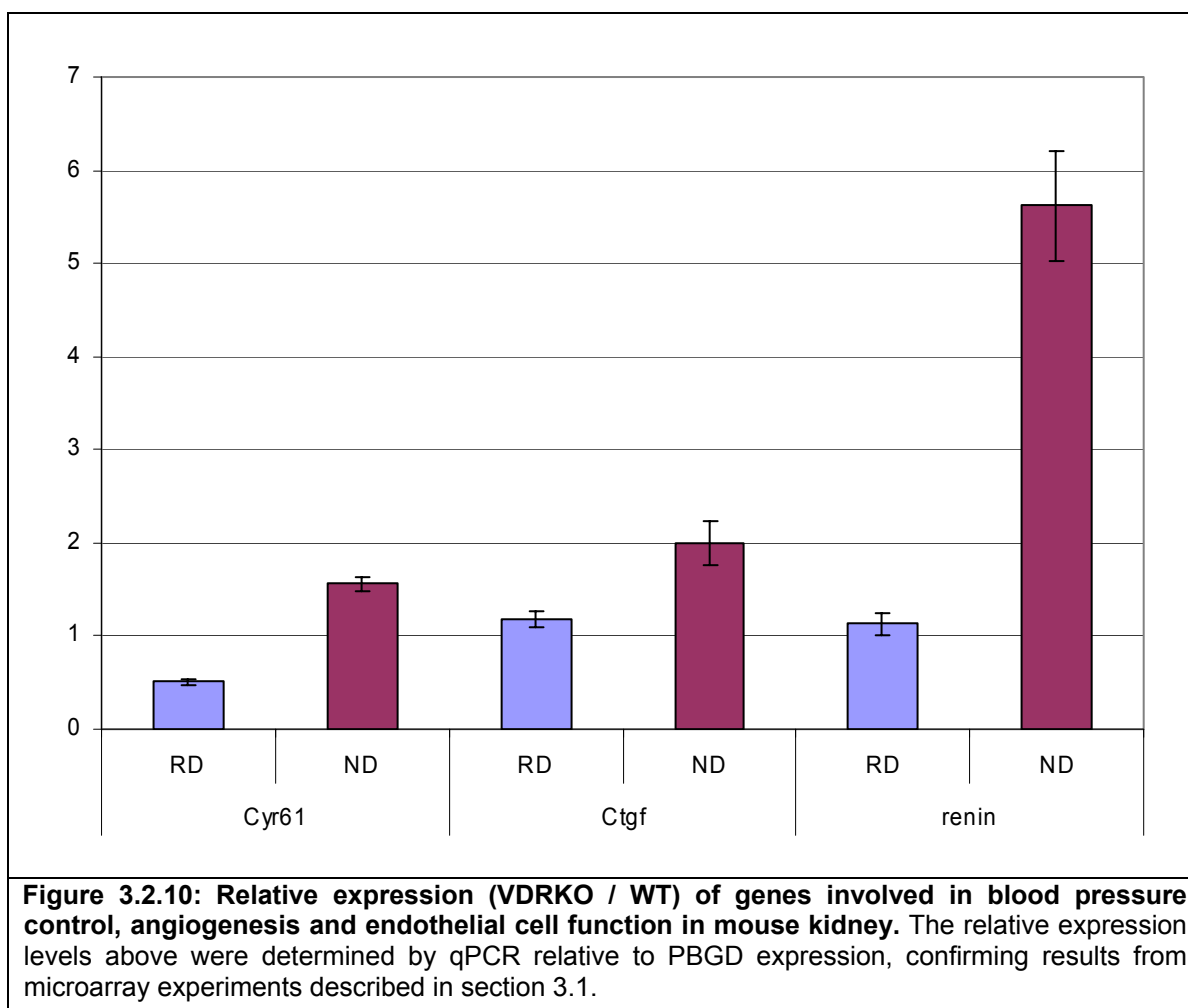
Like diabetes, hypertension is part of the metabolic and cardiovascular diseases, which were for a long time known to be linked to obesity and age. The body-mass index (BMI) is a medical parameter that is widely accepted as a link between these conditions on the macroscopic scale (Sharma 2003). However, on molecular level, the search for biochemical and genetic factors, controlling the mechanism of this linkage, is still ongoing. Recent studies reported dysregulation of intracellular calcium (Zemel 2001) to be one of the major causes, which explains the involvement of the calciotropic hormones vitamin D and PTH as potential key factors in the development of hypertension. The influence of increased dietary intake of calcium on the reduction of blood pressure in a series of clinical studies (McCarron et al. 1982; McCarron 1995) was explained by the suppression of vitamin D synthesis. This in turn reduced vitamin D-mediated influx of calcium through the cellular membrane of vascular smooth muscle cells. Like in adipocytes (Shi et al. 2001b), activation of calcium influx is not mediated by the nuclear vitamin D receptor and occurs as a rapid, non-genomic response (Fleet 1999). Increased intracellular calcium in vascular smooth muscle cells has a positive effect on peripheral vascular resistance, resulting in a rise in blood pressure.

As explained above, parathyroid hormone can stimulate vitamin D synthesis via activation of 1-alpha hydroxylase CYP1 α , which is transcriptionally controlled by

1,25(OH)₂D₃-levels in a VDR-mediated negative feedback loop. Diets with high salt content can induce a decrease in renal calcium reabsorption, activate parathyroid glands to excrete additional PTH, which triggers the mechanism described above, leading to essential hypertension. In mice with ablated nuclear VDR function, both, high PTH levels and a disrupted control of CYP1 α increase the production of 1,25(OH)₂D₃.

An important regulator of blood pressure, electrolyte and volume homeostasis in kidney is the renin-angiotensin system. Renin, a protease synthesized in juxtaglomerular cells of the nephron, cleaves liver-derived angiotensinogen (AGT) in a rate-limiting step to produce angiotensin I, which is then further converted by the angiotensinogen-converting enzyme ACE into angiotensin II (Ang II). Ang II, an important vasoconstrictor, stimulates water and salt uptake in mice (Li et al. 2002) and increased production of Ang II can lead to hypertension and cardiac hypertrophy. Ang II can act as an endocrine hormone or, when synthesized locally in kidney, heart or brain, as an autocrine or paracrine effector (Sigmund 2002). A recent study investigating the effect of VDR gene ablation in mice on the renin-angiotensin system revealed significant up-regulation of renin expression in VDRKO mouse kidney. Blood diastolic and systolic blood pressure in VDRKO mice were significantly elevated, as was the heart weight / body weight ratio, a potential indication for the onset of hypertension-induced cardiac hypertrophy. Treatment of WT mice with active vitamin D and in vitro experiments on mouse glomerular AS4.1 cells, transfected with human VDR and a reporter gene fused to the murine renin 5' promoter region, showed VDR-mediated suppression of renin expression (Li et al. 2002). The disruption of this suppressing mechanism in VDRKO mice explains the up-regulation of renin expression in VDRKO mouse kidney.

Up-regulation of renin mRNA in VDRKO mouse kidney (with respect to WT) was not detected by microarray analysis, but measured by quantitative real-time PCR (qPCR), see figure 3.2.10 below. In contrast to the findings of Li et al., the increase in renin expression was found reduced almost to WT levels in VDRKO mice, supplemented with a calcium-rich rescue diet (Li 2003). Apart from direct regulation by 1,25(OH)₂D₃ via the VDR, renin expression can be suppressed by endothelin-1 signalling via phospholipase C and the release of intracellular calcium (Ryan et al. 2002). Other factors mediating renin expression are renal perfusion pressure, tubular sodium load and vasoconstrictors like vasopressin, adenosine and the product angiotensin II itself via a negative feedback loop. Stimulation of renin production can be induced by vasodilating nitric oxide (NO), prostaglandins and adrenomedullin.



Apart from its role as vasoconstrictor, Angiotensin II was reported to be directly involved in the development of fibrosis in heart and kidney by stimulating the expression of connective tissue growth factor (CTGF) via a calcineurin-dependent pathway (Finckenberg et al. 2003). Increased expression of CTGF was observed in the heart of RD VDRKO mice (see section 4), and in kidneys from ND mice. Although a significant increase of VDRKO mouse heart weight relative to body weight (Li et al. 2002; Erben 2004) might indicate the onset of cardiac hypertrophy, indicators for extracellular matrix accumulation, like increased collagen 1 and 3 production were not detected. As hypertrophy and fibrosis progresses with age, further systematic studies, characterising changes in the histology and expression profiles of VDRKO mouse heart and kidney with age, might be necessary to acquire further evidence about the role of vitamin D action in the development of these diseases. The angiogenic factor Cyr61 (CCN1) was significantly up-regulated in ND mouse kidney ((1.55 +/- 0.16)-fold), but down-regulated in kidneys from normocalcemic VDRKO mice ((0.47 +/- 0.08)-fold), determined by qPCR, respectively. Cyr61 was found overexpressed in several types of cancer, inflammations and in bone during fracture repair, see introduction and section 1.

The induction of CTGF expression via calcineurin is antagonised by calcipressin (DSCR, CSP1). In kidneys of ND VDRKO mice Csp1 was up-regulated by a factor of (2.04 +/- 0.04), in confirmation experiments by qPCR (1.98 +/- 0.12)-fold. Normalisation of calcipressin expression in RD VDRKO mouse kidneys (qPCR: (0.91 +/- 0.12)-fold) indicates indirect regulation of Csp1 via calcium or PTH. Apart from regulating the expression of CTGF, calcineurin is associated with signal transduction

pathways underlying immune response, cardiac hypertrophy and stroke. In transgenic mice lacking the gene encoding Csp1, calcineurin-dependent activation of apoptotic pathways lead to the premature death of T helper type 1 cells (Ryeom et al. 2003). While chronic overexpression of Csp1 *in vivo* was associated with Alzheimer disease (Ermak et al. 2001) and protects against calcineurin-induced cardiac hypertrophy (Rothermel et al. 2001), *in vitro* studies showed a protective effect of Csp1 overexpression against cell death caused by oxidative stress (Ermak et al. 2002). Since oxidative stress is connected to increases of the concentration of intracellular calcium, it is not surprising that Csp1 also can prevent apoptosis in cells exposed to calcium stress (Ermak et al. 2002).

Bradykinin is a prominent member of the peptide hormone family of kinins that confer as vasodilators protection against hypertension, myocardial hypertrophy and fibrosis (Linz et al. 1992). The activity of kinins is, to a large extent, determined by the rate of enzymatic degradation through kininases, such as carboxypeptidase N (CPN), aminopeptidase P (APP) or angiotensin I-converting enzyme (ACE). ACE, which links bradykinin degradation with Ang II formation and CPN are the major factors for kininase activity in human blood serum (Sheikh and Kaplan 1989). This was the reason to develop ACE inhibitors, that are used in the therapeutic treatment of cardiovascular diseases (Linz et al. 1995; Dendorfer et al. 2001). In VDRKO mouse kidney of RD mice with normalised serum calcium levels CPN was found significantly up-regulated by (2.66 +/- 0.22)-fold with respect to WT animals.

As mentioned in section 3.1 above, two enzymes of the cytochrome P450A and CYP4B family were down-regulated in RD VDRKO mouse kidney with respect to WT, which could be verified by qPCR. These enzymes are involved in the metabolism of arachidonic acid to 20-hydroxyeicosatetraenoic acid (20-HETE) and epoxyeicosatrienoic acids (EETs), which promote salt excretion and act as vasodilators, respectively (Linz et al. 1995). Deficiency of 20-HETE generating CYP4A enzymes in renal tubular cells was related to salt-sensitive hypertension in rats (Makita et al. 1994; McGiff and Quilley 1999; Roman 2002).

The previously discussed up-regulation of aquaporin Aqp2 in the kidneys of hypocalcemic ND VDRKO mice by (2.33 +/- 0.11)-fold in comparison to WT kidneys might also contribute to the observed symptoms of increased blood pressure and the onset of fibrosis in this mouse model (Wang, W. et al. 2002).

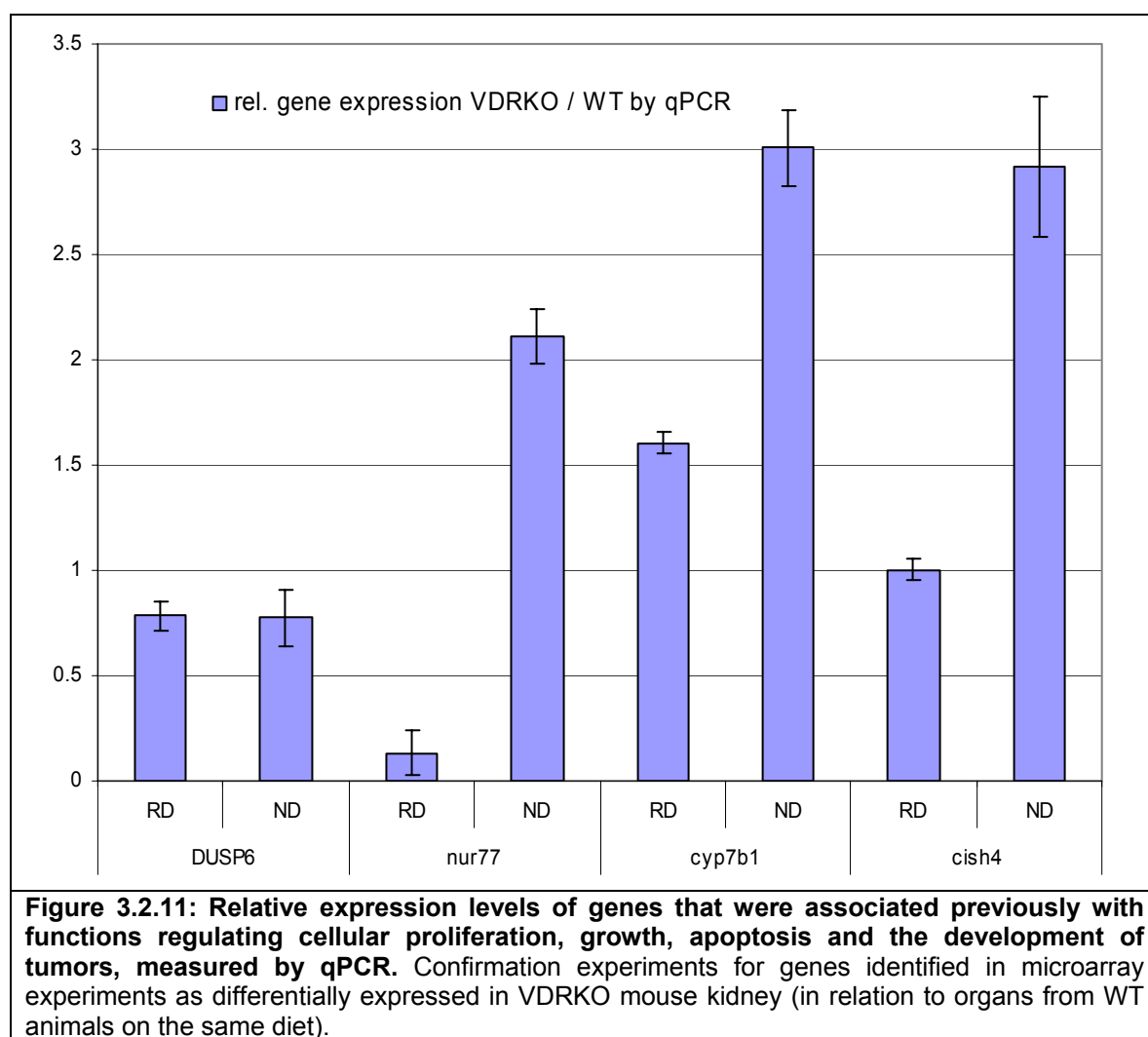
3.2.6 Cell growth, proliferation, apoptosis and cancer

There is an enormous amount of evidence for the chemopreventive effects of 1,25(OH)₂D₃ in cancers (Lin and White 2004), particularly in colon (Grant and Garland 2004) and prostate (Chen and Holick 2003). The antiproliferative effects of vitamin D depend on VDR-mediated transcriptional control, evidenced by overexpression and suppression of VDR in experiments with prostatic cancer cell lines (Miller 1998). Local expression of mitochondrial CYP1 α in prostate cells (Schwartz et al. 1998) and the linkage between circulating levels of 25(OH)D₃ and prostate cancer further supports an important role of vitamin D in cancer prevention. Although *in vitro* experiments revealed a number of vitamin D-responsive genes involved in apoptosis, differentiation and cell-cycle arrest, the precise mechanism of vitamin D - mediated arrest of tumor growth is still unclear. Gene expression profiling of VDRKO mouse kidneys in this work could identify additional vitamin D-responsive

genes involved in processes controlling tumor growth and thus might contribute to the elucidation of pathways and potential targets for drug development.

A prominent member of apoptosis-regulating proteins that target mitochondrial membranes is BCL-2. By controlling the membrane permeability of apoptogenic proteins, members of the BCL-2 protein family can promote or suppress the release of mitochondrial proteins like cytochrome c. Cytochrome c triggers a pathway leading to apoptosis via activation of Apaf-1 and caspase-9. BCL-2 was found up-regulated in different tumors. Calcitriol was reported to induce apoptosis in human prostate cancer LNCaP cells, which could be prevented by overexpression of BCL-2 (Blutt et al. 2000). Vitamin D-induced apoptosis after LNCaP treatment was in parallel with up-regulation of proapoptotic BCL-X_L and down-regulation of protective BCL-2. Paradoxically, BCL-2, known for antiapoptotic functions in models of renal injury or prostate cancer (Saikumar and Venkatachalam 2003), can also promote cell death (Lin et al. 2004). A key factor in the conversion of BCL-2 "from protector to killer" (Lin et al. 2004) seems to be the orphan nuclear receptor Nur77 (TR3, Nr4a1, NGFIB) that induces a conformational change of BCL-2. Nur77 was observed to initiate the release of cytochrome c and apoptosis after translocating from the nucleus to mitochondria in response to apoptotic stimuli (Li et al. 2000). This non-genomic, proapoptotic action of Nur77 is in contrast to its function in modulating transcription as a nuclear hormone receptor: Similar to LXR, PPAR and RAR, Nur77 heterodimerises with retinoid X receptor RXR and initiates transcription after trafficking to the nucleus and binding to RAR-responsive elements (RARE). Transcriptional activity of Nur77 can even promote cell proliferation. Translocation of Nur77 to the mitochondria, but not Nur77 transactivation, seems to be required for the proapoptotic functions of retinoids in cancer cells (Li et al. 2000; Zhang 2002).

Figure 3.2.11 shows that, like in microarray experiments, Nur77 is significantly up-regulated in VDRKO mouse kidneys from hypocalcemic ND animals according to measurements by qPCR. In normocalcemic RD mouse kidneys, however, inactivation of the VDR down-regulates Nur77 expression. Up-regulation of Nur77 in ND VDRKO mouse kidneys might be due to the elevated serum levels of PTH in these animals, as PTH was shown to induce Nur77 expression (Tetradis et al. 2001). Nur77 expression was also reported to respond to increases of intracellular calcium after treatment of cells with a calcium ionophore (Watanabe et al. 2001). In the case of ND VDRKO mice, the ionophore might be either PTH or calcitriol, produced in large amounts due to the inactivated feedback loop controlling calcitriol-activating CYP1 α . In RD mice, serum levels of both, PTH and vitamin D, are lower, reducing cytosolic calcium and activation of Nur77 expression via non-genomic mechanisms. Here, the lack of VDR transactivation might be the reason for the down-regulation of Nur77.



Cytokine-inducible Src homology domain-containing protein CISH was significantly up-regulated in kidneys from male VDRKO mice on normal diet. CISH has been implicated in the suppression of signalling through cytokine receptors. In erythroid progenitor cells, CISH was reported to promote apoptosis by blocking signalling across the STAT5 pathway through the erythropoietin receptor (EpoR) (Ketteler et al. 2003). Interestingly, an EST regulated by erythropoietin, was up-regulated by (6.3 +/- 1.2)-fold in kidneys of ND VDRKO mice. The exact mechanism of the inhibition of proliferation of cell lines through CISH is still poorly understood, but was suggested to be a result of competition of the SH2 domain of CISH with the transcription factor STAT5 for binding to EpoR (Sasaki et al. 2000)

Independent of cytosolic or plasma calcium levels appears to be the expression of the dual-specificity phosphatase6 DUSP6, which was found to be down-regulated in VDRKO mouse kidneys, irrespective of the diet. In primary pancreatic cancer tissues there was a high incidence of loss of heterozygosity observed at chromosome 12q, the position of the gene coding for DUSP6 in humans (Furukawa et al. 1998; Kimura et al. 1998). In cultured pancreatic cancer cells, expression of DUSP6 was lost. DUSP6 is a phosphatase specific for extracellular signal-regulated kinase (ERK). Dephosphorylation of ERK by DUSP6 shuts down growth-stimulating signalling along the mitogen-activated protein kinase (MAPK) pathway, considered as an important feedback loop in cell growth control (Keyse 2000). Downregulation of DUSP6, as in VDRKO mouse kidney, can abrogate this feedback loop and lead, at least in the case of pancreatic carcinoma, to uncontrolled cell growth, carcinogenesis and progression.

Adenovirus-mediated transfection of pancreatic cancer cells with DUSP6 could stop cell growth and induce apoptosis (Furukawa et al. 1998).

As mentioned already in chapter 3.1.2.4, CYP7b1 is involved in cholesterol metabolism, but also can hydroxylate 5α -androstane- 3β - 17β -diol (3 β Adiol), a metabolite of 5α -dihydrotestosterone (DHT). In contrast to kidneys from female VDRKO mice, in kidneys from male VDRKO mice the expression of CYP7b1 is up-regulated for both diets (see results from qPCR in figure 3.2.11 above). Since 3 β Adiol can inhibit androgen-driven proliferation by repressing the expression of androgen receptor in prostate, prostates from CYP7b1 $-/-$ mice were reduced in growth after puberty with respect to those from WT littermates (Weihua et al. 2002). Growth control by 3 β Adiol requires the expression of a functioning estrogen receptor ER β , which explains why ER β expression gets lost in advanced prostate cancer (Royuela et al. 2001). Increase of CYP7b1 expression with VDR ablation in normocalcemic mice might elevate the risk of these animals to hyperproliferative diseases of AR-expressing tissues. If the observations made here for kidney are analogical in prostate, suppression of CYP7b1 expression by vitamin D might a mechanism to prevent the progression of prostate cancer.

4. Expression analysis of VDRKO and WT mouse heart

In the experiments with kidneys from VDRKO and WT mice a number of genes were differentially expressed that previously had been attributed to symptoms of hypertension and cardio-vascular diseases. Therefore and because of several reports in the literature, suggesting an important role of vitamin D action in heart function and disease, I decided to analyse the expression profile of VDRKO mouse heart (Li et al. 2002; Holick 2004).

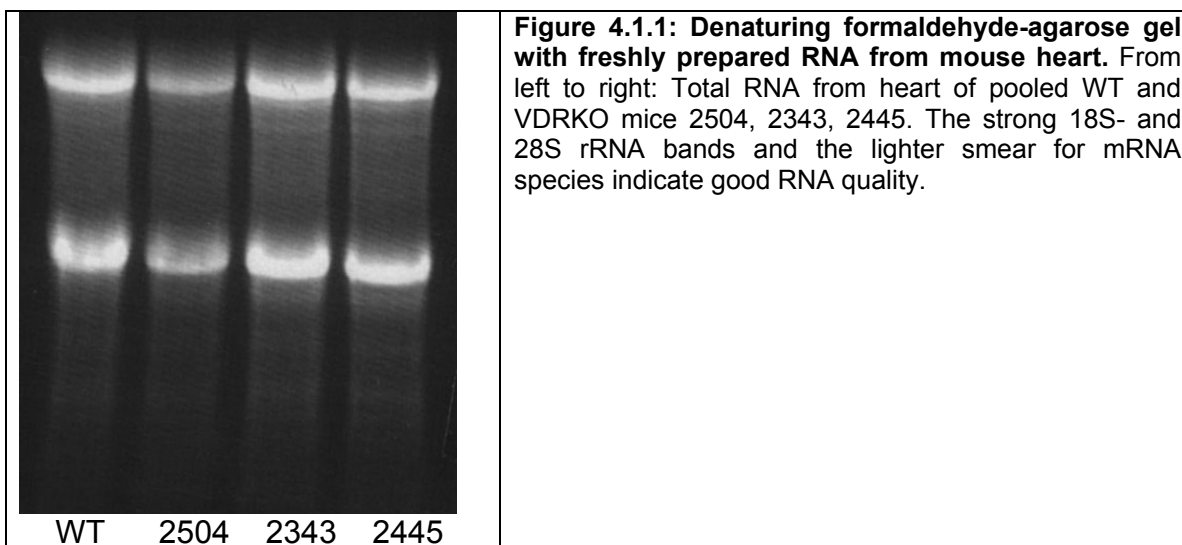
4.1 Microarray experiments: Experimental set-up

Hearts from male age-matched mice, raised on rescue diet (RD) were isolated and frozen at -80° C. For microarray analysis, the RNA extracted from the hearts of four wild type (WT) animals was pooled as reference and labelled indirectly with cyanine 3 / 5 as described above. The RNA from the hearts of three vitamin D receptor knockout (VDRKO) mice was pooled and labelled with cyanine dye, as well.

Table 4.1: Mouse hearts (VDRKO and WT), obtained from K. Weber, University of Munich. Only hearts from age-matched mice fed with a calcium and phosphorous-rich rescue diet (RD) were used for RNA extraction and subsequent gene expression analysis with DNA microarrays and real-time PCR.

Mouse Number	Diet	Sex	Genotype	Age [months]	Heart Weight [g]
2501	RD	m	WT	19	164
2502	RD	m	WT	19	188
2407	RD	m	WT	20	181
2414	RD	m	WT	20	173
2343	RD	m	VDRKO	20	179
2445	RD	m	VDRKO	19	175
2504	RD	m	VDRKO	19	172

In order to reduce experimental variation due to microarray quality, hybridization and wash conditions, gene expression of these RNA pools was directly compared in 5 replicate microarray experiments. To exclude artifacts due to different dye incorporation and fluorescence properties of Cy3 and Cy5, two dye swap experiments were included.



As in experiments with kidneys, the samples were hybridised onto 21K-cDNA mouse arrays overnight in a buffer containing 50% formamide. After a series of stringent washes the slides were scanned on an Axon 4000 instrument with 100% laser power and optimised photomultiplier (PMP) gain. Images were processed with GenePix 3.0 software, intensities measured and attributed to the respective gene identifiers and annotations provided by Lion Biosciences.

Table 4.1.2: Labeling scheme and array probe coverage in 5 replicate experiments of pooled RNA from male WT against VDRKO mouse heart. In three experiments cDNA labeling followed the standard pattern (WT Cy3, KO Cy5). In two experiments, the labeling dyes were exchanged. As expression levels have to be similar in replicate hybridisations, the differences in probe coverage (= percentage of spots giving a signal above background noise) can be attributed predominantly to varying background and signal-to-noise ratios.

experiment	WT labeling	VDRKO labeling	probe coverage %
1_heartQ	Cy5	Cy3	80,1%
2_heartQ	Cy5	Cy3	69,6%
3_heartQ	Cy3	Cy5	69,5%
4_heartQ	Cy3	Cy5	66,6%
5_heartQ	Cy3	Cy5	71,0%

The relative probe coverage indicates the percentage of spots that were identified by the GenePix software as "good" in terms of spot roundness, intensity distribution across the surface and giving a positive fluorescence signal (after background subtraction). Since each spot was scanned twice for each fluorescence channel, also the quality criteria had to be fulfilled for each channel. In experiment 1_heartQ 16947 of the total 21168 analyzed spot positions were flagged as "good", which is 80,1% of the total amount of spots (probes). Experimental artifacts (eg. cross hybridisations) and a small redundancy in the probe set add to the number of "real" expressed genes in the analysed tissue. In the following, the procedure of data analysis, used in the microarray study of mouse heart, is explained at the example of experiment 1_heartQ.

4.2 Analysis of microarray data

Raw data files were converted from the GenePix .gpr format into the .mev format used by the TIGR TM4 software package MIDAS. Scatter plots of the raw data give a first impression about the data quality obtained from each experiment (see figure 4.2.1-5).

To make the data within and between experiments comparable and to attenuate saturation effects and influences of spatial inhomogeneities on the arrays, the data were further filtered and normalised. Blockwise locally weighted linear regression (LOWESS) analysis with a smoothing factor of 0.33 and Cy3 as the standard reference was chosen for normalisation (Quackenbush 2002).

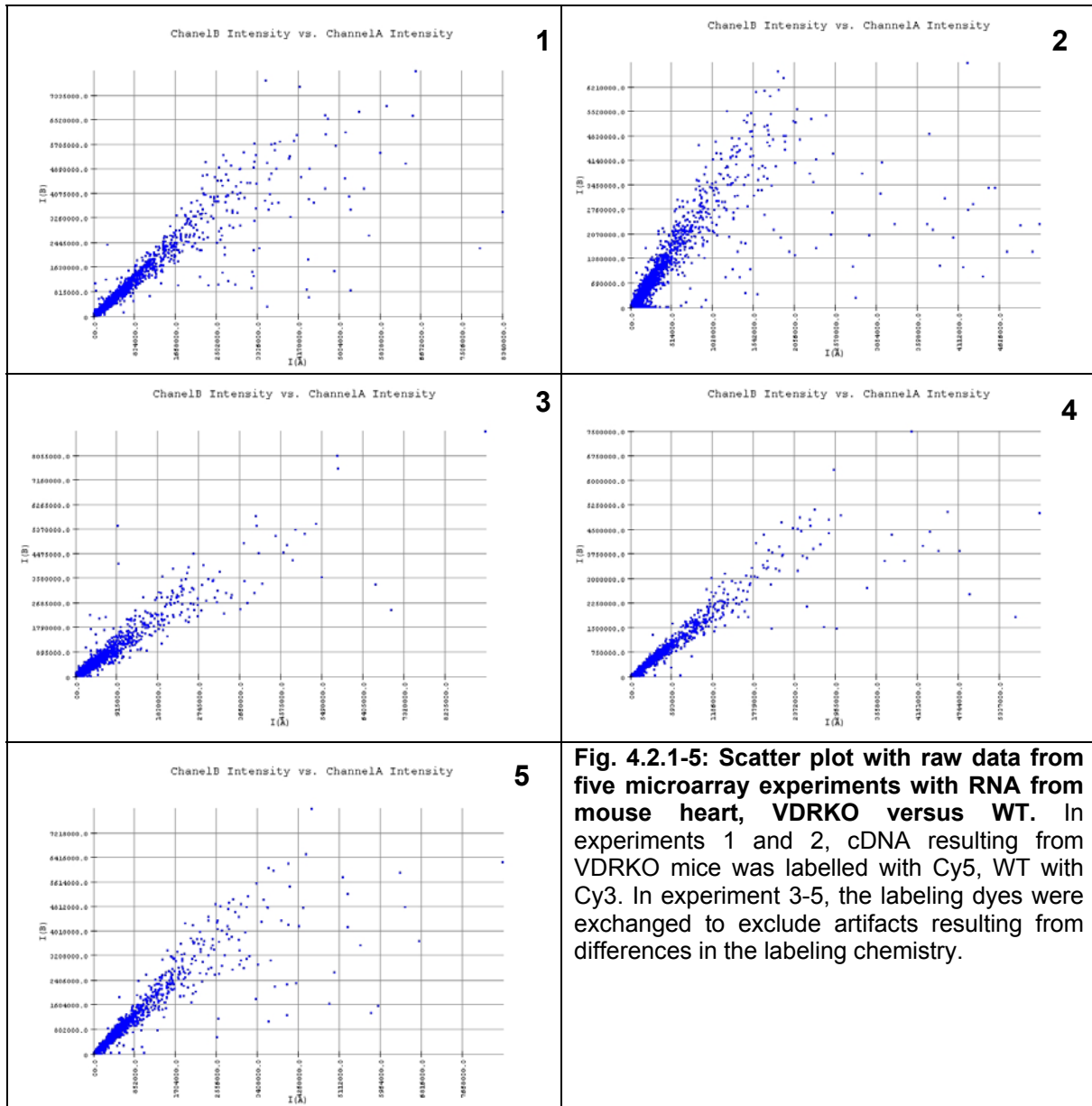
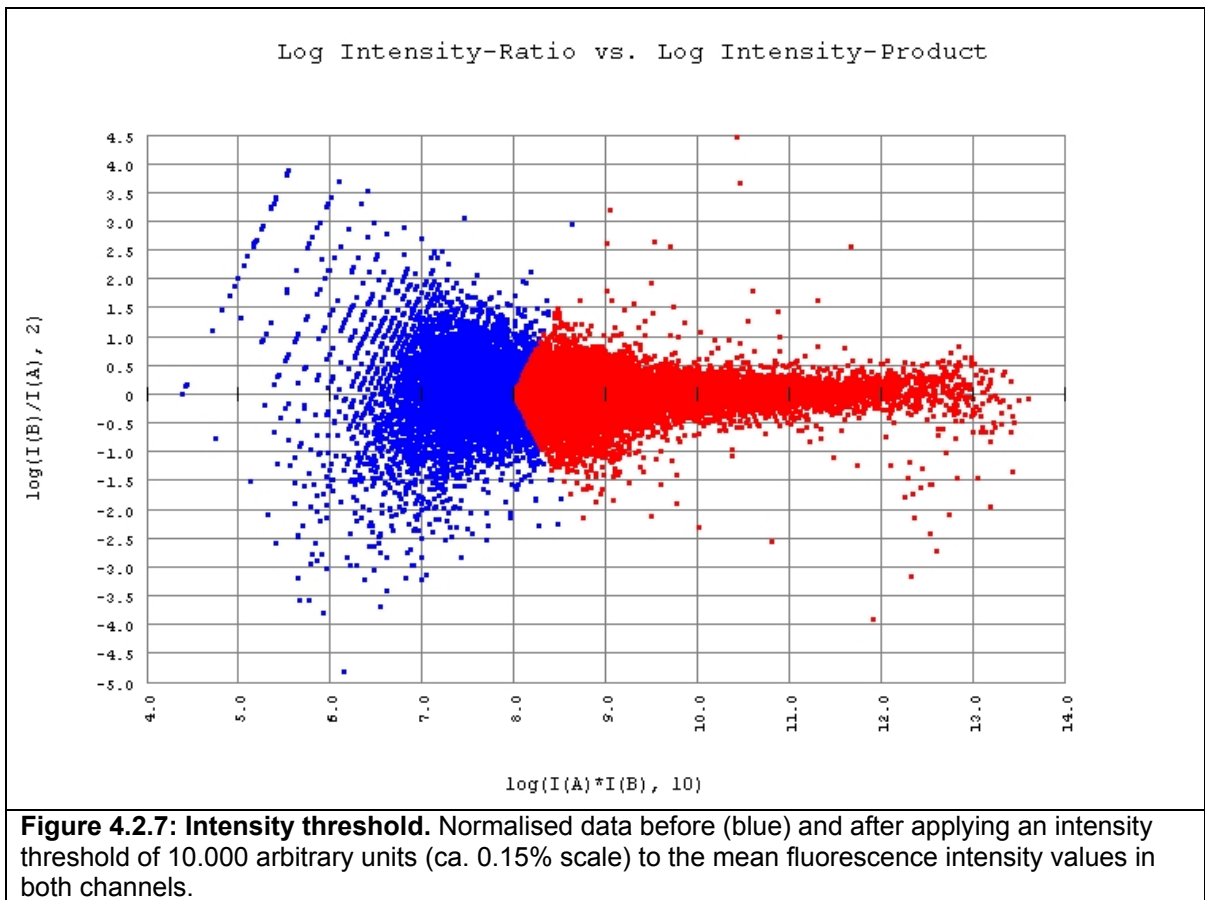
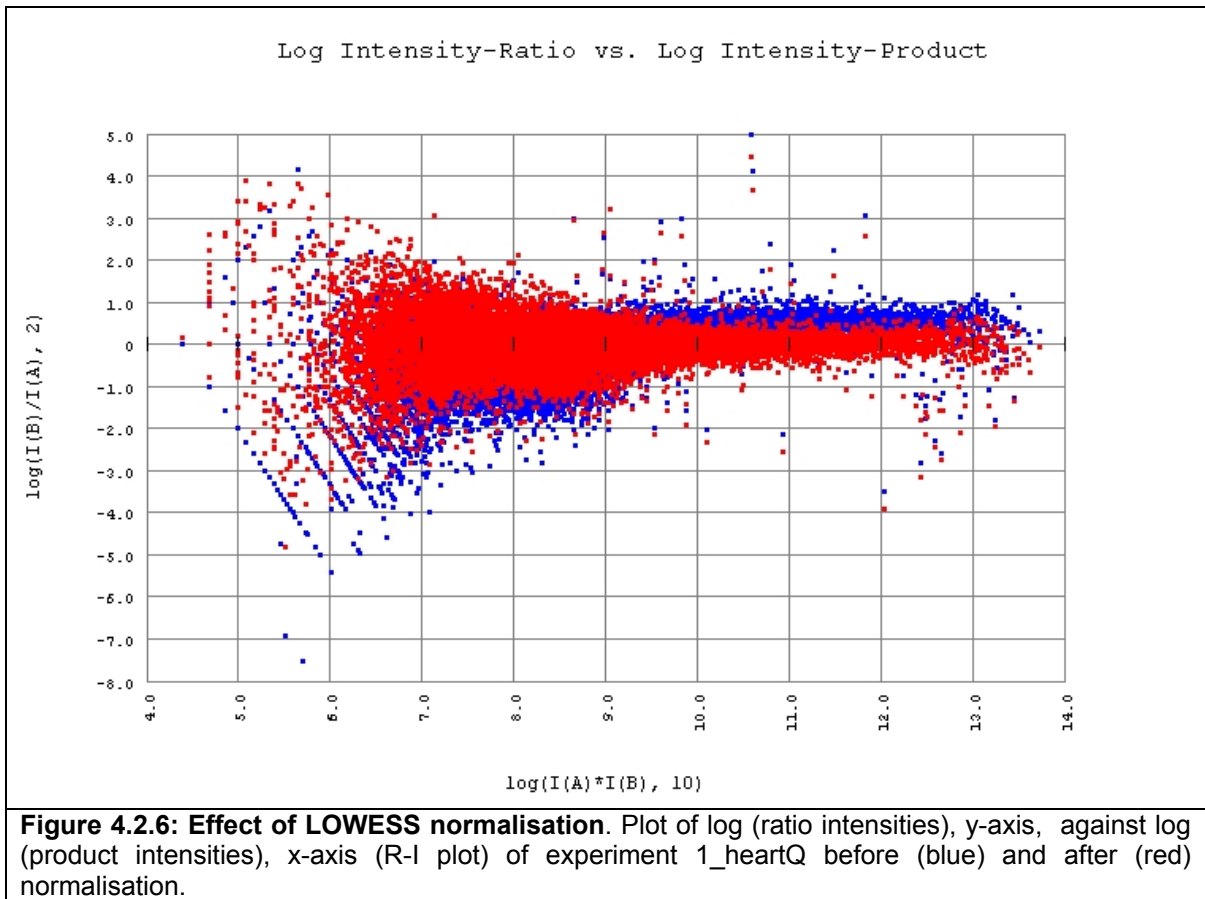


Fig. 4.2.1-5: Scatter plot with raw data from five microarray experiments with RNA from mouse heart, VDRKO versus WT. In experiments 1 and 2, cDNA resulting from VDRKO mice was labelled with Cy5, WT with Cy3. In experiment 3-5, the labeling dyes were exchanged to exclude artifacts resulting from differences in the labeling chemistry.

The example of the dataset of experiment 1_heartQ shows how LOWESS normalisation helps to overcome effects introducing a bias due to different experimental conditions during microarray production, sample preparation, hybridization and scanning. After normalisation, the data group symmetrically around the $\log(\text{ratio intensities}) = 0$ axis. At low intensity values, data cannot be interpreted due to excessive variability. Further data analysis was simplified by cutting out data at intensities below a threshold of 10.000 arbitrary units (approximately 0.1-0.2% of the full range) in at least one of the channels.

Additional to the usual dye bias and the intensity dependence of variability, the raw $\log(\text{ratio intensity})$ data of experiment 1_heartQ seem to have an intensity-dependent shift, which might arise from spatial differences of the background signal (figure 4.2.6). These effects that might distort the resulting gene expression profile can be attenuated by a locally weighted non-linear normalisation algorithm as LOWESS.



Normalisation and intensity filtering reduces noise and data complexity (in experiment 1_heartQ from 16947 signals flagged as "good" down to 14644). This

data set is still too large for complex inter-experiment analysis and contains a large portion of redundant information. Genes that had not changed in expression between WT and VDRKO mouse heart were therefore excluded by Z-score filtering (slice analysis in MIDAS).

As previously explained in the analysis of expression data from mouse kidney, a common Z-score threshold was set for all experiments. In this way, the experimentator can define the stringency of data filtering. As stringency requirements depend on each individual data set and the experimental goal, it has to be adjusted for each study individually. In this study the data set was analyzed several times with lower Z-score thresholds ranging from 1 to 2 local standard deviations, delivering confidence levels between 67 and 97%. A z-score threshold of 2 is very stringent and helps to find the "safest" candidate values while accepting a high number of false negatives, especially among genes which are differentially expressed less than 2.5-fold or in range of low mRNA copy numbers. As mentioned before, due to saturation effects the real expression ratios are generally somewhat larger than those measured in microarray experiments. In the example of experiment 1_heartQ, the number of candidate genes after Z-score filtering with a threshold of two SD is 644, 3,0% of the initial number of 21168 (figure 4.2.9). A threshold of one SD results in 1619 candidate genes (figure 4.2.8).

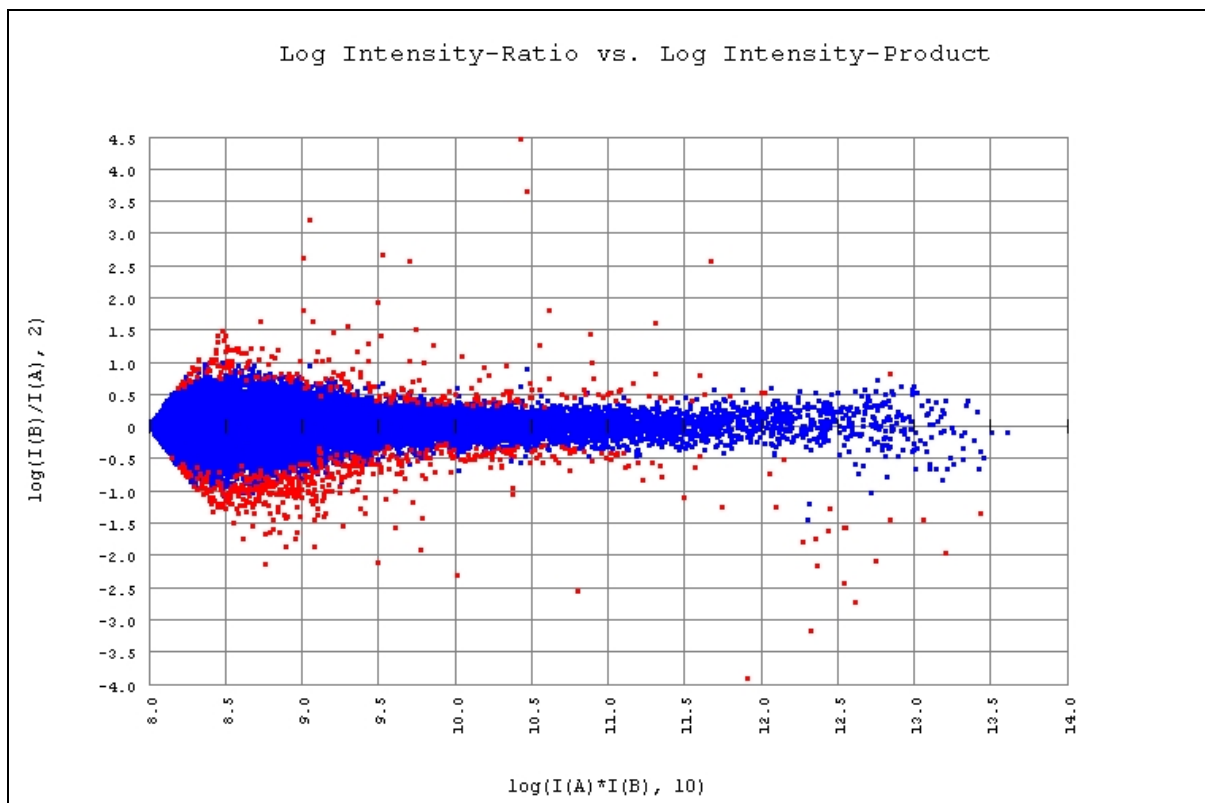
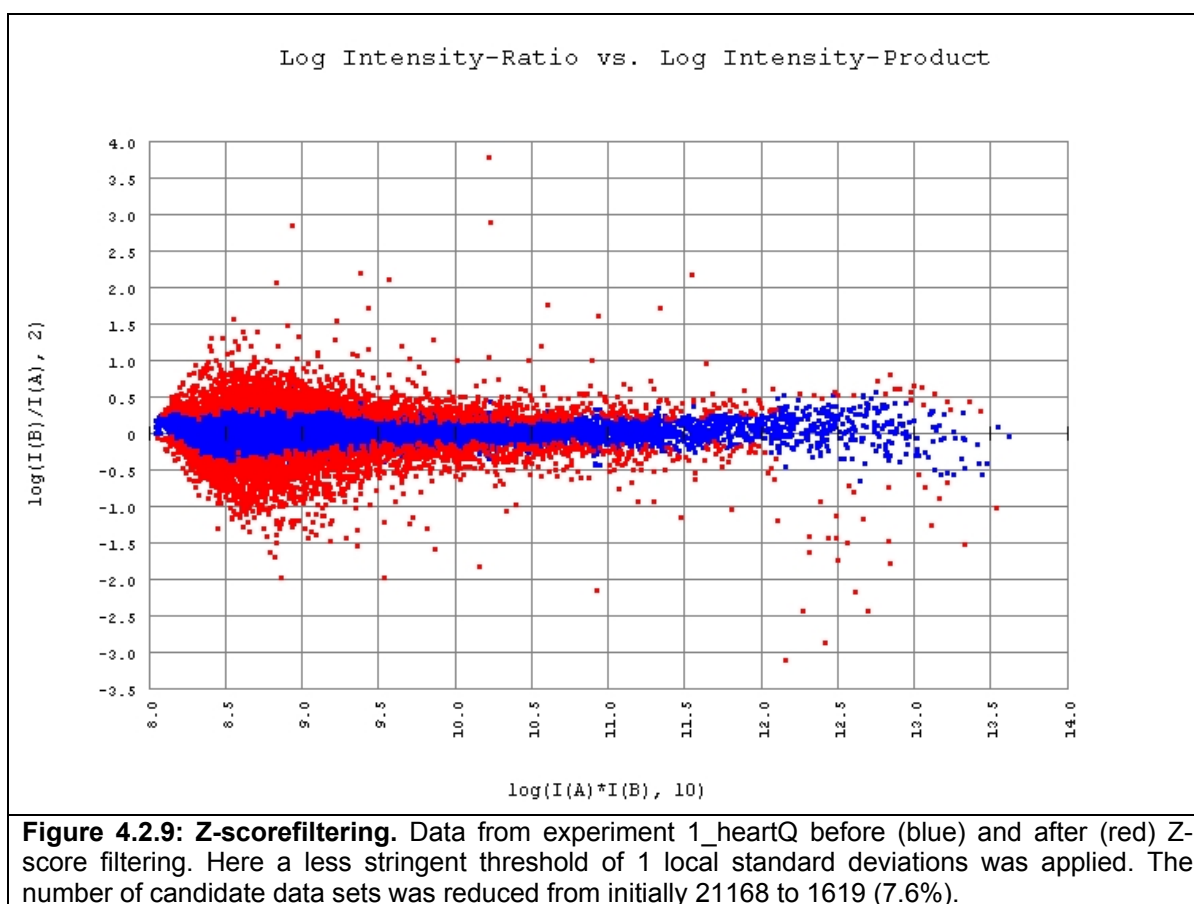


Figure 4.2.8: Z-score filtering. Data from experiment 1_heartQ before (blue) and after (red) Z-score filtering. Here a threshold of 2 local standard deviations was applied. The initial number of 21168 probe sets was reduced to 644 (3.0%).



Technical noise, especially introduced by inhomogeneous spot quality, problems with probe specificity (cross hybridization) and biological noise due to differences between individual animals can still be present in this set of filtered candidate genes. Since the number of sample organs and possible hybridisation experiments were greatly restricted, sample pooling was chosen to average out biological variation. Technical noise, a dominating source of variation for self-made cDNA arrays, was reduced by comparing technical replicates.

The filtered data were exported from MIDAS and imported into the Multiexperiment Viewer (MEV) for data comparison between experiments. As pointed out in section 5, $\log_2(\text{ratio intensities})$ from each experiment build a column in an expression matrix of the whole data set. Genes are assigned to rows in this matrix and can be interpreted as vectors in an n -dimensional space ($n = \text{number of experiments}$). Values filtered out in MIDAS were set to $\log(\text{ratio intensities}) = 0$ and appeared in grey colour in the matrix. These data could be excluded from further analysis in MEV by setting a low minimum threshold (0.1% of scale). Since normal and dye swap experiments form two groups, two-class unpaired significance analysis of microarrays (SAM) was chosen to find genes with significantly different mean expression levels between both sets of experiments.

In significance analysis of microarrays (SAM), the data for each gene are permuted, and a test statistic "d" is computed for both the original and the permuted data, analogous to the t-statistic in a t-test. The value "d" describes the difference between mean expression levels of experimental conditions (here WT and VDRKO), scaled by a measure of variance in the data.

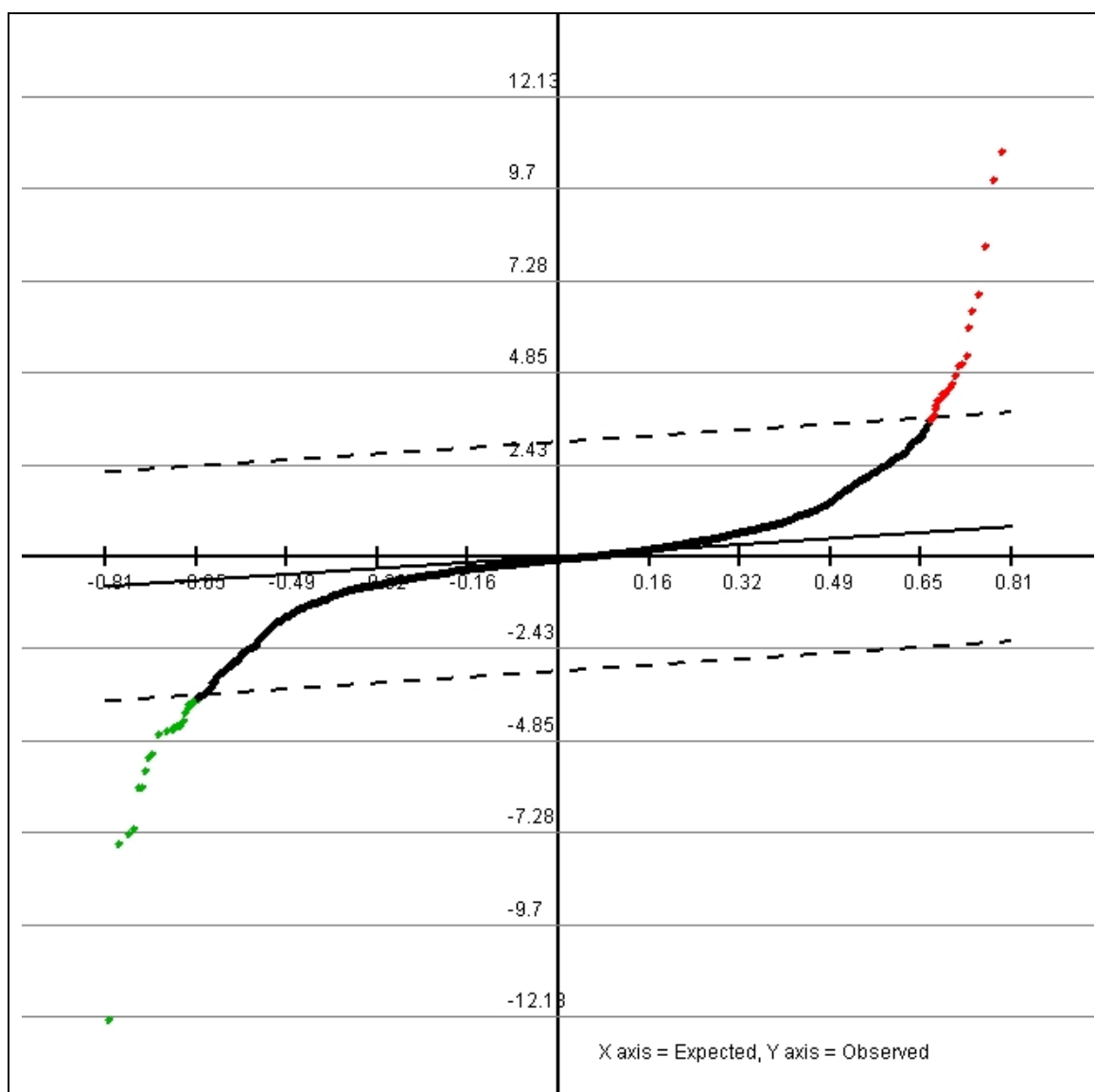


Figure 4.2.10: Selection of differentially expressed genes of 5 experiments VDRKO mouse heart against WT by significance analysis of microarrays (SAM). Plot of the observed (y-axis) against expected (based on permuted data) d-values, as generated by SAM. The two dotted lines represent a region within +/- the vertical distance delta from the solid line of slope 1 (i.e. observed = expected). By choosing delta, the analyst can define the stringency of selection. Black dots represent values considered as non-significant, red ones positive significant and green dots negative significant genes.

SAM is an interactive algorithm that offers the analyst to set the thresholds of significance according to the distribution of the test statistic and to the individual experimental needs. Studies where the goal is to classify samples (e.g. biopsies from cancer tissue) by comparing their gene expression profile to known expression patterns of marker genes would require more stringent selection parameters to avoid false positive candidate genes. In studies aiming at finding new pathways, where a more concise pattern of all candidate genes has to be established, less stringent selection parameters would be appropriate. The threshold of the observed d-values, set by the analyst, is called delta (Δ). Lowering Δ means less stringency and more significant candidate genes. The trade-off of lowering analysis stringency can be described by the false discovery rate (FDR), an estimate for the number of false positives, selected by chance.

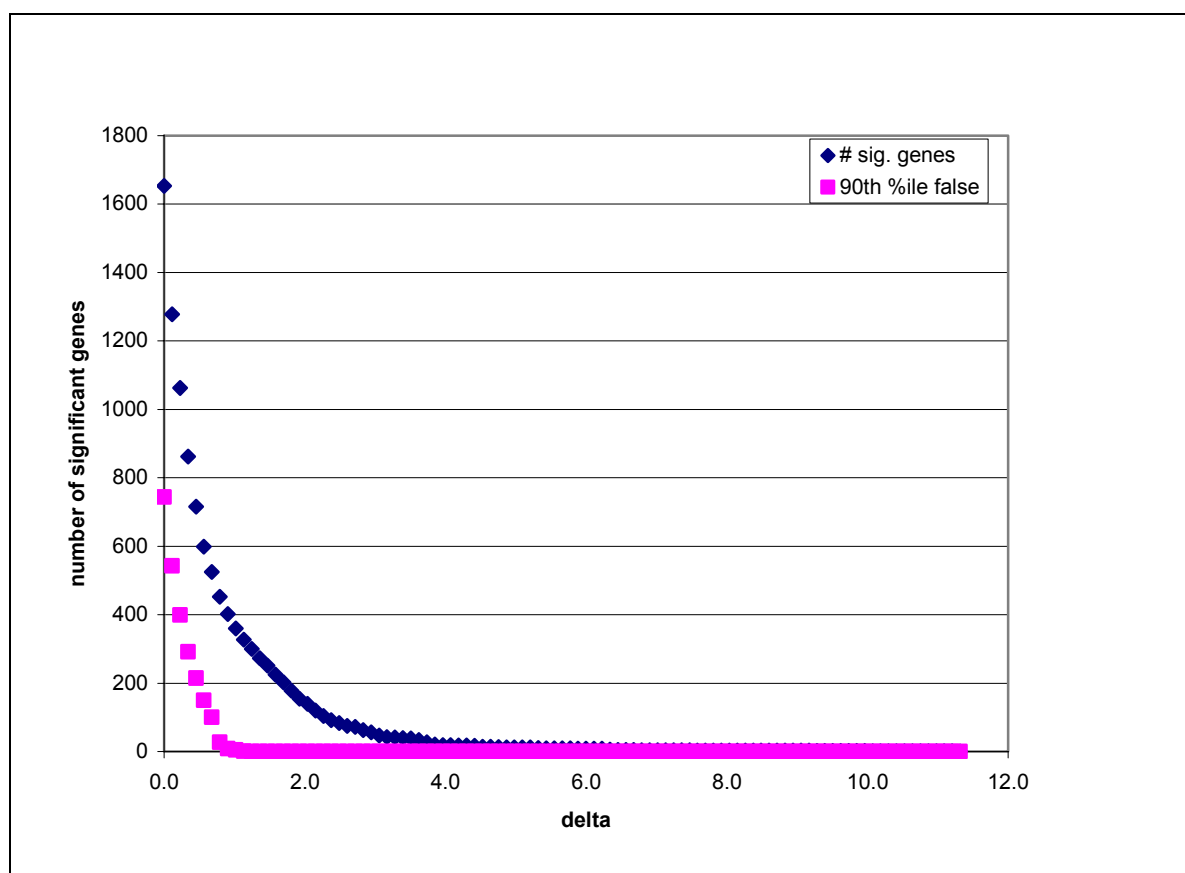


Figure 4.2.11: Dependence of the number of genes, considered by SAM as significantly differentially expressed, on the delta (\square) value. Data set of five gene expression profiling experiments of heart from VDRKO against WT mice. Another measure of significance is the 90%ile false discovery rate (FDR). The number of significant genes selected decreases with delta, the chance to select false positives decreases, as well. For delta values above 1.2, the 90%ile FDR is nearly zero, while the number of significant genes is about 300.

As statistical significance according to statistical test algorithms like SAM does not always correspond to real experimental significance (and even less to biological significance), feedback from control experiments with alternative methods can help to tune the setting of selectivity parameters like delta in SAM. In this study, quantitative real-time PCR was chosen to confirm gene expression data from microarray experiments.

According to figure 4.2.11 above, setting delta at 1.245 would result in a 90%ile FDR of less than 10^{-4} and 300 candidate genes for differential expression. 300 candidates out of 21168 (1.4%) appears as a realistic order of magnitude but is still a far too high number in terms of resources for data interpretation and experimental confirmation. Therefore SAM was applied to the data set repeated times with delta values at 1.819, 2.304 and 3.759, resulting in numbers of (positive and negative) significant genes between 201, 102 and 39, respectively.

In the case of delta = 2.304 the number of positive significant (up-regulated) genes was 49, the negative significant genes were 53, together about 6.3% of the input of 1619 pre-selected genes imported from MIDAS and 0.48% of the probe sets represented on the array (fig. 4.2.11 and tables 4.2.1-2).

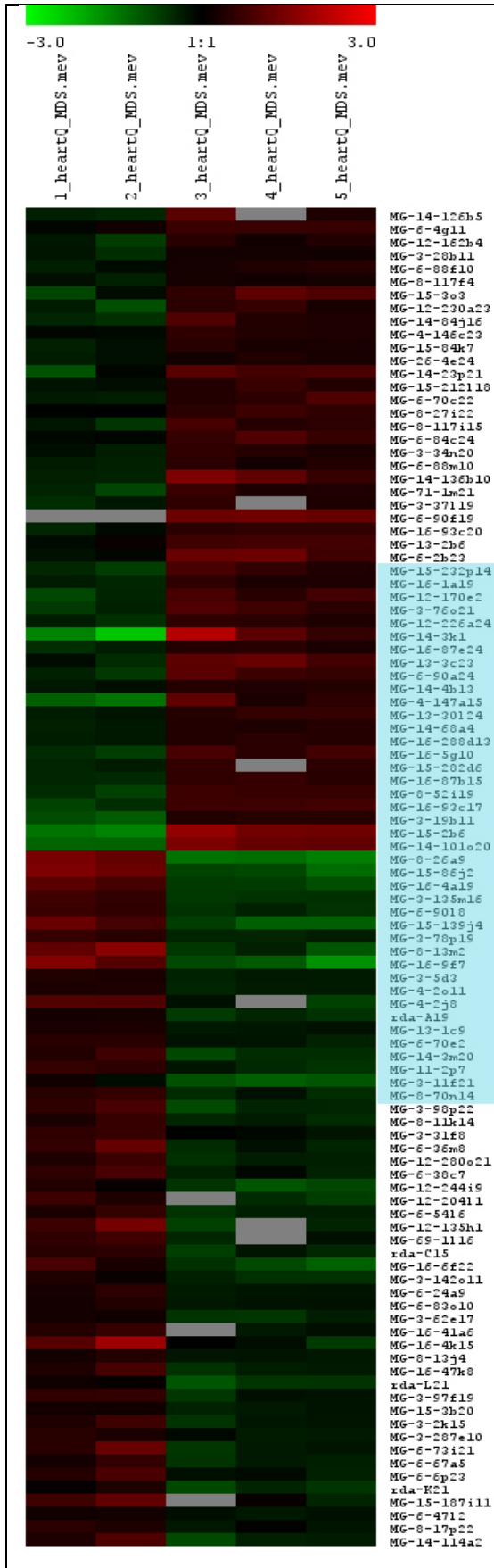


Table 4.2.1: Result table with the 39 most significantly regulated genes. From the left: delta score d, the mean expression (across 5 experiments), the error of the mean expression, and the Lion gene identifier.

score (d)	mean fold	error of mean	Lion ID
4.01	1.54	0.08	MG-15-232p14
4.06	1.33	0.04	MG-16-1a19
4.19	1.62	0.09	MG-12-170e2
4.22	1.60	0.11	MG-3-76o21
4.23	1.39	0.04	MG-12-226a24
4.36	3.22	0.66	MG-14-3k1
4.36	1.35	0.03	MG-16-87e24
4.37	1.75	0.16	MG-13-3c23
4.45	1.65	0.10	MG-6-90a24
4.52	1.28	0.04	MG-14-4b13
4.53	1.93	0.24	MG-4-147a15
4.65	1.38	0.07	MG-13-30l24
4.88	1.30	0.03	MG-14-68a4
5.14	1.32	0.04	MG-16-288d13
5.17	1.62	0.07	MG-16-5g10
5.38	1.39	0.05	MG-15-282d6
6.11	1.44	0.03	MG-16-87b15
6.59	1.58	0.02	MG-8-52i19
7.01	1.65	0.05	MG-16-93c17
8.28	1.62	0.15	MG-3-19b11
10.04	2.78	0.15	MG-15-2b6
10.77	2.37	0.10	MG-14-101o20
-12.13	0.39	0.01	MG-8-26a9
-7.47	0.46	0.04	MG-15-86j2
-7.21	0.56	0.02	MG-16-4a19
-7.10	0.64	0.01	MG-3-135m16
-5.98	0.68	0.02	MG-6-90l8
-5.98	0.50	0.03	MG-15-139j4
-5.54	0.72	0.01	MG-3-78p19
-5.22	0.53	0.08	MG-8-13m2
-5.11	0.43	0.04	MG-16-9f7
-4.62	0.79	0.01	MG-3-5d3
-4.49	0.79	0.01	MG-4-2o11
-4.41	0.82	0.01	MG-13-1c9
-4.38	0.78	0.03	MG-6-70e2
-4.37	0.66	0.03	MG-14-3m20
-4.37	0.71	0.03	MG-11-2p7
-4.27	0.69	0.12	MG-3-11f21
-4.02	0.73	0.04	MG-8-70n14

Figure 4.2.12 (left): Log₂(ratio intensity) plot of significant genes according to SAM with delta = 2.304. The selection criterium was differential expression between the dye swap experiments (exp. 1, 2) and the normally labelled experiments (3-5). In blue the 39 most significant genes with a delta score of +/- 4.0.

Results & Discussion: VDRKO mouse heart

Table 4.2.2: Annotations of the 39 most significant differentially expressed candidate genes (table 4.2.1) in mouse heart VDRKO against WT.

Fold Change	Lion ID	Abreviation	Genbank ID	Gene Name	Function / Remark
1.54	MG-15-232p14	STARS	NM_175456	striated muscle activator of Rho-dependent signalling	serum response factor-dependent transcription
1.33	MG-16-1a19	n.a.	NM_029180	n.a.	n.a.
1.62	MG-12-170e2	CNK1	XM_110525	similar to connector enhancer of KSR-like	Drosophila kinase suppressor of ras.
1.60	MG-3-76o21	Bdh	NM_175177	3-hydroxybutyrate dehydrogenase heart mitochondrial	SCAD; lipid binding
1.39	MG-12-226a24	n.a.	BC047216	n.a.	n.a.
3.22	MG-14-3k1	S100a8 /MRP8	NM_013650	S100 calcium binding protein A8 calgranulin A	calcium ion binding
1.35	MG-16-87e24	P38ip-pending	NM_019995	transcription factor (p38 interacting protein)	mRNA is down-regulated in human prostate cancer, also described as C13
1.75	MG-13-3c23	Rbm3	NM_016809	n RNA binding motif protein 3; Cold Stress-induced mRNA,	Mediates Internal Initiation of Translation with Increased Efficiency under Conditions of Mild Hypothermia.
1.65	MG-6-90a24	Snrpn	NM_013670	Snrpn: small nuclear ribonucleoprotein N	linked to Prader-will Syndrome
1.28	MG-14-4b13	Ant1 / Slc25a4	XM_134169	solute carrier family 25 (mitochondrial carrier), member 4; adenine nucleotide translocase-1	energy mobilization
1.93	MG-4-147a15	S100a8 /MRP8	NM_013650	S100 calcium binding protein A8 (calgranulin A)	immune response
1.38	MG-13-30l24	Fbln2	NM_007992	fibulin 2	calcium ion binding
1.30	MG-14-68a4	Irs1	NM_010570	insulin receptor substrate 1	insulin / IGF signalling
1.32	MG-16-288d13	n.a.	NM_181402	n.a.	n.a.
1.62	MG-16-5g10	Fasn	NM_007988	fatty acid synthase	fatty acid biosynthesis
1.39	MG-15-282d6	Myom2	NM_008664	Myom2: myomesin 2	striated muscle contraction
1.44	MG-16-87b15	ANF; Nppa	XM_131840	similar to atrial natriuretic peptide precursor; ANF peptide ANP Prepronatriodilatin	marker f. hypertension, hypertrophy
1.58	MG-8-52i19	Elov16; FAE, LCE	NM_130450	Fatty acyl elongase (Long-chain fatty-acyl elongase) (Myelination associated SUR4-like protein).	fatty acid biosynthesis
1.65	MG-16-93c17	MPAST2	NM_133838	EH domain containing protein MPAST2	calcium ion binding; ATP binding
1.62	MG-3-19b11	Bdh	NM_175177	3-hydroxybutyrate dehydrogenase heart mitochondrial	SCAD; lipid binding
2.78	MG-15-2b6	S100a9, Cagb, MRP14	NM_009114	S100 calcium-binding protein A9 (calgranulin B)	negatively regulated by glucocorticoids in a c-Fos-dependent manner and overexpressed throughout skin carcinogenesis.
2.37	MG-14-10l020	Ctgf	NM_010217	connective tissue growth factor	fibroblast mitogen and angiogenic factor which plays an important role in wound healing, cancerogenesis and fibrotic and vascular disease
0.39	MG-8-26a9	Car3	NM_007606	carbonic anhydrase 3	pH stabilisation
0.46	MG-15-86j2	Car3	NM_007606	carbonic anhydrase 3	pH stabilisation
0.56	MG-16-4a19	H2-Aa	NM_010378	histocompatibility 2 class II antigen A alpha	immune response; integral to membrane
0.64	MG-3-135m16	n.a.	BX636716	n.a.	n.a.
0.68	MG-6-90l8	n.a.	n.a.	n.a.	n.a.
0.50	MG-15-139j4	Car3	NM_007606	carbonic anhydrase 3	pH stabilisation
0.72	MG-3-78p19	Dhrs4	NM_030686	dehydrogenase reductase SDR family member 4	NADPH-dependent retinol dehydrogenase/reductase
0.53	MG-8-13m2	n.a.	NM_025845	1110021E09Rik protein (fragment).	n.a.
0.43	MG-16-9f7	RETNLA; HIMF, Fizz1, RELMa, c	NM_020509	resistin like alpha	angiogenic and vasoconstrictive properties; hypoxia-induced mitogenic factor which increased pulmonary arterial pressure and vascular resistance
0.79	MG-3-5d3	Grcc10	NM_013535	gene rich cluster C10	n.a.
0.79	MG-4-2o11	FCRN; FCGRT	NM_010189	Fc receptor IgG alpha chain transporter	immune response
0.82	MG-13-1c9	S100a10	NM_009112	S100 calcium binding protein A10 calpactin	EGF-hand calcium binding
0.78	MG-6-70e2	n.a.	XM_127466	similar to solute carrier family 25 (mitochondrial carrier; phosphate carrier), member 3	transport
0.66	MG-14-3m20	Cpt2	NM_009949	carnitine palmitoyltransferase 2	lipid metabolism
0.71	MG-11-2p7	Es1	NM_007954	esterase 1	lipid metabolism
0.69	MG-3-11f21	Prnd	NM_023043	prion protein dublet	n.a.
0.73	MG-8-70n14	Mgll	NM_011844	monoglyceride lipase	lipid metabolism

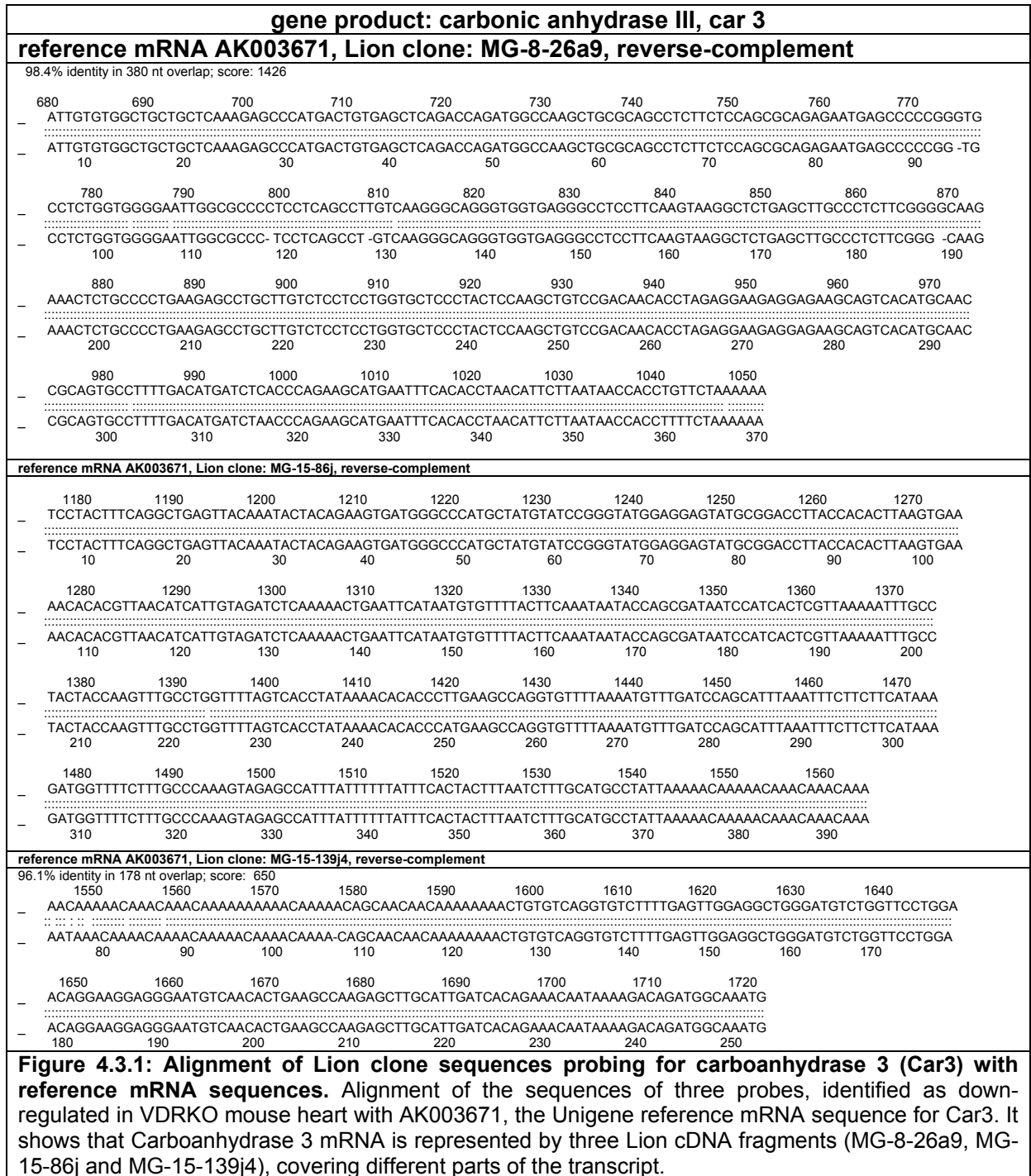
In figure 4.2.12, an expression matrix of the 102 most significant differentially expressed gene candidates with colours representing the \log_2 (ratio intensities) is depicted. The genes are ranked according to the significance score delta from the center to the top (for positive delta values, i.e. up-regulation in VDRKO mouse heart compared to WT) and downwards for negative delta scores (down-regulated genes). Note that the ranking according to delta score is not equivalent to ranking according to fold expression, as significance depends on the local standard deviation of the data population in the neighbourhood of the respective value.

4.3 Annotation of candidate genes

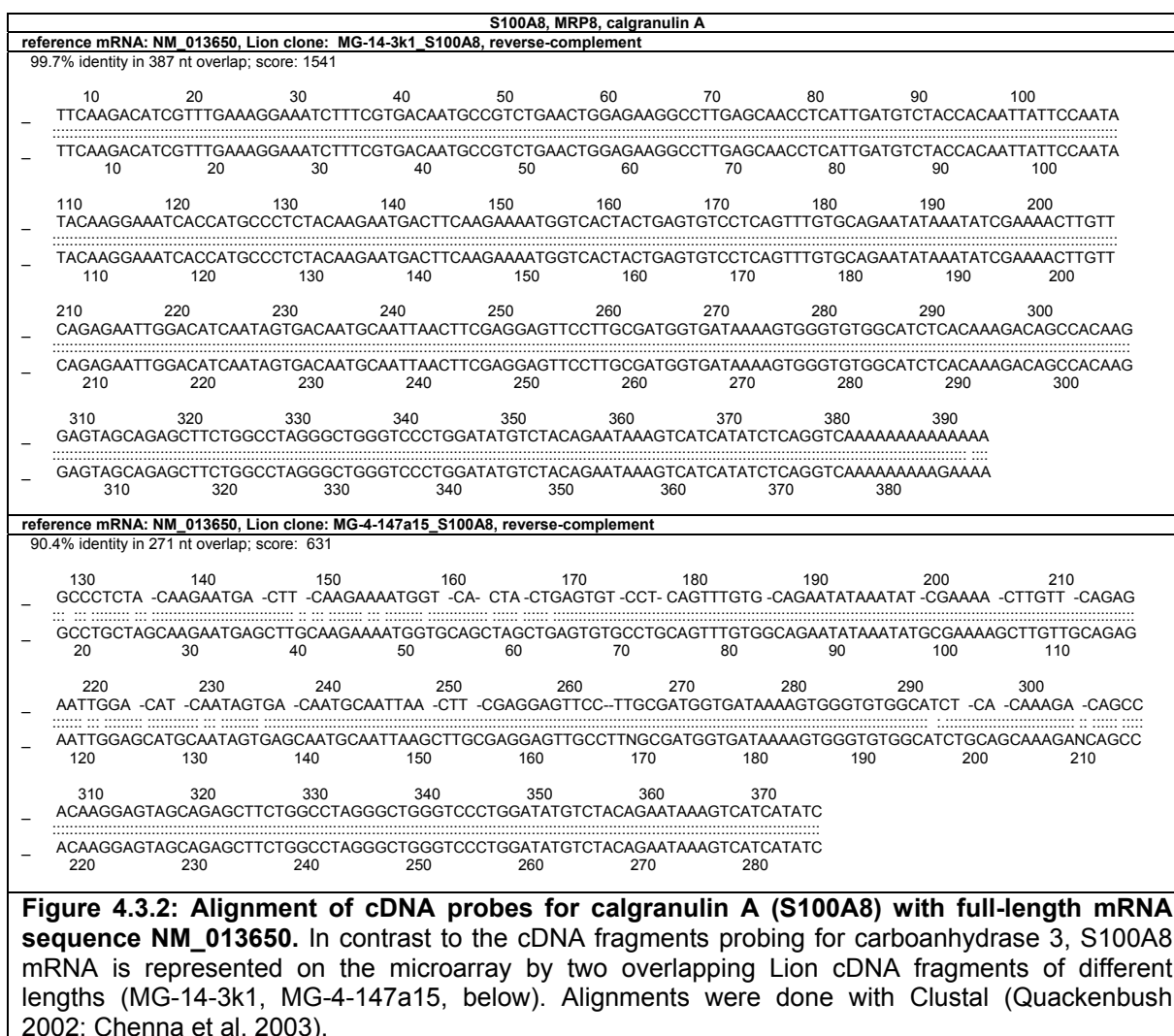
With the help of the SRS database "arrayBase" from Lion Biosciences, Lion clone IDs of these candidates were assigned to the sequences of the spotted probes. A part of the gene annotations were directly extracted from the arrayBase platform, which is linked to other public databases. To explore all relevant information about gene identity, function, gene regulation and related pathways, the sequences were additionally used to by search by BLAST other public and commercial databases like Genbank (NCBI), Ensemble or Celera / Applied Biosystems. Experimental data from previous studies were found from literature databases like PubMed, using search tools as Bibliosphere from Genomatix for each candidate gene.

Since Lion clone IDs only can be related to sequence information through the Lion arrayBase with restricted access, the probe sequences of candidate genes were assigned by BLAST to Unigene reference cDNAs and presented in tables with the respective Genbank IDs. Ambivalent gene names and shortcut identifiers often cause problems in data analysis from large-scale gene expression experiments. Therefore the most current gene names and shortcut identifiers found in literature were included into result tables.

Some of the candidate genes in table 4.2.2 appear twice (in the case of S100A8) or even three times with different Lion clone identifiers. Although all clones in the set printed on the arrays were sequence-verified and redundancy in the set was guaranteed to be low, some genes are represented by two or three cDNA fragments. One of the reasons for this is that gene annotation was far less complete at the time of production of the clone set than it is now. To get more information about this redundant sequences they were compared by BLAST with NCBI nucleotide databases and then aligned with the respective Unigene reference mRNA sequence (see Figure 4.2.13 below). In the case of carbonic anhydrase III, the three probes spotted on the array represent three different parts of the 3' end of the car 3 mRNA.



In the case of S100A8, both clones represent segments of different lengths from the same part of S100A8 mRNA. The fold change value of the longer S100A8 probe MG-14-3k1 is closer to the fold change value obtained by quantitative real-time PCR.



The fact that different cDNA probes representing the same mRNA species gave very similar fold changes confirms the validity of the gene expression data obtained in this microarray study.

4.4 Confirmation of candidate genes by qPCR

Even more robust data confirmation can be achieved by using a different method. Like in the example of kidney, quantitative real-time PCR (qPCR) was chosen for its advantages in terms of accuracy, speed, cost and low sample material consumption. Especially the last criterium was important since in the case of VDRKO mouse heart a very limited amount of sample material was available. To get an impression of the variation in gene expression between VDRKO individuals, only RNA from WT animals was pooled.

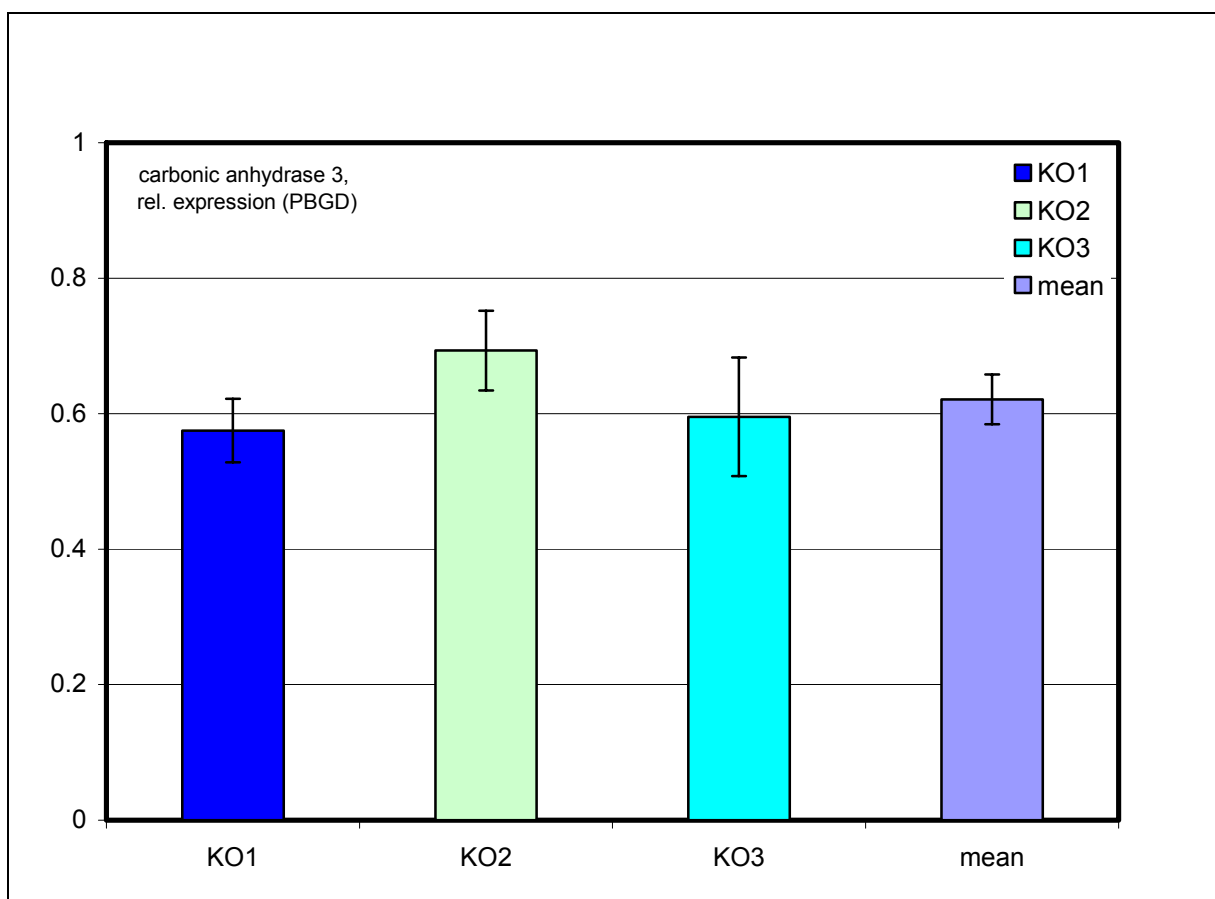


Figure 4.4.1: Validation of gene expression data from microarray experiments by quantitative real-time PCR: Differences between individuals. The example above shows the result for relative gene expression of carbonic anhydrase 3 (Car3) in mouse heart of 3 different VDRKO individuals, relative to a pool of 4 WT mouse hearts, all male and age-matched. Each column represents a value obtained from 12 measurements, 3 technical repeats each for VDRKO reference (here: PBGD) and target gene (here: Car3) and WT. The error bars of (VDR)KO1-3 represent the variation introduced by pipetting (technical noise), calculated by Gaussian error propagation; the error bar of the mean value represents the error of the mean between individuals (biological noise).

The example above shows that both technical noise (due to the pipetting error) and biological variation between individuals are in the range of 10-15%. Technical variability in qPCR results mainly from pipetting and is smaller than in microarray experiments. Normalisation in qPCR is much simpler than in microarray data analysis, since it uses only one reference gene. This makes complicated normalisation procedures obsolete and avoids the danger of skewing the overall gene expression level by mathematical transformations. On the other hand it has to be assured that the reference ("housekeeping") gene is not regulated. In this study, the expression of at least two ubiquitously expressed genes, porphobilinogen deaminase (PBGD) and hypoxanthine-guanine phosphorybosyl transferase (HPRT) was measured in each experiment and taken as reference relative to the target gene.

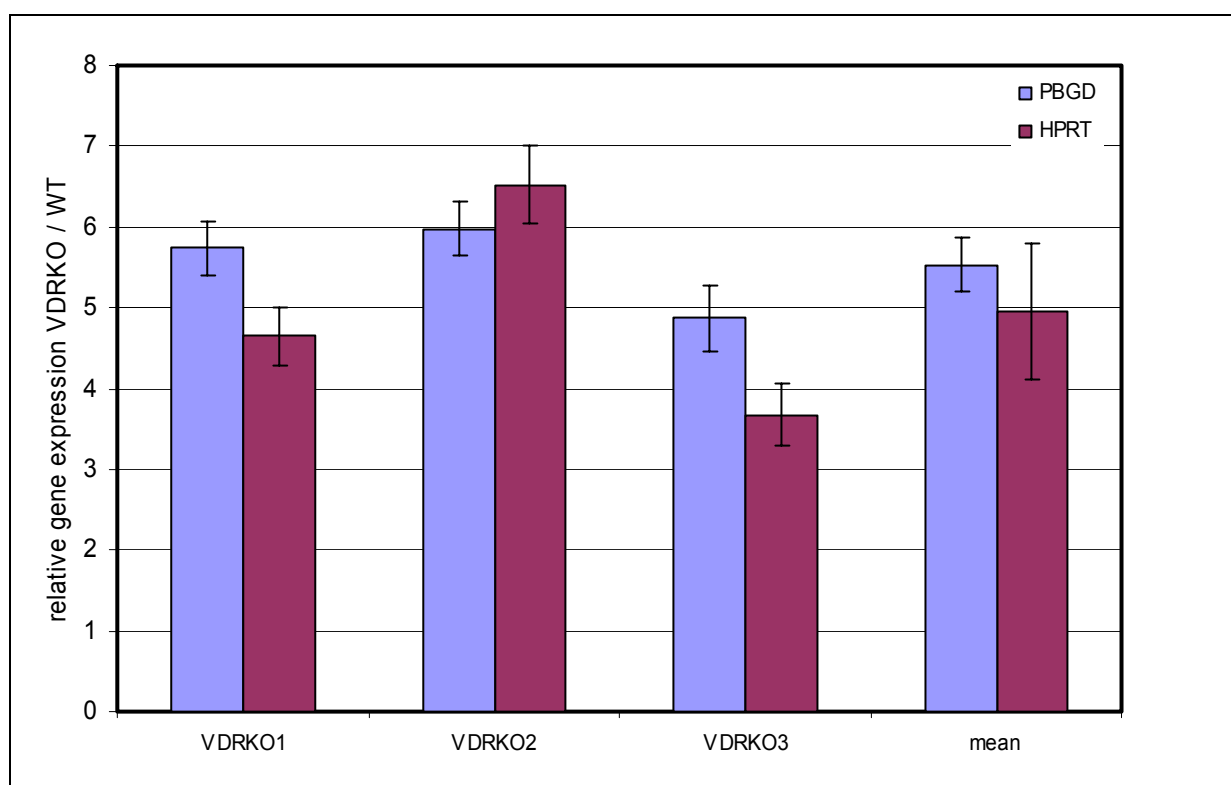


Figure 4.4.2: Comparison of two reference transcripts, HPRT and PBGD. Relative gene expression of S100A9 / MRP14 / calgranulin B, VDRKO vs. WT mouse heart. Like in all measurements with RT-PCR presented here, two reference genes, HPRT and PBGD were used to normalise gene expression between samples. The blue columns represent values normalised with respect to PBGD, the purple columns stand for the same measurements, normalised to HPRT. Both reference genes gave similar values, but as PBGD appeared to be more stable (less variation), it was preferred as reference gene.

Although quantitative real-time PCR is more efficient and precise than classical methods like Northern Blotting or semiquantitative PCR, the number of genes of which the expression can be measured is limited. Here the genes that, according to microarray data, were most significantly expressed were measured (provided that suitable primer pairs or fluorescent Taqman probes could be obtained). Especially genes with annotations that indicate their contribution to important pathways or functions that help to define the VDRKO phenotype were selected.

The direct comparison between relative expression data obtained by microarray experiments with the data obtained by qPCR showed very good correlation (figure 4.4.3 below). There was virtually not a single case of contradicting results, i.e. up-regulated genes in microarray experiments always could be verified as up-regulated by qPCR and down-regulated genes were confirmed as down-regulated, given that the fold regulation was significant (>25%). Sometimes, especially for large differences in expression between VDRKO and WT heart, the fold-change values differed, with a clear tendency to the higher fold-range for qPCR results. This is not surprising, as the dynamic range of qPCR is larger than that of microarray intensity signals, which are more prone to saturation effects. For this reason it can be expected that the values obtained by qPCR are closer to the true expression levels.

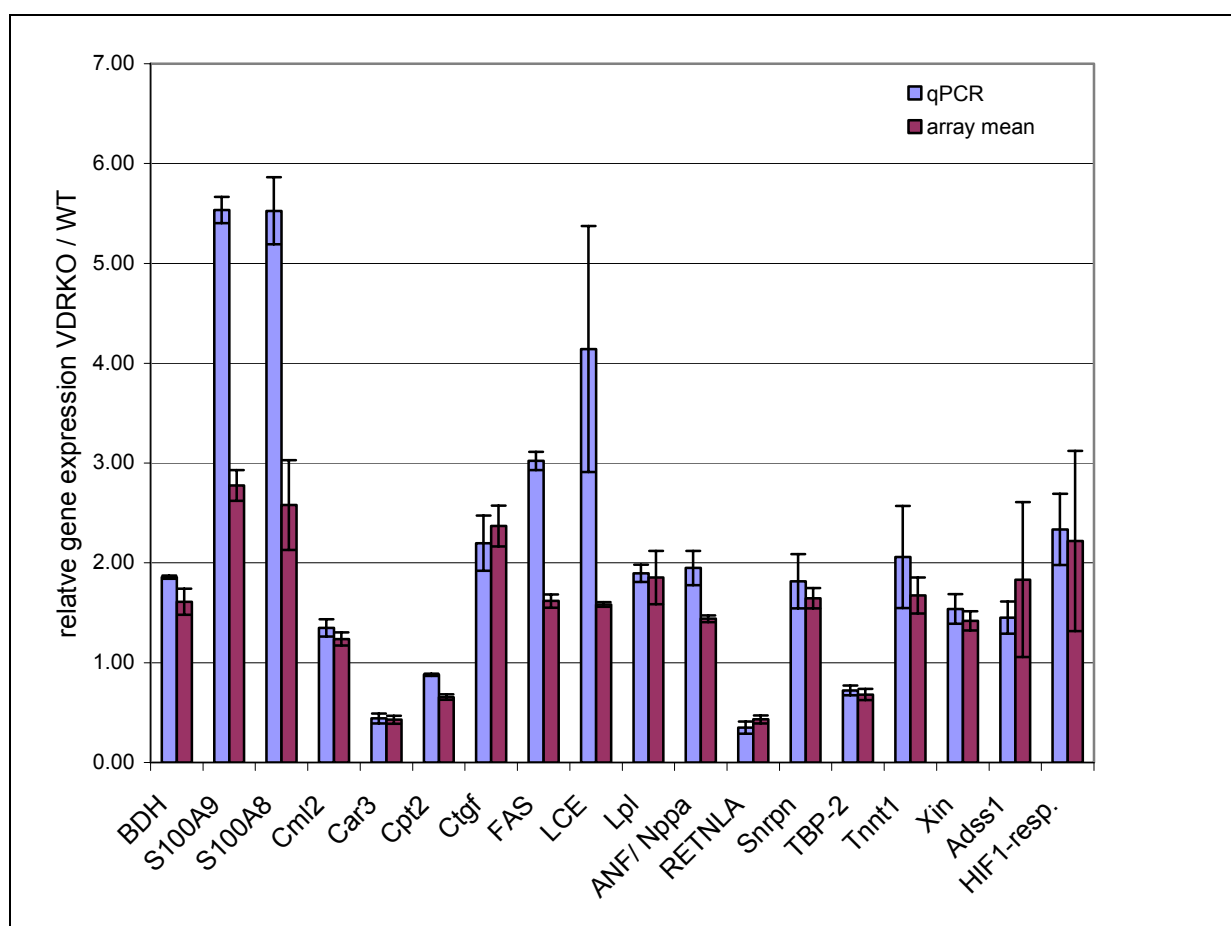


Figure 4.4.3: Validation of selected candidate genes from microarray experiments by quantitative real-time PCR: Comparison between microarray and qPCR data. All values represent the mean relative expression of VDRKO vs. WT mouse heart. This means that values below one represent down-regulated genes. The blue columns are the mean expression values obtained by qPCR from 3 VDRKO individuals, 3 technical repeats each, with error bars indicating the error of the mean between individuals. Purple columns are mean relative expression values obtained by 5 microarray experiments, error bars indicating the error of the mean between experiments.

4.5 Discussion of gene expression profiles and assignment of candidate genes to physiological functions and pathways

Data interpretation takes into account the 200 genes that were most significantly differentially expressed between VDRKO and WT mouse heart. Since the discussion of all candidate genes would not be possible, special focus will be given on the 39 most significantly expressed gene candidates (the central blue fraction in fig. 4.2.12 and table 4.2.1, annotations in table 4.2.2). Gene annotations and literature were searched for common functions / pathways for the 22 most significantly up-regulated candidate genes (in pink colour in table 4.2.2) and the 17 most significantly down-regulated candidates (in green in table 4.2.2).

Among these candidate genes, a big part has functions in the regulation of the immune system, lipid metabolism, transport, or were reported to be induced in cardiovascular diseases, hypertension or by hypoxia. As in kidney, a number of genes with calcium-binding protein products are differentially expressed, although systemic serum calcium levels were normalised through the diet in VDRKO and WT mice.

4.5.1 Candidate genes involved in the immune system

Predominant among up-regulated calcium-binding genes were S100A8 (MRP8, calgranulin A) and S100A9 (MRP14, calgranulin B), two members of the S100 gene family. They contain two EF-hand domains that bind each two Ca^{2+} ions (compare Calb3, section 3). Both genes cluster in mouse on chromosome 3 and the gene products were found to dimerise and to be often co-regulated (Nacken et al. 2003), a fact that is in line with the expression profiles found in this study.

Previously, S100A8/9 were reported to be predominantly expressed in neutrophils and their induction was associated to inflammatory diseases and innate immunity response (Nacken et al. 2003). The names of the proteins, myeloid-related protein (MRP) 8 /14 indicate their main site of expression, neutrophils and monocytes. In these cell types, they form heterodimers and constitute about 45% and 1% of the total cytosolic proteins, respectively (Edgeworth et al. 1991). In the human promyelocytic leukemia cell line HL-60, $1,25(\text{OH})_2\text{D}_3$ induces differentiation into cells of the monocytic lineage, in parallel with increased expression of S100A8/9 (Kuwayama et al. 1993). S100A8/9 expression is repressed by retinoids inhibiting the enhancer action of nuclear factor-interleukin-6 (NF-IL6). While normally located in the cytoplasm of monocytes and granulocytes, elevation of the intracellular calcium level through stimulation by vitamin D or inflammatory processes triggers the translocation of S100A8/9 to the plasma membrane, where they can be anchored on the surface or secreted. The secretion of the S100A8/9 complex seems to be mediated by protein kinase C and was observed in sera from patients with inflammatory diseases, like cystic fibrosis, rheumatoid arthritis and sarcoidosis (Nacken et al. 2003).

Another interesting feature of the S100A8/9 complex is its ability to bind unsaturated fatty acids in a Ca^{2+} -dependent manner, especially arachidonic acid (AA). As the intracellular calcium concentration rises, reversibly bound AA is transported to the cell membrane and secreted. Interaction of the AA/S100A8/9 complex with the fatty acid transporter FAT/CD36 accelerates its dissociation. Taken up by target cells, AA gets metabolized into eicosanoids, which in turn have been shown to regulate smooth muscle contractility and to modulate the adhesion of monocytes and neutrophils to endothelium (Nacken et al. 2003). To sum up, the strong up-regulation S100A8 and S100A9 indicates an inflammatory condition of the heart of VDRKO mice and / or alterations in the regulation of muscle contractility. Induction of calgranulins might also be a result of elevated intracellular calcium levels and VDR-independent stimulation by $1,25(\text{OH})_2\text{D}_3$, which was detected at significantly elevated serum levels in VDRKO mice (Erben et al. 2002).

Like in kidney, carboxypeptidase N (CPN) was found up-regulated in VDRKO mouse heart. CPN cleaves the carboxyterminal arginin from bradykinin and kallikinin, two peptides that increase vascular permeability and act through the G-protein coupled receptor B2 in the acute phase of inflammatory response. The cleavage products are specific to the B1 receptor, active in the chronic phase of inflammatory response. This means that CPN can cause a shift of kinin peptides in their physiological activity of mediating blood pressure and inflammatory response (Matthews et al. 2004).

Vitamin D-binding protein (DBP, Gc protein) was strongly up-regulated in the heart of VDRKO mice. The role of DBP in the transport and renal reabsorption of vitamin D metabolites was discussed in section 3. DBP also is required for the activation of macrophages in inflammation (Yamamoto and Naraparaju 1996). DBP was shown to

be converted into macrophage activating factor by B-cells. Activated macrophages were reported to express 25-hydroxyvitamin D₃-1 α hydroxylase (CYP1 α), which can locally produce the hormonal active form of vitamin D. Active 1,25(OH)₂D₃ can then act in a paracrine fashion in target cells expressing high levels of VDR, like T-lymphocytes or immature immune cells of the thymus (Deluca and Cantorna 2001).

The effect of vitamin D deficiency on increasing the severity of autoimmune diseases has been shown at the example of inflammatory bowel disease (IBD). IL-10 knockout mice, a model for IBD, progress much more rapidly and develop more severe inflammations in the gastrointestinal tract when crossed with VDRKO mice resulting in VDR/IL-10 double KO mice (Froicu et al. 2003).

The onset of autoimmune diseases in animal models for multiple sclerosis (MS) and type I diabetes was either attenuated or completely prevented by vitamin D treatment (Deluca and Cantorna 2001). Although the mechanism is unclear, it seems to depend on VDR expression and serum calcium levels. The most possible mechanisms of immune response modulation by vitamin D include a paracrine feedback loop to resolve inflammation, to regulate the differentiation of activated CD4 T cells or to enhance suppressor T cell activity (Hayes et al. 2003).

Mice suffering from experimental autoimmune encephalomyelitis (EAE), a widely used model for human MS, were successfully treated with vitamin D. Examination of the lymph nodes of treated animals showed significantly increased expression of TGF β -1 and IL-4 transcripts. Ablating IL-4 expression makes mice affected by EAE resistant to treatment with vitamin D. (Deluca and Cantorna 2001). TGF β -1 is recognized as an anti-inflammatory cytokine that might have an important role in immunological self-tolerance (Prud'homme and Piccirillo 2000).

Table 4.5.1: Genes identified as differentially expressed by 5 microarray experiments with RD VDRKO vs. WT mouse heart that were related to functions in the immune response.

Mean Fold	Error	Lion ID	Abbreviation	Genbank	Name
3.22	0.66	MG-14-3k1	S100a8 /MRP8	NM_013650	S100 calcium binding protein A8 calgranulin A
1.93	0.24	MG-4-147a15	S100a8 /MRP8	NM_013650	S100 calcium binding protein A8 (calgranulin A)
2.78	0.15	MG-15-2b6	S100a9, MRP14	NM_009114	S100 calcium-binding protein A9 (calgranulin B)
0.56	0.02	MG-16-4a19	H2-Aa	NM_010378	histocompatibility 2 class II antigen A alpha
0.79	0.01	MG-4-2o11	FCRN; FCGRT	NM_010189	Fc receptor IgG alpha chain transporter
0.61	0.06	MG-16-6f22	Ii	NM_010545	Ia-associated invariant chain
0.60	0.09	MG-14-2n18	Ccl21a,b,c, ALP; SLC; CKb9; Tca4; Scya21;	NM_011124	chemokine C-C motif ligand 21a serine
0.70	0.07	MG-6-431	Ii	NM_010545	Hemopexin; Ia-associated invariant chain

Table 4.5.2: Results from qPCR: Differentially expressed genes in VDRKO mouse heart, relative to WT, involved in the immune response. These measurements by qPCR confirmed the results from microarray experiments. CPN and GC / DBP, were measured because they were differentially expressed in VDRKO mouse kidney. Measurements were done in triplicates with mRNA from three different VDRKO mouse hearts, normalised to PBGD expression and compared to a pool of mRNA from 4 WT mouse hearts.

Fold change	Error	Name	Abbreviation	Genbank Reference
5.54	0.13	calgranulin A / MRP8	S100A8	NM_013650
5.53	0.34	calgranulin B / MRP14	S100A9	NM_009114
1.39	0.12	carboxypeptidase N	CPN	<u>NM_030703</u>
6.49	1.84	vitamin D binding protein	GC / DBP	<u>NM_008096</u>

4.5.2 Lipid metabolism and energy mobilization

Increased intracellular calcium levels might be the explanation for the up-regulation of genes related to lipid biosynthesis. Among the 17 most significantly up-regulated genes in table 4.2.2 there is fatty acid synthase (FAS) and long-chain fatty-acyl elongase (LCE). FAS catalyses the synthesis of fatty acids up to a length of C-16 (palmitate) in the cytosol, using acetyl-CoA as substrate. The synthesis of longer fatty acids is located in the endoplasmatic reticulum and catalyzed by a system of enzymes that have been best characterised in yeast. The rate-controlling first condensation step of microsomal fatty acyl elongation, catalyzed by LCE, was shown to be - like FAS -regulated by insulin via transcription factors of the SREBP family.

Inhibition of fatty acid synthase expression by vitamin D was recently confirmed in prostate cancer cells (Qiao et al. 2003). The authors of this study found that the effect of vitamin D treatment was abolished by androgen blockers. Stimulation of lipid biosynthesis in adipocytes by vitamin D through the elevation of Ca^{2+} influx was observed in kidney (see section 3 and (Shi et al. 2001b)). The up-regulation of genes involved in lipogenesis in VDRKO mouse kidney and heart is in accordance with the model they proposed:

Table 4.5.3: Measurements of genes involved in lipid metabolism and energy mobilisation in VDRKO mouse heart by qPCR. As before, the fold-change values are relative to WT heart and normalised to PBGD expression.

Fold change	Error	Name	Abbreviation	Genbank Reference
3.02	0.09	fatty acid synthase	FAS	NM_007988
1.90	0.09	lipoprotein lipase	LPL	NM_008509
1.86	0.02	3-hydroxybutyrate dehydrogenase heart mitochondrial	BDH	NM_175177
1.00	0.26	uncoupling protein 1	UCP-1	<u>NM_009463</u>
1.45	0.16	adenylosuccinate synthetase muscle	Adss1	<u>NM_007421</u>
0.88	0.01	carnitine palmitoyltransferase 2	Cpt2	NM_009949
0.43	0.04	resistin-like protein alpha	FIZZ1; RETNLA	<u>NM_020509</u>

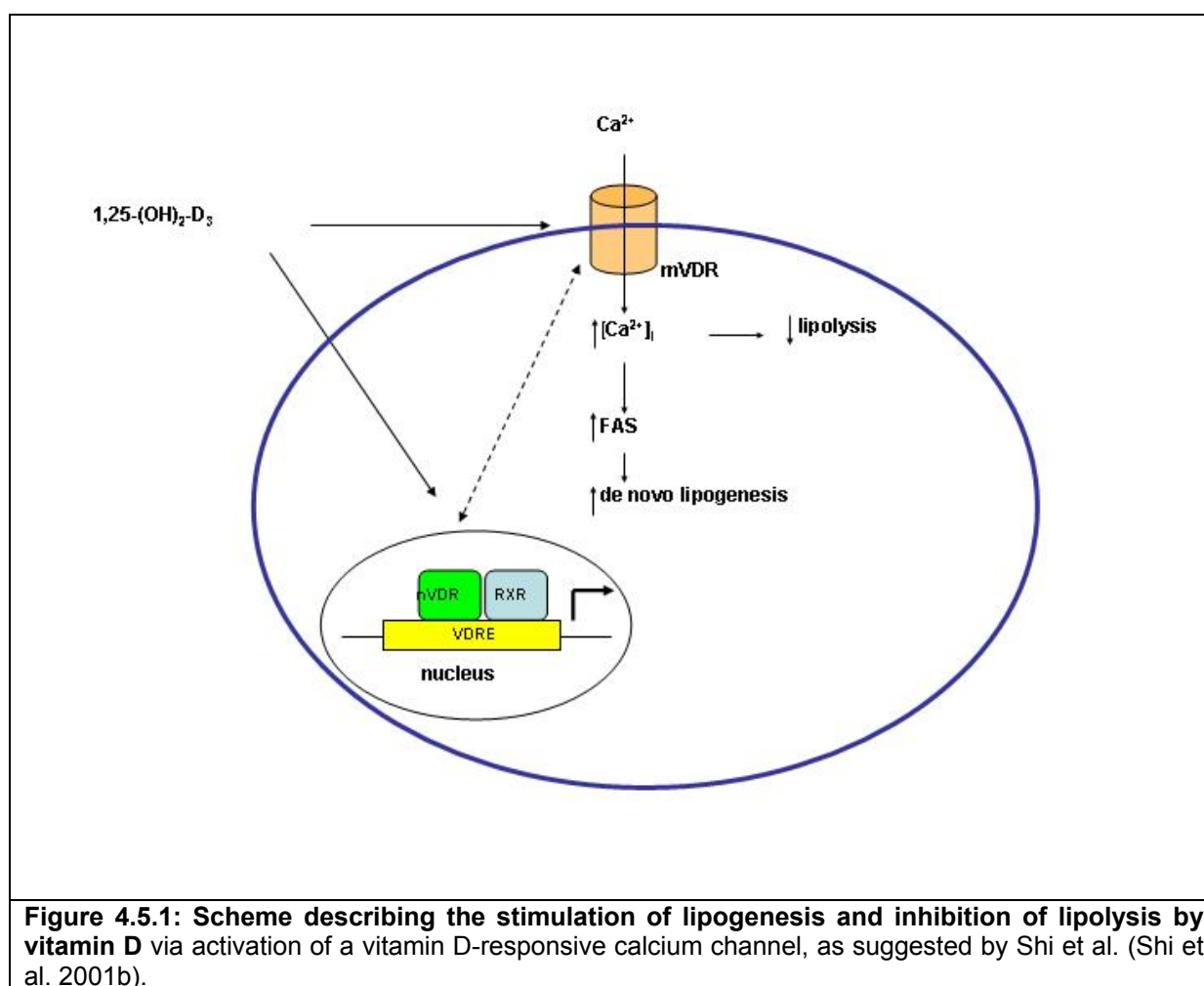


Figure 4.5.1: Scheme describing the stimulation of lipogenesis and inhibition of lipolysis by vitamin D via activation of a vitamin D-responsive calcium channel, as suggested by Shi et al. (Shi et al. 2001b).

To explain the vitamin D-induced, VDR-independent increase of calcium influx into the cells and secondary stimulation of lipogenesis, Shi et al. suggested the existence of vitamin D-responsive calcium channels. These apparently contradictory roles of vitamin D in lipogenesis in prostate cancer cells and in adipocytes is explained by the differences in its mode of action: While the androgen-dependent inhibition of lipogenesis in cancer cells appears to be the result of a genomic effect via VDR, FAS activation in adipocytes was shown to be non-genomic and regulated by intracellular calcium levels (see scheme in figure 4.5.1 and discussion in section 3).

Down-regulation of two genes with products involved in lipolysis and lipid metabolism, carnitine palmitoyltransferase 2 (Cpt2) and monoglyceride lipase (MglI) might confirm this model. On the other hand, lipoprotein lipase (LPL), which is known to be expressed in the capillary endothelium of adipose tissue, skeletal muscle and heart, and which has a central role in the metabolism of triglycerides, was up-regulated in VDRKO mouse heart. Previous studies found up-regulation of LPL by treatment of adipocytes with calcitriol, an effect which is antagonized by PTH (Querfeld et al. 1999). Interestingly, the antagonizing effect of PTH could be prevented by the calcium channel blocker verapamil, again supporting the putative role of vitamin D on stimulating calcium influx into the cytosol. A more recent study showed that LPL was not only active on the endothelial surface of vascular lumen, but also on the surface of cardiomyocytes (Yagyu et al. 2003). The authors showed that a fraction of triglycerides can pass the endothelial barrier and interacts with LPL, bound to the myocyte surface. With LPL action, partly lipolysed triglyceride-rich particles can enter the myocytes, where they are deposited as core lipids or

cholesteryl and retinyl esters. Excess lipid uptake can lead to pathogenic conditions like cardiomyopathy, as it is also known in the setting of diabetes mellitus and obesity (Finck et al. 2002).

Mitochondrial 3-hydroxybutyrate dehydrogenase (BDH), represented on the array by two different probes, was clearly up-regulated in the hearts of VDRKO mice. Across 5 hybridisations, the fold-change for both probes was almost identical: (1.62 + / - 0.15)-fold for probe MG-3-19b11 and (1.60 +/- 0.11)-fold for probe MG-3-76o21, showing again the reproducibility of the data. BDH is a lipid-requiring enzyme that uses phosphatidylcholine as an allosteric activator for the binding of NADH (Adami, P 863). It belongs to the short-chain alcohol dehydrogenase superfamily (SCAD, recently renamed as SDR).

One of the clearly down-regulated transcripts in microarray and qPCR experiments in VDRKO mouse heart codes for resistin-like protein a (Retnla). Resistin-like peptides are mainly expressed in adipose tissue and circulate in the blood. The observation that resistin is increased in diet-induced obese mice and decreased by anti-diabetic drugs led to the conclusion that resistin is a hormone that links obesity to diabetes (Steppan et al. 2001). Administration of resistin to normal mice impaired glucose tolerance and insulin action, while treatment of obese and insulin-resistant mice with an antibody neutralizing resistin action enhanced insulin sensitivity in these animals. A number of recent publications, however, questioned the suggested antagonistic role of resistin and insulin, by linking insulin resistance, obesity and elevated levels of free fatty acids to decreased expression of resistin (Juan et al. 2001; Way et al. 2001). Although recent research revealed several factors of resistin regulation (Ukkola 2002) and a new, non-secretable splice isoform (Del Arco et al. 2003), the nature of the receptor molecule and the precise metabolic function of hormones of the resistin family remain to be investigated.

If decreased activity of resistin increases insulin signalling, the increase of insulin receptor substrate 1 (IRS-1) expression in VDRKO mouse hearts might further enhance this effect. IRS-1 and IRS-2 are scaffold proteins that couple insulin and IGF receptors to the phosphatidylinositol-3-kinase (PI3-kinase) and extracellular signal-regulated kinase (ERK) cascades (White, MF E413). Transgenic IRS-1 deficient mice were retarded in growth. IRS-1 expression appeared to be a pre-requisite for IGF-1 induced growth of various organs (Pete et al. 1999). Attenuation of IRS-1 activity by serine phosphorylation is suspected to contribute to insulin resistance and type 2 diabetes (Tanti et al. 2004). IRS-1 also is necessary to induce uncoupling protein-1 (UCP-1) expression in brown adipocytes (Valverde et al. 2003). Unlike in VDRKO mouse kidneys, where UCP-1 expression was strongly up-regulated, no difference in expression of UCP-1 between VDRKO and WT mice was detected in heart.

Among the up-regulated heart-specific energy metabolic enzymes in VDRKO mice was adenylosuccinate synthetase 1 (Adss1). Adss1 is a member of the purine nucleotide cycle (PNC) and regulates the adenine pool during periods of increased workload. Especially under hypoxic conditions enzymes of the PNC are activated to provide additional ATP (Lewis et al. 1999). Increased expression of Adss1 also was observed in cultured neonatal rat cardiomyocytes after addition of glutamine, a major energy resource of the heart. This cellular response was associated with the induction of adult forms of contractile proteins, like α -myosin heavy chain and α -actin, markers for the non-pathological, reversible form of physiological hypertrophy (Xia et al. 2003). In contrast to physiological hypertrophy, an adaptive response to increased

energy demand during postnatal life or maternity, pathological hypertrophy is often secondary to hypertension and is characterised by the induction of fetal genes, like b-MHC and skeletal α -actin (Schwartz et al. 1986). Further evidence for a role of *Adss1* in the development of cardiac hypertrophy was provided by a study that reported *Adss1* expression to be up-regulated in *in vivo* rodent models of surgically induced cardiac hypertrophy (Wen et al. 2002).

Table 4.5.4: Candidate genes involved in lipid metabolism / energy mobilisation, differentially expressed in VDRKO mouse heart compared to WT heart. The fold change values are the mean of five technical repeats, given with the error of the mean.

Fold change	Error	Lion ID	Abbreviation	Genbank ID	Name	Function
1.85	0.27	MG-14-136b10	Lpl	NM_008509	lipoprotein lipase	heparin binding; lipid metabolism; cardiomyopathy
1.83	0.37	MG-6-29h14	ADSS1	NM_007421	adenylosuccinate synthetase muscle	purine nucleotide biosynthesis
1.62	0.15	MG-3-19b11	Bdh	NM_175177	3-hydroxybutyrate dehydrogenase heart mitochondrial	SDR; lipid binding
1.62	0.07	MG-16-5g10	Fas	NM_007988	fatty acid synthase	fatty acid biosynthesis
1.60	0.11	MG-3-76o21	Bdh	NM_175177	3-hydroxybutyrate dehydrogenase heart mitochondrial	SCAD; lipid binding
1.58	0.02	MG-8-52i19	FAE, LCE	NM_130450	fatty acyl elongase (Long-chain fatty-acyl elongase)	Myelination associated SUR4-like protein
1.30	0.03	MG-14-68a4	Irs1	NM_010570	insulin receptor substrate 1	insulin signalling
1.28	0.04	MG-14-4b13	Ant1 Slc25a4	XM_134169	solute carrier family 25 member 4; adenine nucleotide translocase-1	energy mobilization
1.25	0.06	MG-4-146c23	Pcyt1a	NM_009981	phosphate cytidyltransferase 1	phospholipid biosynthesis
1.22	0.10	MG-6-52b15	Gls	XM_129846	Gls: Glutaminase	mitochondrial inner membrane
1.19	0.02	MG-8-35m2	LCE	XM_133979	fatty acyl elongase (Long-chain fatty-acyl elongase)	Myelination associated SUR4-like protein
0.73	0.04	MG-8-70n14	Mgll	NM_011844	monoglyceride lipase	lipid metabolism
0.71	0.04	MG-3-7f21	ECH1	NM_016772	enoyl coenzyme A hydratase 1, peroxisomal	Delta3, β -oxidation
0.66	0.03	MG-14-3m20	Cpt2	NM_009949	carnitine palmitoyltransferase 2	lipid metabolism
0.58	0.07	MG-12-135h1	Gpam	NM_008149	glycerol-3-phosphate acyltransferase mitochondrial	fatty acid metabolism; phospholipid biosynthesis
0.43	0.04	MG-16-9f7	FIZZ1; RETNLA	NM_020509	resistin-like protein alpha	mitogenic factor

4.5.3 Ion transport processes

Strongly down-regulated in the heart of VDRKO mice was carbonic anhydrase type III (*Car3*). Carbonic anhydrase is responsible for the hydration of CO_2 and the removal of protons from ATPases (Dzeja et al. 1999). The myocardium of failing hearts is characterised by reduced activity of *Car3*, together with creatine kinase and adenylate kinase, which promote the removal of ADP, P_i and H^+ from extracellular ATPases (Dzeja et al. 2000). Another function attributed to *Car3* in muscle was to protect proteins from oxidation, catalysed by iron-containing degradation products of haemoglobin and myoglobin (Wistrand 2002).

Also a group of genes coding for proteins involved in trans-membrane ion transport was differentially expressed in VDRKO mouse heart. Among these were two ATPases, the Na^+/K^+ -ATPase *Atp1b1* and the H^+/K^+ -ATPase *Atp4a*, which were both slightly up-regulated. Na^+/K^+ -ATPases establish and maintain the electrochemical gradients of Na and K ions across the plasma membrane. While the subunit alpha

contains the catalytic center, the glycosylated beta subunit determines the number of sodium ion pumps transported to the plasma membrane and the localisation of the enzyme. H⁺/K⁺-ATPases mediate the electroneutral exchange of intracellular H⁺ and extracellular K⁺.

Transmembrane lipid transport is the function of ATP binding cassette (ABC) transporters. The expression of ABCA6 was significantly increased in the heart of VDRKO mice. Although the detailed role of ABC6 transporter is presently unknown, it was reported to be responsive to cholesterol and up-regulated during monocyte differentiation into macrophages (Kaminski et al. 2001). In concert with other cholesterol-responsive ABC subclass A transporters it might regulate functions in lipid export.

Calmodulin is an ubiquitous intracellular calcium-binding protein, that plays an important role in calcium signalling. The isoform calmodulin 2 (Calm2) was slightly up-regulated in hearts of VDRKO mice, which might be associated to higher intracellular calcium concentrations in cardiac myocytes.

Table 4.5.5: Genes involved in transport processes, differentially expressed in VDRKO vs. WT mouse heart, measured in 5 microarray experiments

Fold change	Error	Lion ID	Abbreviation	Genbank ID	Name
0.39	0.07	MG-8-26a9	Car3	NM_007606	carbonic anhydrase 3
1.31	0.09	MG-6-69k15	Atp1b1	NM_009721	ATPase Na K transporting beta 1 polypeptide
1.23	0.03	MG-26-4e24	Atp4a	NM_018731	Atp4a: ATPase, H ⁺ /K ⁺ transporting, alpha polypeptide
1.24	0.06	MG-13-2f24	Calm2	NM_007590	calmodulin 2
1.32	0.11	MG-8-27i22	Abca6	NM_147218	Abca6: ATP-binding cassette, sub-family A (ABC1), member 6
1.48	0.14	MG-6-18c1	Slc2a1, Glut1;	NM_011400	solute carrier family 2 facilitated glucose transporter member 1
1.35	0.09	by qPCR:	Calm2,	NM_007590	calmodulin 2

4.5.4 Marker genes for hypertension and cardiac hypertrophy

Increased lipogenesis and decreased lipolysis generally are regulated by insulin in response to caloric excess. In cardiac hypertrophy, the increased utilisation of glucose instead of fatty acids as energy source is a metabolic shift in response to pressure overload (Allard et al. 1994). In the face of increased and prolonged stress through hypertension, terminally differentiated cardiomyocytes enlarge, increasing weight and volume of the heart, that eventually progresses to severe disease and failure.

Hypertension in VDRKO mice might be the result of an up-regulation of the renin-angiotensin system in kidney, as detected in this study in section 3 and by Li et al. (Li 2003). Renin, cleaving angiotensin I from angiotensinogen, was highly up-regulated in VDRKO mouse kidney (section 3). In heart, renin is expressed only in marginal concentrations and was even slightly down-regulated. However, angiotensinogen mRNA and endothelin receptor, not represented on the array, were found significantly up-regulated in qPCR measurements. Endothelin is known as a powerful vasoconstrictor, inducing hypertension, fibrosis, arterial remodelling and atherosclerosis (Touyz and Schiffrin 2003). A sign for hypertrophy, apart from elevated blood pressure, is the increased heart weight of VDRKO mice, relative to the body mass. (Li et al. 2002). Although further morphological studies in the hearts

of mice of different ages have to confirm the disease pattern of cardiac hypertrophy, a number of genes, characteristic for the onset of this disease condition were found in this study.

Increased utilisation of glucose in cardiac hypertrophy has been related to up-regulated expression of the glucose transporter GLUT1 (Montessuit and Thorburn 1999). In neonatal rat ventricular myocytes (NRVM)s, GLUT1 overexpression was found necessary, but not sufficient for the development of hypertrophy and increased expression of marker genes for hypertension and cardiac hypertrophy, like atrial natriuretic peptide (ANP). GLUT1 up-regulation also seemed to have a protective effect for myocytes against apoptosis (Morissette et al. 2003). In the hearts of VDRKO mice GLUT1 and ANP were found significantly up-regulated. Up-regulation of ANP, verified by qPCR, appears to be a logic consequence of the ablation of VDR function: Vitamin D was shown previously to suppress ANP expression via a genomic, VDR-mediated mechanism (Chen et al. 1998; Chen et al. 1999).

Cardiovascular stress can not only result in hypertrophic growth and enhanced glucose demand, but also induces myocardial angiogenesis and, in a chronic state, fibrosis. Important regulators of angiogenesis, myocardial fibrosis and atherosclerosis are growth factors of the CCN family, like Cyr61 (CCN1), up-regulated in kidneys of VDRKO mice (section 3) or connective tissue growth factor (CTGF, CCN2), significantly up-regulated in hearts from VDRKO mice. CTGF up-regulation was measured in tissue of rats with myocardial remodelling heart failure and seemed to be induced by angiotensin II via the AT1 receptor (Ahmed et al. 2004). CTGF expression was reported to respond positively to TGF β via protein kinase C and RAS/MEK/ERK cascades (Leask et al. 2003).

As can be concluded from its name, the expression of vitamin D₃ up-regulated protein 1, (VDUP1, thioredoxin-binding protein-2, TBP-2) is induced Vitamin D. By binding specifically to the reduced state of thioredoxin, TBP-2 blocks its function as oxido-reductase to control the cellular redox balance (Nishiyama et al. 1999; Schulze et al. 2002). In vascular smooth muscle cells, thioredoxin (TRX) overexpression results in increased proliferation, as was observed in several malignomas (Gasdaska et al. 1994). Elevated activity of TRX also was observed to be induced by oxidative stress, either mediated through intracellular pathways of PDGF signalling (Sundaresan et al. 1995) or by treatment with H₂O₂. This increased activity of TRX as a scavenger for reactive oxiditive species (Del Arco et al.) can be inhibited by TBP-2 overexpression or treatment with vitamin D.

Increased ROS production and TRX activation was observed as a side effect of angiotensin II signalling (Schulze et al. 2002). Since angiotensin is a potent vasoconstrictor, a positive correlation between hypertension, oxidative stress and TRX expression can be expected. Increased cardiac hypertrophy and oxidative stress markers in transgenic mice expressing dysfunctional TRX confirms this conclusion. Mice overexpressing wild type TRX were less prone to hypertrophy and the expression of markers for oxidative stress (Yamamoto et al. 2003).

Recently, this finding was challenged by a study that observed reduced levels of TRX expression in spontaneous hypertensive and stroke-prone rats, in spite of increased markers for oxidative stress in these rats (Tanito et al. 2004). It appears that in these rat strains TRX expression is suppressed due to a different mechanism. Reduced levels of TRX make these animals more vulnerable to oxidative stress and

cardiovascular diseases. Furthermore, expression levels of TRX protein were reduced in myocardium after ischemic stroke. Through exposure to repeated short periods of ischemia, the heart can be preconditioned and protected against heart failure through ischemic stroke. This preconditioning process increased TRX expression. Hearts from transgenic mice overexpressing TRX were more resistant to ischemic injury as compared to hearts from WT mice (Das 2004).

Since vitamin D induces the expression of TBP-2, it can suppress the protective effects of TRX against oxidative stress, hypertension, ischemia and cardiac hypertrophy. Down-regulation of TBP-2 in the hearts of VDRKO mice can be expected to make them less vulnerable to these pathological conditions and might be a protective reaction.

Table 4.5.6: Genes involved in the development of hypertension and cardiac hypertrophy. The expression in VDRKO mice was measured by microarray expression profiling and / or by qPCR, normalised to PBGD expression. The fold change values calculated relative to WT mouse heart.					
Fold change	Error	Method	Abbreviation	Genbank ID	Name
1.95	0.17	qPCR	ANP / ANF	XP_131840	atrial natriuretic peptide precursor
1.44	0.03	array	ANP / ANF	XP_131840	atrial natriuretic peptide precursor
1.48	0.14	array	Slc2a1, GLUT1	NM_011400	solute carrier family 2 facilitated glucose transporter member 1
2.20	0.28	qPCR	CTGF	NM_010217	connective tissue growth factor
2.37	0.10	array	CTGF	NM_010217	connective tissue growth factor
0.72	0.05	qPCR	TBP-2 / VDUP1	AF173681	thioredoxin interacting protein
0.68	0.06	array	TBP-2 / VDUP1	AF173681	thioredoxin interacting protein
2.97	0.65	qPCR	AGT	NM_007428	angiotensinogen
1.33	0.16	qPCR	Ednrb	NM_007904	endothelin receptor B
1.03	0.25	qPCR	Cyr61 /CCN1	NM_010516	cystein rich protein 61
0.59	0.08	qPCR	renin	NM_031192	renin

4.5.5 Genes induced in ischemic insult and cardiac hypoxia

Cardiac troponin T is a protein integral to the function of cardiac muscle. In the heart of VDRKO mice the slow skeletal muscle isoform (Tnnt1) was clearly up-regulated, which was confirmed by qPCR. Cardiac troponins are released from necrosing myocardium in a time-specific manner, peaking at 16-18 hours post infarction (Sarko and Pollack 2002). The quick decrease of troponin levels in serum are an indicator for successful reperfusion and can be used as a prognostic marker for a favourable disease outcome, similar to creatine kinase MB (CK-MB). Creatine kinase was found up-regulated in the kidneys of hypocalcemic VDRKO mice. Although the physiological interpretation of elevated mRNA levels of Tnnt1 in the heart of VDRKO mice requires further histological studies, it might indicate ischemic cardiac lesions.

In fact many of the genes induced in VDRKO mouse heart, like GLUT1, ANP, CTGF or hypoxia-inducible factor-(HIF)-responsive RTP801 were observed up-regulated in heart tissue after ischemic stroke. While ischemic stroke often causes lethal injuries, brief episodes of hypoxic stress / ischemia can protect the heart from future ischemic insult, a mechanism called preconditioning (Cai et al. 2003). Under hypoxic conditions, a number of genes involved in glucose metabolism, cell proliferation and erythropoiesis are induced, many of them in response to the activation of the HIF-1 transcriptional complex (Harris, AL 38). While in the absence of oxygen the HIF complex binds to hypoxia-response elements to induce transcription, in the presence

of oxygen HIF binds to the tumor suppressor von Hippel-Lindau protein, becomes ubiquitinated and degrades rapidly (Maxwell et al. 1999).

A recently published microarray study aimed to find target genes and pathways, induced in the 4 hours following a brief period of ischemia. This preconditioning of rat hearts mimicks a condition comparable to mild angina pectoris (Simkhovich et al. 2003). Hearts from rats were subjected to ischemia by proximal coronary occlusion. After 4 hours of reperfusion, the hearts were excised, frozen and their expression profile compared to the hearts of untreated rats. Surprisingly, some the genes which were strongly induced by ischemia-reperfusion were also found strongly up-regulated in the hearts of VDRKO mice, like S100A8 and S100A9 (calgranulin A / B).

Among the genes up-regulated in VDRKO mouse heart was a cold stress-responsive protein, called RNA binding motif protein 3 (RBM3). RBM3 was recently identified to be responsive to hypoxia by a HIF-1-independent mechanism (Wellmann et al. 2004). Cold stress in turn is a condition that induces hypertension in humans and rodents (Zhu et al. 2002) and was used in wild type rats as a model to study hypertension without further treatment. *In vitro* RBM-3 was found to prevent cell death in various cell lines (Kita et al. 2002).

Fold change	Error	Lion ID	Abbreviatio	Genbank ID	Name	Function
2.22	0.41	MG-13-134p22	Rtp801-pending	NM_02908	HIF-1 responsive RTP801	expressed after ischemic stroke
1.67	0.18	MG-15-3o3	Tnnt1	NM_01161	Slow skeletal muscle troponin T.	regulation of muscle contraction
2.06	0.51	qPCR	Tnnt1	NM_01161	Slow skeletal muscle troponin T.	regulation of muscle contraction
1.75	0.16	MG-13-3c23	Rbm3	NM_01680	mRNA binding motif protein 3	cold stress-induced mRNA, mediates internal initiation of translation with increased efficiency under conditions of mild hypothermia.

5. Conclusions

5.1 Establishing microarray technology

As a first step to establish cDNA microarray technology for gene expression profiling, protocols for the production and use of “low density arrays” were tested and optimised. This included the selection of *E.coli* clones with 4-800 bp long cDNA fragments in silico and the verification of their identity by gel electrophoresis and re-sequencing. Procedures for efficient and quality-controlled amplification by PCR and purification were adapted to automation with liquid-handling robotics. Uniform morphology of probe spots on the array, stable binding to the surface and low background are essential to produce reproducible microarray data. Therefore, a major effort was invested to optimise the printing process. Whereas ring and pin systems worked well for low-density arrays, split pin printing delivered the best results in the production of high density arrays. A crucial role has the combination of surface coating of the glass substrate and spotting buffer. Epoxy and aldehyde coatings with low hydrophobicity and buffers containing high salt concentrations gave the most uniform probe spots. Spotted probes bind covalently to these coatings. Blocking protocols prevent unspecific binding.

The performance of these low and medium-density arrays was tested with osteosarcoma cells that were induced to differentiate into osteoblast-like cells by the steroid hormones vitamin D, dexamethasone and estradiol. Differentiation stages of these cells that ultimately agglomerate to nodules, express alkaline phosphatase and excrete bone matrix could be distinguished by light microscopy. Analysis of untreated and treated cells with microarrays delivered clear and reproducible changes in gene expression pattern. These experiments were sufficient to validate the method. However, the changes in gene expression were difficult to normalise data and interpret.

5.2 Treatment of osteoblast with CCN1 induces processes as in bone fracture repair

Treatment of human fetal osteoblast (hfOB) precursor cells with CCN1, a factor that previously was identified as induced by vitamin D treatment delivered more focused changes in gene expression. CCN1 expression is associated with bone growth and wound healing especially during fracture repair (Hadjiargyrou et al. 2000), as was confirmed by the activation of several genes that earlier had been identified as markers for these processes: The elevated expression of the Notch2 transcript was detected by microarray analysis and confirmed by RT-PCR. The transcripts of the Notch downstream effectors Hey2 and Hes1 were also measured in elevated concentrations by the collaborating partner N. Schütze in hfOB after treatment with CCN1. Activation of IGF2 and genes from the hedgehog signalling pathway additionally enhanced the anabolic effect of Notch signalling on bone growth. During bone fracture repair, growth arrest and terminal differentiation of osteoblasts has to be reversed. Down-regulation of genes related to growth control, like Gadd45 or inhibin alpha, and markers for late stages of chondrocyte differentiation characterise the transcriptional events in parallel to this process. Although further experiments with the protein products of CCN1 target genes have to confirm their specific role in bone growth and fracture repair, this study can be seen as a first step to elucidate the underlying molecular control mechanisms. In the meantime, further studies are on

their way which might establish CCN1 as therapeutic agent to accelerate the growth of bone tissue after implantations (Schutze, personal communication 2003).

5.3 Pancreatic beta cells respond to glucocorticoid treatment with transcriptional changes characteristic for a pre-diabetic condition

The success of these preliminary experiments provided confidence to scale up probe production and create high-density mouse cDNA arrays in collaboration with scientists from the new gene expression profiling group at the IEG. With nearly 21.000 probes these arrays cover an important part of the mouse genome. These 21K arrays were tested with RNA samples extracted from murine osteoblast-like MC3T3 cells and tissue from different organs. Their first application was studying transcriptional changes induced by treatment of pancreatic beta-cells with high doses of corticosterone, the murine analog of cortisol. Analysis of five microarray experiments with RNA extracted from two sets of independently treated aliquots of cells resulted in a list of reproducibly up- or down-regulated genes. Our collaborating partners M. Hult and U. Opperman from the Karolinska Institute in Stockholm confirmed the regulation of a selection of these genes by quantitative PCR.

The observation that the short-term reaction of beta cells to glucocorticoid treatment includes elevated secretion rates of insulin was in line with the activation of genes that previously were associated to increased insulin secretion, such as amiloride-sensitive cation channel, phosphatidylinositol 3-kinase, growth receptor binding protein 10 or lipoprotein lipase (Hult 2004). Increased secretion rates of insulin can be interpreted as a stress reaction, which after chronic exposure to glucocorticoids can result in insulin resistance and diabetes (Lenzen and Bailey 1984). This previously established association was corroborated here by the activation of stress markers, like FK506 binding protein 5 (FKBP51). FKBP51 confers protection against stress mediated by exposure to glucocorticoids by lowering the affinity of the glucocorticoid receptor to its ligand. Several genes, previously associated with immune response and inflammation of the pancreas, including heat shock protein 1/25, integral membrane-associated protein 1 (Itmap1), or lipocalcin 2 (Lcn2), were activated by glucocorticoid treatment. In contrast, trefoil factor 2 (TFF2), known to attenuate symptoms of inflammation, was clearly down-regulated after treatment with corticosterone. Furthermore, alpha-1 proteinase inhibitor (Api or Serpina12), an acute phase protein specific for pre-diabetic conditions, was clearly induced by glucocorticoid treatment. IL-1 β an antagonist of Api was strongly down-regulated.

A pre-diabetic condition of pancreatic beta cells, after exposure to elevated concentrations of glucocorticoids was reflected in elevated insulin secretion, and increased expression of marker genes for stress and inflammation. Extended over longer time periods, this stress condition might result in glucose insensitivity and a decrease in insulin production. To our knowledge this was the first study that investigated direct effects of glucocorticoid treatment of pancreatic beta cells from lean mice on gene expression level.

5.4 Gene expression profiling of kidneys of mice with inactivated vitamin D receptor (VDRKO)

Ablation of the function of the vitamin D receptor in mice created an excellent model of type II human hereditary rickets and provided options to study the molecular biology of vitamin D signalling. The comparison of gene expression profiles of

kidneys of VDRKO mice with WT animals, grown under identical conditions, showed that a large number of genes were differentially expressed, including genes that were published recently from a similar study (Li et al. 2003). Not surprisingly, some of the protein products of the most strongly regulated genes like calbindin D9k (CalbD9k) are involved in calcium and phosphate transport in renal glomeruli. Strong suppression of CalbD9k in VDRKO mice reflects impaired renal reabsorption of calcium and severe hypocalcemia. Low serum calcium levels in turn cause a number of malfunctions diagnosed in the VDRKO phenotype, like osteomalacia and growth retardation.

Apart from the classical function of vitamin D in the regulation of serum calcium levels, gene expression profiling of kidneys from VDRKO mice revealed genes involved in other processes. Physiological functions as lipogenesis, blood pressure regulation or immune response, were often associated with vitamin D signalling, but the molecular mechanisms of these effects of vitamin D actions remained elusive (Zemel 1998; Zemel 2004). These transcriptional changes were difficult to interpret because of the strong impact of hypocalcemia and hyperparathyroidism, which might overlap with the effect of VDR ablation on transcriptional regulation.

5.4.1 Influence of covariate factors: Gender and diet

To distinguish the influence of various conditions on changes of the expression profile of tissue from VDRKO mouse kidneys, a second study was conducted. In this study organs from mice of different gender which were raised either on normal diet or on food additionally supplemented with calcium and phosphate ("rescue diet", RD) were analysed. Different strategies and clustering algorithms were employed to group genes and sample groups according to functions and experimental conditions. Hierarchical clustering showed that microarray experiments clustered spontaneously according to the four sample animal groups. The gender effect outweighed the influences due to different diets. Supervised methods, like k-means clustering and significance analysis of microarrays (SAM) were used to group genes that were regulated by both, VDR function and gender.

Prominent examples of VDR and sex-dependent genes are two forms of glutathione S-transferases, *Gsta2* and *Gsta4*, which were up-regulated in female mice and have an important protective function against reactive oxygen species (ROS). Cytochrome P4504b1 (*CYP4β1*) was strongly down-regulated in all VDRKO animal groups, whereas the related *CYP4α14* was up-regulated in females and down-regulated in males. Since *CYP4α14* indirectly can influence the regulation of the vascular tone, different expression according to gender might explain the elevated risk of males to develop hypertension and heart diseases, as observed in multiple studies (Reckelhoff 2001). A more efficient protection of vascular endothelia of females against hemodynamic shear stress can result from increased expression of macrophage-capping protein (Capg), a member of the gelsolin-like family of proteins. These proteins interact with vitamin D binding protein (DBP), and are up-regulated in VDRKO mouse kidney and heart. Cytochrome P450 *CYP7b1* was only in the kidneys of female mice down-regulated, while it was strongly up-regulated in male VDRKO mice, compared to WT. The dependence of *CYP7b1* expression on VDR action and gender is reasonable, if one considers its role in the catabolism of 5α androstane- $3\beta,17\beta$ -diol and its capacity to suppress androgen-controlled growth processes.

5.4.2 Altered gene expression in tissues from normocalcemic VDRKO

A separate analysis of changes in gene expression profiles in kidneys from male RD mice excluded influences of sex steroids, hypocalcemia and hyperparathyroidism. Especially genes that previously were associated with important physiological functions were selected and their relative changes in expression confirmed by quantitative real-time PCR (qPCR). Results from qPCR experiments correlate strongly with microarray data and confirm the quality of the experiments and strategies for data analysis. As observed previously, qPCR has a higher dynamic measurement range and suffers less from signal compression due to saturation effects.

Supplementation of VDRKO mice with a diet enriched in calcium and phosphate (RD) increases intestinal calcium absorption rates and balances the losses due to impaired renal reabsorption (Erben et al. 2002). Many genes, involved the maintenance of systemic ion concentrations, like the sodium-dependent phosphate cotransporter Npt4 or the sulfate transporter NaS1, were down-regulated in kidneys only from ND VDRKO mice. Vasopressin-sensitive Aquaporin 2, regulating electrolyte volume and previously identified as suppressed in rat kidney by vitamin D treatment, was up-regulated exclusively in ND VDRKO mice. On the other hand, the strong down-regulation of cabindin D9k independent of the diet confirmed observations that in RD mice calcium transport processes remained impaired (Li, Y. C. et al. 2001).

5.4.3 Ligand-independent action of VDR

The expression of the truncated VDR was down-regulated in male ND VDRKO mouse kidneys, which is in line with the observation that VDR expression can be induced by increased exposure to vitamin D. Ligand-independent functions of the receptor complex, like in the case of hair growth correspond to the fact that with increased concentrations of receptor and ligand the level of unliganded VDR remains stable (Strom et al. 1989).

The disrupted transcriptional feedback control of vitamin D biosynthesis in VDRKO mice, leads to dramatically increased serum levels of active $1,25(\text{OH})_2\text{D}_3$ (Erben et al. 2002). In kidneys of ND VDRKO mice vitamin D-activating CYP1 α was increased by a factor of (158,4 +/- 10,7) fold, in RD VDRKO mice by (5,4 +/-1,1) fold with respect to WT animals on the same diet. While VDR-dependent transcriptional control of vitamin D is disrupted in VDRKO mice, the elevated levels of $1,25(\text{OH})_2\text{D}_3$ can result in increased non-genomic action of vitamin D. In the case of alopecia, it has previously been shown that hair growth exclusively depends on the availability of the VDR-RXR receptor complex, independent from vitamin D ligand (Sakai et al. 2001).

5.4.4 Non-genomic and genomic actions of vitamin D influence lipid metabolism

On the other hand, there is substantial evidence for non-genomic actions of vitamin D and its derivatives. The high proportion of genes involved in lipid metabolism and cellular energy supply among differentially expressed genes in kidney indicate major metabolic changes in the VDRKO mouse phenotype. A general trend of induction of genes involved in lipogenesis and repression of lipid catabolism, as can be seen especially in the case of ND VDRKO mice, correlates with numerous studies conducted by Zemel et al (Zemel 2001; Zemel 2002; Zemel 2004). They found that

high systemic vitamin D concentrations, which can be attenuated with calcium-enriched diets, stimulate lipogenesis and suppress lipolysis in rodents and humans. Significant activation of fatty acid synthase (FAS) and long-chain fatty acyl elongase (Lcfae) in ND VDRKO mouse kidneys and down-regulation of lipoprotein lipase (Lpl) or cytosolic acetyl-CoA hydrolase (Cach) in kidneys of mice on both diets confirm and further extend this model. It was shown previously that this effect is based on interaction of vitamin D with a putative membrane receptor, which can activate the import of calcium ions into the cytosol. Increased intracellular calcium levels activate lipogenesis and decreases sensitivity to insulin signalling.

Simultaneously, disrupted genomic action of vitamin D abrogates suppression of uncoupling protein 1 (UCP1) in mice on both diets. Enhanced mitochondrial uncoupling increases energy expenditure at the cost of ATP production. A decrease in ATP supply in turn compromises insulin signalling and numerous other essential cellular functions. Two members of the Cide family of proteins, Cidea and FSP27, were strongly up-regulated in VDRKO mouse kidney. Only recently a functional association of the protein products of the Cidea and the UCP1 gene was found: By binding to UCP1, Cidea seems to inhibit uncoupling and increased dissipation of energy (Lin and Li 2004). Whether increased expression of Cidea in kidneys of VDRKO mice is a protective mechanism in response to excessive uncoupling needs to be further investigated. The interaction of UCP1 with Cidea appears to be a key event in the development of obesity and diabetes (Zhou et al. 2003). A function of vitamin D in the regulation of this important metabolic switch was for the first time discovered in this study.

5.4.5 Vitamin D and growth control / apoptosis

Cide proteins also function as apoptotic inducers. The role of vitamin D action in the control of growth and apoptosis was substantiated especially in the case of tumors like breast and prostate cancer *in vitro* and *in vivo*. Apoptosis is initiated by the release of cytochrome C from the mitochondria. This can be triggered by the nuclear orphan receptor Nur77/TR3, which was significantly up-regulated in hypocalcemic ND VDRKO mouse kidneys but down-regulated in kidneys from RD VDRKO mice. While down-regulation of Nur77 in RD mouse kidneys can be due to the lack of transcriptional activation through the VDR, elevated PTH serum levels in ND mice might cause up-regulation of Nur77 via non-genomic actions (Tetradis et al. 2001). The complex system regulating Nur77 activity via multiple factors might be the reason why the use of vitamin D derivatives in tumor therapy so far was little successful. The loss of the expression of dual-specificity phosphatase 6 (DUSP6) in tumor tissue is associated with uncontrolled growth. Dephosphorylation of ERK by DUSP6 inhibits growth stimuli through the MAPK pathway. Down-regulation of dual-specific phosphatase 6 (DUSP6) in kidneys of VDRKO mice further supports the role of vitamin D action in the control of growth and carcinogenesis.

5.4.6 VDRKO mice and hypertension

Similar as in lipogenesis and weight control, the influence of calcium and vitamin D on blood pressure control becomes more and more clear. As mentioned before, up-regulation of aquaporin 2 in VDRKO mouse kidneys indicate increased susceptibility of these mice to develop hypertension. Hyperparathyroidism and increased cytosolic calcium concentrations are further risk factors for the development of hypertension. On the transcriptional level, activation of the renin – angiotensin system, as found in

this study and by others, appears to be a mechanism which promotes elevated blood pressure in the animal models and humans suffering from type 2 hereditary rickets. The suppression of renin biosynthesis found to be regulated by a genomic, VDR-dependent mechanism (Li et al. 2004). In this study, however, increased expression of renin was restricted to kidneys from hypocalcemic ND mice, suggesting at least an influence of PTH or non-genomic effects via calcium. Up-regulation of bradykinin-metabolising carboxypeptidase N (CPN) shortens the half-life time of the kinin peptide, which is widely known as vasodilator and protector against hypertension. The cleavage products of bradykinin act through a different G-coupled receptor, active in the chronic phase of inflammatory response.

Chronic hypertension can result in cardiac hypertrophy, fibrosis and other types of cardiovascular diseases. Although systematic measurements of blood pressure and heart weight were not possible within this project, elevation of these macroscopic indicators were recently stated by others (Li 2003). The description of a cardiovascular disease VDRKO phenotype and activated gene expression of marker genes for hypertension observed in VDRKO mouse kidneys were the motivation to conduct gene expression analysis in VDRKO mouse heart, as well.

5.5 Gene expression profiling of VDRKO and WT mouse heart

To find changes in the expression profile of hearts from VDRKO and WT mice, RNA from 3 VDRKO mouse hearts, raised on a calcium-enriched RD diet, were pooled and hybridised in 5 microarray experiments against a reference RNA from WT mouse hearts. Differentially expressed genes were identified after normalisation and Z-score filtering by significance analysis of microarrays (SAM) on the criterion whether they follow the dye swap. Genes that changed significantly between WT and VDRKO mice were grouped according to their functional annotations and the expression of selected genes verified by qPCR. Most of these genes have functions in immune response, lipid metabolism and energy mobilisation, ion transport or are known as marker genes for cardiovascular diseases, including hypertension, hypertrophy or ischemia.

5.5.1 Changes in the immune response in VDRKO mouse heart

Drastically up-regulated were calgranulin A and B (S100A8/9), which previously were reported to be induced in response to inflammatory diseases. Like in kidney, carboxypeptidase N (CPN) and vitamin D-binding protein (DBP) were significantly up-regulated in VDRKO mouse heart. Apart from its role as transporter for vitamin D metabolites, DBP is involved in the activation of macrophages in inflammation (Yamamoto and Naraparaju 1996). Increased expression of immune response markers indicates an inflammatory condition of VDRKO mouse hearts. The impact of vitamin D signalling on the immune system has long been recognised. In animal models for autoimmune diseases, like multiple sclerosis, inflammatory bowel disease or type I diabetes, vitamin D treatment attenuated or completely inhibited the onset of the disease.

5.5.2 Impaired lipid metabolism can compromise heart function

Like in kidney, the largest part of differentially expressed genes in VDRKO mouse heart can be associated to functions in lipid metabolism and energy supply. Again fatty acid synthase (FAS) belonged to the most strongly up-regulated genes, confirming the scheme proposed by Si et al. (Shi et al. 2001b). Up-regulation of lipoprotein lipase on the surface of cardiomyocytes can facilitate the entry of triglyceride-rich particles into the cytosol (Yagyu et al. 2003). Accumulation of glyceride particles in cardiomyocytes leads to lipotoxic effects and pathogenic conditions as known in cardiomyopathy, diabetes mellitus and obesity (Finck et al. 2002). Down-regulation of enzymes involved in lipolysis like carnitine palmitoyltransferase Cpt II or monoglyceride lipase might indicate a metabolic shift from lipolysis to other energy carriers like carbohydrates or glutamine. Increased metabolism of glutamine in stress phases and during the onset of cardiac hypertrophy is paralleled by the up-regulation of adenylysuccinate synthetase 1 (Adss1) (Lewis et al. 1999). Activation of the glucose transporter GLUT1 was previously associated with increased utilisation of glucose in cardiac hypertrophy (Montessuit and Thorburn 1999). In this study, the expression of Adss1 and GLUT1 in hearts of VDRKO mice was identified as significantly increased. Other markers for cardiac hypertrophy and fibrosis, like atrial natriuretic peptide (ANP) and connective tissue growth factor (CCN2) were strongly up-regulated, as well.

Metabolic processes create reactive oxygen species (ROS) as side products. Thioredoxin can attenuate oxidative stress exerted by ROS. Vitamin D up-regulated protein 1 (TBP-2, VDUBP1) was significantly down-regulated in VDRKO mouse heart, showing that activation of this gene has to be mediated by VDR via genomic action. Since TBP-2 inhibits thioredoxin function, VDRKO mouse hearts are probably less vulnerable to oxidative stress. On the other hand, with cardiac troponin T, HIF-1-responsive RTP801 and Rbm3 markers for ischemia, hypoxia and cold stress were activated. Exposure of rodents to cold stress is a non-invasive method to create animal models for hypertension.

Carbonic anhydrase 3, responsible for the removal of CO₂ and protons from ATPases was significantly down-regulated. Decreased activity of carbonic anhydrase, creatine kinase and adenylate kinase characterise the myocardium of failing hearts (Dzeja et al. 2000).

5.6 Summary

To sum up, gene expression profiling of VDRKO mouse kidney and heart and the comparison to organs from WT animals showed impairments in the regulation of diverse physiological functions and biochemical pathways. Especially the high number of differentially expressed genes with functions in lipid metabolism and blood pressure control is striking and confirms the long suspected association between vitamin D action and metabolic diseases. Disturbances in blood pressure control and lipid metabolism are also reflected in the alterations of the transcription profile from the hearts of VDRKO mice. Activation of genetic markers for inflammatory diseases, cardiac hypertrophy and ischemia might be secondary to these disturbances, caused by ablated genomic VDR function and non-genomic action of vitamin D.

6. Methods

Although there are a number of companies selling cDNA arrays, most commercial applications of DNA microarray technology base on oligonucleotide arrays due to the better conditions for standardisation, quality control and mass production. In academic research, the financially more accessible cDNA arrays technology prevails, which is the method of choice for this project.

Whereas on oligonucleotide arrays each gene is usually represented by several probes with a defined length between 20 and 70 base pairs, on cDNA arrays one single cDNA fragment with a length of several hundred base pairs are intended to bind specifically to one gene transcript. The longer fragment sizes of cDNA probes and their variation in length and G/C content imply limitations of cDNA arrays to distinguish between partly homologous transcription products (e.g. different splice forms), less stringent hybridisation and wash conditions and problems that might arise from secondary structures of long DNA fragments. In contrast to the oligonucleotides produced by chemical synthesis, the probes for cDNA array production are generally amplified by PCR from cDNA fragments cloned into *E.coli*.

6.1 Microarray production and analysis

6.1.1 Clone selection, storage and verification

To establish the method, small and medium-sized cDNA arrays were produced from *E.coli* clones obtained from the German Resource Center (RZPD). In later studies a genome-wide mouse array was produced using a cDNA clone collection obtained from Lion Biosciences Inc. (Lion 2001).

6.1.1.1 The Human cDNA array

For the human array, genes and gene families, known to be involved in steroid biosynthesis, cholesterol metabolism, bone growth and –turnover (Ho et al. 2000; Jia et al. 2001), cell adhesion, (bone) matrix production, and the development of osteoporosis, were chosen, as well as genes from two UNIGENE bone tissue cDNA libraries. The corresponding cDNA clones were found by aligning mRNA or EST sequences to the NCBI human EST data base (EST Blast) or from the UNIGENE data base. If available, cDNA clones were ordered from the RZPD in Berlin. Before ordering, the identity and specificity of the cDNA clone inserts was re-confirmed by comparing the sequences by (non-redundant) Blast with all ESTs in the NCBI EST data base.

Since sample RNA was transcribed using oligo (dT) primers, the 3' end of mRNA sequences was the preferred region from which EST clones were selected. To obtain a uniform melting range of probes, allowing more stringent hybridisation and washing conditions, generally a probe length between 400 to 800bp was chosen, in some cases up to 1200bp.

The gene annotations and clone identifiers (IDs) were stored in Excel sheets. While Excel provides an easy-to use platform for small microarray projects, safety considerations, memory size and feasibility issues speak against their use for data storage and -management for middle-sized or genome-wide clone data bases.

Commercial packages or data bases like ACCESS are better suitable to manage large clone databases. For the 21K-mouse chip the GSF obtained the Lion mouse arrayBASE, a web-interfaced data base containing clone annotations and links to other resources, like the NCBI.

Once the *E.coli* clones were obtained, the identity of their cDNA inserts was verified by re-sequencing and by comparing insert lengths of the corresponding PCR products, as read from agarose gels, to the lengths (partially) provided in the databases. In the case of human RZPD clones, ca. 25% of the clones didn't have the expected sequence inserts and further 20% were difficult to amplify by PCR. In the meantime, the RZPD has reacted to complaints and offers a non-redundant, sequence-verified UNIGENE 3.1 set of 36.400 human cDNA clones.

6.1.1.2 The Mouse 21k-array

At the end of the year 2001, the mouse arrayTag clone collection, from Lion Biosciences AG became available and was used in cooperation with the group of Dr. Johannes Beckers, IEG, to produce microarrays containing over 20.000 sequence-verified mouse cDNAs. For the productions of this array methods and materials developed and tested during the development of the smaller human array were used. To meet the needs of high-throughput microarray probe production, the protocols were adapted to liquid-handling robotics.

6.1.2 Template production

E.coli clones were delivered as LB-medium agarose cultures (RZPD) or as glycerol stocks (Lion AG), recently in 96-well format. While the first hundreds of clones were picked and plated one-by-one, the 96-well format allowed quick and safe transfer of bacterial clones with a stainless steel comb into 96-deep well plates, containing ca. 800 µl of LB medium with 50µg/µl ampicilin. The plates were covered with a gas permeable membrane and incubated in a heated shaker for 24-30 hours at 37 °C.

Initially, purified bacterial plasmids were use as PCR templates. The tedious, cost- and work-intensive plasmid purification on midi or mini-columns (Quiagen, Macherey & Nagel) were later replaced by bacterial lysates. Like plasmid preps, lysates can be produced efficiently with the help of liquid-handling robots in the 96-well format: An aliquot of bacterial suspension was diluted 1:10 in water and heated in a thermocycler block for 10 min. at 95°C. The cell debris was removed by centrifugation for 3 minutes at ca. 1200xg. Generally, two copies were made of this lysate plate and stored at -80°C for later use to avoid repeated thawing and freezing of glycerol stocks. Two more aliquots were taken from the bacterial solution for archiving as 10% glycerol stocks and frozen at -80°C.

6.1.3 Amplification of probes by PCR

Gene expression can be quantified by microarray technology only if the probe (the PCR product) is available in excess on the coated glass substrate, achieving an hybridisation reaction of first order kinetics. Various experiments within this project, as well as the experience from other groups showed that a concentration range of 200-500 ng/µl DNA in the spotting buffer is recommendable. To achieve this

concentration (in 30µl spotting solution) over a wide range of reactions with differing amplification efficiencies, 3 replicates of 100µl PCR reactions were pooled.

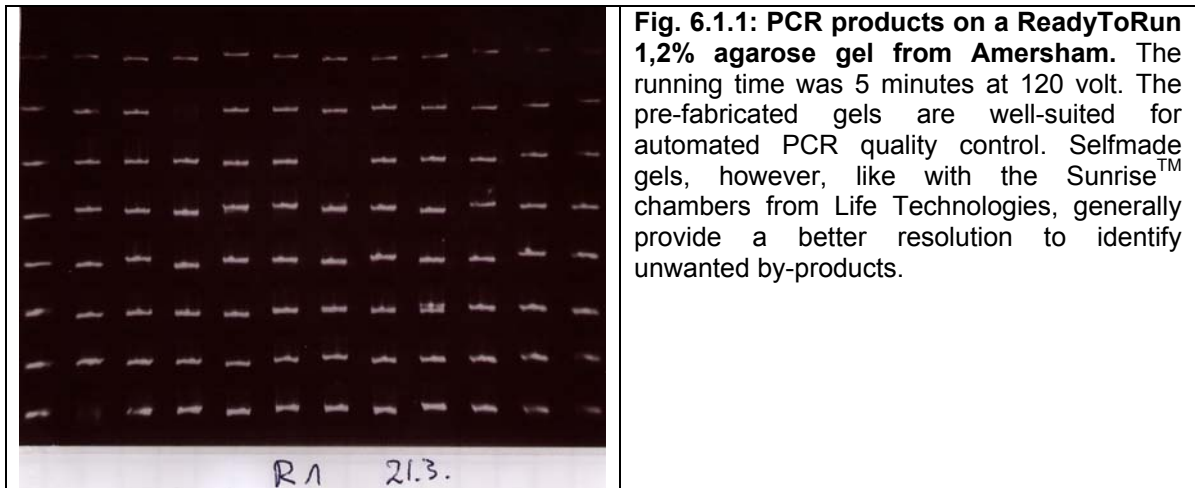
PCR master mix for one 96-well plate:

Ampuwa water	8,74ml
10xPCR buffer	1ml
MgCl ₂ (250mM)	100µl
M13 forward primer (100µM)	20µl
M13 reverse primer (100µM)	20µl
dNTP mix (25mM per dNTP)	80µl
Taq polymerase	40µl
total volume	10ml

100 µl of this master mix and 3 µl of template (bacterial lysate) were pipetted into 96 well thermoplates and sealed. The reactions were amplified in a thermocycler (MJ Resarch; PTC-225 Tetrad) using the following cycling programme:

95°	3 min	} 37x	initial denaturation
95°	30 sec		denaturation
52°	30 sec		annealing
72°	1:30		extension
72°	5 min		
6°	unlimited		

After amplification, the products were checked on 1,2% agarose gels for by-products and the concentration estimated. For the enormous numbers of PCR reactions to be checked, this step can be very time consuming and has to be done in high throughput format. In this study, large gels for 2x96 samples (Sunrise™, Life Technologies) or up to 8x96 wells (Owl Scientific, Woburn MA, USA) and 12 channel pipettes were used. At a later stage, pre-fabricated Ready-to-Run agarose gels from Amersham were used (this format can be processed by lab robots), as the separation time is just 5 min. at 120V.



Before spotting, unincorporated dNTPs and primers had to be removed. For this step, an automated protocol was developed for the Biomek 2000 lab robot (Beckman Instruments Inc.). Initially the PCR products were purified on silica columns (Macherey&Nagel AG), later on cheaper Millipore Multiscreen™ 96 well plates.



Figure 6.1.2: Biomek 2000 pipetting robot. Producing DNA probes for microarray production has to be done in high-throughput format. Programming new protocols for this machine is time consuming but worthwhile for large sample batches (like the 70.000 PCR reactions for the 21k mouse array).

The automated cleaning programme developed for the Multiscreen plates can be summarised as follows:

- pooling of 3 100 µl PCR reactions in 96 well plates onto one Multiscreen™ plate
- filtering by applying a vacuum of 400 mbar for 10 min.
- washing with 120 µl MilliQ water
- filtering on a vacuum of 400 mbar for 7 min.

- resuspension in 160 µl MilliQ water (in two steps)
- transfer into clean 96 well plate

The concentrations of purified DNA solutions were measured on a 96 well plate spectrophotometer at 260 nm. If the yield / reaction was above 6 µg, the DNA was concentrated in a speedvac to dryness and resuspended in spotting buffer.

6.1.4 Printing of DNA microarrays

As pointed out in section 2, good quality microarrays need careful matching of the spotting buffer, the printing technology and substrate surface coating. Ring-and pin systems work well with 50% DMSO in water, whereas contact printers with split pins perform better with buffers of high salt concentrations (eg 3xSSC, or SSC / betaine) and traces of surfactants. For the human array best results were achieved with Epoxy coated slides (Quantifoil) and the printing buffer 1 from Quantifoil, whereas the mouse array was generally printed on silylated (aldehyde-) slides with a buffer containing 3xSSC.

The volume of DNA solution deposited on each spot is about 10^{-9} l (1nl). Depending on the hydrophobicity of the surface and the nature of the buffer, the droplets were either small and spherical or large and flat in shape. Instant drying of these small droplets often results in spots of irregular shape and thickness (“donoughts”). A more uniform spot morphology and better attachment of DNA to the surface was achieved by re-hydrating the printed slides in a humid atmosphere during >48 hours. Useful for this purpose were empty pipet tip boxes. The bottom of the boxes was covered with a solution of 50% glycerol / water (to reduce the steam pressure and avoid merging of droplets), the slides deposited on the plastic tip rack and the box closed and sealed with parafilm.

Rehydrated slides were stored in boxes for microscope slides for up to 6 months. On the day of use, the microarrays were treated according to a protocol including several steps for washing, denaturing, blocking and pre-hybridisation, specific for the type of coating (tables 5.1.3-4)

Except of the denaturing step, which is done in a 500ml beaker glass, all washing steps were performed in 50ml disposable Falcon tubes (one slide per tube). In these tubes the slides can be shaken vigorously without harming the printed slide surface. The volume of solution /tube (usually 40-45ml) and the way of shaking (most steps were done per hand, longer shaking times with the help of an orbital shaker) has a big impact on the result. Care has to be taken that the slide surface is not touched and that it never dries between washing steps. After this procedure the slides were dried in Falcon tubes in a centrifuge (at ca. 1000rpm for 5min.), pre-warmed to 42°C and hybridised immediately.

In the course of this work, various slide surfaces have been tested. Here the protocols for the two mostly used surface types will be described:

Table 6.1.3: Processing microarrays printed on QMT epoxy slides (Quantifoil)

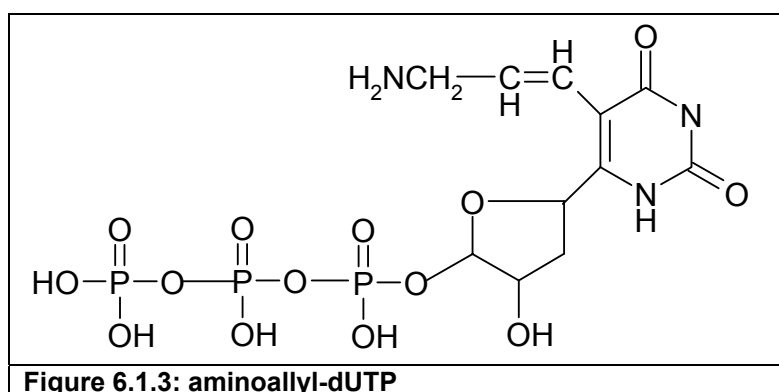
step number	repeats	incubation time	buffer	mixing
1	1	3	0,1% Triton-X 100	vigorously shaking
2	1	2	100µL HCl (37%) in 1000mL H ₂ O	smoothly shaking
3	1	3	100mM KCl	smoothly shaking
4	1	2	boiling H ₂ O (Millipore)	slowly stirring
5	1	2	H ₂ O (Millipore) at RT	smoothly shaking
6	1	15	1x QMT blocking solution (Quantifoil)	smoothly shaking (orbital shaker)
7	2	1	H ₂ O (Millipore) at RT	smoothly shaking
8	1	30-50 min	pre-hybridisation solution at 42°C	smoothly shaking
9	3	1	H ₂ O (Millipore) at RT	vigorously shaking

Table 6.1.4: Processing microarrays printed on aldehyde slides (Cell Associates)

step number	repeats	incubation time	buffer	mixing
1	1	3	0,1% SDS	vigorously shaking
2	1	2	H ₂ O (Millipore) at RT	smoothly shaking
3	1	2	boiling H ₂ O (Millipore)	slowly stirring
4	1	2	H ₂ O (Millipore) at RT	smoothly shaking
5	1	15	1x Aldehyde blocking solution (see list)	smoothly shaking (orbital shaker)
6	2	1	H ₂ O (Millipore) at RT	smoothly shaking
7	1	30-50 min	pre-hybridisation solution at 42°C	smoothly shaking
8	3	1	H ₂ O (Millipore) at RT	vigorously shaking

6.1.5 Aminoallyl Labeling für RNA Microarrays

This method, often referred to as indirect labeling, is based on the incorporation of dTTP/dUTP containing an aminoallyl moiety



that can bind covalently to the N-hydroxysuccinimide moiety attached to the cyanine dyes:

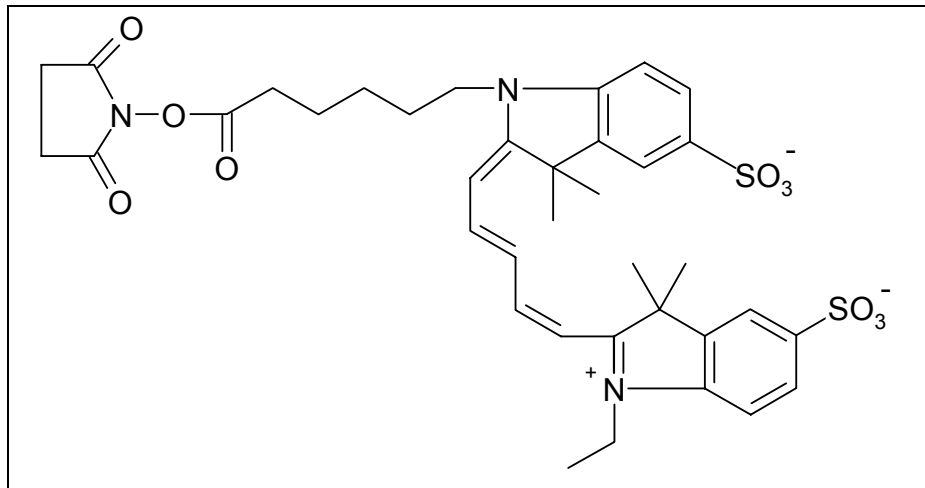


Figure 6.1.4: Cyanine 5 (Cy5)

Cyanine 5 is a red fluorescing cyanine dye with an absorbance maximum at 649 nm and an emission maximum at 670 nm. It was used in the form of an NHS-ester.

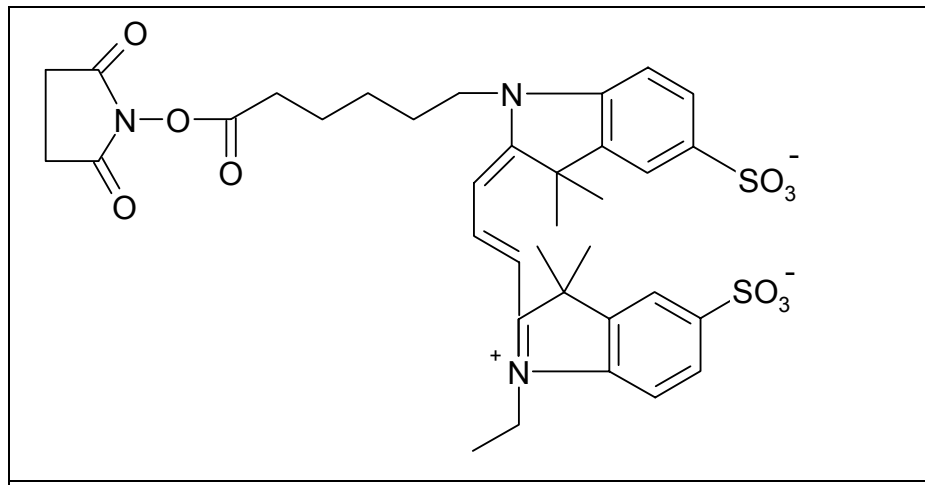


Figure 6.1.5: Cyanine 3 (Cy3)

Cyanine 3 is a green-blue fluorescent cyanine dye with an absorbance maximum at 550 nm and an emission maximum at 570 nm. Note that the conjugated system of Cy 3 is one allyl moiety shorter than that of Cy5.

While the direct incorporation of cyanine-labeled dNTPs allows the incorporation of only 2-3 dye molecules per 1000 bps, the sterically favourable aa-dUTP allows the introduction of 10-12 cyanine molecules in 1000 bps. This signal enhancement makes it possible to work with smaller RNA samples.

The following protocol was developed for the transcription of RNA into cDNA that can be indirectly labelled with cyanine dyes:

a) cDNA preparation

- In 200µL PCR vials ca. 20µg total RNA was combined with 2µl oligo (dT) mix, containing each 100µM (dT)₁₂₋₂₀ and filled up to 16µl with ddH₂O. The RNA was denatured at 80°C for 3 min and immediately cooled on ice.
- 14,3 µL of a RT-PCR master mix was added containing:

6µl 5x First Strand Buffer
 3µl dTT 0,1M
 3µl aminoallyl L(abelling)dNTP Mix
 2µl Superscript II RT (200U/µl)
 0.3µL RNAse inhibitor

- Mixing was performed by pipetting (the enzyme is prone to denature when mixed vigorously) and incubated in a PCR cycler at 42°C for 2,5 hours before inactivating the RT polymerase by heating to 80°C for five minutes.
- The RNA template has to be degraded to get single-stranded cDNA probes. This was easily be achieved by incubating with RNAseH for 15 min. at 37°C
- By adding 10µL 3M sodium acetate pH 5,2 and 250µl of 100% ethanol, the cDNA was precipitated over night in the freezer at -20°C. cDNA can be stored in ethanolic solution at -20°C for extended periods of time.

compound	final concentration in LdNTP	for 400µl solution B add 100 mM stock dNTP	add 382µl solution B to vial with 1mg lyophilised AA-dUTP (Sigma) and dissolve: vortex, shake, centrifuge)	add 3µl LdNTP to each labeling reaction of 15-25µg of RNA
AA-dUTP	5mM	--	Aliquot (eg 53µl for 17 samples (17x3=51µl) and freeze at 20°C	
dTTP	5mM	20µl		
dATP	10mM	40µl		
dGTP	10mM	40µl		
dCTP	10mM	40µl		
H ₂ O		260µl		

b) Dye coupling

- The cDNA was pelleted by centrifugation for 20 min. at 14 000rpm and 4°C and washed twice with 70% ethanol
- the pellet was dried subsequently in a vacuum centrifuge and desolved in 6µL 0,1M Na₂CO₃ pH 9
- Cyanine dye pellets were dissolved in 25 µl dry and ultrapure DMSO, vortexed and spinned down by centrifugation
- 6µl of dye solution was added to the samples, mixed by pipetting and incubated at room temperature in the dark for 1,5 hours
- 58ml of 0,1M HOAc pH 5,2 were added and the labelled cDNA purified on Quiagen PCR purification columns according to the manufacturer's instructions. The washed cDNA was eluted from the membrane four times with 40µl of the provided elution buffer to avoid any losses. The combined eluate can then be used for immediate hybridisation or stored at -20°C.

c) Quality control of the labeled sample cDNA

The success of the labeling reaction was determined photometrically either with a Beckman DU 530 UV/VIS or a Uvikon 933 (Kontron Instruments) double beam UV/VIS spectrophotometer in 1cm quartz cuvettes.

Undiluted labeled cDNA samples were measured at 260, 280, 550 and 650 nm while taking care to minimise exposure to light to avoid photobleaching. The total amount of synthesized cDNA was calculated according to the formula

$$\frac{OD_{260} * \text{volume } \mu\text{l} * 37\text{ng}/\mu\text{l} * 1000 \text{ pg/ng}}{324,5 \text{ pg/pmol}} = \text{pmol nucleotides}$$

with 1 OD₂₆₀ = 37ng/μl for cDNA; 324,5pg/pmol average molecular weight of dNTPs

and the amount of incorporated Cy3/5 was calculated as:

$$\frac{OD_{550} * \text{Volumen } (\mu\text{l})}{0.15} = \text{pmol Cy3} \quad \text{and} \quad \frac{OD_{650} * \text{Volumen } (\mu\text{l})}{0.25} = \text{pmol Cy5}$$

The (inverse) efficiency of dye incorporation was then calculated as

$$E = \frac{\text{pmol cDNA}}{\text{pmol cyanin dye}}$$

> 200 pmol of dye incorporation per sample and a ratio of less than 50 nucleotides/dye molecules is optimal for hybridisations

The labelled sample was then either frozen at -20°C in 1.5 ml vials and stored until usage or directly used for hybridisation on cDNA microarrays:

6.1.6 Hybridisation

- The labelled cDNA samples were combined (eg. wt-Cy3 and mutant-Cy5), 2μl salmon sperm DNA and 20μl Poly(dA) added and dried in a vacuum centrifuge at 45°C (ca. 2,5 hours).
- In the meantime the rehydrated arrays were washed and blocked according to the protocols in table 5.1.3-4. Instead of spinning the slides to dryness, the wet slides were incubated in prehybridisation buffer for ca. 40 min. at 42°C.
- The slides were then washed twice with ddH₂O and dried in 50ml Falcon tubes by centrifugation at 1000rpm for 5 min. Cover slides were washed in 0,1% SDS, twice in ddH₂O and dried in the centrifuge at ca. 1000 rpm for 3 min.
- The cDNA was dissolved in 50μl hybridisation buffer (table 5.1.6) in a heated shaker at 50°C, denatured at 90°C for three minutes and then cooled to 45°C
- The hybridisation mix was pipetted onto the prewashed glass cover slides and the arrays applied cautiously onto the cover slide face-to-solution, taking care to avoid air bubbles. The arrays were incubated in the dark in humidified incubation chambers for 17-20 hours at 42°C.

During the hybridisation process the labelled cDNA fragments have to be distributed evenly over the surface area by diffusion, which can be a problem especially with big arrays and small sample volumes (typically 50μl on 20 x 55mm). Several

commercially available hybridisation stations have peristaltic micro-pumps installed to provide optimal mixing. Pumps have the disadvantage of increasing the hybridisation volume due to introduced dead volume. Increased volumes of hybridisation solution logically require larger amounts of labelled sample cDNA to obtain the same degree of sensitivity. In this project, several automated and semi-automated hybridisation systems and -chambers were tested. In our hands the only technique that could improve results obtained by manual hybridisation with glass or plastic cover slides was a system from Advalytix AG (now on the market under the name ArrayBooster™). By inducing surface acoustic waves to produce microagitation, it requires only moderately larger volumes (100µl instead of 50 µl) of hybridisation solution than conventional hybridisation with glass cover slips..

Prehyb buffer	volume	stock solution	Hybridisation- buffer	volume	stock solution
6xSSC	15ml	20xSSC	50% Formamide	500µl	Formamide
0,5%SDS	2,5ml	10%SDS	6xSSC	300µl	20xSSC
1%BSA	5ml	10%BSA	0,5%SDS	50µl	10%SDS
	27,5ml	ddH ₂ O	5x Denhardt's	100µl	50xDenhardt's
				50µl	ddH ₂ O
	50ml	total		1000µl	total

Prehybridisation (Prehyb) buffer and hybridisation buffer can be aliquoted and stored at -20°C.

6.1.7 Procedure for stringent washing of slides

The slides were taken from the hybridisation chambers and immediately immersed in wash buffer 1, prewarmed to 45 degrees. Gentle shaking makes the cover slides drop of the array without applying any force, which might result in scratches. The uncovered slides were transferred into a new 50ml tube with wash buffer 1 at 45°C and shaken for 5 min.

To avoid drying of the surface, the slides were quickly transferred into new 50ml tubes containing the more stringend wash buffer 2 and shaken during 10 min. Vigorous shaking by hand twice for 1-2 min in wash buffer 3 purifies the surface from detergents (SDS) and particles.

After the last wash the slides were immediately centrifuged in 50ml Falcon tubes at ca. 1100 rpm and room temperature for 5 min. and let stand to dry in the dark for another 15 min. before scanning.

solution	composition	preparation
washing solution 1	0,1% SDS, 1xSSC	10 ml 10%SDS + 50ml 20xSSC + 940ml ddH ₂ O
washing solution 2	0,1% SDS, 0,1xSSC	10ml 10%SDS + 5ml 20xSSC + 985ml ddH ₂ O
washing solution 3	0,1xSSC	5ml 20xSSC + 995ml ddH ₂ O

The washing procedure seems to be trivial but has in fact a major impact on the quality of the data produced.

The aim is to remove in a series of washes with increasing stringency labelled cDNA, which is bound unspecifically and thus lowers the overall signal-to noise ratio. Additionally, particles and remains of salts and detergents, altering the background fluorescence, have to be removed uniformly over the array surface. Only cDNA annealed to the complementary probes on the array should remain. In this project, all washings were performed manually in 50 ml Falcon tubes, employing an orbital shaker for longer shaking steps. The amount of washing buffer in the tubes and the force applied when shaking (like temperature, shaking time or buffer composition, etc.) affect significantly signal quality.

Automated wash stations have recently been developed to ease the use of microarrays and to provide better comparability between experiments. Personal communications from collaborating groups (Seltmann 2003) indicate problems adapting these devices to current protocols. The results produced by automated wash stations were generally poorer than those produced by trained laboratory staff.

6.1.8 Signal enhancement using dendrimer technology

The amount of sample RNA often restricts the number of possible microarray experiments below of what might be desirable in terms of statistics to obtain confidence through technical repeats. Tissue from microdissections or rare cell types often provide often far less RNA than necessary for a single experiment using direct or indirect labeling techniques. This problem can be circumvented either by amplifying the sample RNA through linear PCR methods, or with more effective labeling techniques, like radioactively labeled nucleotides.

Fluorescent signals can be enhanced using dendrimers, as provided from Genisphere Inc. Dendrimers are highly branched molecules, that can be synthesized from oligonucleotides in a series of self-assembling and crosslinking steps:

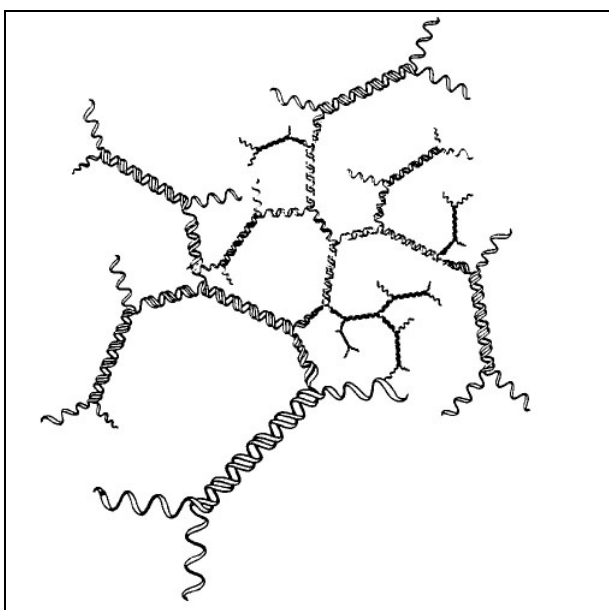


Figure 6.1.6: Second layer of assembled oligonucleotides

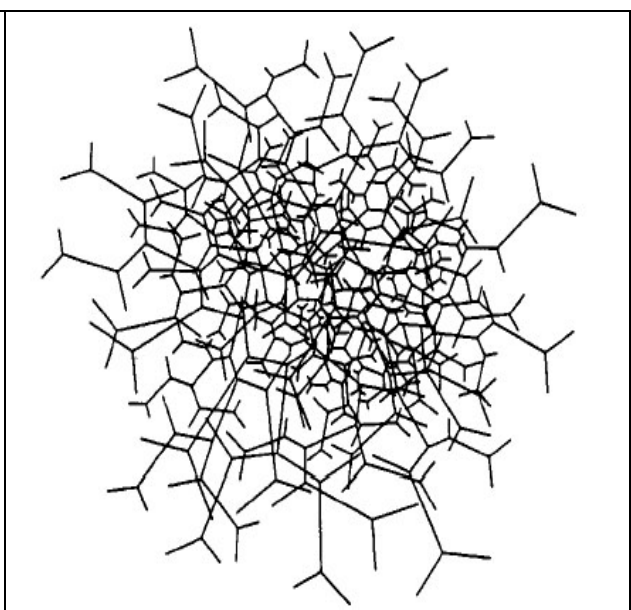


Figure 6.1.7: The fourth layer of assembled oligonucleotides builds the core structure

The outer branches of the dendrimers are ligated to oligonucleotides containing fluorophores, like Cyanine 3 or Cyanine 5, and to oligonucleotide conjugates. The latter contain a specific "capture" sequence that can hybridize to sample cDNA. Sample cDNA was produced with primers containing a sequence, which is complementary to the capture sequence. Each of these branched "tree" molecules contains more than 200 fluorophores, leading to a remarkable signal amplification. The original protocol provided by Genisphere was changed and adapted to the specific experimental conditions. Especially the procedure for sample purification was simplified.

cDNA synthesis

For cDNA Synthesis, the following primers, specific for the respective labeling dye were used:

Cy3: 5'-GGC CGA CTC ACT GCG CGT CTT CTG TCC CGC C-(dT)18-22

Cy5: 5'-CCT GTT GCT CTA TTT CCC GTG CCG CTC CGG T-(dT)18-22

- 5µg of mammalian total RNA were combined with 1µl of a 5mM solution of the respective oligo(dT) primer and made up to 10µl with dd H₂O
- the RNA-primer mix was spun down, denatured at 80°C for 5 min. and chilled for 30 seconds on ice.
- for each reaction, 10 ml of a master mix, containing 4ml 5X Superscript II RT buffer, 1ml dNTP mix (10mM each for dATP, dCTP, dGTP, dTTP), 2µl 0,1M dithiothreitol (DTT), 1µl Superscript II RT polymerase (200U), 1µl H₂O and 1µl RNase Inhibitor were added, mixed by pipetting, spun down and incubated for 2 hours at 42°C
- the enzyme was inactivated by heating the mixture to 80°C for 5 min. The RNA template was then degraded by adding 0.3µl of RNaseH and incubated for 15 min. at 37°C.

The cDNA had to be purified from enzymes, excess dNTPs and primers that would mask later the labeling dendrimers.

- The reaction products were transferred to a 1,5ml vial containing 50µl of 0,1M sodium acetate buffer at pH 5,2. 350µl of Quiagen binding buffer were added and mixed before applying the mixture onto Quiquick PCR purification columns and centrifuged at 3000rpm for 3 min.
- The spin columns were washed three times with 400µl ethanolic Quiagen wash buffer, the throughflow discarded and spun dry for additional 3 min at 10 000 rpm.
- The columns were placed in a clean 1,5ml microcentrifuge tube and the purified cDNA eluted with 30µl elution buffer, applied to the center of the column membrane. After incubation for 3 min., the columns were centrifuged at 8000 rpm for 1 min. This step was repeated three times.
- The combined cDNA eluate was then stored at -20°C until usage or dried in the vacuum centrifuge at 45°C (1-2 hours).

Hybridisation

- For experiments with the 21k mouse array (ca 50x20 mm), 2µl of dT blocking agent (provided by Genisphere) and 50µl hybridisation buffer (table 5.1.6)

were added to the dried sample cDNA pellet. The cDNA was redissolved in a shaking incubator at 50°C for 15 min

- In the meantime, the arrays were washed, denatured, blocked, pre-hybridized, washed, dried and prewarmed at 45°C
- Glass cover slides were washed in 0,1% SDS, twice in ddH₂O and dried in Falcon tubes by centrifugation at 1000 rpm for 2 min
- The hybridisation solution was heated to 80°C for 5min and then incubated at 45°C, before applying it onto the glass cover slides
- the pre-warmed arrays were placed onto the cover slides and incubated in warm (45°C) hybridisation chambers, containing additional 80µl of hybridisation buffer to create a saturated humid atmosphere for 18-22 hours.

Washing

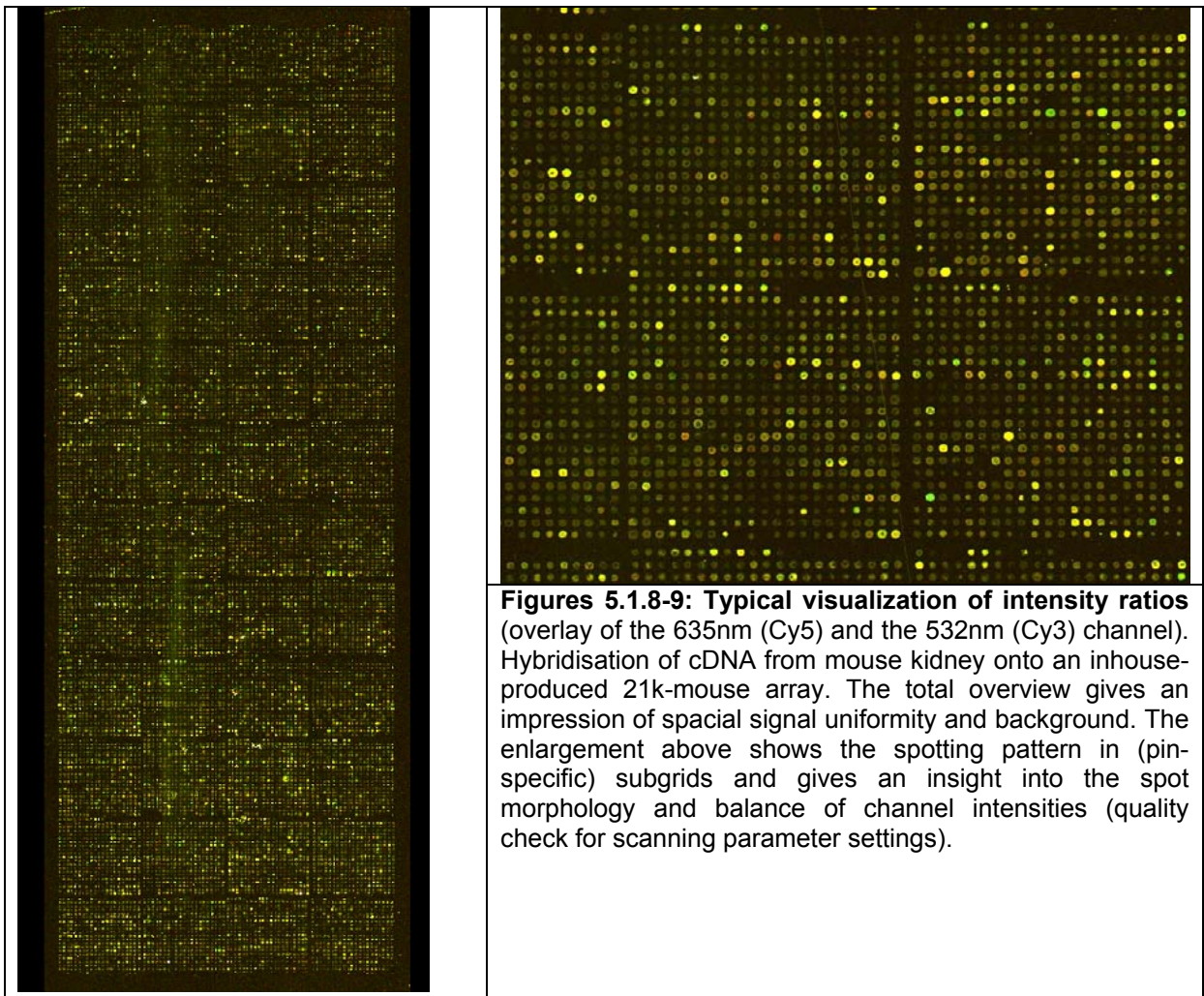
The washing procedure is analog to the procedure for indirect labeling with aminoallyl-dUTP. The washed slides were spinned to dryness in 50ml Falcon tubes at 1100rpm for 5 min., prewarmed at 45°C and incubated in the dye reagent solution immediately afterwards.

Second hybridisation with dendrimer labeling reagents

- The dendrimer reagents were thawed and homogenised according to the Genisphere protocol
- A hybridisation mix was prepared, containing 2,5 µl of Cy3- and Cy5-dendrimer each, 1µl differential enhancer (provided by Genisphere) and 45 µl of the hybridisation buffer (table 5.1.6), incubated for 10 min. at 80°C and then for 10 min. at 45 °C
- Like in the first hybridisation step the mix was applied onto prewashed glass cover slides and the glass array put upside down onto the cover slide
- The slides were subsequently washed as described in 5.1.7, dried and scanned.

6.1.9 Scanning

Scanning was usually performed with an Axon GenePix 4000A epifluorescent scanner, equipped with two excitation lasers, emitting at 532nm and 635nm, respectively. While the laser power was always set to 100%, the photomultiplier gain was adjusted to achieve a wide dynamic range of signal intensities. According to the manufacturer, the linear response of the scanner stretches over approximately three orders of magnitude, about two orders of magnitude less than the real biological dynamic range (app. 10^5). A few (<0,5%) signals usually exceeded the saturation limit of 65.000 units. As the overall signal intensity generally differs between the two channels, the PMT gain was regulated to balance labeling and background effects and thus facilitate normalisation. On the other hand, big changes in hardware settings of the scanner were avoided within one set of experiments. Generally, there was a considerable day-to-day variation observed in terms of overall signal-to-noise ratio and optimum PMT settings, which might be related to differences in chip quality, labeling and washing.



The image quality depends on fluorescence background, signal intensity, spot morphology, uniformity of spatial signal distribution, the signal intensity range and the balance between the Cy3 and the Cy5 channel. The latter two parameters can be optimised during scanning by selecting the appropriate photomultiplier gain for each channel. In a well-optimised scan only few spots appear as saturated (white, $> 2^{16} =$

65.000 intensity units), whereas the majority of the spots show up in yellow (equal intensities in both channels, not regulated).

6.1.10 Image processing

In this project, two different software packages for image analysis were tested: AIDA (Raytest) and GenePix (Axon). While the first was originally designed for large filters (macroarrays), the latter package turned out to be well-suited for fast and standardised analysis of two-channel microarray images. Especially the overlay of the images recorded at 532nm and 635nm excitation wavelength and the spot finding procedures were found to be efficient with GenePix 3.0 and the improved versions 4.0 and 4.1. Apart from tools for scanning, GenePix provides tools for image processing, spot identification, quantification of intensity signals, spot-clone ID annotation and the first steps of data quality control and -filtering.

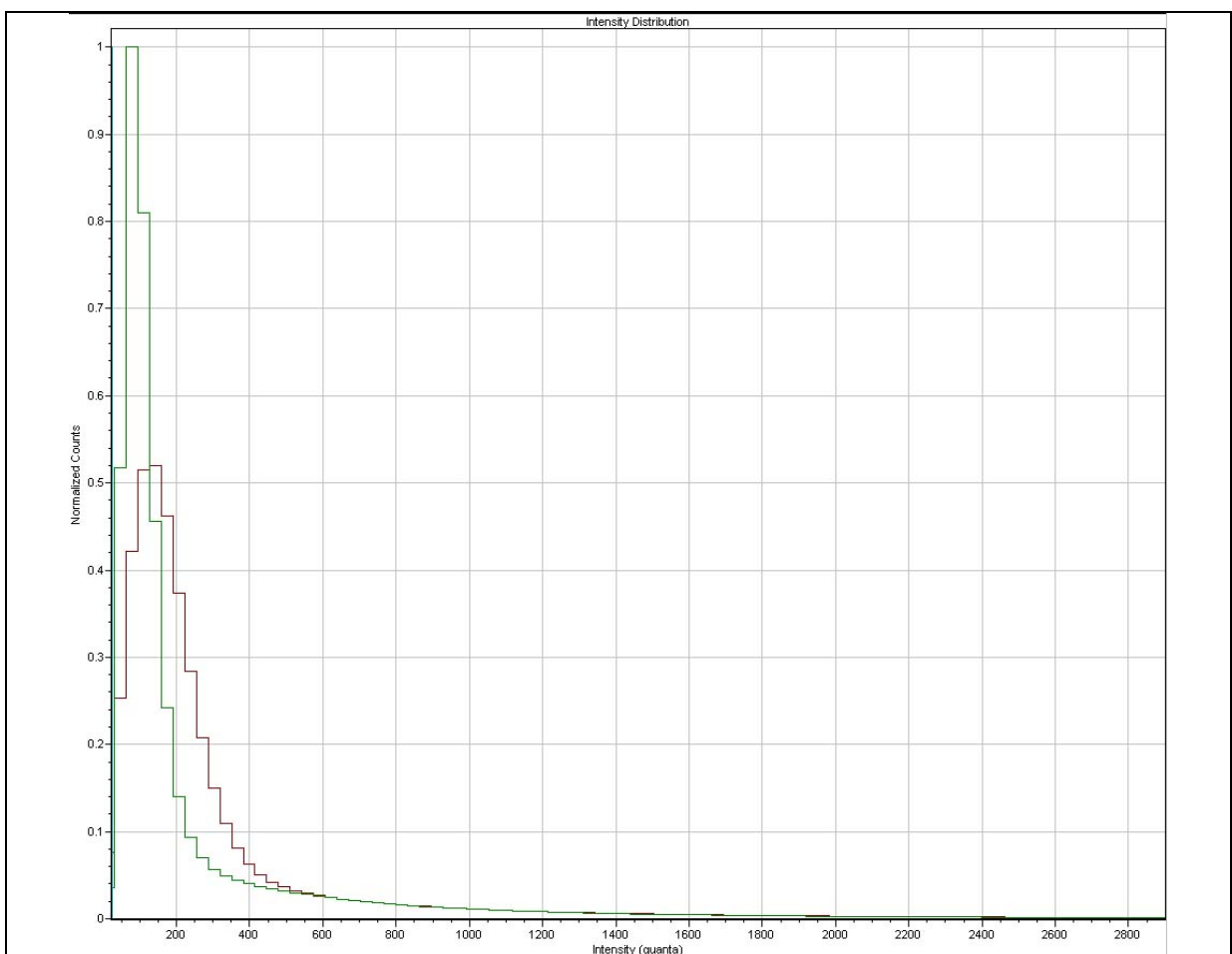


Figure 6.1.9: Histogram showing the intensity distribution of signals detected on the Cy3 (Singh-Gasson et al.) and the Cy5-channel (red). Small differences are only visible in the range of very low intensities (<600). Intensity values in this region are subjected to large variability and were therefore excluded in later steps of analysis.

Spot identification, signal integration and raw data export with GenePix

The following steps for data evaluation are spot finding and identification. Like in most other software packages for microarray image analysis, in GenePix this task is done by defining the spotting pattern as a grid. Each position in the grid is assigned to an identifier that represents the respective clone or EST sequence on the array. This grid is stored as a text file (extension .tas in GenePix) and can be used for all experiments with arrays, spotted in this pattern. The grid can be positioned on the scanned image and an spot-finding algorithms adjusts the area of detection to each spot shape and size. The area surrounding each spot is defined as the local background, which can then be subtracted from the spot intensity value. Good quality software packages can handle a non-uniform background or identify non-circular spots as artefacts (eg. dust particles).

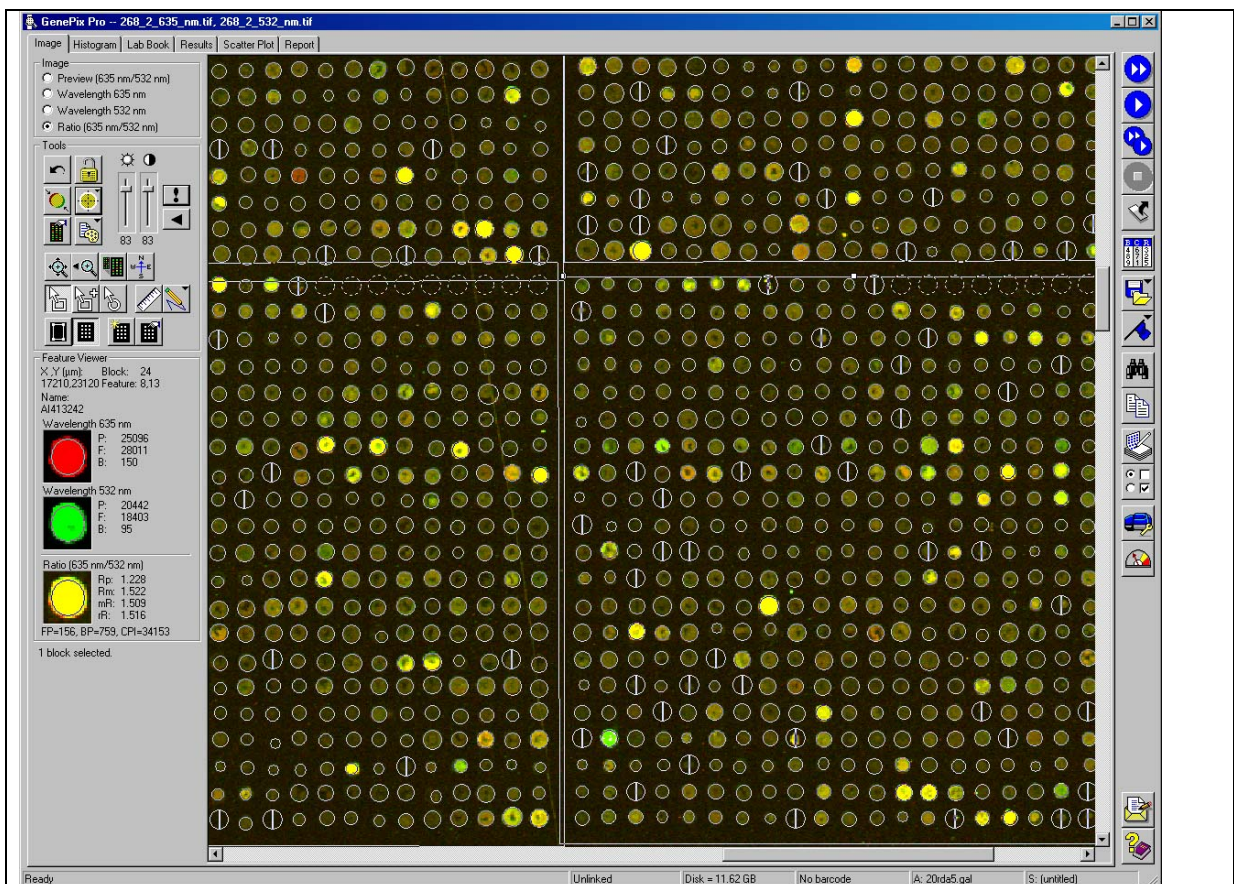
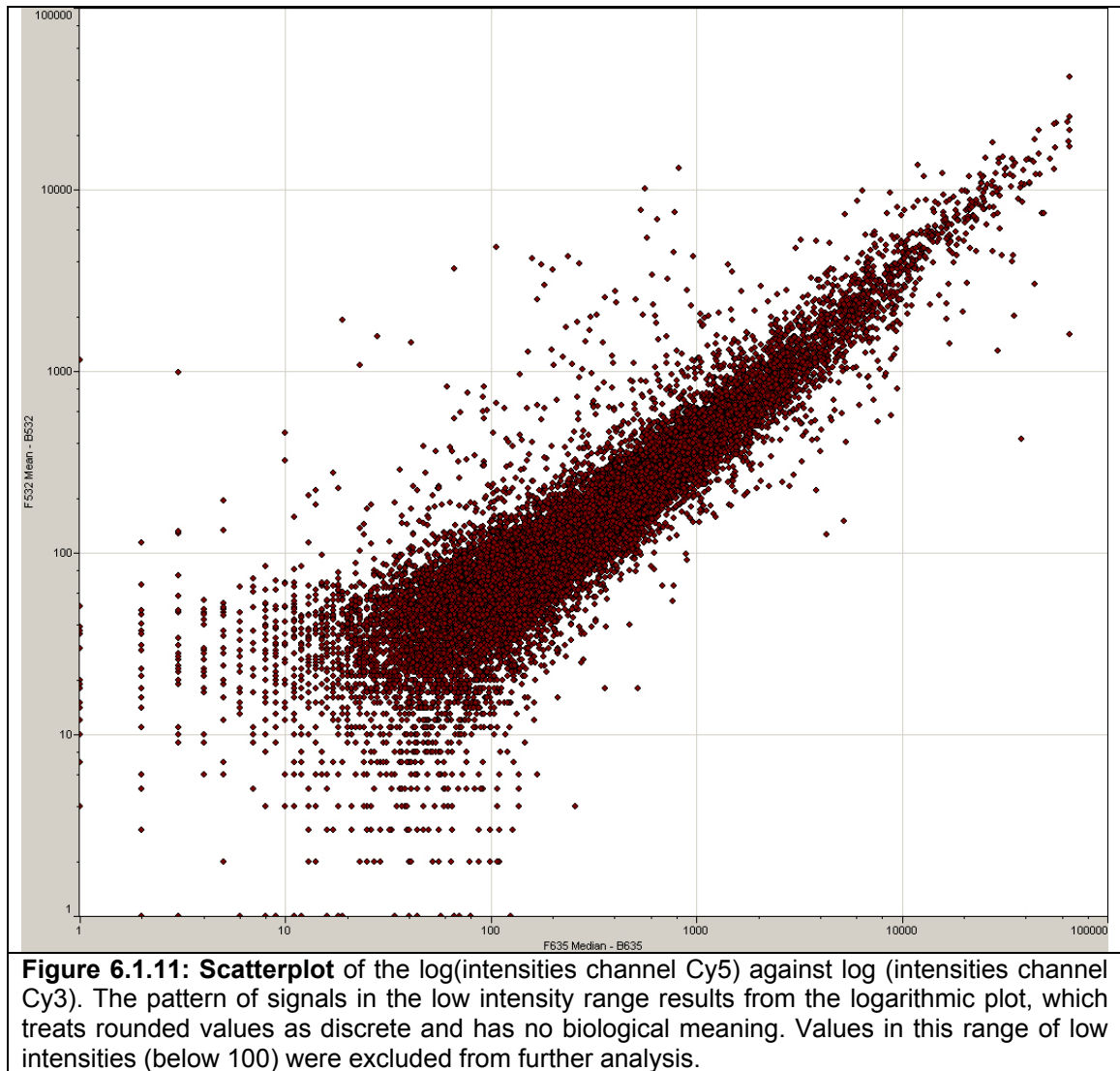


Figure 6.1.10: Section of a scanned image (21k mouse array) with grid overlay after activation of the spot finding function in GenePix. Here the borders of 4 subgrids can be seen. Spots with signals below a pre-defined threshold are flagged and excluded from further analysis. For each spot, signal intensities of both channels can be seen (see spot enlargement on the left panel).

The fluorescence signal intensities are then integrated over the spot surface. EST identifiers, spot coordinates, mean or median signal intensities, background fluorescence intensities, intensity ratios, etc. are then calculated and stored as text (GenePix: .gpr) files.

These data tables contain several 10.000 values for each single microarray experiment. Data visualization is therefore a very helpful tool to control data quality and to interpret the results as an entity. A simple, but informative way to present the results of one microarray experiment is the log-log scatterplot.



6.1.11 Data normalisation, filtering and extraction

In microarray experiments, the expression of several thousand genes of one or (like here in dual-colour experiments) two samples are tested under the same conditions. In fact one microarray experiments can be regarded as the combination of thousands of sub-experiments. This results in the problem of introducing errors (multiple testing). There are several sources of variation of experimental conditions that might introduce systematic errors:

- different shapes of pin tips produce spots with differing sizes and morphologies (“doughnut spots”)
- different concentrations of probes in the spotting source plate
- inhomogeneities in the coating of the substrate
- different binding properties of probes
- unequal quantities of starting RNA samples
- unequal distribution of sample solution during hybridisation
- inhomogenous washing
- different fluorescence efficiencies between fluorophores (Cy3 and Cy5)

- different incorporation rates of fluorophores (Cy5 is more “bulky”- sterical hinderance)

All these sources of error make the development of well-optimised and standardised experimental protocols necessary. It is nevertheless impossible to exclude all sources of experimental bias in one experiment and between experiments. Some of these biases can be overcome by mathematical transformation of result values, based on assumptions (normalisation). One principal assumption is that generally there is only a small fraction of genes (<5%) that changes in expression in response to different experimental conditions. As a consequence, the mean ratio of expression (or fluorescence intensity) signals has to be equal to one (the 45° axis in the scatterplot). In the scatterplot, the majority of log (ratio intensity) values should therefore group symmetrically around the 45° axis in the scatterplot. If there is a systematic bias towards one channel (eg towards Cy3), it can be corrected by multiplying all ratio intensity values by a constant factor:

Figure 6.1.12: Formula to calculate a global normalisation factor	
$N_{total} = \frac{\sum_{i=1}^n R_i}{\sum_{i=1}^n G_i};$	n : number of elements (ESTs) on the array R _i : fluorescence intensities channel Cy5 (red) G _i : fluorescence intensities channel Cy3 (Singh-Gasson et al.) N _{total} : global normalisation factor

Global intensity normalisation only accounts for systematic effects that affect all values in the same way, independent from signal intensity or localisation on the array, like the labeling dye chemistry. Other effects, like variations due to differences in printing (pins), non-uniform coating of the substrate, unefficient sample mixing during hybridisation, etc., as well as intensity-dependent effects cannot be corrected by global normalisation.

The software package MIDAS, a component of the TM4 software package provided by the TIGR institute (Saeed et al. 2003), offers other options for normalisation, data filtering, visualization and extraction. To import gene expression raw data from GenePix .gpr files into MIDAS, the files had to be converted into the right format, which was accomplished with the tool Express Converter. Midas allows to treat data from a series of microarray experiments according to a user-defined protocol and helps to keep track of all transformations in a workflow.

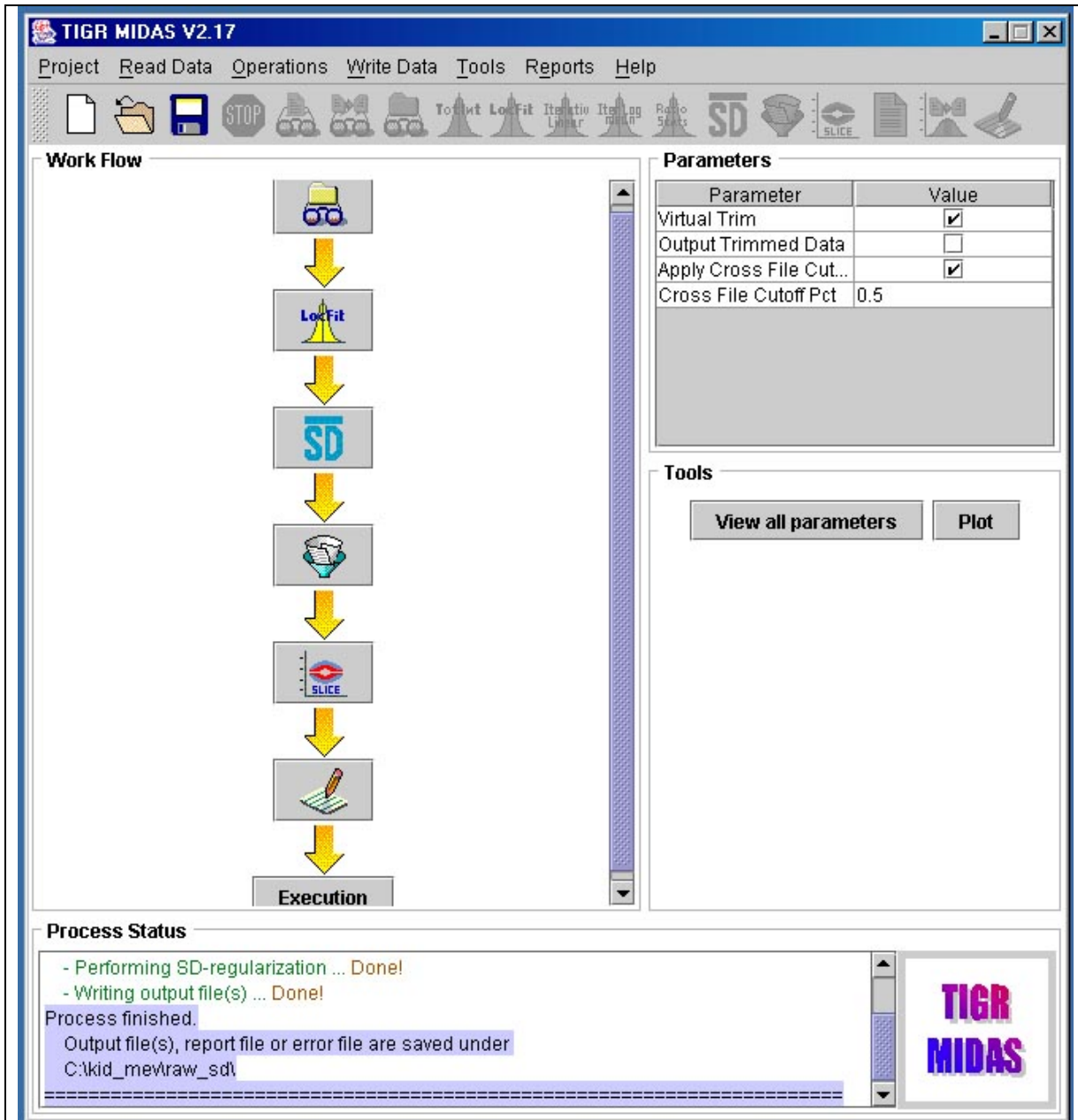


Figure 6.1.13: Typical workflow for data analysis with MIDAS, as used in the following studies. First, data from a series of experiments were imported. Then the data underwent subsequently LOWESS normalisation, blockwise standard deviation regularization, low intensity filtering and slice analysis. Finally the processed data and the documentation of intermediate steps were stored as text files.

Another way to represent the data is the R-I plot (log ratio intensities / log product intensities). In this form intensity-dependent systematic effects become visible, as can be seen in the R-I plots of microarray experiments with mouse kidney (section 3) and heart (section 4). This systematic effect (Quackenbush 2002) can be corrected with locally weighted linear regression analysis (LOWESS). Lowess carries out a local linear regression as a function of the log (product intensities) and subtracts the calculated best-fit average $\log_2(\text{ratio intensities})$ from the experimentally observed ratio for each data point. Array elements that are far from each data point are deemphasised by a weight function.

Another normalisation method provided by MIDAS and used in these studies is called standard deviation regularization. This method bases on the assumption that all

spots within each block of a slide should have the same spread for $\log_2(R_i/G_i)$. The algorithm scales the intensities of both channels of each spot so that within each block of a slide the values will have the same standard deviation for the $\log_2(R_i/G_i)$ distribution.

After normalisation, data with intensities below a certain threshold can be excluded from further analysis. Considered that the variability of data increase as intensities decrease, it makes sense to skip data that only add random noise to the experiment. In the following studies, the threshold was set at 10.000 units (ranging from 0 to $2^{16} = 65.535$).

A more sophisticated way to reduce the data amount and extract candidates for differentially expressed genes is called “slice analysis” in MIDAS. Like low intensity filtering, slice analysis also takes into account that variability in the measured \log_2 (ratio) values depends inversely on intensity. As visualized in the R-I plot, intensity values are transformed into $\log_2(R_i/G_i)$ vs. $\log_{10}(R_i*G_i)$ data sets. Dynamic “sliding windows”, containing a user-defined number of values (slice data population) are generated and the mean and standard deviation of the \log_2 (ratio intensity) values for the data points within the window are calculated. Differentially expressed genes are selected with an algorithm that calculates the local standard deviation of each array element. Dividing the \log_2 (ratio intensity) values $\log_2(T_i)$ by the local standard deviation $\sigma_{\log_2(T_i)}^{local}$ gives a measure for differential expression, (Z-score) for each data point. Differentially expressed genes can then be automatically extracted by setting the Z-score threshold to 1, 1.5 or 1.96, depending on the statistical level of confidence to be obtained. Generally a Z-score of 1.96 (95% level of confidence) was chosen.

This Z-score selection with

$$Z_i^{local} = \frac{\log_2(T_i)}{\sigma_{\log_2(T_i)}^{local}}; |Z_i^{local}| > 1.96$$

has been shown to be more reliable than setting rigid global \log (ratio intensity) levels for the extraction of differentially expressed data (Quackenbush 2002). The results of these normalisation and filtering processes in MIDAS are stored in a text file (.tav or .mev) that can then be imported into another element of the TM4 software package, the Multi Experiment Viewer (MeV).

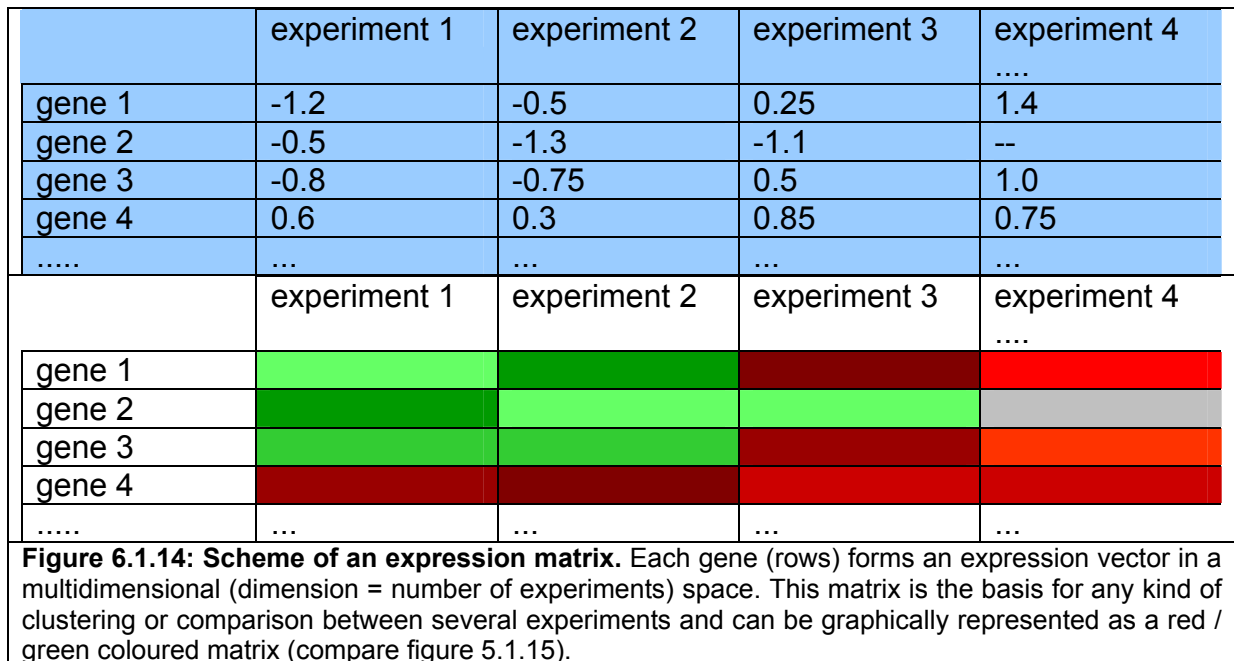
Comparison between several microarray experiments

Single microarray experiments give results with only little confidence for several reasons:

- biological variability between individuals (animals, cell populations)
- technical variation from a multitude of error sources due to the complex protocol
- the statistical problem of testing one (or two) sample(s) with many probes (“multiple testing”). For most experiments the situation is inverse: Several (or many) sample are tested with a single probe.

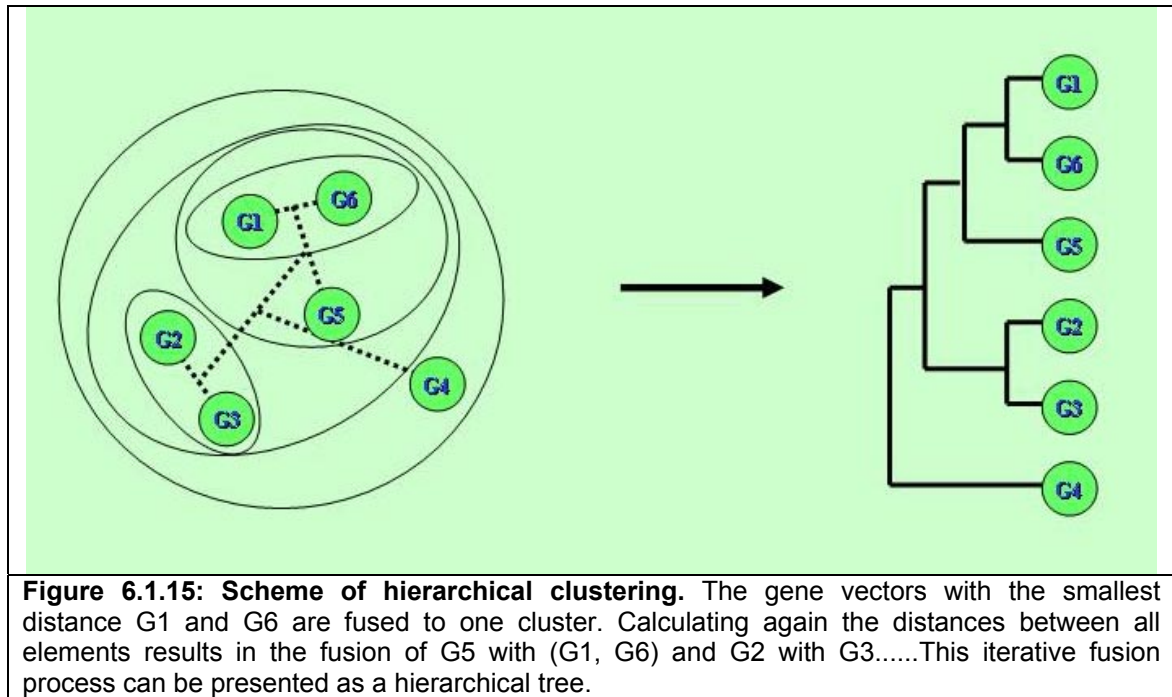
To improve confidence the in data, studies always have to include several experiments, either as technical (same samples) or as biological repeats. These can be compared to each other with the help of the MultiExperimentViewer (MeV).

The size of result files of microarray experiments easily exceeds computing memory and time during cluster analysis. It is therefore necessary to reduce the data amount significantly in advance, with filtering tools as provided in MIDAS. Once imported into MeV, the pre-selected data from several experiments can be aggregated as an expression matrix



The log (ratio intensity) values in the matrix above are represented as red (for positive), green (negative), dark (nearly 0: equal intensities) or gray (missing data, filtered out) and give an intuitive impression of genes / experiments that behave similarly and can be aggregated to clusters. There are several ways (Euclidean distance, Pearson correlation coefficient(s), Manhattan distance, ...) to calculate the distance (inverse similarity) between expression vectors. According to these distances, similar genes/experiments can be grouped into clusters.

A widely used, almost classic way to sort genes is hierarchical clustering, as described by Eisen (Eisen et al. 1998): In hierarchical clustering, vectors with the smallest distance are fused as a cluster. Then the distances between this cluster and all other elements are calculated and the closest elements fused to a new cluster. This procedure is repeated until all clusters are fused. The result can be drawn as a hierarchical tree:



Another clustering method used in this project is K-means clustering. The user defines *a priori* the number of clusters the gene expression vectors should be attributed to. Then the genes are randomly assigned to the clusters and the mean expression profile of each cluster is calculated. The genes are then re-distributed among clusters such that the gene's expression profile is closest to the cluster it is assigned to. Then the mean expression profile of each cluster is calculated again and the process is iterated either for a pre-defined number of times or until the genes can't be reshuffled any more. Examples for data analysis by k-means clustering are given in section 3. It is a simple method to bring some kind of order into gene expression matrices, especially when there are *a priori* assumptions about the number of clusters to be created.

Significance analysis of microarray data (SAM), developed by Tusher et al. (Tusher et al. 2001) is useful to pick out significant genes based on differential expression between sets of experiments. SAM can be successfully applied if there is an *a priori* hypothesis that some genes will be differentially regulated between sets of samples, e.g. kidneys from VDRKO and WT mice in the case of one-colour labeling or between male and female VDRKO mice with two-colour labeling, see section 3. By calculation of a false discovery rate (FDR), SAM can give an estimate to quantify the chance of identifying "significant" genes by chance.

The data for each gene are permuted and a test statistic d is calculated for the permuted and the calculated data for each gene, analogous to a t-statistic in a t-test. d captures the difference among mean expression levels of experimental conditions, scaled by a measure of variance in the data. In an interactive plot d -values, based on observed data are plotted against those calculated from permuted data. The vertical distance from the line of slope 1 (where observed = expected d -values) is the threshold value δ . By setting δ , the user can define the stringency of data filtering. Values above δ are regarded as positive significant, below as negative significant to distinguish the two sample groups. Practical examples for the application of SAM, as it is implemented in the MeV package, are given in sections 3 and 4.

MeV offers many more clustering and testing methods, like bootstrapping, jackknifing, self-organising maps, etc. In this study there was no need for sophisticated clustering methods due to the small number of experiments and experimental conditions.

Since any kind of data transformation or filtering influences the result, various software packages, methods and conditions have been tested and compared with data from previous experiments and published studies. It is generally impossible to carry out enough of microarray experiments to obtain statistical confidence without subsequent confirmation experiments. In the studies described here the quality of the data analysis procedure was continuously confirmed with quantitative real-time PCR.

6.2 Quantitative Real-time PCR

Microarray technology is a powerful screening method to analyze expression profiles of thousands of genes in parallel. The pay-off is a lack of precision and sensitivity, compared with other methods that measure gene expression one-by-one, like Northern Blotting or reverse transcription polymerase chain reaction (RT-PCR). Northern Blotting is a well-established method based on electrophoretic separation of cDNA products on a gel, followed by detection of the species of interest by radioactively labelled cDNA probes. Northern Blotting is fairly precise but requires large amounts of sample RNA and is labour and cost-intensive. RT-PCR offers a greater sensitivity but is less precise since small variations in amplification efficiencies between reference and target gene can cause significant changes in PCR product yield. It is often difficult to determine optimum PCR conditions for several different amplification products and avoid saturation effects.

Quantitative real-time PCR (qPCR) combines the great sensitivity of PCR based methods with a high degree of precision, as the amplification process can be controlled on-line and easily be optimised. In recent years a wide range of quantification strategies for qPCR has been developed. For the verification of microarray results, detection of double-stranded PCR products with SYBR Green fluorescent dye was chosen as a universal and relatively cost-efficient method. Quantification of target genes was measured relative to the expression to the expression of a reference gene. The instruments used were the Light Cycler system developed by Roche and the Taqman 9700 from Applied Biosystems.

6.2.1 Principle of relative quantification

During PCR, the number of copies of a DNA strand is increased according to the following formula:

$$N = N_0 \cdot E^{C_n}$$

with N = Number of DNA molecules at PCR cycle n
 N_0 = Number of DNA molecules at PCR cycle 0
 E = Efficiency of amplification
 C_n = Cycle number

Ideally, the efficiency $E = 2$, which means doubling of the DNA copy number after every cycle. This assumption holds under optimised conditions and can be used for

relative quantification, but has to be verified experimentally by measuring a dilution series of cDNA samples. At a pre-defined point t , e.g. where the second derivative of the signal amplification curve (see figure 5.1) is zero, the intensity (and concentration) of the target gene N_t^T and the reference gene N_t^R are equal, and the number of cycles is measured, giving the crossing point C_R of the reference and the target gene C_T . The original concentration of the target gene T can then be calculated as:

$$N_t^T = N_t^R; \frac{N_0^T}{N_0^R} = 2^{C_R - C_T}; \text{ or } \frac{N_0^T}{N_0^R} = \frac{E_R^{C_R}}{E_T^{C_T}} \text{ for } E_R \neq E_T \text{ and } E_R, E_T \neq 2$$

- with
- N_t^T = Number of copies of target gene T at time t
 - N_t^R = Number of copies of reference gene R at time t
 - N_0^T = Number of copies of target gene T at time 0
 - N_0^R = Number of copies of reference gene R at time 0
 - C_R = crossing point of reference gene R
 - C_T = crossing point of target gene T
 - E_T = amplification efficiency of target gene T
 - E_R = amplification efficiency of reference gene R

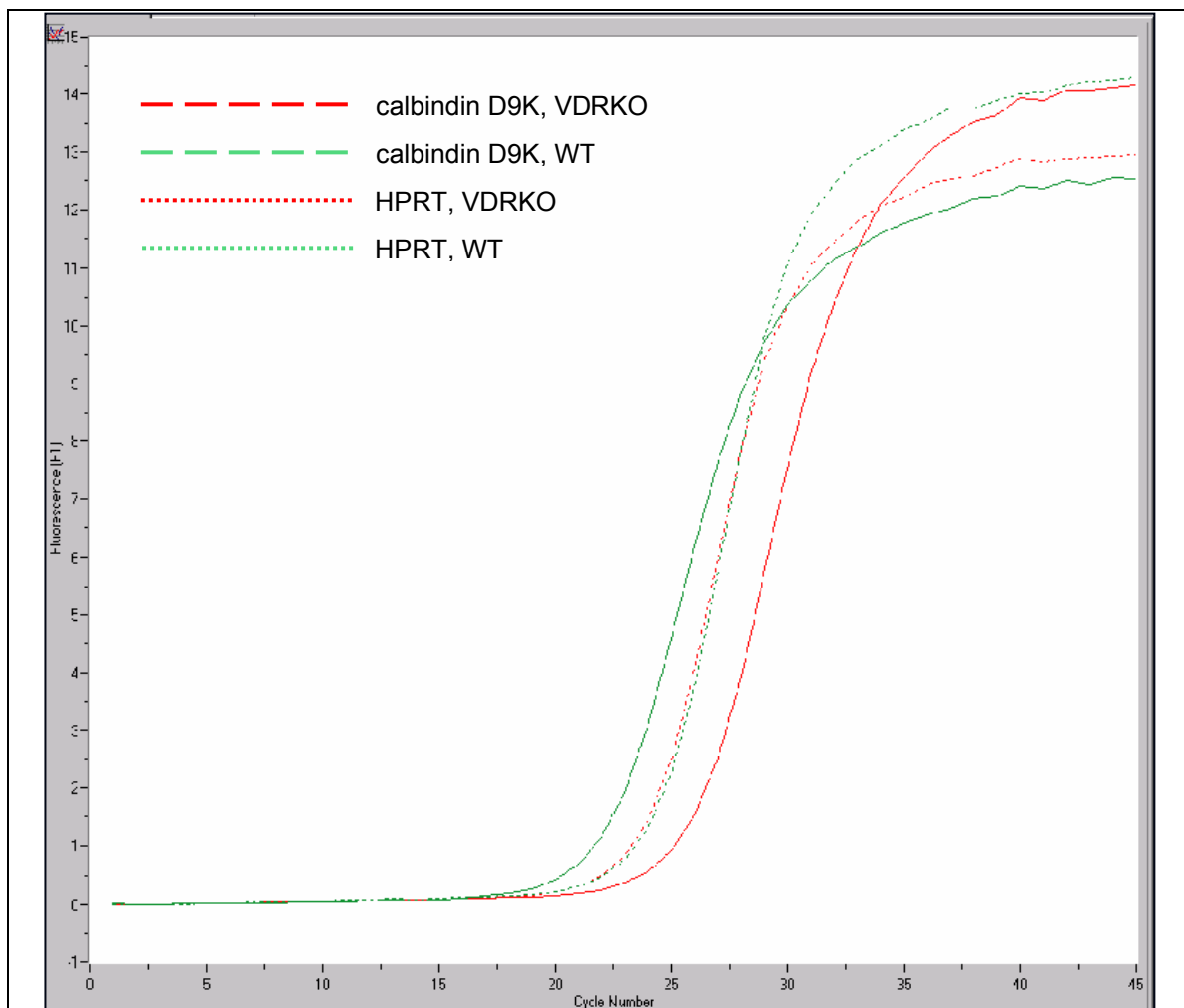


Figure 6.2.1: Fluorescence signal of target and reference gene during amplification by qPCR. Signal amplification plot of 4 qPCR reactions, showing the fluorescence signal of SYBR Green, in relation to the cycle number. The target gene calbindin D9K and the reference gene HPRT were measured in cDNA from VDRKO mouse kidney and compared to transcript concentrations in WT mouse kidney.

In some cases, especially at very high or low concentrations of DNA molecules, the efficiency differs significantly, e.g. due to inhibition effects. In those cases, it is safer to determine the efficiency for the amplification of the target gene ET and the reference gene ER experimentally with a standard curve, measured over 4-6 orders of magnitude of template DNA concentration and 4 replicates for each concentration. By linear regression the dependence of efficiency on template concentration can then be determined and expressed as a polynomial function, which can be used to determine the concentration of the target gene according to the formula above.

In most experiments, the relative change in transcript copy number of RNA from VDRKO mouse tissue was calculated with respect to RNA from WT tissue. The relative change in copy number is then

$$R_{VDRKO,WT}^T = \frac{\frac{N_{VDRKO}^T}{N_{VDRKO}^R}}{\frac{N_{WT}^T}{N_{WT}^R}} \approx 2^{(C_{VDRKO}^T - C_{VDRKO}^R - C_{WT}^T + C_{WT}^R)}$$

All C_p values were determined in triplicate experiments to account for the pipetting errors. Pipetting is generally the most significant source of technical variation. It was estimated by Gaussian error propagation of the ΔC_p values:

$$(\Delta R_{VDRKO,WT}^T)^2 = (R_{VDRKO,WT}^T \cdot \ln 2)^2 \cdot \sum_{i,j} (\Delta C_i^j)^2;$$

The biological variation due to differences in the expression profiles is discussed in section 3 and 4.

6.2.2 Sample cDNA preparation

Prior to qPCR analysis, total RNA was transcribed into the more stable cDNA, following standard protocols. First, a master mix was prepared:

quantity / reaction [μ l]	compound	concentration stock	company
4	5x First Strand Buffer	5X	Life Technologies
2	10x DTT	0.1M	Life Technologies
1	RNAse inhibitor	40U/l	Roche
1	20x 4dNTP	10mM each	Applied Biosystems
1	Superscript II MMLV RT	200U/l	Life Technologies
9	total volume		

1 μ g total RNA in 10 μ l volume per reaction and 1 μ l random nonamers (0.2M) were pipetted into 200 μ l PCR reaction tubes. The tubes were closed and heated for 5 min. at 80°C and chilled in a cold metal block. 9 μ l master mix (table 5.2.1) was added to each reaction, mixed by pipetting, let stand at RT for 3 min., incubated in a PCR cyclor for 90 minutes at 42°C and then for 15 minutes at 70 °C to inactivate the Superscript II RT polymerase. Depending on the level of expression of the genes to be measured, a dilution of the cDNA reaction products between 1:10 and 1:50 generally gave the best results.

6.2.3 Amplification protocols

As amplification of target and reference gene occurs simultaneously in separate reactions, the PCR reaction has to occur under standardised conditions. In this study, the standard amplification protocol for the Light Cycler was the following:

process	activation of hot-start Taq	annealing	amplification	denaturation	melting curve
temperature [°C]	95	58	60	95	40-95
time [sec]	600	15	45	10	600
cycles	1	40			1

For qPCR measurements with the Taqman 9700 from Applied Biosystems the protocol was similar, just annealing and amplification were combined in one step:

process	activation of hot-start Taq	annealing + amplification	denaturation	denaturation	annealing/ amplification	melting curve
temperature [°C]	95	60	95	95	60	60-95
time [sec]	600	60	15	15	60	600
cycles	1	40		1	1	1

All reactions were performed using the standard magnesium concentration as recommended by the manufacturer of the detection kit (6mM).

6.2.4 Primer selection and testing

To achieve comparable amplification efficiencies for all transcripts, the primers were designed according to standardised PCR conditions. Using the open-source programme primer3 from the Whitehead Institute for Biomedical Research (Rozen and Skaletsky 2000), primers were selected by setting the following parameters:

parameter	target	product size	max. 3' stability	max. mispriming	pair max. mispriming	primer size
range	X, 20 ¹	120-220	7	10	20	18-22
parameter	primer T _m	primer GC %	max. self complementarity	max. 3' self complementarity	mispriming library:	max. T _m difference
entry	58-61	45-56	6	2	rodent	1.5

¹X represents an exon-intron border minus 10bp. The following 20 bp had to be included in the amplified product.

Prior to qPCR analysis, all primer pairs were tested, using a dilution series of the sample cDNA spanning 3-4 orders of magnitude of cDNA concentration to test the specificity and linearity of the reaction and to estimate the amplification efficiency.

The specificity can be tested by comparing the melting curves of the amplification products of qPCR reactions at different concentration ranges. The derivative of the melting curves should be single peaks with a maximum that determines a well-

defined melting point. Shoulders in the derivative curves or shifts in the melting temperature indicate unwanted by-products.

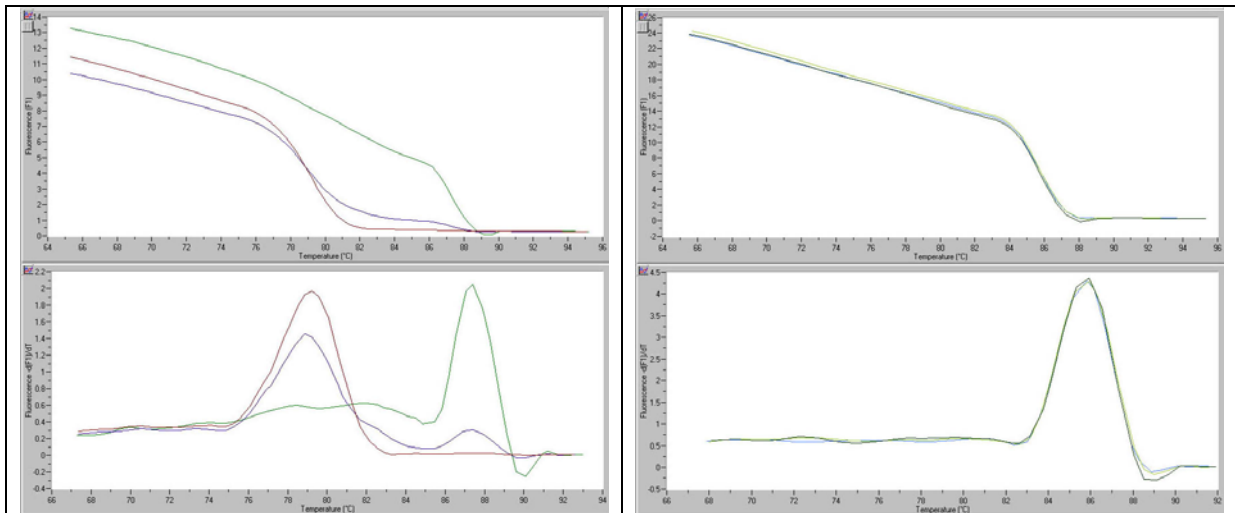


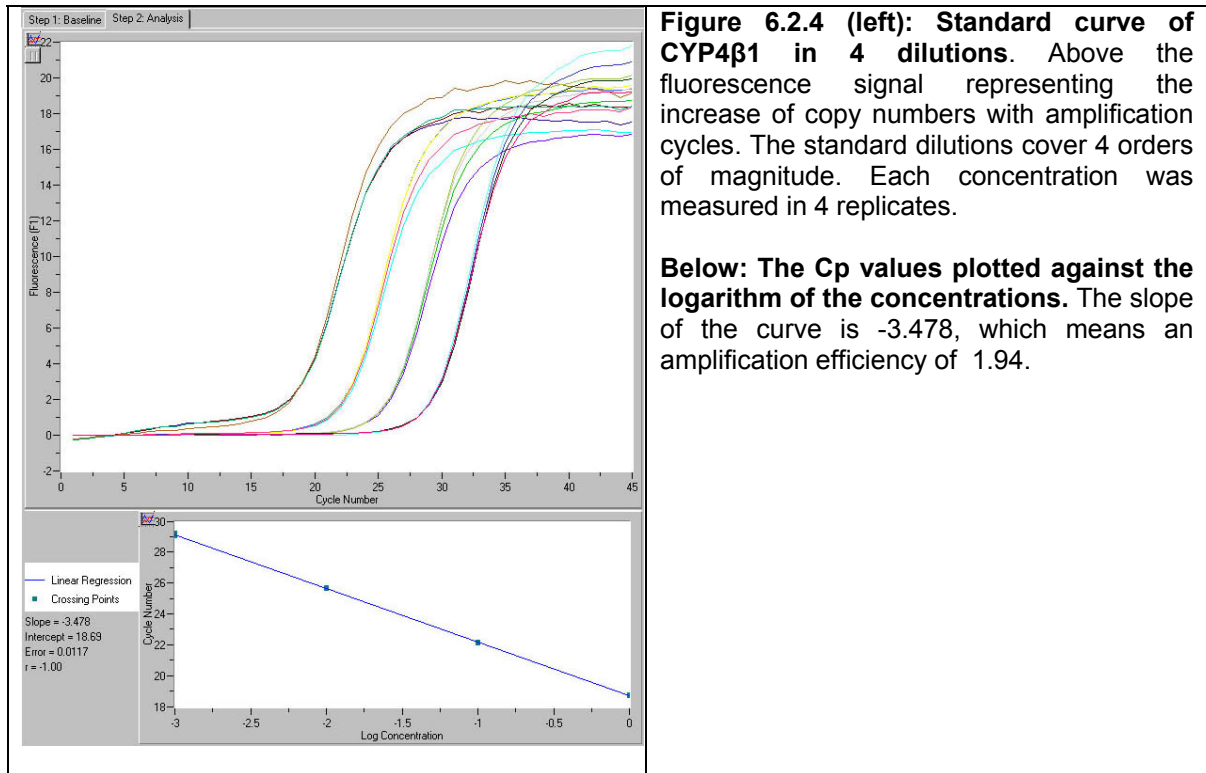
Figure 6.2.2: Melting curves of fatty acid synthase (FAS) amplification with the Light Cycler. FAS was measured in three dilutions of cDNA, covering 3 orders of magnitude. While the highest cDNA concentration the melting curve shows a relatively pure product, at lower concentrations the signal from by-products becomes stronger and the derivative melting curve shifts to a different melting point. Since the reaction has to be specific for one defined product over the whole measurement range, a different primer pair was chosen to determine the relative copy numbers of FAS

Figure 6.2.3: Melting curves of CYP4β1 over three orders of magnitude of cDNA concentration. The melting curves of three cDNA sample dilutions and the derivatives overlay nicely and describe the melting of a single PCR product with a well-defined melting point (peak of the derivative melting curves below).

A plot of the logarithm of cDNA concentration versus Cp values should deliver a linear line with a negative slope. From the slope, the efficiency can be calculated according to the formula

$$E = 10^{\frac{1}{\text{slope}}};$$

For a efficiency between 1.9 and 2.1 the slope has to be in the range between -3.10 and -3.59. Relative quantification with and without efficiency correction was tested. If the efficiency was constant in the range of sample concentrations and close to 2, the differences between both methods were marginal.



6.2.5 Choice of the reference gene

The reference gene should have the properties of a "housekeeping gene", i.e. not be regulated between two experimental conditions (e.g. WT and VDRKO mouse kidney). The expression of the reference gene should be in the range of the target gene. Since there are no *a priori* "housekeeping genes", a set of potential reference genes had to be tested for each set of samples and the relative concentrations to be calculated (Schmid et al. 2003). If the relative concentration of a transcript is similar in all samples with respect to several reference genes, it can be assumed to be a valuable reference.

In this study hypoxanthine guanine phosphoribosyl transferase (HPRT) and porphobilinogen deaminase (PBGD) were almost constant between samples and delivered nearly identical results. Since genes acting as housekeeping genes in one biological system can be regulated in a different system, it is recommendable to include two or more potential reference genes in each set of measurements. This opens the possibility to compare the relative copy numbers of reference genes and avoid erroneous results due to regulation of the reference gene. Good reference genes have copy numbers in the median measurement range and give a linear signal over several orders of magnitude.

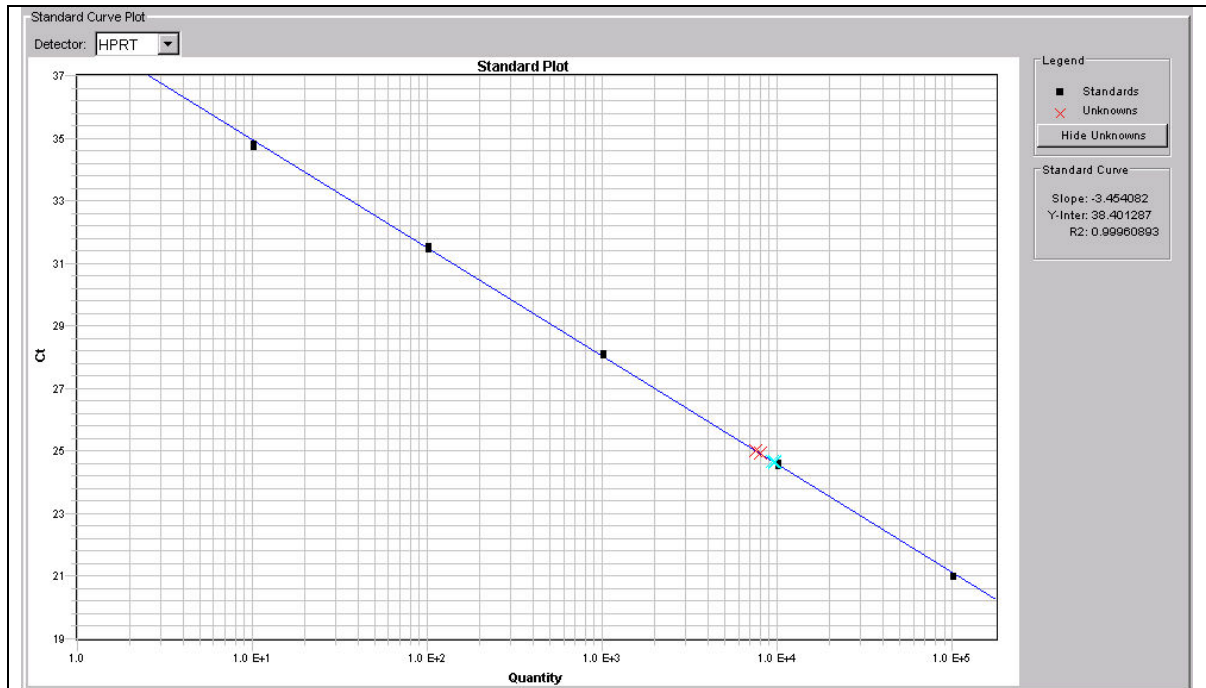


Figure 6.2.5: Standard curve of HPRT in dilutions of mouse heart cDNA over 5 orders of magnitude. The black boxes represent the Cp values of HPRT in the standard dilutions, measured in triplicates, the red crosses the Cp values in a cDNA sample of VDRKO mouse heart, the blue crosses in cDNA from WT mouse heart.

Initially for experiments with the Light Cycler HPRT was used. The data were verified in experiments with the Taqman 9700 using both, PBGD and HPRT. Other reference genes tested were GAPDH and S18. As in some cases HPRT seemed to be slightly regulated, most of the results from qPCR experiments presented in this thesis were calculated relative to PBGD expression.

6.3 Cell culture conditions

Name cell line	Medium	Splitting ratio
Mg-63	DMEM, 2mM glutamine, 10% FBS	1:4
SAOS-2	85% McCoy's, 15% FBS	1:3
MC3T3	DMEM, 2mM glutamine, 10% FBS	1:3
hfOB	DMEM/F12 1:1, 2mM glutamine, 10% FBS	1:4

All cell lines except hfOB were incubated at 37°C and 5% CO₂. In the case of hfOB the temperature was 34°C. To identify the influence of treatment with steroid hormones on the gene expression profile, sample (treated) and reference cells always were cultured under identical conditions for the same time and number of passages before harvesting and RNA extraction. For RNA extraction, cells were washed briefly with PBS, lysed with Trizol and homogenised with a syringe carrying a 18G needle.

7. Materials

7.1 Chemicals

7.1.1 Chemicals for Microarray analysis

Blocking agent	Salmon Sperm DNA	Sigma
Blocking agent	Poly(dA)	Sigma
Blocking agent	Blocking solution	Quantifoil
Filter columns	Microcon-YM-30	Millipore
Labeling dye	Cy3 / Cy5-dUTP	Amersham
Labeling nucleotides	5-(3-Aminoallyl)-2'-Deoxyuridine 5'-Triphosphate (AA-dUTP)	Sigma
Microarray glass substrates	CSS-100 silylated slides (aldehyde)	Cel Associates / Telechem
Microarray glass substrates	Sigma screen coated slides	Sigma
Microarray glass substrates	Gaps II aminosilane coated slides	Corning
Microarray glass substrates	Epoxi slides	Quantifoil
Monoreactive labeling dye	AA-Cy3/Cy5-dUTP	Amersham
PCR probe amplification	Taq DNA Polymerase (recombinant, 1u/μL)	MBI Fermentas
RNAse	RNAseH, E.coli	Biozym/Epicentre
RNAse cleaning agent	RNAse OUT Ribonuclease Inhibitor (Recombinant)	Gibco BRL
RT Polymerase	Superscript II RNAseH ⁻ Reverse Transcriptase	Invitrogen

7.1.2 General chemicals

Acetic acid	Merck
Acrylamide (30% with 0.8% Bisacrylamide)	Roth
Agar	Difco
Agarose	Biozym
Agarose (NuSieve)	Biowhittaker
Alcian blue	Sigma
APS (Ammonium peroxodisulfate)	Merck
Ampicillin	Sigma
Boric acid	Sigma
Bromophenol Blue	Sigma
BSA (Bovine serum albumine)	Sigma
Calcium chloride (dihydrate)	Sigma
Chloroform	Merck
DEPC (Diethylpyrocarbonate)	Aldrich

Materials

DMF (N,N-Dimethyl formamide)	Sigma
DMSO (Dimethyl sulfoxide)	Sigma
dNTPs	MBI Fermentas, Roche
EDTA (Ethylenediamine tetraacetic acid)	Sigma
Ethanol	Merck
Ethidium bromide	Sigma
Eukitt	Fluka
Formamide	Fluka
Glycerol	Sigma
Heparin	Sigma
HEPES (N-2-Hydroxyethylpiperazine-N'-2-ethanesulfonic acid)	Sigma
Hydrochloric acid	Merck
Hydrogen peroxide	Sigma
Isopropanol	Merck
Kanamycin	Sigma
Magnesium chloride	Sigma
β -mercaptoethanol	Sigma
Methanol	Merck
Methylene blue	Sigma
Mineral oil	Sigma
PFA (Paraformaldehyde)	Sigma
Phenol	Biosolve
Potassium acetate	Sigma
Potassium chloride	Sigma
Potassium hydroxide	Sigma
PTU (1-Phenyl-2-thio-urea)	Sigma
SDS (Sodium dodecyl sulfate)	Sigma
Sodium acetate	Sigma
Sodium chloride	Sigma
Sodium citrate	Sigma
Sodium dihydrogen phosphate	Sigma
Sodium hydrogen phosphate	Sigma
Sodium phosphate	Sigma
TEMED (N, N, N', N'-Tetramethylethylenediamine)	Sigma
Toluidine blue	Sigma
Tris	Sigma
Triton X-100	Sigma
Tween-20	Merck

7.2 Buffers and Solutions

- DEPC-H₂O 0.1% (v/v) DEPC in dH₂O
- Ethidium bromide stock solution 10 mg Ethidium bromide/ml dH₂O
- 1x PBS buffer (pH 7.5)
 - 140 mM NaCl
 - 8.1 mM Na₂HPO₄
 - 1.5 mM KH₂PO₄
 - 2.5 mM KCl
- 1x PBT buffer 0.1% Tween-20 in PBS
- 20x SSC (pH 7.0) buffer
 - 300 mM Sodium citrate
 - 3 M NaCl
- 1x TE buffer (pH 8.0)
 - 10 mM Tris-HCl, pH 8.0
 - 1 mM EDTA
- 10x TBE buffer
 - 1.4 M Tris-HCl, pH 8.3 – 8.7
 - 45 mM Boric acid
 - 25 mM EDTA

7.3 Kits

Microarray cDNA labeling	Genisphere 3DNA Submicro EX Expression Array Kit Cy3 / Cy5 labeled	Genisphere
Microarray cDNA labeling	Atlas Glass Fluorescent Labeling kit	Clontech
mRNA purification	Oligotec mRNA Midi kit	Quiagen
PCR product + Microarray sample purification	Quiaquick PCR purif.	Quiagen
PCR product purification	Nucleospin 96-well	Macherey-Nagel
PCR product purification	Multiscreen PCR 96-well filtration	Amicon
quantitative real-time PCR detection	iTaq Sybr Green Supermix with ROX	Bio-Rad
quantitative real-time PCR detection	LightCycler FastStart DNA Master Sybr Green I	Roche
RNA purification	RNAeasy Midi, Maxi	Quiagen
RNA purification	Trizol	Life Technologies

7.4 Primers

7.4.1 Primers for microarray analysis

reverse transcription of RNA samples	random9	nnn nnn nnn
reverse transcription of RNA samples	Oligo(dT)mix	0.2mM (dT) ₁₂₋₂₂
amplification of probes for spotting	M13-NH _{2_fw}	H ₂ N(CH ₂) ₆ -gtt ttc cca gtc acg acg ttg
	M13-NH _{2_fw}	H ₂ N(CH ₂) ₆ -tga gcg gat aac aat ttc aca cag

7.4.2 Primers for qPCR

Gene name	Forward	Reverse
Adamts1	ggg aat gag ccc act gta ga	atc aca gcc agc ttt cac ac
Adh1	gcc aag gcc aaa gag ttg	tcc tac gac gac gct tac ac
Adss1	tag gcg atg tgt atg gtg tg	agt gaa gcc att gac cat gt
ANP	tgg ctt cca ggc cat att	ggg cat gac ctc atc ttc ta
ApoE	gtg gca aag caa cca acc	agc tgt tcc tcc agc tcc tt
ApoH	gga tga ggg tga aga tcc ag	ctt cag cag ggt gtc agt tc
Aqp2	ttc gag ctg cct tct acg	tgc atg gtc agg aag agc
Atg	ccc agt tct tgc cac tga	tcc agg cag ctg aga gaa
Atp11A1	tcc tca aga agg tcc tgt gt	acc tgg agc aca caa ctc tc
Bdh1	gtg acc gac tga gaa cca tc	gtc tcc atc ctg gtg aac tc
C3	gct ggc ctc tgg agt aga ta	ttg aag gtc agg cag tct tc
CalbD28K	tgc cag caa ctg aag tcc	gcc atc tct gtc agt tcc ag
CalbD9K	gct ctc caa gga gga gct aa	ggg gct gtt gga act cct tc
calmodulin 1	ggg tca gaa ccc aac aga	ctg ccg cac tga tgt aac
calreticulin	ata caa ggg cga gtg gaa ac	tct gca tag gcc tca tca tt
Car3	tct gaa gca gcc tga tgg	tcc aat agt ccc ggc aag
Cidea	gtg gtg gac aca gag gag tt	ttg aga cag ccg agg aag
Cish	gtc cag gca gag aat gaa cc	gtg ggt gct gtc tcg aac ta
Cml-2	ccc tga aga gga aac aga ag	ctg gta ctg tcg gat gtg at
Col1A	atc gtg gtg aga ctg gtc ct	gag acc gtt gag tcc gtc tt
Cpn1	tcc cgg gta ctt act ctg tc	gag atg agc ttc gct tga gt
Cpt2	gct cgc tca gga taa aca ga	gtg tct tca gaa acc gca ct
CRADL	cct ggc ttc ttc ctg act	ggg cct tgt tgc acc tct
Ctgf	agc tgg gag aac tgt gta cg	agc tgc ttt gga agg act c
CYP1alpha	tca gtc aag ccc tgc atc	tct ctg ttg cac ttg ggg
CYP24	aca gag gaa gaa gcc ctg ac	ggg aat atc tct cta ggc gg
CYP2A4	tat gct ggg ctc tgt gct	agt tcc atc cta gcc agt cc
CYP2d9	ctt tgg gga cat tgt tcc ag	ggc atc gaa gtg ttc agg at
CYP4α14	ctc acc ata gcc atg ctt atc t	gga tcc cat tct tgg act tc
CYP4β1	ctg acc cag agg tct ttg ac	gct gtg acc acc ttc atc tc
CYP7b1	cgg cat cct gaa gct atg	tct cgg atg atg ctg gag
Cyr61	ggc atc tcc aca cga gtt ac	gac tgg ttc tgg gga ttt ct
DAP	cag ccc acc taa acc aac	gtc act tgc gag gct gtt
Desm	gga gcg tga caa cct gat ag	aag ctc acg gat ctc ctc tt
Dscr1	ccg ttg gct gga aac aag	tgg gct tgg gtc tct tca
DTR	ttc ttg tca tcg tgg gac tt	cggt gta acg aac cac tgt ctc
DUSP6	gac tct tcc tcg gac att ga	tct tcc aac acg tcc aag tt
Ebag9c	ttt ggt gtc cca gat ggt ag	ctt ccc acg cat tgc tat t
EndothelinR	ggc cct tgg aga cct tat	ggg tca aga cgg tga tgc

Materials

Fabp3	gca tga cca agc cta cta cc	ccc att cca ctt ctg cac
FAS	gct acc aag cca agc aca tt	att tgg gct tgt tga cat cc
FGF1	ctg aag ggg aga tca caa cc	ccg gtc tcc gta ccc ttt at
FGF2	caa ccg gta cct tgc tat ga	agt tcg ttt cag tgc cac at
Fsp27	cct ttc cca gaa gcc aac	cat gct gaa gag ggt cca
FXR	acc act aca acg cgc tca	agc caa cat ccc cat ctc
Gaddg45g	ctt gct gtt cgt gga tcg	act ttg gcg gac tcg tag ac
Gclc	gac caa tgg agg tgc agt ta	taa aac atc ccc tgc aag ac
GC-VDB	ctg cag ctc aca gat tga tg	ctt gga agg cca tct ct
HIFR	tgg aca gca aca gtg	cat cag gtt ggc aca cag
HNF4	tgg cag atg atc gaa cag a	gtc cat tgc tga ggt gag ag
HPRT	gtt gga tac agg cca gac ttt gt	cac agg act aga aca cct gc
HSD3B2	caa gca tca agg tga cag tg	aag atg aag gct ggc aca c
HSP70A1	tgg act caa gcc tac gtc ac	aaa ggt gtg tgg ata at
Ian6	gaa gaa tcc cac aag gca gt	ctt tct gga atg tcg tgg tc
Irs1	gac gct cca gtg agg att ta	gtg agg tcc tgg ttg tga at
Lcfae	agg cgc aga gaa cac gta	gcg tac agc gca gaa aac
Lpl	ctg ctg agt cct ttc cct tc	gag gtg gac atc gga gaa ct
mGLA	acc cga gac acc atg aag ag	gct gag ggg aca taa agg tg
Nephr2	gcc tta gat gca gtg acc tg	cag cct ttt ccc ctt ctg
NSD1	tcc act tgg agt gcc ttg	ggt ggg tac ttc tgg aca ca
Nur77	aac atc ctg gcc ttc tca c	gta gcc atg tgc tcc ttc a
Odc	tcc aga ggc caa aca tct ac	tgc agc caa gag cta caa g
Osta	gag gac tct gat ctg gag tag	ttc cac cat gac cat cat c
Osteopontin	agc ctg cac cca gat cct at	tcc gag tcc aca gaa tcc tc
Pafah1b1/LIS1	gca agc ctg gac ctt tct	gag ggt ctt gtc atc agc ac
PBGD	gcc tac cat act acc tcc tg	gca ctg aat tcc tgc agc tc
Pde1a1	ggc taa agg cctg tga tga tt	cgt gtc aac tcc tgg ata gaa
PGC1a	ttc gct gct ctt gag aat g	gtt acc tgc gca agc ttc t
PGC1b1	tcg aaa tct ctc cag tga ca	tga aca ccg gaa ggt gat a
Pparα-1	gac atc atg gaa ccc aag tt	ggg aag agg aag gtg tca tc
Pparγ-1	gcg atc ttg aca gga aag ac	gat ctc ttg cac ggc ttc ta
Ptgds	gcc tca atc tca cct cta cc	gca gag cgt act cgt cat ag
Renin	gtc ctt gca cct tca gtc tc	cgc cgt agt act ggg tat tc
Retnla	gct gat ggt ccc agt gaa tac	gga ggc cca tct gtt cat agt
S100A14	tac cag gaa cga tgg gac ag	cac agt tgc tcg gca tga
S100A8	tca cca tgc cct cta caa ga	tgg ctg tct ttg tga gat gc
S100A9	tcg gct ttg aca gag tgc	gtc cag gtc ctc cat gat gt
S2	ggg tta ctg gag cgt caa	gtc aag tca agg ggc aga
TGFb2	aac aat tcc tgg cgt tac ct	ttg ctg tca caa gag cag tg
TMP6	ccg gca tat gga ctg tgt	tga ggg cca cca taa cag
Tnnt1	agc gtg tgg att ttg atg ac	gct cct ttt ccg ttc tga ag
Ttr	ggc tca cca cag atg aga ag	gta gga gta tgg gct gag ca
Txnip	att cct gat gga cgt gtg tc	tga gga cag ctt ctg agt ga
Ucp-1	gtc ccc tgc cat tta ctg tc	acc cga gtc gca gaa aag
Uromodullin	gac caa ctg cta tgc cac ac	ctg gca aac cgg aac atc
VDR	gtt cac ctg ccc ctt caa	gcc tct tcc tcc ttc ctc tt
Xin	caa ggc tag aca ccc aaa ag	tgg aac ttg gag aag gtt tc

7.5 Hardware

Centrifuge	5415	Eppendorf
Centrifuge	Universal 32R	Hettich
Centrifuge	4-15C	Sigma/Qiagen
Gel chamber	Mini-Sub Cell GT	BioRad
Gel chamber	Sub Cell GT	BioRad
Gel chamber	Gator A3-1	Owl
Gel chamber	ReadyToRun 96-well	Amersham
Gel chamber	Sunrise	Gibco BRL
Hybridisation Chamber	HybChamber	Gene Machines
Hybridization oven	7601	GFL
Incubator	BK-600	Heraeus Instruments
Incubator	Innova 4400	New Brunswick Scientific
Incubator	Innova 4230	New Brunswick Scientific
Liquid-Handling Robot	Biomek 2000	Beckman
Micro Spotting Pins	Stealth SMP4 and SMP3	ArrayIt / Telechem
Overhead Shaker	Heidolph Reax2	Heidolph
PCR Thermocycler	Robocycler 96	Stratagene
PCR Thermocycler	PTC-225 Tetrad	MJ Research
Platform shaker	Polymax 1040	Heidolph
Power supply	PowerPac 300	BioRad
Power supply	PowerPac 3000	BioRad
Robotic Spotter	GMS417	Affymetrix
Robotic Spotter	Microgrid II Pro	BioRobotics
Scanner	FLA-8000	Fujifilm
Scanner	Axon 4000	Axon Instruments
Slide camera system	AxioCam MRm	Zeiss
Spectrophotometer	Double Beam UV/VIS	Uvikon
Spectrophotometer	DU 530	Beckman
Stereo microscope	Axiovert40 CFL	Zeiss
Thermocycler qPCR	Light Cycler	Roche
Thermocycler qPCR	TaqMan 7900 HAT	Applied Biosystems
Transilluminator	TFX-35M	Vilber Lourmat
Vacuumconcentrator	Concentrator 5301	Eppendorf
Vacuumconcentrator 96-well	Univapo 150 ECH	UniEquip
Waterbath	Ecoline E100	Lauda

7.6 Software

Interactive Technical Computing environment	Matlab	Mathworks
Microarray Data Analysis Software	MIDAS	TIGR Institute of Genomics Research
Microarray Data Analysis Software	MeV	TIGR Institute of Genomics Research
Microarray Data Analysis Software	Bioconductor	Bioconductor.org
Microarray Image Analysis Software	GenePix Pro 4.0	Axon Instruments

7.7 Bacterial strains

- *E.coli* DH5a
- *E.coli* DH10B

7.8 Cell lines

Name	Description	Provider
Mg-63	Human osteosarcoma	ECACC
Saos-2	Human primary osteogenic sarcoma	ECACC
MC3T3-E1	Murine osteoblast precursor	DSMZ
hFOB 1.19	Human osteoblast; SV40 large T antigen transfected	ATCC

7.9 Media for Cell Culture

Description	Provider
DMEM without Phenol red	Gibco
Mc Coy's 5A	Gibco
DMEM/F12 1:1 without Phenol red	Gibco
FBS	Biochrom
charcoal-stripped FCS	Hyclone
L-Glutamin	Gibco
Trypsin/EDTA	Gibco
Penicilin/Streptavidin	Gibco
1,25(OH) ₂ D ₃	Solvay Pharmaceuticals
Estradiol	Sigma
ICI 182 780	Zeneca

8. Appendix

8.1 Frequently used abbreviations

1,25(OH) ₂ D ₃	calcitriol, active vitamin D
25(OH)D ₃	calcidiol, 25-HydroxyvitaminD ₃
μl	microliter
bp	base pair
Ca ²⁺	calcium ion (concentration)
CCN1, Cyr61	cystein-rich protein 1
cDNA	complementary DNA
CTGF, CCN2	connective tissue growth factor
Cy3, Cy5	cyanine 3, cyanine 5
CYP1α	25-HydroxyvitaminD ₃ -1alpha-hydroxylase
CYP24	25-hydroxyvitamin D ₃ -24-hydroxylase
CYP27	vitamin D ₃ -25-hydroxylase
CYP4β1	cytochrome P4504B1
DBP, Gc	vitamin D-binding protein
DNA	deoxyribonucleic acid
dNTP	deoxyribonucleotriphosphate
mg	miligram
ml	milliliter
mRNA	messenger RNA
n.a.	not annotated
ND	normal diet
ng	nanogram
nm	nanometer
OD	optical density
PCR	polymerase chain reaction
PTH	parathyroid hormone
qPCR	quantitative real-time PCR
RD	rescue diet, enriched with calcium and phosphate
RNA	ribonucleic acid
RT-PCR	reverse transcription PCR
RXR	retinoic X receptor
SAM	significance analysis of microarray (data)
VDR	vitamin D receptor
VDRKO	vitamin D receptor knockout
WT	wild type

Further abbreviations are explained in the text.

8.2 Curriculum vitae

persönliche Daten

geboren am 10.06.1969 in
Marktbreit / Lkr.
Kitzingen
Familiennamen Graedler
Name Florian Alois
Kontaktadresse Ponschabastr. 7
83512 Wasserburg
Deutschland
Mobiltelefon 0049-8071 4801
Email: graedler@gmx.com



Abschlüsse

2004/5 GSF Forschungszentrum für Umwelt und Gesundheit, Institut für Experimentelle Genetik / Technische Universität München, Fakultät WZW für Ernährung, Landnutzung und Umwelt **Promotion (Dr. rer. nat.)**, Prüfung mit 1,1 (magna cum laude) abgeschlossen).
1998 Universität Regensburg: **Chemie Diplom**
1994 Universität Aberdeen (UK) / Rowett Research Institute: **Master of Science (M.Sc.)** in Analytischer Chemie
1992 Universität Regensburg: **Vordiplom Chemie**
1989 Luitpoldgymnasium Wasserburg a. Inn: **Allgemeine Hochschulreife** (Abitur)

Arbeitserfahrung

seit 01.11.2004 **Affymetrix UK Ltd.**, Applikations Support Spezialist. Aufgaben: Durchführung von Pilotstudien, Schulung und Beratung von Kunden in der Anwendung von Affymetrix Produkten (DNA-Microarrays, GeneChip Array Plattform, Software Anwendungen) in Forschung, Entwicklung und Diagnostik. Pre- und Postsales Support. Interaktion mit Sales, Marketing und F&E.
2000-2004 **GSF Forschungszentrum für Umwelt und Gesundheit GmbH, München-Neuherberg**: Wiss. Assistent am Institut für Experimentelle Genetik (IEG). Aufgaben: Forschung (Funktionelle Genomanalyse, Datenanalyse, Laborautomation, Anleitung von Studenten).
1999 **École Polytechnique Fédérale de Lausanne (EPFL)**: Wissenschaftl. Assistent am Institut für Umweltwissenschaften. Aufgaben: Forschung, Koordination eines Kooperationsprojekts mit Pharmacia /Stockholm, Seminarbetreuung.
1998 **Centro de Estudios Ambientales del Mediterraneo (CEAM), Valencia (E)** und **Universität Wuppertal**, Fakultät für Physikal. Chemie: Wissenschaftliche Hilfskraft. Forschung (Spurenanalytik von Photooxidationsprodukten in der Atmosphäre), Praktikumsbetreuung.

Fähigkeiten/Techniken

Molekularbiologie/Genomics Standardmethoden, Zellkulturtechniken, Transfektion, DNA - Sequenzierung, Genexpressionsanalyse mit DNA Microarrays, 2D-Gelelektrophorese, bioinformatische tools zur Datenanalyse, quantitative PCR.

Appendix

Analytische Chemie Methoden der organischen und biochemischen Analytik, Proteinanalytik, Massenspektrometrie, Kapillarelektrophorese, Chromatographie (GC, HPLC, FPLC), Spektrometrie (UV, AAS, FT-IR, NMR), statistische Methoden

EDV Office (Word, Excel, PowerPoint), Grafikprogramme (Photoshop, Illustrator, Corel), Statistik- und Clusterprogramme zur Auswertung von Microarray Daten, Maximiser Kundendatenbank, JDE Customer Service Package, ...

Sprachen

Deutsch	Muttersprache
Englisch	verhandlungsfähig mündlich und schriftlich
Spanisch	verhandlungsfähig mündlich und schriftlich
Französisch	sehr gute Kenntnisse
Italienisch	gute Grundkenntnisse
Russisch	geringe Grundkenntnisse

Weiterbildung

2005	Stratagene Schulung bei Affymetrix, High Wycombe, UK: Einführung in das Software Packet Array Assist
2005	Reed Trainingscenter, London, UK: Professional Telephone Techniques und Advanced Presentation Skills
2004	GSF Forschungszentrum München-Neuherberg: Workshop zur praktischen Einführung in das GenChip System von Affymetrix
2003	Max Planck Institut für Molekulare Genetik, Berlin: NGFN Kurs zur Statistik und Bioinformatik von Daten aus Experimenten mit DNA Microarrays
2003	European Bioinformatics Institute (EBI) in Hinxton/Cambridge, UK: EMBO Workshop über die Analyse von Microarray Daten
2002	GSF Forschungszentrum Neuherberg: Schulung Vortragstechnik mit Powerpoint
2002	Akademie der Bayerischen Presse: Workshop Wissenschaftsjournalismus
2002	Biorobotics, Inc., Cambridge, UK: Practical course in microarray production and - analysis.
2001	Beckman Instruments, Unterschleißheim: Kurs im Programmieren von Laborrobotern (Biomek 2000)
2000	GSF Forschungszentrum Neuherberg: Schulung zur Gestaltung von Datenbanken mit ACCESS
2000	Bruker Daltonics GmbH, Bremen: Workshop Proteinidentifikation durch MALDI-Massenspektrometrie
1998	University College Dublin, IR: Intensivkurs Grundlagen der Volks- und Betriebswirtschaftslehre

Hobbies & Interessen

Leben und arbeiten in einem offenen, internationalen Umfeld, reisen, tauchen, kochen, Film, Literatur

Engagement für AEGEE, eine EU-geförderte internationale Organisation von jungen Berufstätigen und Studenten zur Förderung des Austausches und der europäischen Integration

8.3 Publications

8.3.1 Manuscripts:

Kappler, R.; Calzada-Wack, J.; Schnitzbauer, U.; Koleva, M.; Herwig, A.; Piontek, G.; **Graedler, F.**; Adamski, J.; Heinzmann, U.; Schlegel, J.; Hemmerlein, B.; Quintanilla-Martinez, L. and Hahn, H.: Molecular characterization of Patched-associated rhabdomyosarcoma. *J Pathol* 200, 348-56 (2003)

Hult, M.; Ortsäter, H.; Schuster, G.; **Graedler, F.**; Adamski, J.; Ploner, A.; Jörnvall¹, H.; Bergsten, P.; and Oppermann, U.: Glucocorticoids increase insulin secretion in lean mice through multiple pathways and mechanisms. *J. Endocrinol.* submitted

Graedler F.; Horsch M.; Zeitz U.; Adamski J.: Gene expression profiling of hearts and kidneys from vitamin D receptor knockout mice reveals new functions of the vitamin D, in preparation.

8.3.2 Posters

Graedler, F.; Zeitz, U; Möller, G; Erben, RG; Adamski, J: Large-scale gene expression profiling of vitamin D receptor knock-out mouse tissue. 1st Wittgenstein conference on Bone Genetics and Development, Lucca, Italy, October 12-15, 2002

Schütze, N; **Graedler, F.**; Kunz, M; Balling, S; Hendrich, C; Eulert, J; Adamski, J; Jakob, F: The extracellular matrix protein hCYR61 (CCN1) affects signal transduction pathways associated with cell differentiation and proliferation in human osteoblasts. Osteologie-Tagung, Göttingen, March 26-29, 2003

Graedler, F.; Zeitz, U; Möller, G; Erben, RG; Adamski, J: Gene expression profiling reveals new functions of vitamin D. European Symposium on Calcified Tissues Rome, Italy, May 8-12, 2003

Schütze, N; **Graedler, F.**; Kunz, M; Balling, S; Hendrich, C; Eulert, J; Adamski J; Jakob F: The extracellular matrix protein hCYR61 (CCN1) modulates signal transduction pathways associated with cell differentiation and proliferation in human osteoblasts. 25th Annual Meeting of the American Society of Bone and Mineral Research (ASBMR), Minneapolis, Minnesota, USA, September 19-23, 2003

Graedler, F.; Zeitz, U; Möller, G; Beckers J; Erben, RG; Adamski, J: Gene expression profiling characterizes vitamin D receptor function. German Conference on Bioinformatics, GSF, Neuherberg, Germany, October 12-14, 2003

Schütze, N; **Graedler, F.**; Kunzi-Rapp, K; Jaschinski, D; Balling, S; Hendrich, C; Eulert, J; Adamski, J; Jakob F: The extracellular matrix signalling protein hCYR61 affects components of signal transduction pathways associated with cell differentiation in human osteoblasts. Orthopaedic Research Society, Orthopaedic Research Society 50th Annual Meeting, San Francisco, CA, USA, March 7-10, 2004

8.4 Acknowledgements / Danksagung

Ich möchte mich bei allen bedanken, die direkt oder indirekt zum Gelingen dieser Arbeit beigetragen haben: Bei meinem Betreuer PD Dr. Adamski für die großzügige und freundliche Unterstützung, sowie für die wissenschaftliche Freiheit bei der Entstehung dieser Arbeit, die mir als Chemiker einen tiefen Einblick in die Molekularbiologie ermöglichte. Gabriele Zieglmeier nahm mich als "Labormutter" gleich zu Anfang unter ihre Fittiche und half mir mit unglaublicher Effizienz und Geduld, wenn mich das Arbeitspensum zu überrollen drohte. Sehr viel verdanke ich auch Dr. Gabriele Möller, die sich immer Zeit nahm, wissenschaftlichen Problemen mit Rat und Tat zu begegnen.

Dr. Roland Kappler und Dr. Heidi Hahn halfen mir bei den ersten Schritten zur Etablierung der Microarray Technologie. Dies war der Anfang einer erfolgreichen Zusammenarbeit mit dem Institut für molekulare Pathologie, die später durch meine Kollegen und Freunde Dr. Jan Smida und Holger Laux fortgeführt wurde. Auch der Austausch mit Kollegen vom Institut für Biochemische Pflanzenpathologie, insbesondere mit Dr. Oliver Thulke und Dr. Olaf Neuschäfer-Rube war oft sehr hilfreich. Bei der späteren Entwicklung und Produktion der 21K Maus Microarrays war die Zusammenarbeit mit Dr. Matthias Seltmann, Dr. Marion Horsch, Dr. Alexei Drobyshev, Tomek Michalski und Christine Machka von der AG Dr. Beckers essentiell. Dr. Hutzler möchte ich danken für seine Hilfe am Konfokal-Mikroskop.

Die Kooperation mit auswärtigen Gruppen brachte Unterstützung und neue Ideen in meine Arbeit. Besonders danken möchte ich dabei Dr. Norbert Schütze und Prof. Dr. Franz Jakob vom Universitätsklinikum Würzburg für ihre engagierte Zusammenarbeit bei der Untersuchung der Wirkung von Cyr61 auf Osteoblasten. Mein Dank gilt auch Dr. Malin Hult und Prof. Dr. Udo Oppermann, die murine Inselzellen in mühevoller Arbeit isolierten, kultivierten und mit Glukokortikoiden behandelten, und sie mir zur Untersuchung mit Microarray Technologie überließen. Sehr zum Gelingen dieser Arbeit trugen auch Dr. Ute Zeitz, Dr. Karin Weber und PD Dr. Reinhold Erben vom veterinärmedizinischen Institut der Universität München bei, die mir Mäuse aus der VDRKO Linie zur Verfügung stellten.

Besonders möchte ich mich auch bei allen bedanken, die mich auch in schwierigen Phasen ermutigten und motivierten. Außer den bereits oben erwähnten seien hier Frau Prof. Dr. Eckhardt-Schupp, Dr. Eleonora Minina, meine Eltern Gert und Gisela Graedler und viele nette Kollegen vom GSF Forschungszentrum zu erwähnen. Die freundliche Atmosphäre unter den Kollegen in der AG Dr. Adamski und aus den benachbarten Arbeitsgruppen am IEG, IHG, IDG und dem Institut für Epidemiologie sorgte dafür, daß ich meist mit Freude und großer Motivation an der GSF arbeiten konnte. Dabei gewann ich viele Freunde, hoffentlich nicht nur für die Zeit an der GSF, sondern auch fürs Leben.

9. References

- Adachi, R., Shulman, A. I., Yamamoto, K., Shimomura, I., Yamada, S., Mangelsdorf, D. J. and Makishima, M. (2004). "Structural determinants for vitamin D receptor response to endocrine and xenobiotic signals." *Mol Endocrinol* **18**(1): 43-52.
- Adams, J. S., Chen, H., Chun, R. F., Nguyen, L., Wu, S., Ren, S. Y., Barsony, J. and Gacad, M. A. (2003). "Novel regulators of vitamin D action and metabolism: Lessons learned at the Los Angeles zoo." *J Cell Biochem* **88**(2): 308-14.
- Ahmed, M. S., Oie, E., Vinge, L. E., Yndestad, A., Oystein Andersen, G., Andersson, Y., Attramadal, T. and Attramadal, H. (2004). "Connective tissue growth factor--a novel mediator of angiotensin II-stimulated cardiac fibroblast activation in heart failure in rats." *J Mol Cell Cardiol* **36**(3): 393-404.
- Alagol, F., Shihadeh, Y., Boztepe, H., Tanakol, R., Yarman, S., Azizlerli, H. and Sandalci, O. (2000). "Sunlight exposure and vitamin D deficiency in Turkish women." *J Endocrinol Invest* **23**(3): 173-7.
- Allard, M. F., Schonekess, B. O., Henning, S. L., English, D. R. and Lopaschuk, G. D. (1994). "Contribution of oxidative metabolism and glycolysis to ATP production in hypertrophied hearts." *Am J Physiol* **267**(2 Pt 2): H742-50.
- Amersham (2002). Technical Service, Personal communication. F. Graedler.
- Amsterdam, A., Keren-Tal, I., Aharoni, D., Dantes, A., Land-Bracha, A., Rimon, E., Sasson, R. and Hirsh, L. (2003). "Steroidogenesis and apoptosis in the mammalian ovary." *Steroids* **68**(10-13): 861-7.
- Anisfeld, A. M., Kast-Woelbern, H. R., Meyer, M. E., Jones, S. A., Zhang, Y., Williams, K. J., Willson, T. and Edwards, P. A. (2003). "Syndecan-1 expression is regulated in an isoform-specific manner by the farnesoid-X receptor." *J Biol Chem* **278**(22): 20420-8.
- Argani, P., Rosty, C., Reiter, R. E., Wilentz, R. E., Murugesan, S. R., Leach, S. D., Ryu, B., Skinner, H. G., Goggins, M., Jaffee, E. M., Yeo, C. J., Cameron, J. L., Kern, S. E. and Hruban, R. H. (2001). "Discovery of new markers of cancer through serial analysis of gene expression: prostate stem cell antigen is overexpressed in pancreatic adenocarcinoma." *Cancer Res* **61**(11): 4320-4.
- Ashcroft, F. M., Proks, P., Smith, P. A., Ammala, C., Bokvist, K. and Rorsman, P. (1994). "Stimulus-secretion coupling in pancreatic beta cells." *J Cell Biochem* **55** Suppl: 54-65.
- Augenlicht, L. H., Wahrman, M. Z., Halsey, H., Anderson, L., Taylor, J. and Lipkin, M. (1987). "Expression of cloned sequences in biopsies of human colonic tissue and in colonic carcinoma cells induced to differentiate in vitro." *Cancer Res* **47**(22): 6017-21.
- Babic, A. M., Chen, C. C. and Lau, L. F. (1999). "Fisp12/mouse connective tissue growth factor mediates endothelial cell adhesion and migration through integrin alphavbeta3, promotes endothelial cell survival, and induces angiogenesis in vivo." *Mol Cell Biol* **19**(4): 2958-66.
- Babic, A. M., Kireeva, M. L., Kolesnikova, T. V. and Lau, L. F. (1998). "CYR61, a product of a growth factor-inducible immediate early gene, promotes angiogenesis and tumor growth." *Proc Natl Acad Sci U S A* **95**(11): 6355-60.
- Ballock, R. T., Zhou, X., Mink, L. M., Chen, D. H. and Mita, B. C. (2001). "Both retinoic acid and 1,25(OH)₂ vitamin D₃ inhibit thyroid hormone-induced terminal differentiation of growth plate chondrocytes." *J Orthop Res* **19**(1): 43-9.
- Bao, P., Frutos, A. G., Greef, C., Lahiri, J., Muller, U., Peterson, T. C., Warden, L. and Xie, X. (2002). "High-sensitivity detection of DNA hybridization on microarrays using resonance light scattering." *Anal Chem* **74**(8): 1792-7.
- Baron, M., Aslam, H., Flasz, M., Fostier, M., Higgs, J. E., Mazaleyrat, S. L. and Wilkin, M. B. (2002). "Multiple levels of Notch signal regulation (review)." *Mol Membr Biol* **19**(1): 27-38.

References

- Bastie, J. N., Balitrand, N., Guidez, F., Guillemot, I., Larghero, J., Calabresse, C., Chomienne, C. and Delva, L. (2004). "1 α ,25-Dihydroxyvitamin D₃ Transrepresses Retinoic Acid Transcriptional Activity via Vitamin D Receptor in Myeloid Cells." *Mol Endocrinol*.
- Beck, L. and Markovich, D. (2000). "The mouse Na(+)-sulfate cotransporter gene Nas1. Cloning, tissue distribution, gene structure, chromosomal assignment, and transcriptional regulation by vitamin D." *J Biol Chem* **275**(16): 11880-90.
- Becker, K. G. (2001). "The sharing of cDNA microarray data." *Nat Rev Neurosci* **2**(6): 438-40.
- Blutt, S. E., McDonnell, T. J., Polek, T. C. and Weigel, N. L. (2000). "Calcitriol-induced apoptosis in LNCaP cells is blocked by overexpression of Bcl-2." *Endocrinology* **141**(1): 10-7.
- Boheler, K. R. and Stern, M. D. (2003). "The new role of SAGE in gene discovery." *Trends Biotechnol* **21**(2): 55-7; discussion 57-8.
- Bolt, M. J., Liu, W., Qiao, G., Kong, J., Zheng, W., Krausz, T., Cs-Szabo, G., Sitrin, M. D. and Li, Y. C. (2004). "Critical Role of Vitamin D in Sulfate Homeostasis: Regulation of the Sodium-Sulfate Co-transporter by 1,25-Dihydroxyvitamin D₃." *Am J Physiol Endocrinol Metab*.
- Boute, N., Gribouval, O., Roselli, S., Benessy, F., Lee, H., Fuchshuber, A., Dahan, K., Gubler, M. C., Niaudet, P. and Antignac, C. (2000). "NPHS2, encoding the glomerular protein podocin, is mutated in autosomal recessive steroid-resistant nephrotic syndrome." *Nat Genet* **24**(4): 349-54.
- Brazma, A., Hingamp, P., Quackenbush, J., Sherlock, G., Spellman, P., Stoeckert, C., Aach, J., Ansorge, W., Ball, C. A., Causton, H. C., Gaasterland, T., Glenisson, P., Holstege, F. C., Kim, I. F., Markowitz, V., Matese, J. C., Parkinson, H., Robinson, A., Sarkans, U., Schulze-Kremer, S., Stewart, J., Taylor, R., Vilo, J. and Vingron, M. (2001). "Minimum information about a microarray experiment (MIAME)-toward standards for microarray data." *Nat Genet* **29**(4): 365-71.
- Brigstock, D. R. (2003). "The CCN family: a new stimulus package." *J Endocrinol* **178**(2): 169-75.
- Brown, M. S. and Goldstein, J. L. (1997). "The SREBP pathway: regulation of cholesterol metabolism by proteolysis of a membrane-bound transcription factor." *Cell* **89**(3): 331-40.
- Brown, P. O. e. a. (1999). "The MGuide. Version 2.0." [online publication](#).
- Bubb, M. R., Yarmola, E. G., Gibson, B. G. and Southwick, F. S. (2003). "Depolymerization of actin filaments by profilin. Effects of profilin on capping protein function." *J Biol Chem* **278**(27): 24629-35.
- Byyny, R. L., LoVerde, M., Lloyd, S., Mitchell, W. and Draznin, B. (1992). "Cytosolic calcium and insulin resistance in elderly patients with essential hypertension." *Am J Hypertens* **5**(7): 459-64.
- Cai, Z., Manalo, D. J., Wei, G., Rodriguez, E. R., Fox-Talbot, K., Lu, H., Zweier, J. L. and Semenza, G. L. (2003). "Hearts from rodents exposed to intermittent hypoxia or erythropoietin are protected against ischemia-reperfusion injury." *Circulation* **108**(1): 79-85.
- Cantorna, M. T., Hayes, C. E. and DeLuca, H. F. (1996). "1,25-Dihydroxyvitamin D₃ reversibly blocks the progression of relapsing encephalomyelitis, a model of multiple sclerosis." *Proc Natl Acad Sci U S A* **93**(15): 7861-4.
- Cantorna, M. T., Hayes, C. E. and DeLuca, H. F. (1998). "1,25-Dihydroxycholecalciferol inhibits the progression of arthritis in murine models of human arthritis." *J Nutr* **128**(1): 68-72.

- Carruth, B. R. and Skinner, J. D. (2001). "The role of dietary calcium and other nutrients in moderating body fat in preschool children." *Int J Obes Relat Metab Disord* **25**(4): 559-66.
- Chang, B. L., Zheng, S. L., Hawkins, G. A., Isaacs, S. D., Wiley, K. E., Turner, A., Carpten, J. D., Bleecker, E. R., Walsh, P. C., Trent, J. M., Meyers, D. A., Isaacs, W. B. and Xu, J. (2002). "Joint effect of HSD3B1 and HSD3B2 genes is associated with hereditary and sporadic prostate cancer susceptibility." *Cancer Res* **62**(6): 1784-9.
- Chen, H., Hu, B., Allegretto, E. A. and Adams, J. S. (2000). "The vitamin D response element-binding protein. A novel dominant-negative regulator of vitamin D-directed transactivation." *J Biol Chem* **275**(45): 35557-64.
- Chen, K. S. and DeLuca, H. F. (1995). "Cloning of the human 1 alpha,25-dihydroxyvitamin D-3 24-hydroxylase gene promoter and identification of two vitamin D-responsive elements." *Biochim Biophys Acta* **1263**(1): 1-9.
- Chen, S., Costa, C. H., Nakamura, K., Ribeiro, R. C. and Gardner, D. G. (1999). "Vitamin D-dependent suppression of human atrial natriuretic peptide gene promoter activity requires heterodimer assembly." *J Biol Chem* **274**(16): 11260-6.
- Chen, S., Wu, J., Hsieh, J. C., Whitfield, G. K., Jurutka, P. W., Haussler, M. R. and Gardner, D. G. (1998). "Suppression of ANP gene transcription by liganded vitamin D receptor: involvement of specific receptor domains." *Hypertension* **31**(6): 1338-42.
- Chen, T. C. and Holick, M. F. (2003). "Vitamin D and prostate cancer prevention and treatment." *Trends Endocrinol Metab* **14**(9): 423-30.
- Chenna, R., Sugawara, H., Koike, T., Lopez, R., Gibson, T. J., Higgins, D. G. and Thompson, J. D. (2003). "Multiple sequence alignment with the Clustal series of programs." *Nucleic Acids Res* **31**(13): 3497-500.
- Cheret, C., Doyen, A., Yaniv, M. and Pontoglio, M. (2002). "Hepatocyte nuclear factor 1 alpha controls renal expression of the Npt1-Npt4 anionic transporter locus." *J Mol Biol* **322**(5): 929-41.
- Christakos, S., Barletta, F., Huening, M., Dhawan, P., Liu, Y., Porta, A. and Peng, X. (2003). "Vitamin D target proteins: function and regulation." *J Cell Biochem* **88**(2): 238-44.
- Churchill, G. A. (2002). "Fundamentals of experimental design for cDNA microarrays." *Nat Genet* **32 Suppl**: 490-5.
- Clemens, T. L., Adams, J. S., Henderson, S. L. and Holick, M. F. (1982). "Increased skin pigment reduces the capacity of skin to synthesise vitamin D3." *Lancet* **1**(8263): 74-6.
- Colantuoni, C., Henry, G., Zeger, S. and Pevsner, J. (2002). "Local mean normalization of microarray element signal intensities across an array surface: quality control and correction of spatially systematic artifacts." *Biotechniques* **32**(6): 1316-20.
- Cross, H. S., Bareis, P., Hofer, H., Bischof, M. G., Bajna, E., Kriwanek, S., Bonner, E. and Peterlik, M. (2001). "25-Hydroxyvitamin D(3)-1alpha-hydroxylase and vitamin D receptor gene expression in human colonic mucosa is elevated during early cancerogenesis." *Steroids* **66**(3-5): 287-92.
- Crowe, R., Zikherman, J. and Niswander, L. (1999). "Delta-1 negatively regulates the transition from prehypertrophic to hypertrophic chondrocytes during cartilage formation." *Development* **126**(5): 987-98.
- Dahlquist, K. D., Salomonis, N., Vranizan, K., Lawlor, S. C. and Conklin, B. R. (2002). "GenMAPP, a new tool for viewing and analyzing microarray data on biological pathways." *Nat Genet* **31**(1): 19-20.
- Dallas, D. J., Genever, P. G., Patton, A. J., Millichip, M. I., McKie, N. and Skerry, T. M. (1999). "Localization of ADAM10 and Notch receptors in bone." *Bone* **25**(1): 9-15.
- Das, D. K. (2004). "Thioredoxin regulation of ischemic preconditioning." *Antioxid Redox Signal* **6**(2): 405-12.
- Davani, B., Khan, A., Hult, M., Martensson, E., Okret, S., Efendic, S., Jornvall, H. and Oppermann, U. C. (2000). "Type 1 11beta -hydroxysteroid dehydrogenase mediates

References

- glucocorticoid activation and insulin release in pancreatic islets." *J Biol Chem* **275**(45): 34841-4.
- Davies, K. M., Heaney, R. P., Recker, R. R., Lappe, J. M., Barger-Lux, M. J., Rafferty, K. and Hinders, S. (2000). "Calcium intake and body weight." *J Clin Endocrinol Metab* **85**(12): 4635-8.
- Del Arco, A., Peralta, S., Carrascosa, J. M., Ros, M., Andres, A. and Arribas, C. (2003). "Alternative splicing generates a novel non-secretable resistin isoform in Wistar rats." *FEBS Lett* **555**(2): 243-9.
- Delaunay, F., Khan, A., Cintra, A., Davani, B., Ling, Z. C., Andersson, A., Ostenson, C. G., Gustafsson, J., Efendic, S. and Okret, S. (1997). "Pancreatic beta cells are important targets for the diabetogenic effects of glucocorticoids." *J Clin Invest* **100**(8): 2094-8.
- Deluca, H. F. and Cantorna, M. T. (2001). "Vitamin D: its role and uses in immunology." *Faseb J* **15**(14): 2579-85.
- Dendorfer, A., Wolfrum, S., Wagemann, M., Qadri, F. and Dominiak, P. (2001). "Pathways of bradykinin degradation in blood and plasma of normotensive and hypertensive rats." *Am J Physiol Heart Circ Physiol* **280**(5): H2182-8.
- Deng, Y., Bhattacharya, S., Swamy, O. R., Tandon, R., Wang, Y., Janda, R. and Riedel, H. (2003). "Growth factor receptor-binding protein 10 (Grb10) as a partner of phosphatidylinositol 3-kinase in metabolic insulin action." *J Biol Chem* **278**(41): 39311-22.
- Denny, W. B., Valentine, D. L., Reynolds, P. D., Smith, D. F. and Scammell, J. G. (2000). "Squirrel monkey immunophilin FKBP51 is a potent inhibitor of glucocorticoid receptor binding." *Endocrinology* **141**(11): 4107-13.
- Diehl, F., Grahlmann, S., Beier, M. and Hoheisel, J. D. (2001). "Manufacturing DNA microarrays of high spot homogeneity and reduced background signal." *Nucleic Acids Res* **29**(7): E38.
- Doniger, S. W., Salomonis, N., Dahlquist, K. D., Vranizan, K., Lawlor, S. C. and Conklin, B. R. (2003). "MAPPFinder: using Gene Ontology and GenMAPP to create a global gene-expression profile from microarray data." *Genome Biol* **4**(1): R7.
- Dooley, T. P., Curto, E. V., Reddy, S. P., Davis, R. L., Lambert, G. W., Wilborn, T. W. and Elson, C. O. (2004). "Regulation of gene expression in inflammatory bowel disease and correlation with IBD drugs: screening by DNA microarrays." *Inflamm Bowel Dis* **10**(1): 1-14.
- Draznin, B., Sussman, K. E., Eckel, R. H., Kao, M., Yost, T. and Sherman, N. A. (1988). "Possible role of cytosolic free calcium concentrations in mediating insulin resistance of obesity and hyperinsulinemia." *J Clin Invest* **82**(6): 1848-52.
- Dudoit, S., Gentleman, R. C. and Quackenbush, J. (2003). "Open source software for the analysis of microarray data." *Biotechniques Suppl*: 45-51.
- Dzeja, P. P., Pucar, D., Redfield, M. M., Burnett, J. C. and Terzic, A. (1999). "Reduced activity of enzymes coupling ATP-generating with ATP-consuming processes in the failing myocardium." *Mol Cell Biochem* **201**(1-2): 33-40.
- Dzeja, P. P., Redfield, M. M., Burnett, J. C. and Terzic, A. (2000). "Failing energetics in failing hearts." *Curr Cardiol Rep* **2**(3): 212-7.
- Edgeworth, J., Gorman, M., Bennett, R., Freemont, P. and Hogg, N. (1991). "Identification of p8,14 as a highly abundant heterodimeric calcium binding protein complex of myeloid cells." *J Biol Chem* **266**(12): 7706-13.
- Eisen, M. B., Spellman, P. T., Brown, P. O. and Botstein, D. (1998). "Cluster analysis and display of genome-wide expression patterns." *Proc Natl Acad Sci U S A* **95**(25): 14863-8.
- Ellis, P. D., Chen, Q., Barker, P. J., Metcalfe, J. C. and Kemp, P. R. (2000). "Nov gene encodes adhesion factor for vascular smooth muscle cells and is dynamically regulated in response to vascular injury." *Arterioscler Thromb Vasc Biol* **20**(8): 1912-9.

References

- Erben, R. G. (2004). personal communication.
- Erben, R. G., Soegiarto, D. W., Weber, K., Zeitz, U., Lieberherr, M., Gniadecki, R., Moller, G., Adamski, J. and Balling, R. (2002). "Deletion of deoxyribonucleic acid binding domain of the vitamin D receptor abrogates genomic and nongenomic functions of vitamin D." *Mol Endocrinol* **16**(7): 1524-37.
- Ermak, G., Harris, C. D. and Davies, K. J. (2002). "The DSCR1 (Adapt78) isoform 1 protein calcipressin 1 inhibits calcineurin and protects against acute calcium-mediated stress damage, including transient oxidative stress." *Faseb J* **16**(8): 814-24.
- Ermak, G., Morgan, T. E. and Davies, K. J. (2001). "Chronic overexpression of the calcineurin inhibitory gene DSCR1 (Adapt78) is associated with Alzheimer's disease." *J Biol Chem* **276**(42): 38787-94.
- Evdokiou, A. and Cowled, P. A. (1998). "Growth-regulatory activity of the growth arrest-specific gene, GAS1, in NIH3T3 fibroblasts." *Exp Cell Res* **240**(2): 359-67.
- Feldman, A. L., Costouros, N. G., Wang, E., Qian, M., Marincola, F. M., Alexander, H. R. and Libutti, S. K. (2002). "Advantages of mRNA amplification for microarray analysis." *Biotechniques* **33**(4): 906-12, 914.
- Fernandes, I., Hampson, G., Cahours, X., Morin, P., Coureau, C., Couette, S., Prie, D., Biber, J., Murer, H., Friedlander, G. and Silve, C. (1997). "Abnormal sulfate metabolism in vitamin D-deficient rats." *J Clin Invest* **100**(9): 2196-203.
- Finck, B. N., Lehman, J. J., Leone, T. C., Welch, M. J., Bennett, M. J., Kovacs, A., Han, X., Gross, R. W., Kozak, R., Lopaschuk, G. D. and Kelly, D. P. (2002). "The cardiac phenotype induced by PPARalpha overexpression mimics that caused by diabetes mellitus." *J Clin Invest* **109**(1): 121-30.
- Finckenberg, P., Inkinen, K., Ahonen, J., Merasto, S., Louhelainen, M., Vapaatalo, H., Muller, D., Ganten, D., Luft, F. and Mervaala, E. (2003). "Angiotensin II induces connective tissue growth factor gene expression via calcineurin-dependent pathways." *Am J Pathol* **163**(1): 355-66.
- Fleet, J. C. (1999). "Vitamin D receptors: not just in the nucleus anymore." *Nutr Rev* **57**(2): 60-2.
- Fodor, S. P., Read, J. L., Pirrung, M. C., Stryer, L., Lu, A. T. and Solas, D. (1991). "Light-directed, spatially addressable parallel chemical synthesis." *Science* **251**(4995): 767-73.
- Froicu, M., Weaver, V., Wynn, T. A., McDowell, M. A., Welsh, J. E. and Cantorna, M. T. (2003). "A crucial role for the vitamin D receptor in experimental inflammatory bowel diseases." *Mol Endocrinol* **17**(12): 2386-92.
- Furukawa, T., Yatsuoka, T., Youssef, E. M., Abe, T., Yokoyama, T., Fukushige, S., Soeda, E., Hoshi, M., Hayashi, Y., Sunamura, M., Kobari, M. and Horii, A. (1998). "Genomic analysis of DUSP6, a dual specificity MAP kinase phosphatase, in pancreatic cancer." *Cytogenet Cell Genet* **82**(3-4): 156-9.
- Garland, C. F., Garland, F. C. and Gorham, E. D. (1999). "Calcium and vitamin D. Their potential roles in colon and breast cancer prevention." *Ann N Y Acad Sci* **889**: 107-19.
- Gasdaska, P. Y., Oblong, J. E., Cotgreave, I. A. and Powis, G. (1994). "The predicted amino acid sequence of human thioredoxin is identical to that of the autocrine growth factor human adult T-cell derived factor (ADF): thioredoxin mRNA is elevated in some human tumors." *Biochim Biophys Acta* **1218**(3): 292-6.
- Gohda, T., Makita, Y., Shike, T., Tanimoto, M., Funabiki, K., Horikoshi, S. and Tomino, Y. (2003). "Identification of epistatic interaction involved in obesity using the KK/Ta mouse as a Type 2 diabetes model: is Zn-alpha2 glycoprotein-1 a candidate gene for obesity?" *Diabetes* **52**(8): 2175-81.
- Grant, W. B. and Garland, C. F. (2004). "Reviews: A Critical Review of Studies on Vitamin D in Relation to Colorectal Cancer." *Nutr Cancer* **48**(2): 115-123.

- Gregori, S., Giarratana, N., Smioldo, S., Uskokovic, M. and Adorini, L. (2002). "A 1alpha,25-dihydroxyvitamin D(3) analog enhances regulatory T-cells and arrests autoimmune diabetes in NOD mice." *Diabetes* **51**(5): 1367-74.
- Guan, X., Fisher, M. B., Lang, D. H., Zheng, Y. M., Koop, D. R. and Rettie, A. E. (1998). "Cytochrome P450-dependent desaturation of lauric acid: isoform selectivity and mechanism of formation of 11-dodecenoic acid." *Chem Biol Interact* **110**(1-2): 103-21.
- Gurlek, A. and Kumar, R. (2001). "Regulation of osteoblast growth by interactions between transforming growth factor-beta and 1alpha,25-dihydroxyvitamin D3." *Crit Rev Eukaryot Gene Expr* **11**(4): 299-317.
- Hadjiargyrou, M., Ahrens, W. and Rubin, C. T. (2000). "Temporal expression of the chondrogenic and angiogenic growth factor CYR61 during fracture repair." *J Bone Miner Res* **15**(6): 1014-23.
- Halgren, R. G., Fielden, M. R., Fong, C. J. and Zacharewski, T. R. (2001). "Assessment of clone identity and sequence fidelity for 1189 IMAGE cDNA clones." *Nucleic Acids Res* **29**(2): 582-8.
- Harris, S. A., Enger, R. J., Riggs, B. L. and Spelsberg, T. C. (1995). "Development and characterization of a conditionally immortalized human fetal osteoblastic cell line." *J Bone Miner Res* **10**(2): 178-86.
- Haussler, M. R., Jurutka, P. W., Hsieh, J. C., Thompson, P. D., Selznick, S. H., Haussler, C. A. and Whitfield, G. K. (1995). "New understanding of the molecular mechanism of receptor-mediated genomic actions of the vitamin D hormone." *Bone* **17**(2 Suppl): 33S-38S.
- Hayes, C. E., Nashold, F. E., Spach, K. M. and Pedersen, L. B. (2003). "The immunological functions of the vitamin D endocrine system." *Cell Mol Biol (Noisy-le-grand)* **49**(2): 277-300.
- Hegde, P., Qi, R., Abernathy, K., Gay, C., Dharap, S., Gaspard, R., Hughes, J. E., Snesrud, E., Lee, N. and Quackenbush, J. (2000). "A concise guide to cDNA microarray analysis." *Biotechniques* **29**(3): 548-50, 552-4, 556 passim.
- Heng, Y. M., Kuo, C. S., Jones, P. S., Savory, R., Schulz, R. M., Tomlinson, S. R., Gray, T. J. and Bell, D. R. (1997). "A novel murine P-450 gene, CYP4 α 14, is part of a cluster of CYP4 α and CYP4 β , but not of CYP4F, genes in mouse and humans." *Biochem J* **325** (Pt 3): 741-9.
- Hida, Y., Kawada, T., Kayahashi, S., Ishihara, T. and Fushiki, T. (1998). "Counteraction of retinoic acid and 1,25-dihydroxyvitamin D3 on up-regulation of adipocyte differentiation with PPAR γ ligand, an antidiabetic thiazolidinedione, in 3T3-L1 cells." *Life Sci* **62**(14): PL205-11.
- Hippler, M., Hädrich, A. (2004). Surface Analysis - Imaging Ellipsometry, Nanofilm Technologies GmbH. **2004**.
- Ho, N. C., Jia, L., Driscoll, C. C., Gutter, E. M. and Francomano, C. A. (2000). "A skeletal gene database." *J Bone Miner Res* **15**(11): 2095-122.
- Hoenderop, J. G., Dardenne, O., Van Abel, M., Van Der Kemp, A. W., Van Os, C. H., St - Arnaud, R. and Bindels, R. J. (2002). "Modulation of renal Ca²⁺ transport protein genes by dietary Ca²⁺ and 1,25-dihydroxyvitamin D3 in 25-hydroxyvitamin D3-1alpha-hydroxylase knockout mice." *Faseb J* **16**(11): 1398-406.
- Hofmann, W. K., de Vos, S., Komor, M., Hoelzer, D., Wachsman, W. and Koeffler, H. P. (2002). "Characterization of gene expression of CD34+ cells from normal and myelodysplastic bone marrow." *Blood* **100**(10): 3553-60.
- Holick, M. F. (1989). Phylogenetic and evolutionary aspects of vitamin D from phytoplankton to humans. *Vertebrate Endocrinology: fundamentals and biochemical implications*. P. Pang, Schreibman, MP. Orlando, Academic Press. **3**: 7-43.
- Holick, M. F. (2003). "Vitamin D: A millenium perspective." *J Cell Biochem* **88**(2): 296-307.

References

- Holick, M. F. (2004). "Vitamin D: importance in the prevention of cancers, type 1 diabetes, heart disease, and osteoporosis." *Am J Clin Nutr* **79**(3): 362-71.
- Holla, V. R., Adas, F., Imig, J. D., Zhao, X., Price, E., Jr., Olsen, N., Kovacs, W. J., Magnuson, M. A., Keeney, D. S., Breyer, M. D., Falck, J. R., Waterman, M. R. and Capdevila, J. H. (2001). "Alterations in the regulation of androgen-sensitive Cyp 4a monooxygenases cause hypertension." *Proc Natl Acad Sci U S A* **98**(9): 5211-6.
- Hult, M., Ortsäter, H., Schuster, G., Graedler, F., Adamski, J., Ploner, A., Jörnvall, H., Bergsten P., Oppermann, U. (2004). "Glucocorticoids increase insulin secretion in lean mice through multiple pathways and mechanisms." *submitted*.
- Hypponen, E., Laara, E., Reunanen, A., Jarvelin, M. R. and Virtanen, S. M. (2001). "Intake of vitamin D and risk of type 1 diabetes: a birth-cohort study." *Lancet* **358**(9292): 1500-3.
- Ichikawa, I. and Fogo, A. (1996). "Focal segmental glomerulosclerosis." *Pediatr Nephrol* **10**(3): 374-91.
- Imamura, T., Asada, M., Vogt, S. K., Rudnick, D. A., Lowe, M. E. and Muglia, L. J. (2002). "Protection from pancreatitis by the zymogen granule membrane protein integral membrane-associated protein-1." *J Biol Chem* **277**(52): 50725-33.
- Imaoka, S., Hiroi, T., Tamura, Y., Yamazaki, H., Shimada, T., Komori, M., Degawa, M. and Funae, Y. (1995). "Mutagenic activation of 3-methoxy-4-aminoazobenzene by mouse renal cytochrome P450 CYP4B1: cloning and characterization of mouse CYP4B1." *Arch Biochem Biophys* **321**(1): 255-62.
- Imaoka, S., Yoneda, Y., Sugimoto, T., Ikemoto, S., Hiroi, T., Yamamoto, K., Nakatani, T. and Funae, Y. (2001a). "Androgen regulation of CYP4B1 responsible for mutagenic activation of bladder carcinogens in the rat bladder: detection of CYP4B1 mRNA by competitive reverse transcription-polymerase chain reaction." *Cancer Lett* **166**(2): 119-23.
- Imaoka, S., Yoneda, Y., Sugimoto, T., Ikemoto, S., Hiroi, T., Yamamoto, K., Nakatani, T. and Funae, Y. (2001b). "Androgen regulation of CYP4B1 responsible for mutagenic activation of bladder carcinogens in the rat bladder: detection of CYP4B1 mRNA by competitive reverse transcription-polymerase chain reaction." *Cancer Lett* **166**(2): 119-23.
- Inohara, N., Koseki, T., Chen, S., Wu, X. and Nunez, G. (1998). "CIDE, a novel family of cell death activators with homology to the 45 kDa subunit of the DNA fragmentation factor." *Embo J* **17**(9): 2526-33.
- Ito, H., Akiyama, H., Shigeno, C., Iyama, K., Matsuoka, H. and Nakamura, T. (1999). "Hedgehog signaling molecules in bone marrow cells at the initial stage of fracture repair." *Biochem Biophys Res Commun* **262**(2): 443-51.
- Itoh, N. and Okamoto, H. (1980). "Translational control of proinsulin synthesis by glucose." *Nature* **283**(5742): 100-2.
- Iyer, V. R., Eisen, M. B., Ross, D. T., Schuler, G., Moore, T., Lee, J. C., Trent, J. M., Staudt, L. M., Hudson, J., Jr., Boguski, M. S., Lashkari, D., Shalon, D., Botstein, D. and Brown, P. O. (1999). "The transcriptional program in the response of human fibroblasts to serum." *Science* **283**(5398): 83-7.
- Jezek, P. (1999). "Fatty acid interaction with mitochondrial uncoupling proteins." *J Bioenerg Biomembr* **31**(5): 457-66.
- Jezek, P., Engstova, H., Zackova, M., Vercesi, A. E., Costa, A. D., Arruda, P. and Garlid, K. D. (1998). "Fatty acid cycling mechanism and mitochondrial uncoupling proteins." *Biochim Biophys Acta* **1365**(1-2): 319-27.
- Jezek, P. and Garlid, K. D. (1998). "Mammalian mitochondrial uncoupling proteins." *Int J Biochem Cell Biol* **30**(11): 1163-8.
- Jezek, P., Zackova, M., Ruzicka, M., Skobisova, E. and Jaburek, M. (2004). "Mitochondrial uncoupling proteins - facts and fantasies." *Physiol Res* **53** Suppl 1: S199-211.

References

- Jia, L., Ho, N. C., Park, S. S., Powell, J. and Francomano, C. A. (2001). "Comprehensive resource: Skeletal gene database." *Am J Med Genet* **106**(4): 275-81.
- Jones, G., Strugnell, S. A. and DeLuca, H. F. (1998). "Current understanding of the molecular actions of vitamin D." *Physiol Rev* **78**(4): 1193-231.
- Juan, C. C., Au, L. C., Fang, V. S., Kang, S. F., Ko, Y. H., Kuo, S. F., Hsu, Y. P., Kwok, C. F. and Ho, L. T. (2001). "Suppressed gene expression of adipocyte resistin in an insulin-resistant rat model probably by elevated free fatty acids." *Biochem Biophys Res Commun* **289**(5): 1328-33.
- Kaminski, W. E., Wenzel, J. J., Piehler, A., Langmann, T. and Schmitz, G. (2001). "ABCA6, a novel a subclass ABC transporter." *Biochem Biophys Res Commun* **285**(5): 1295-301.
- Kappler, R., Calzada-Wack, J., Schnitzbauer, U., Koleva, M., Herwig, A., Piontek, G., Graedler, F., Adamski, J., Heinzmann, U., Schlegel, J., Hemmerlein, B., Quintanilla-Martinez, L. and Hahn, H. (2003). "Molecular characterization of Patched-associated rhabdomyosarcoma." *J Pathol* **200**(3): 348-56.
- Karle, S. M., Uetz, B., Ronner, V., Glaeser, L., Hildebrandt, F. and Fuchshuber, A. (2002). "Novel mutations in NPHS2 detected in both familial and sporadic steroid-resistant nephrotic syndrome." *J Am Soc Nephrol* **13**(2): 388-93.
- Karsten, S. L., Van Deerlin, V. M., Sabatti, C., Gill, L. H. and Geschwind, D. H. (2002). "An evaluation of tyramide signal amplification and archived fixed and frozen tissue in microarray gene expression analysis." *Nucleic Acids Res* **30**(2): E4.
- Kawada, T., Kamei, Y., Fujita, A., Hida, Y., Takahashi, N., Sugimoto, E. and Fushiki, T. (2000). "Carotenoids and retinoids as suppressors on adipocyte differentiation via nuclear receptors." *Biofactors* **13**(1-4): 103-9.
- Ketteler, R., Moghraby, C. S., Hsiao, J. G., Sandra, O., Lodish, H. F. and Klingmuller, U. (2003). "The cytokine-inducible Scr homology domain-containing protein negatively regulates signaling by promoting apoptosis in erythroid progenitor cells." *J Biol Chem* **278**(4): 2654-60.
- Keyse, S. M. (2000). "Protein phosphatases and the regulation of mitogen-activated protein kinase signalling." *Curr Opin Cell Biol* **12**(2): 186-92.
- Khan, A., Ostenson, C. G., Berggren, P. O. and Efendic, S. (1992). "Glucocorticoid increases glucose cycling and inhibits insulin release in pancreatic islets of ob/ob mice." *Am J Physiol* **263**(4 Pt 1): E663-6.
- Kimura, M., Furukawa, T., Abe, T., Yatsuoka, T., Youssef, E. M., Yokoyama, T., Ouyang, H., Ohnishi, Y., Sunamura, M., Kobari, M., Matsuno, S. and Horii, A. (1998). "Identification of two common regions of allelic loss in chromosome arm 12q in human pancreatic cancer." *Cancer Res* **58**(11): 2456-60.
- Kita, H., Carmichael, J., Swartz, J., Muro, S., Wyttenbach, A., Matsubara, K., Rubinsztein, D. C. and Kato, K. (2002). "Modulation of polyglutamine-induced cell death by genes identified by expression profiling." *Hum Mol Genet* **11**(19): 2279-87.
- Kitazawa, R. and Kitazawa, S. (2002). "Vitamin D(3) augments osteoclastogenesis via vitamin D-responsive element of mouse RANKL gene promoter." *Biochem Biophys Res Commun* **290**(2): 650-5.
- Koizumi, K., Nakajima, M., Yuasa, S., Saga, Y., Sakai, T., Kuriyama, T., Shirasawa, T. and Koseki, H. (2001). "The role of presenilin 1 during somite segmentation." *Development* **128**(8): 1391-402.
- Kragballe, K., Beck, H. I. and Sogaard, H. (1988). "Improvement of psoriasis by a topical vitamin D3 analogue (MC 903) in a double-blind study." *Br J Dermatol* **119**(2): 223-30.
- Krause, R., Buhning, M., Hopfenmuller, W., Holick, M. F. and Sharma, A. M. (1998). "Ultraviolet B and blood pressure." *Lancet* **352**(9129): 709-10.

References

- Krishnan, A. V., Peehl, D. M. and Feldman, D. (2003). "The role of vitamin D in prostate cancer." Recent Results Cancer Res **164**: 205-21.
- Kumar, S., Hand, A. T., Connor, J. R., Dodds, R. A., Ryan, P. J., Trill, J. J., Fisher, S. M., Nuttall, M. E., Lipshutz, D. B., Zou, C., Hwang, S. M., Votta, B. J., James, I. E., Rieman, D. J., Gowen, M. and Lee, J. C. (1999). "Identification and cloning of a connective tissue growth factor-like cDNA from human osteoblasts encoding a novel regulator of osteoblast functions." J Biol Chem **274**(24): 17123-31.
- Kuwayama, A., Kuruto, R., Horie, N., Takeishi, K. and Nozawa, R. (1993). "Appearance of nuclear factors that interact with genes for myeloid calcium binding proteins (MRP-8 and MRP-14) in differentiated HL-60 cells." Blood **81**(11): 3116-21.
- Lai, E. C. (2004). "Notch signaling: control of cell communication and cell fate." Development **131**(5): 965-73.
- Lambillotte, C., Gilon, P. and Henquin, J. C. (1997). "Direct glucocorticoid inhibition of insulin secretion. An in vitro study of dexamethasone effects in mouse islets." J Clin Invest **99**(3): 414-23.
- Lau, W. K., Chiu, S. K., Ma, J. T. and Tzeng, C. M. (2002). "Linear amplification of catalyzed reporter deposition technology on nylon membrane microarray." Biotechniques **33**(3): 564, 566-70.
- Leask, A., Holmes, A., Black, C. M. and Abraham, D. J. (2003). "Connective tissue growth factor gene regulation. Requirements for its induction by transforming growth factor-beta 2 in fibroblasts." J Biol Chem **278**(15): 13008-15.
- Lechner, A., Schutze, N., Siggelkow, H., Seufert, J. and Jakob, F. (2000). "The immediate early gene product hCYR61 localizes to the secretory pathway in human osteoblasts." Bone **27**(1): 53-60.
- Lehste, J. R., Melsen, F., Wellner, M., Jansen, P., Schlichting, U., Renner-Muller, I., Andreassen, T. T., Wolf, E., Bachmann, S., Nykjaer, A. and Willnow, T. E. (2003). "Hypocalcemia and osteopathy in mice with kidney-specific megalin gene defect." Faseb J **17**(2): 247-9.
- Lenzen, S. and Bailey, C. J. (1984). "Thyroid hormones, gonadal and adrenocortical steroids and the function of the islets of Langerhans." Endocr Rev **5**(3): 411-34.
- Lewis, A. L., Xia, Y., Datta, S. K., McMillin, J. and Kellems, R. E. (1999). "Combinatorial interactions regulate cardiac expression of the murine adenylosuccinate synthetase 1 gene." J Biol Chem **274**(20): 14188-97.
- Li, H., Kolluri, S. K., Gu, J., Dawson, M. I., Cao, X., Hobbs, P. D., Lin, B., Chen, G., Lu, J., Lin, F., Xie, Z., Fontana, J. A., Reed, J. C. and Zhang, X. (2000). "Cytochrome c release and apoptosis induced by mitochondrial targeting of nuclear orphan receptor TR3." Science **289**(5482): 1159-64.
- Li, M., Chiba, H., Warot, X., Messaddeq, N., Gerard, C., Chambon, P. and Metzger, D. (2001). "RXR-alpha ablation in skin keratinocytes results in alopecia and epidermal alterations." Development **128**(5): 675-88.
- Li, X., Zheng, W. and Li, Y. C. (2003). "Altered gene expression profile in the kidney of vitamin D receptor knockout mice." J Cell Biochem **89**(4): 709-19.
- Li, Y. C. (2003). "Vitamin D regulation of the renin-angiotensin system." J Cell Biochem **88**(2): 327-31.
- Li, Y. C., Amling, M., Pirro, A. E., Priemel, M., Meuse, J., Baron, R., Delling, G. and Demay, M. B. (1998a). "Normalization of mineral ion homeostasis by dietary means prevents hyperparathyroidism, rickets, and osteomalacia, but not alopecia in vitamin D receptor-ablated mice." Endocrinology **139**(10): 4391-6.
- Li, Y. C., Bolt, M. J., Cao, L. P. and Sitrin, M. D. (2001). "Effects of vitamin D receptor inactivation on the expression of calbindins and calcium metabolism." Am J Physiol Endocrinol Metab **281**(3): E558-64.

References

- Li, Y. C., Kong, J., Wei, M., Chen, Z. F., Liu, S. Q. and Cao, L. P. (2002). "1,25-Dihydroxyvitamin D(3) is a negative endocrine regulator of the renin-angiotensin system." *J Clin Invest* **110**(2): 229-38.
- Li, Y. C., Pirro, A. E., Amling, M., Dellling, G., Baron, R., Bronson, R. and Demay, M. B. (1997). "Targeted ablation of the vitamin D receptor: an animal model of vitamin D-dependent rickets type II with alopecia." *Proc Natl Acad Sci U S A* **94**(18): 9831-5.
- Li, Y. C., Pirro, A. E. and Demay, M. B. (1998b). "Analysis of vitamin D-dependent calcium-binding protein messenger ribonucleic acid expression in mice lacking the vitamin D receptor." *Endocrinology* **139**(3): 847-51.
- Li, Y. C., Qiao, G., Uskokovic, M., Xiang, W., Zheng, W. and Kong, J. (2004). "Vitamin D: a negative endocrine regulator of the renin-angiotensin system and blood pressure." *J Steroid Biochem Mol Biol* **89-90**(1-5): 387-92.
- Lin, B., Kolluri, S. K., Lin, F., Liu, W., Han, Y. H., Cao, X., Dawson, M. I., Reed, J. C. and Zhang, X. K. (2004). "Conversion of Bcl-2 from protector to killer by interaction with nuclear orphan receptor Nur77/TR3." *Cell* **116**(4): 527-40.
- Lin, R. and White, J. H. (2004). "The pleiotropic actions of vitamin D." *Bioessays* **26**(1): 21-8.
- Lin, S. C. and Li, P. (2004). "CIDE-A, a novel link between brown adipose tissue and obesity." *Trends Mol Med* **10**(9): 434-9.
- Linz, W., Schaper, J., Wiemer, G., Albus, U. and Scholkens, B. A. (1992). "Ramipril prevents left ventricular hypertrophy with myocardial fibrosis without blood pressure reduction: a one year study in rats." *Br J Pharmacol* **107**(4): 970-5.
- Linz, W., Wiemer, G., Gohlke, P., Unger, T. and Scholkens, B. A. (1995). "Contribution of kinins to the cardiovascular actions of angiotensin-converting enzyme inhibitors." *Pharmacol Rev* **47**(1): 25-49.
- Lion (2001). electronic source:
http://www.dhgp.de/media/xpress/genomxpress01_03/rzpd.html, Lion Biosciences AG. **2004**.
- MacBeath, G. (2002). "Protein microarrays and proteomics." *Nat Genet* **32 Suppl**: 526-32.
- Madsen, S. A., Chang, L. C., Hickey, M. C., Rosa, G. J., Coussens, P. M. and Burton, J. L. (2004). "Microarray analysis of gene expression in blood neutrophils of parturient cows." *Physiol Genomics* **16**(2): 212-21.
- Mahonen, A., Jukkola, A., Risteli, L., Risteli, J. and Maenpaa, P. H. (1998). "Type I procollagen synthesis is regulated by steroids and related hormones in human osteosarcoma cells." *J Cell Biochem* **68**(2): 151-63.
- Mahonen, A. and Maenpaa, P. H. (1994). "Steroid hormone modulation of vitamin D receptor levels in human MG-63 osteosarcoma cells." *Biochem Biophys Res Commun* **205**(2): 1179-86.
- Makishima, M., Lu, T. T., Xie, W., Whitfield, G. K., Domoto, H., Evans, R. M., Haussler, M. R. and Mangelsdorf, D. J. (2002). "Vitamin D receptor as an intestinal bile acid sensor." *Science* **296**(5571): 1313-6.
- Makita, K., Takahashi, K., Karara, A., Jacobson, H. R., Falck, J. R. and Capdevila, J. H. (1994). "Experimental and/or genetically controlled alterations of the renal microsomal cytochrome P450 epoxygenase induce hypertension in rats fed a high salt diet." *J Clin Invest* **94**(6): 2414-20.
- Mastyugin, V., Mezentsev, A., Zhang, W. X., Ashkar, S., Dunn, M. W. and Laniado-Schwartzman, M. (2004). "Promoter activity and regulation of the corneal CYP4β1 gene by hypoxia." *J Cell Biochem* **91**(6): 1218-38.
- Mathieu, C., Van Etten, E., Gysemans, C., Decallonne, B., Kato, S., Laureys, J., Depovere, J., Valckx, D., Verstuyf, A. and Bouillon, R. (2001). "In vitro and in vivo analysis of the immune system of vitamin D receptor knockout mice." *J Bone Miner Res* **16**(11): 2057-65.

References

- Matsunaga, T., Isohashi, F., Nakanishi, Y. and Sakamoto, Y. (1985). "Physiological changes in the activities of extramitochondrial acetyl-CoA hydrolase in the liver of rats under various metabolic conditions." Eur J Biochem **152**(2): 331-6.
- Matsuoka, L. Y., Wortsman, J., Hanifan, N. and Holick, M. F. (1988). "Chronic sunscreen use decreases circulating concentrations of 25-hydroxyvitamin D. A preliminary study." Arch Dermatol **124**(12): 1802-4.
- Matthews, K. W., Mueller-Ortiz, S. L. and Wetsel, R. A. (2004). "Carboxypeptidase N: a pleiotropic regulator of inflammation." Mol Immunol **40**(11): 785-93.
- Maxwell, P. H., Wiesener, M. S., Chang, G. W., Clifford, S. C., Vaux, E. C., Cockman, M. E., Wykoff, C. C., Pugh, C. W., Maher, E. R. and Ratcliffe, P. J. (1999). "The tumour suppressor protein VHL targets hypoxia-inducible factors for oxygen-dependent proteolysis." Nature **399**(6733): 271-5.
- McCarron, D. A. (1995). "Calcium metabolism in hypertension." Keio J Med **44**(4): 105-14.
- McCarron, D. A., Morris, C. D. and Cole, C. (1982). "Dietary calcium in human hypertension." Science **217**(4556): 267-9.
- McDonnell, D. P., Mangelsdorf, D. J., Pike, J. W., Haussler, M. R. and O'Malley, B. W. (1987). "Molecular cloning of complementary DNA encoding the avian receptor for vitamin D." Science **235**(4793): 1214-7.
- McGiff, J. C. and Quilley, J. (1999). "20-HETE and the kidney: resolution of old problems and new beginnings." Am J Physiol **277**(3 Pt 2): R607-23.
- Miller, G. J. (1998). "Vitamin D and prostate cancer: biologic interactions and clinical potentials." Cancer Metastasis Rev **17**(4): 353-60.
- Mishal, A. A. (2001). "Effects of different dress styles on vitamin D levels in healthy young Jordanian women." Osteoporos Int **12**(11): 931-5.
- Mishina, Y., Starbuck, M. W., Gentile, M. A., Fukuda, T., Kasparcova, V., Seedor, G. J., Hanks, M. C., Amling, M., Pinero, G. J., Harada, S. I. and Behringer, R. R. (2004). "BMP type IA receptor signaling regulates postnatal osteoblast function and bone remodeling." J Biol Chem.
- Monaco, H. L. (2000). "The transthyretin-retinol-binding protein complex." Biochim Biophys Acta **1482**(1-2): 65-72.
- Montessuit, C. and Thorburn, A. (1999). "Transcriptional activation of the glucose transporter GLUT1 in ventricular cardiac myocytes by hypertrophic agonists." J Biol Chem **274**(13): 9006-12.
- Morissette, M. R., Howes, A. L., Zhang, T. and Heller Brown, J. (2003). "Upregulation of GLUT1 expression is necessary for hypertrophy and survival of neonatal rat cardiomyocytes." J Mol Cell Cardiol **35**(10): 1217-27.
- Muller, D. N., Theuer, J., Shagdarsuren, E., Kaergel, E., Honeck, H., Park, J. K., Markovic, M., Barbosa-Sicard, E., Dechend, R., Wellner, M., Kirsch, T., Fiebeler, A., Rothe, M., Haller, H., Luft, F. C. and Schunck, W. H. (2004). "A peroxisome proliferator-activated receptor- α activator induces renal CYP2C23 activity and protects from angiotensin II-induced renal injury." Am J Pathol **164**(2): 521-32.
- Nacken, W., Roth, J., Sorg, C. and Kerkhoff, C. (2003). "S100A9/S100A8: Myeloid representatives of the S100 protein family as prominent players in innate immunity." Microsc Res Tech **60**(6): 569-80.
- Nakamura, T., Aikawa, T., Iwamoto-Enomoto, M., Iwamoto, M., Higuchi, Y., Pacifici, M., Kinto, N., Yamaguchi, A., Noji, S., Kurisu, K., Matsuya, T. and Maurizio, P. (1997). "Induction of osteogenic differentiation by hedgehog proteins." Biochem Biophys Res Commun **237**(2): 465-9.
- Newswire, P. (2004). World's First Diagnostic Microarray System Launched by Affymetrix in European Union, Belga Press. **2004**.
- Nishiyama, A., Matsui, M., Iwata, S., Hirota, K., Masutani, H., Nakamura, H., Takagi, Y., Sono, H., Gon, Y. and Yodoi, J. (1999). "Identification of thioredoxin-binding protein-

References

- 2/vitamin D(3) up-regulated protein 1 as a negative regulator of thioredoxin function and expression." *J Biol Chem* **274**(31): 21645-50.
- O'Kelly, J. and Koefler, H. P. (2003). "Vitamin D analogs and breast cancer." *Recent Results Cancer Res* **164**: 333-48.
- Otsuki, M., Gao, H., Dahlman-Wright, K., Ohlsson, C., Eguchi, N., Urade, Y. and Gustafsson, J. A. (2003). "Specific regulation of lipocalin-type prostaglandin D synthase in mouse heart by estrogen receptor beta." *Mol Endocrinol* **17**(9): 1844-55.
- Otterbein, L. R., Cosio, C., Graceffa, P. and Dominguez, R. (2002). "Crystal structures of the vitamin D-binding protein and its complex with actin: structural basis of the actin-scavenger system." *Proc Natl Acad Sci U S A* **99**(12): 8003-8.
- Owen, R. W., Dodo, M., Thompson, M. H. and Hill, M. J. (1987). "Fecal steroids and colorectal cancer." *Nutr Cancer* **9**(2-3): 73-80.
- Pan, W., Lin, J. and Le, C. T. (2002). "How many replicates of arrays are required to detect gene expression changes in microarray experiments? A mixture model approach." *Genome Biol* **3**(5): research0022.
- Papa, S., Zazzeroni, F., Bubici, C., Jayawardena, S., Alvarez, K., Matsuda, S., Nguyen, D. U., Pham, C. G., Nelsbach, A. H., Melis, T., De Smaele, E., Tang, W. J., D'Adamio, L. and Franzoso, G. (2004). "Gadd45 beta mediates the NF-kappa B suppression of JNK signalling by targeting MKK7/JNKK2." *Nat Cell Biol* **6**(2): 146-53.
- Park, T., Yi, S. G., Kang, S. H., Lee, S., Lee, Y. S. and Simon, R. (2003). "Evaluation of normalization methods for microarray data." *BMC Bioinformatics* **4**(1): 33.
- Pellieux, C., Desgeorges, A., Pigeon, C. H., Chambaz, C., Yin, H., Hayoz, D. and Silacci, P. (2003). "Cap G, a gelsolin family protein modulating protective effects of unidirectional shear stress." *J Biol Chem* **278**(31): 29136-44.
- Pete, G., Fuller, C. R., Oldham, J. M., Smith, D. R., D'Ercole, A. J., Kahn, C. R. and Lund, P. K. (1999). "Postnatal growth responses to insulin-like growth factor I in insulin receptor substrate-1-deficient mice." *Endocrinology* **140**(12): 5478-87.
- Peterfy, M., Phan, J., Xu, P. and Reue, K. (2001). "Lipodystrophy in the fld mouse results from mutation of a new gene encoding a nuclear protein, lipin." *Nat Genet* **27**(1): 121-4.
- Phan, J., Peterfy, M. and Reue, K. (2004). "Lipin Expression Preceding Peroxisome Proliferator-activated Receptor- γ Is Critical for Adipogenesis in Vivo and in Vitro." *J Biol Chem* **279**(28): 29558-29564.
- Picotto, G. (2001). "Rapid effects of calciotropic hormones on female rat enterocytes: combined actions of 1,25(OH)₂-vitamin D₃, PTH and 17beta-estradiol on intracellular Ca²⁺ regulation." *Horm Metab Res* **33**(12): 733-8.
- Prud'homme, G. J. and Piccirillo, C. A. (2000). "The inhibitory effects of transforming growth factor-beta-1 (TGF-beta1) in autoimmune diseases." *J Autoimmun* **14**(1): 23-42.
- Prufer, K. and Barsony, J. (2002). "Retinoid X receptor dominates the nuclear import and export of the unliganded vitamin D receptor." *Mol Endocrinol* **16**(8): 1738-51.
- Qiao, S., Pennanen, P., Nazarova, N., Lou, Y. R. and Tuohimaa, P. (2003). "Inhibition of fatty acid synthase expression by 1alpha,25-dihydroxyvitamin D₃ in prostate cancer cells." *J Steroid Biochem Mol Biol* **85**(1): 1-8.
- Quackenbush, J. (2002). "Microarray data normalization and transformation." *Nat Genet* **32**(Suppl): 496-501.
- Querfeld, U., Hoffmann, M. M., Klaus, G., Eifinger, F., Ackerschott, M., Michalk, D. and Kern, P. A. (1999). "Antagonistic effects of vitamin D and parathyroid hormone on lipoprotein lipase in cultured adipocytes." *J Am Soc Nephrol* **10**(10): 2158-64.
- Rabahi, F., Brule, S., Sirois, J., Beckers, J. F., Silversides, D. W. and Lussier, J. G. (1999). "High expression of bovine alpha glutathione S-transferase (GSTA1, GSTA2) subunits is mainly associated with steroidogenically active cells and regulated by gonadotropins in bovine ovarian follicles." *Endocrinology* **140**(8): 3507-17.

References

- Rapoport, R., Sklan, D. and Hanukoglu, I. (1995). "Electron leakage from the adrenal cortex mitochondrial P450_{scc} and P450_{c11} systems: NADPH and steroid dependence." Arch Biochem Biophys **317**(2): 412-6.
- Reckelhoff, J. F. (2001). "Gender differences in the regulation of blood pressure." Hypertension **37**(5): 1199-208.
- Rickman, D. S., Herbert, C. J. and Aggerbeck, L. P. (2003). "Optimizing spotting solutions for increased reproducibility of cDNA microarrays." Nucleic Acids Res **31**(18): e109.
- Rida, P. C., Le Minh, N. and Jiang, Y. J. (2004). "A Notch feeling of somite segmentation and beyond." Dev Biol **265**(1): 2-22.
- Robin, M. A., Prabu, S. K., Raza, H., Anandatheerthavarada, H. K. and Avadhani, N. G. (2003). "Phosphorylation enhances mitochondrial targeting of GSTA4-4 through increased affinity for binding to cytoplasmic Hsp70." J Biol Chem **278**(21): 18960-70.
- Robinson, W. H., DiGennaro, C., Hueber, W., Haab, B. B., Kamachi, M., Dean, E. J., Fournel, S., Fong, D., Genovese, M. C., de Vegvar, H. E., Skriner, K., Hirschberg, D. L., Morris, R. I., Muller, S., Pruijn, G. J., van Venrooij, W. J., Smolen, J. S., Brown, P. O., Steinman, L. and Utz, P. J. (2002). "Autoantigen microarrays for multiplex characterization of autoantibody responses." Nat Med **8**(3): 295-301.
- Rochel, N. (2000). Euro J Biochem **268**: 971-979.
- Roman, R. J. (2002). "P-450 metabolites of arachidonic acid in the control of cardiovascular function." Physiol Rev **82**(1): 131-85.
- Ropeleski, M. J., Tang, J., Walsh-Reitz, M. M., Musch, M. W. and Chang, E. B. (2003). "Interleukin-11-induced heat shock protein 25 confers intestinal epithelial-specific cytoprotection from oxidant stress." Gastroenterology **124**(5): 1358-68.
- Rose, D. (2000). Microfluidic technologies and instrumentation for printing DNA microarrays. Natick, MA, Eaton Publishing.
- Roselli, S., Heidet, L., Sich, M., Henger, A., Kretzler, M., Gubler, M. C. and Antignac, C. (2004). "Early glomerular filtration defect and severe renal disease in podocin-deficient mice." Mol Cell Biol **24**(2): 550-60.
- Rothermel, B. A., McKinsey, T. A., Vega, R. B., Nicol, R. L., Mammen, P., Yang, J., Antos, C. L., Shelton, J. M., Bassel-Duby, R., Olson, E. N. and Williams, R. S. (2001). "Myocyte-enriched calcineurin-interacting protein, MCIP1, inhibits cardiac hypertrophy in vivo." Proc Natl Acad Sci U S A **98**(6): 3328-33.
- Royuela, M., de Miguel, M. P., Bethencourt, F. R., Sanchez-Chapado, M., Fraile, B., Arenas, M. I. and Paniagua, R. (2001). "Estrogen receptors alpha and beta in the normal, hyperplastic and carcinomatous human prostate." J Endocrinol **168**(3): 447-54.
- Rozen, S. and Skaletsky, H. (2000). "Primer3 on the WWW for general users and for biologist programmers." Methods Mol Biol **132**: 365-86.
- Ryan, M. J., Black, T. A., Millard, S. L., Gross, K. W. and Hajduczuk, G. (2002). "Endothelin-1 increases calcium and attenuates renin gene expression in As4.1 cells." Am J Physiol Heart Circ Physiol **283**(6): H2458-65.
- Ryeom, S., Greenwald, R. J., Sharpe, A. H. and McKeon, F. (2003). "The threshold pattern of calcineurin-dependent gene expression is altered by loss of the endogenous inhibitor calcipressin." Nat Immunol **4**(9): 874-81.
- Saal, L. H., Troein, C., Vallon-Christersson, J., Gruvberger, S., Borg, A. and Peterson, C. (2002). "BioArray Software Environment (BASE): a platform for comprehensive management and analysis of microarray data." Genome Biol **3**(8): SOFTWARE0003.
- Saeed, A. I., Sharov, V., White, J., Li, J., Liang, W., Bhagabati, N., Braisted, J., Klapa, M., Currier, T., Thiagarajan, M., Sturn, A., Snuffin, M., Rezantsev, A., Popov, D., Ryltsov, A., Kostukovich, E., Borisovsky, I., Liu, Z., Vinsavich, A., Trush, V. and Quackenbush, J. (2003). "TM4: a free, open-source system for microarray data management and analysis." Biotechniques **34**(2): 374-8.

References

- Safadi, F. F., Thornton, P., Magiera, H., Hollis, B. W., Gentile, M., Haddad, J. G., Liebhaber, S. A. and Cooke, N. E. (1999). "Osteopathy and resistance to vitamin D toxicity in mice null for vitamin D binding protein." *J Clin Invest* **103**(2): 239-51.
- Saikumar, P. and Venkatachalam, M. A. (2003). "Role of apoptosis in hypoxic/ischemic damage in the kidney." *Semin Nephrol* **23**(6): 511-21.
- Sakai, Y. and Demay, M. B. (2000). "Evaluation of keratinocyte proliferation and differentiation in vitamin D receptor knockout mice." *Endocrinology* **141**(6): 2043-9.
- Sakai, Y., Kishimoto, J. and Demay, M. B. (2001). "Metabolic and cellular analysis of alopecia in vitamin D receptor knockout mice." *J Clin Invest* **107**(8): 961-6.
- Sakuma, T., Miyamoto, T., Jiang, W., Kakizawa, T., Nishio, S. I., Suzuki, S., Takeda, T., Oiwa, A. and Hashizume, K. (2003). "Inhibition of peroxisome proliferator-activated receptor alpha signaling by vitamin D receptor." *Biochem Biophys Res Commun* **312**(2): 513-9.
- Sarko, J. and Pollack, C. V., Jr. (2002). "Cardiac troponins." *J Emerg Med* **23**(1): 57-65.
- Sasaki, A., Yasukawa, H., Shouda, T., Kitamura, T., Dikic, I. and Yoshimura, A. (2000). "CIS3/SOCS-3 suppresses erythropoietin (EPO) signaling by binding the EPO receptor and JAK2." *J Biol Chem* **275**(38): 29338-47.
- Schena, M., Shalon, D., Davis, R. W. and Brown, P. O. (1995). "Quantitative monitoring of gene expression patterns with a complementary DNA microarray." *Science* **270**(5235): 467-70.
- Schena, M., Shalon, D., Heller, R., Chai, A., Brown, P. O. and Davis, R. W. (1996). "Parallel human genome analysis: microarray-based expression monitoring of 1000 genes." *Proc Natl Acad Sci U S A* **93**(20): 10614-9.
- Schmid, H., Cohen, C. D., Henger, A., Irrgang, S., Schlondorff, D. and Kretzler, M. (2003). "Validation of endogenous controls for gene expression analysis in microdissected human renal biopsies." *Kidney Int* **64**(1): 356-60.
- Schober, J. M., Chen, N., Grzeszkiewicz, T. M., Jovanovic, I., Emeson, E. E., Ugarova, T. P., Ye, R. D., Lau, L. F. and Lam, S. C. (2002). "Identification of integrin alpha(M)beta(2) as an adhesion receptor on peripheral blood monocytes for Cyr61 (CCN1) and connective tissue growth factor (CCN2): immediate-early gene products expressed in atherosclerotic lesions." *Blood* **99**(12): 4457-65.
- Schroeder, N. J. and Cunningham, J. (2000). "What's new in vitamin D for the nephrologist?" *Nephrol Dial Transplant* **15**(4): 460-6.
- Schulze, P. C., De Keulenaer, G. W., Yoshioka, J., Kassik, K. A. and Lee, R. T. (2002). "Vitamin D3-upregulated protein-1 (VDUP-1) regulates redox-dependent vascular smooth muscle cell proliferation through interaction with thioredoxin." *Circ Res* **91**(8): 689-95.
- Schütze, N. (2003). The extracellular matrix protein hCYR61 (CCN1) modulates signal transduction pathways associated with cell differentiation and proliferation in human osteoblasts. *25th Annual Meeting of the American Society of Bone and Mineral Research (ASBMR)*. F. K. Graedler, M; Balling, S; Hendrich, C; Eulert, J; Adamski J; Jakob F. Minneapolis, Minnesota, USA.
- Schütze, N. (2004). Personal communication. F. Graedler.
- Schutze, N., Lechner, A., Groll, C., Siggelkow, H., Hufner, M., Kohrle, J. and Jakob, F. (1998). "The human analog of murine cystein rich protein 61 [correction of 16] is a 1alpha,25-dihydroxyvitamin D3 responsive immediate early gene in human fetal osteoblasts: regulation by cytokines, growth factors, and serum." *Endocrinology* **139**(4): 1761-70.
- Schütze, N. G., F; Kunz, M; Balling, S; Hendrich, C; Eulert, J; Adamski J; Jakob F (2003). The extracellular matrix protein hCYR61 (CCN1) affects signal transduction pathways associated with cell differentiation and proliferation in human osteoblasts. Osteologie-Tagung, Göttingen.

References

- Schütze, N. G., F; Kunzi-Rapp, K; Jaschinski, D; Balling, S; Hendrich, C; Eulert, J; Adamski, J; Jakob, F (2004). The extracellular matrix signalling protein hCYR61 affects components of signal transduction pathways associated with cell differentiation in human osteoblasts. Orthopaedic Research Society 50th Annual Meeting, San Francisco, CA, USA.
- Schwartz, G. G., Whitlatch, L. W., Chen, T. C., Lokeshwar, B. L. and Holick, M. F. (1998). "Human prostate cells synthesize 1,25-dihydroxyvitamin D₃ from 25-hydroxyvitamin D₃." Cancer Epidemiol Biomarkers Prev **7**(5): 391-5.
- Schwartz, K., de la Bastie, D., Bouveret, P., Oliviero, P., Alonso, S. and Buckingham, M. (1986). "Alpha-skeletal muscle actin mRNA's accumulate in hypertrophied adult rat hearts." Circ Res **59**(5): 551-5.
- Sciaudone, M., Gazzero, E., Priest, L., Delany, A. M. and Canalis, E. (2003). "Notch 1 impairs osteoblastic cell differentiation." Endocrinology **144**(12): 5631-9.
- Sekiya, I., Vuoristo, J. T., Larson, B. L. and Prockop, D. J. (2002). "In vitro cartilage formation by human adult stem cells from bone marrow stroma defines the sequence of cellular and molecular events during chondrogenesis." Proc Natl Acad Sci U S A **99**(7): 4397-402.
- Seltmann, M. (2003). personal communication. F. Graedler.
- Seward, D. J., Koh, A. S., Boyer, J. L. and Ballatori, N. (2003). "Functional complementation between a novel mammalian polygenic transport complex and an evolutionarily ancient organic solute transporter, OSTalpha-OSTbeta." J Biol Chem **278**(30): 27473-82.
- Sharma, A. M. (2003). "Obesity and cardiovascular risk." Growth Horm IGF Res **13 Suppl A**: S10-7.
- Sheikh, I. A. and Kaplan, A. P. (1989). "Mechanism of digestion of bradykinin and lysylbradykinin (kallidin) in human serum. Role of carboxypeptidase, angiotensin-converting enzyme and determination of final degradation products." Biochem Pharmacol **38**(6): 993-1000.
- Shi, H., Dirienzo, D. and Zemel, M. B. (2001a). "Effects of dietary calcium on adipocyte lipid metabolism and body weight regulation in energy-restricted aP2-agouti transgenic mice." Faseb J **15**(2): 291-3.
- Shi, H., Norman, A. W., Okamura, W. H., Sen, A. and Zemel, M. B. (2001b). "1alpha,25-Dihydroxyvitamin D₃ modulates human adipocyte metabolism via nongenomic action." Faseb J **15**(14): 2751-3.
- Sigmund, C. D. (2002). "Regulation of renin expression and blood pressure by vitamin D(3)." J Clin Invest **110**(2): 155-6.
- Simkhovich, B. Z., Marjoram, P., Poizat, C., Kedes, L. and Kloner, R. A. (2003). "Brief episode of ischemia activates protective genetic program in rat heart: a gene chip study." Cardiovasc Res **59**(2): 450-9.
- Sinal, C. J., Tohkin, M., Miyata, M., Ward, J. M., Lambert, G. and Gonzalez, F. J. (2000). "Targeted disruption of the nuclear receptor FXR/BAR impairs bile acid and lipid homeostasis." Cell **102**(6): 731-44.
- Singh-Gasson, S., Green, R. D., Yue, Y., Nelson, C., Blattner, F., Sussman, M. R. and Cerrina, F. (1999). "Maskless fabrication of light-directed oligonucleotide microarrays using a digital micromirror array." Nat Biotechnol **17**(10): 974-8.
- Skott, O. (2003). "Androgen-induced activation of 20-HETE production may contribute to gender differences in blood pressure regulation." Am J Physiol Regul Integr Comp Physiol **284**(4): R1053-4.
- Soriano-Izquierdo, A., Gironella, M., Massaguer, A., May, F. E., Salas, A., Sans, M., Poulson, R., Thim, L., Pique, J. M. and Panes, J. (2004). "Trefoil peptide TFF2 treatment reduces VCAM-1 expression and leukocyte recruitment in experimental intestinal inflammation." J Leukoc Biol **75**(2): 214-23.

References

- Soukas, A., Cohen, P., Socci, N. D. and Friedman, J. M. (2000). "Leptin-specific patterns of gene expression in white adipose tissue." *Genes Dev* **14**(8): 963-80.
- Soulet, D. and Rivest, S. (2002). "Perspective: how to make microarray, serial analysis of gene expression, and proteomic relevant to day-to-day endocrine problems and physiological systems." *Endocrinology* **143**(6): 1995-2001.
- Sousa, M. M., Norden, A. G., Jacobsen, C., Willnow, T. E., Christensen, E. I., Thakker, R. V., Verroust, P. J., Moestrup, S. K. and Saraiva, M. J. (2000). "Evidence for the role of megalin in renal uptake of transthyretin." *J Biol Chem* **275**(49): 38176-81.
- Southern, E. M. (2000). "Blotting at 25." *Trends Biochem Sci* **25**(12): 585-8.
- Spellman, P. T., Miller, M., Stewart, J., Troup, C., Sarkans, U., Chervitz, S., Bernhart, D., Sherlock, G., Ball, C., Lepage, M., Swiatek, M., Marks, W. L., Goncalves, J., Markel, S., Iordan, D., Shojatalab, M., Pizarro, A., White, J., Hubley, R., Deutsch, E., Senger, M., Aronow, B. J., Robinson, A., Bassett, D., Stoeckert, C. J., Jr. and Brazma, A. (2002). "Design and implementation of microarray gene expression markup language (MAGE-ML)." *Genome Biol* **3**(9): RESEARCH0046.
- Stears, R. L., Getts, R. C. and Gullans, S. R. (2000). "A novel, sensitive detection system for high-density microarrays using dendrimer technology." *Physiol Genomics* **3**(2): 93-9.
- Stears, R. L., Martinsky, T. and Schena, M. (2003). "Trends in microarray analysis." *Nat Med* **9**(1): 140-5.
- Steppan, C. M., Bailey, S. T., Bhat, S., Brown, E. J., Banerjee, R. R., Wright, C. M., Patel, H. R., Ahima, R. S. and Lazar, M. A. (2001). "The hormone resistin links obesity to diabetes." *Nature* **409**(6818): 307-12.
- Stewart, K., Walsh, S., Screen, J., Jefferiss, C. M., Chainey, J., Jordan, G. R. and Beresford, J. N. (1999). "Further characterization of cells expressing STRO-1 in cultures of adult human bone marrow stromal cells." *J Bone Miner Res* **14**(8): 1345-56.
- Stillman, B. A. and Tonkinson, J. L. (2001). "Expression microarray hybridization kinetics depend on length of the immobilized DNA but are independent of immobilization substrate." *Anal Biochem* **295**(2): 149-57.
- Strom, M., Sandgren, M. E., Brown, T. A. and DeLuca, H. F. (1989). "1,25-Dihydroxyvitamin D3 up-regulates the 1,25-dihydroxyvitamin D3 receptor in vivo." *Proc Natl Acad Sci U S A* **86**(24): 9770-3.
- Suematsu, N., Okamoto, K. and Isohashi, F. (2002). "Mouse cytosolic acetyl-CoA hydrolase, a novel candidate for a key enzyme involved in fat metabolism: cDNA cloning, sequencing and functional expression." *Acta Biochim Pol* **49**(4): 937-45.
- Sun, X. and Zemel, M. B. (2003). "Effects of mitochondrial uncoupling on adipocyte intracellular Ca(2+) and lipid metabolism." *J Nutr Biochem* **14**(4): 219-26.
- Sundaresan, M., Yu, Z. X., Ferrans, V. J., Irani, K. and Finkel, T. (1995). "Requirement for generation of H2O2 for platelet-derived growth factor signal transduction." *Science* **270**(5234): 296-9.
- Sutton, A. L. and MacDonald, P. N. (2003). "Vitamin D: more than a "bone-a-fide" hormone." *Mol Endocrinol* **17**(5): 777-91.
- Takeda, S., Yoshizawa, T., Nagai, Y., Yamato, H., Fukumoto, S., Sekine, K., Kato, S., Matsumoto, T. and Fujita, T. (1999). "Stimulation of osteoclast formation by 1,25-dihydroxyvitamin D requires its binding to vitamin D receptor (VDR) in osteoblastic cells: studies using VDR knockout mice." *Endocrinology* **140**(2): 1005-8.
- Takekawa, M. and Saito, H. (1998). "A family of stress-inducible GADD45-like proteins mediate activation of the stress-responsive MTK1/MEKK4 MAPKKK." *Cell* **95**(4): 521-30.
- Takeyama, K., Kitanaka, S., Sato, T., Kobori, M., Yanagisawa, J. and Kato, S. (1997). "25-Hydroxyvitamin D3 1alpha-hydroxylase and vitamin D synthesis." *Science* **277**(5333): 1827-30.

References

- Tangpricha, V., Flanagan, J. N., Whitlatch, L. W., Tseng, C. C., Chen, T. C., Holt, P. R., Lipkin, M. S. and Holick, M. F. (2001). "25-hydroxyvitamin D-1 α -hydroxylase in normal and malignant colon tissue." *Lancet* **357**(9269): 1673-4.
- Tanito, M., Nakamura, H., Kwon, Y. W., Teratani, A., Masutani, H., Shioji, K., Kishimoto, C., Ohira, A., Horie, R. and Yodoi, J. (2004). "Enhanced oxidative stress and impaired thioredoxin expression in spontaneously hypertensive rats." *Antioxid Redox Signal* **6**(1): 89-97.
- Tanti, J. F., Gual, P., Gremeaux, T., Gonzalez, T., Barres, R. and Le Marchand-Brustel, Y. (2004). "Alteration in insulin action: role of IRS-1 serine phosphorylation in the retroregulation of insulin signalling." *Ann Endocrinol (Paris)* **65**(1): 43-8.
- Tenenhouse, H. S., Gauthier, C., Chau, H. and St-Arnaud, R. (2004). "1 α -Hydroxylase gene ablation and Pi supplementation inhibit renal calcification in mice homozygous for the disrupted Npt2a gene." *Am J Physiol Renal Physiol* **286**(4): F675-81.
- Tetradis, S., Bezouglaia, O., Tsingotjidou, A. and Vila, A. (2001). "Regulation of the nuclear orphan receptor Nur77 in bone by parathyroid hormone." *Biochem Biophys Res Commun* **281**(4): 913-6.
- Tezuka, K., Yasuda, M., Watanabe, N., Morimura, N., Kuroda, K., Miyatani, S. and Hozumi, N. (2002). "Stimulation of osteoblastic cell differentiation by Notch." *J Bone Miner Res* **17**(2): 231-9.
- Thomasset, M., Parkes, C. O. and Cuisinier-Gleizes, P. (1982). "Rat calcium-binding proteins: distribution, development, and vitamin D dependence." *Am J Physiol* **243**(6): E483-8.
- Todd, R., Lingen, M. W. and Kuo, W. P. (2002). "Gene expression profiling using laser capture microdissection." *Expert Rev Mol Diagn* **2**(5): 497-507.
- Touyz, R. M. and Schiffrin, E. L. (2003). "Role of endothelin in human hypertension." *Can J Physiol Pharmacol* **81**(6): 533-41.
- Tusher, V. G., Tibshirani, R. and Chu, G. (2001). "Significance analysis of microarrays applied to the ionizing radiation response." *Proc Natl Acad Sci U S A* **98**(9): 5116-21.
- Ukkola, O. (2002). "Resistin - a mediator of obesity-associated insulin resistance or an innocent bystander?" *Eur J Endocrinol* **147**(5): 571-4.
- Valverde, A. M., Arribas, M., Mur, C., Navarro, P., Pons, S., Cassard-Doulcier, A. M., Kahn, C. R. and Benito, M. (2003). "Insulin-induced up-regulated uncoupling protein-1 expression is mediated by insulin receptor substrate 1 through the phosphatidylinositol 3-kinase/Akt signaling pathway in fetal brown adipocytes." *J Biol Chem* **278**(12): 10221-31.
- van de Peppel, J., Kemmeren, P., van Bakel, H., Radonjic, M., van Leenen, D. and Holstege, F. C. (2003). "Monitoring global messenger RNA changes in externally controlled microarray experiments." *EMBO Rep* **4**(4): 387-93.
- Vukmirovic, O. G. and Tilghman, S. M. (2000). "Exploring genome space." *Nature* **405**(6788): 820-2.
- Walsh, S., Jordan, G. R., Jefferiss, C., Stewart, K. and Beresford, J. N. (2001). "High concentrations of dexamethasone suppress the proliferation but not the differentiation or further maturation of human osteoblast precursors in vitro: relevance to glucocorticoid-induced osteoporosis." *Rheumatology (Oxford)* **40**(1): 74-83.
- Wang, D., Liu, S., Trummer, B. J., Deng, C. and Wang, A. (2002). "Carbohydrate microarrays for the recognition of cross-reactive molecular markers of microbes and host cells." *Nat Biotechnol* **20**(3): 275-81.
- Wang, W., Li, C., Kwon, T. H., Knepper, M. A., Frokiaer, J. and Nielsen, S. (2002). "AQP3, p-AQP2, and AQP2 expression is reduced in polyuric rats with hypercalcemia: prevention by cAMP-PDE inhibitors." *Am J Physiol Renal Physiol* **283**(6): F1313-25.
- Watanabe, T., Yoshizumi, M., Akishita, M., Eto, M., Toba, K., Hashimoto, M., Nagano, K., Liang, Y. Q., Ohike, Y., Iijima, K., Sudoh, N., Kim, S., Nakaoka, T., Yamashita, N., Ako, J. and Ouchi, Y. (2001). "Induction of nuclear orphan receptor NGFI-B gene and

References

- apoptosis in rat vascular smooth muscle cells treated with pyrrolidinedithiocarbamate." *Arterioscler Thromb Vasc Biol* **21**(11): 1738-44.
- Way, J. M., Gorgun, C. Z., Tong, Q., Uysal, K. T., Brown, K. K., Harrington, W. W., Oliver, W. R., Jr., Willson, T. M., Klierer, S. A. and Hotamisligil, G. S. (2001). "Adipose tissue resistin expression is severely suppressed in obesity and stimulated by peroxisome proliferator-activated receptor gamma agonists." *J Biol Chem* **276**(28): 25651-3.
- Webb, A. R., Kline, L. and Holick, M. F. (1988). "Influence of season and latitude on the cutaneous synthesis of vitamin D3: exposure to winter sunlight in Boston and Edmonton will not promote vitamin D3 synthesis in human skin." *J Clin Endocrinol Metab* **67**(2): 373-8.
- Weihua, Z., Lathe, R., Warner, M. and Gustafsson, J. A. (2002). "An endocrine pathway in the prostate, ERbeta, AR, 5alpha-androstane-3beta,17beta-diol, and CYP7B1, regulates prostate growth." *Proc Natl Acad Sci U S A* **99**(21): 13589-94.
- Wellmann, S., Buhner, C., Moderegger, E., Zelmer, A., Kirschner, R., Koehne, P., Fujita, J. and Seeger, K. (2004). "Oxygen-regulated expression of the RNA-binding proteins RBM3 and CIRP by a HIF-1-independent mechanism." *J Cell Sci* **117**(Pt 9): 1785-94.
- Wen, H. Y., Xia, Y., Young, M. E., Taegtmeier, H. and Kellems, R. E. (2002). "The adenylosuccinate synthetase-1 gene is activated in the hypertrophied heart." *J Cell Mol Med* **6**(2): 235-43.
- White, P. and Cooke, N. (2000). "The multifunctional properties and characteristics of vitamin D-binding protein." *Trends Endocrinol Metab* **11**(8): 320-7.
- Wistrand, P. J. (2002). "Carbonic anhydrase III in liver and muscle of male rats purification and properties." *Ups J Med Sci* **107**(2): 77-88.
- Wu, Z. and Chiang, J. Y. (2001). "Transcriptional regulation of human oxysterol 7 alpha-hydroxylase gene (CYP7B1) by Sp1." *Gene* **272**(1-2): 191-7.
- Wu, Z., Martin, K. O., Javitt, N. B. and Chiang, J. Y. (1999). "Structure and functions of human oxysterol 7alpha-hydroxylase cDNAs and gene CYP7B1." *J Lipid Res* **40**(12): 2195-203.
- Wu-Wong, J. R., Tian, J. and Goltzman, D. (2004). "Vitamin D analogs as therapeutic agents: a clinical study update." *Curr Opin Investig Drugs* **5**(3): 320-6.
- Xia, Y., Wen, H. Y., Young, M. E., Guthrie, P. H., Taegtmeier, H. and Kellems, R. E. (2003). "Mammalian target of rapamycin and protein kinase A signaling mediate the cardiac transcriptional response to glutamine." *J Biol Chem* **278**(15): 13143-50.
- Xiang, C. C., Chen, M., Kozhich, O. A., Phan, Q. N., Inman, J. M., Chen, Y. and Brownstein, M. J. (2003). "Probe generation directly from small numbers of cells for DNA microarray studies." *Biotechniques* **34**(2): 386-8, 390, 392-3.
- Xue, B., Moustaid, N., Wilkison, W. O. and Zemmel, M. B. (1998). "The agouti gene product inhibits lipolysis in human adipocytes via a Ca²⁺-dependent mechanism." *Faseb J* **12**(13): 1391-6.
- Yagyu, H., Chen, G., Yokoyama, M., Hirata, K., Augustus, A., Kako, Y., Seo, T., Hu, Y., Lutz, E. P., Merkel, M., Bensadoun, A., Homma, S. and Goldberg, I. J. (2003). "Lipoprotein lipase (LpL) on the surface of cardiomyocytes increases lipid uptake and produces a cardiomyopathy." *J Clin Invest* **111**(3): 419-26.
- Yamamoto, M., Yang, G., Hong, C., Liu, J., Holle, E., Yu, X., Wagner, T., Vatner, S. F. and Sadoshima, J. (2003). "Inhibition of endogenous thioredoxin in the heart increases oxidative stress and cardiac hypertrophy." *J Clin Invest* **112**(9): 1395-406.
- Yamamoto, N. and Naraparaju, V. R. (1996). "Vitamin D3-binding protein as a precursor for macrophage activating factor in the inflammation-primed macrophage activation cascade in rats." *Cell Immunol* **170**(2): 161-7.

References

- Yanase, T., Mu, Y. M., Nishi, Y., Goto, K., Nomura, M., Okabe, T., Takayanagi, R. and Nawata, H. (2001). "Regulation of aromatase by nuclear receptors." J Steroid Biochem Mol Biol **79**(1-5): 187-92.
- Yoshizawa, T., Handa, Y., Uematsu, Y., Takeda, S., Sekine, K., Yoshihara, Y., Kawakami, T., Arioka, K., Sato, H., Uchiyama, Y., Masushige, S., Fukamizu, A., Matsumoto, T. and Kato, S. (1997). "Mice lacking the vitamin D receptor exhibit impaired bone formation, uterine hypoplasia and growth retardation after weaning." Nat Genet **16**(4): 391-6.
- Zeititz, U., Weber, K., Soegiarto, D. W., Wolf, E., Balling, R. and Erben, R. G. (2003). "Impaired insulin secretory capacity in mice lacking a functional vitamin D receptor." Faseb J **17**(3): 509-11.
- Zella, J. B., McCary, L. C. and DeLuca, H. F. (2003). "Oral administration of 1,25-dihydroxyvitamin D3 completely protects NOD mice from insulin-dependent diabetes mellitus." Arch Biochem Biophys **417**(1): 77-80.
- Zemel, M. B. (1998). "Nutritional and endocrine modulation of intracellular calcium: implications in obesity, insulin resistance and hypertension." Mol Cell Biochem **188**(1-2): 129-36.
- Zemel, M. B. (2001). "Calcium modulation of hypertension and obesity: mechanisms and implications." J Am Coll Nutr **20**(5 Suppl): 428S-435S; discussion 440S-442S.
- Zemel, M. B. (2002). "Regulation of adiposity and obesity risk by dietary calcium: mechanisms and implications." J Am Coll Nutr **21**(2): 146S-151S.
- Zemel, M. B. (2004). "Role of calcium and dairy products in energy partitioning and weight management." Am J Clin Nutr **79**(5): 907S-12S.
- Zemel, M. B., Shi, H., Greer, B., Dirienzo, D. and Zemel, P. C. (2000). "Regulation of adiposity by dietary calcium." Faseb J **14**(9): 1132-8.
- Zhang, X. K. (2002). "Vitamin A and apoptosis in prostate cancer." Endocr Relat Cancer **9**(2): 87-102.
- Zhao, Y. and Pan, W. (2003). "Modified nonparametric approaches to detecting differentially expressed genes in replicated microarray experiments." Bioinformatics **19**(9): 1046-54.
- Zhou, Z., Yon Toh, S., Chen, Z., Guo, K., Ng, C. P., Ponniah, S., Lin, S. C., Hong, W. and Li, P. (2003). "Cidea-deficient mice have lean phenotype and are resistant to obesity." Nat Genet **35**(1): 49-56.
- Zhu, Z., Zhu, S., Zhu, J., van der Giet, M. and Tepel, M. (2002). "Endothelial dysfunction in cold-induced hypertensive rats." Am J Hypertens **15**(2 Pt 1): 176-80.
- Zittermann, A. (2003). "Vitamin D in preventive medicine: are we ignoring the evidence?" Br J Nutr **89**(5): 552-72.
- Zou, J., Young, S., Zhu, F., Gheyas, F., Skeans, S., Wan, Y., Wang, L., Ding, W., Billah, M., McClanahan, T., Coffman, R. L., Egan, R. and Umland, S. (2002). "Microarray profile of differentially expressed genes in a monkey model of allergic asthma." Genome Biol **3**(5): research0020.